THE ASTRONOMICAL JOURNAL

PUBLISHED BY THE AMERICAN INSTITUTE OF PHYSICS
FOR THE AMERICAN ASTRONOMICAL SOCIETY

VOLUME 65 1960 June ~ No. 1280 *NUMBER 5*

Conference on Astronomical Observations from Above the Earth's Atmosphere

SPONSORED BY

THE AMERICAN ASTRONOMICAL SOCIETY

AND

THE NATIONAL SCIENCE FOUNDATION

DECEMBER 30, 1959

CASE INSTITUTE OF TECHNOLOGY

For the last few years it has been customary to hold a conference or a symposium during the regular meetings f the American Astronomical Society. Since the Society was scheduled to meet at the Case Institute of Technolgy on December 28 to 30, 1959,the staff of the Warner and Swasey Observatory proposed such a conference uring this period. The subject chosen by us, and approved by the Society, was "Astronomical Observations from bove the Earth's Atmosphere." Our aim was a presentation of suggestions for extending the terrestrial methods f observation to the instrumentation required and problems to be solved by observations from above the atmoshere. We wished to limit the discussion of observational material already obtained from rockets and satellites. Vith this in mind, we sought the advice of the Committee on Astronomy of the Space Science Board. We are inebted to Professor Leo Goldberg, the chairman, for the suggestions made to us by the Board.

The papers presented at this meeting are included in the current issue of the *Astronomical Journal* .These have ulfilled in an admirable way the aim of the conference. They include a summary of the vehicles and payloads hich will be made available together with a complete and detailed design of a space telescope. The observations uggested range from gravitational astronomy of the solar system to extragalactic studies. The wavelengths of adiation to be utilized range from γ rays to the infrared.

The following persons participated during the one-day program which was held on December 30, 1959:

Presiding: Fred Hoyle, St. John's College, Cambridge University

"Vehicles and Plans," Nancy G. Roman, National Aeronautics and Space Administration
"Space Telescopes and Components," Lyman Spitzer, Jr., Princeton University Observatory
"Recent Experiments from Rockets and Satellites," Herbert Friedman, U. S. Naval Research Laboratory
"Controlled Experiments in Celestial Mechanics," G. M. Clemence, U. S. Naval Observatory
"Solar Experiments," Leo Goldberg, The Observatory, University of Michigan
"Stellar Astronomy from a Space Vehicle," Arthur D. Code, Washburn Observatory, University of Wisconsin
"Proposed Stellar and Interstellar Survey," Fred L. Whipple and Robert J. Davis, Smithsonian Astrophysical Observatory, Cambridge, Massachusetts

Ve are indebted to the National Science Foundation for the grant to defray the expenses incurred for the conference and for the publication cost of these papers.

J. J. NASSAU
Conference Chairman

March 21, 1960

Vehicles and Plans

NANCY G. ROMAN
National Aeronautics and Space Administration, Washington 25, D. C.
(Received March 24, 1960)

ASTRONOMERS are understandably excited about the possibilities of making observations from beyond the terrestrial atmosphere. At the present time, astronomical observations are limited to the relatively small visual window, the somewhat more broken near-infrared region, and a broader, more newly exploited radio region. This means that many important astronomical data are hidden. For example, the solar corona emits strongly in the ultraviolet and in the long-wave region. The disturbed sun flares strongly in Lyman-Alpha and in low radio frequencies. Emission nebulae are bright in Lyman-Alpha and in high radio frequencies. Planetary radiations reach a maximum in the far infrared where they are now masked by the terrestrial atmosphere. Very hot stars are bright in the ultraviolet; interstellar dust should shine by its own emission in the far infrared. Finally, in distant galaxies, we now see only the portion of the spectra which for the nearer galaxies is in the hidden ultraviolet region of the spectrum. Observations of the distant and near galaxies in comparable spectral regions will permit a study of possible galactic aging effects. For all of these objects, and many others, we anticipate that observations in the now hidden spectral regions will be of great interest and great importance to the future of astrophysical development.

Of the vehicles which have been used to place American satellites in orbit, the Jupiter C, the Juno II, and the Vanguard will soon be replaced by systems more specifically designed for space research. The first of these will be the Delta and the Scout. The Delta will be used in about a year for an Orbiting Solar Observatory, a satellite weighing approximately 350 lb with a stabilization system designed to permit the continual accurate pointing of optical equipment to the solar disk. The Scout will permit the orbiting of somewhat smaller payloads and will be particularly useful for high altitude rockets and for low altitude, monitoring satellites. Later the Delta will be replaced by the Agena B boosted by either a Thor or an Atlas. The latter will be used to place multi-ton payloads in earth orbits and usable payloads near the moon. The Centaur, Saturn, and Nova will provide successively larger payloads at increasing distances from the earth.

The ultimate aim of the Lunar Science Program is to place a manned scientific station on the moon. In the meantime, we hope to learn as much as possible about the lunar atmosphere, surface, and interior from lunar orbiters, impacts, and hard and soft landings. The lunar surface will be mapped spectrophotometrically by a radar altimeter and by vidicon; the surface composition will be analyzed by gamma-ray spectrometry and teste for natural beta and gamma radioactivity, and surfac hardness will be determined by a penetrometer. Instru mentation for studying the lunar environment will mak measurements of the density, ionization, and the mag netic field in the lunar atmosphere, the plasma densit and temperature of the lunar ionosphere, soft and ene getic particles fluxes, and cosmic radiation and micr meteorites. Some of the early experiments which ar being prepared are a rubidium-vapor magnetometer, plasma probe, a seismograph, a penetrometer, and radiation complex to measure cosmic radiation in th vicinity of the moon.

The aim of the NASA Solar Physics Program is t obtain an understanding of the solar atmosphere and the solar-planetary relationships by studies from eart satellites in the ultraviolet, x-ray, gamma-ray, and radi region of the spectra, and by probe instrumentation t measure the composition of the solar atmosphere an eventually atmospheric activity on other planets. Th Orbiting Solar Observatory is mentioned above. Th Observatory will carry ultraviolet spectrographs, ultra violet and x-ray photometers, a gamma-ray telescop and other equipment for measuring solar and geophys cal quantities. Instrumentation for a later version the solar observatory is expected to include a coron graph, a spectroheliograph, and other equipment f studying the sun in greater detail than will be possib from the first solar satellite.

The Observational Astronomy Program includes fiv projects. The largest is the Orbiting Astronomical Ob servatories Project, in which a satellite containing moderately large optical telescope is planned. Satelli stabilization and guidance will permit tracking a sta or star field within a small fraction of a second of ar This project will be discussed in greater detail in oth papers in this symposium. However, important featur should be mentioned. The satellite can have a large pr mary mirror for spectroscopy and/or smaller objectiv for photometry and mapping in various regions of th spectrum. A finder telescope system will permit th identification of the star field under observation fro the earth; an independent system for determining th orientation of the telescope objective in space will b provided as well. Solar cells will provide power for th vehicle through its lifetime of at least one year. Of course, antennas to transmit the large amount of in formation obtained back to the terrestrial tracking an data centers will be needed.

There are four other projects in the Observation

Astronomy Program. The first of the astronomical satellite launchings will occur sometime later this year in the Gamma-Ray Astronomy Project. This satellite will be launched by a Juno II and will be instrumented to measure the spatial distribution of 100-mev gamma-ray radiation. Later experiments will provide increased sensitivity and finer energy and spatial resolution for photometry, mapping and monitoring in the gamma-ray region.

In the orbiting Radio Astronomy Project, instrumentation is currently being developed for measuring the cosmic noise background in the region normally reflected by the terrestrial atmosphere, that is, between 0.2 and 20 Mc. Later we hope that this project will also include instrumentation to bridge the present gap between radio and optical astronomy by making possible observations in the wavelengths shorter than 4 mm. Far-infrared observations are contemplated in the Orbiting Astronomical Observatories Project.

The Relativity Investigations Project includes an atomic clock experiment on which work is well underway, a satellite to monitor the earth's gravitational field for secular and periodic changes, and an artificial planet carrying a radar transponder to measure more accurately the size and shape of the earth's and the planetoid's orbits.

Finally, the Advanced Galactic Investigations Project includes astronomical plans for the future which have not yet been implemented. This will include, for both the solar and the galactic investigations, advanced orbiting optical and radio instrumentation, instrumentation on the moon, and finally in the distant future, manned lunar observatories.

A fundamental part of all of these plans is the participation of the entire astronomical community. NASA will act as a coordinating agency to enable astronomers to obtain the basic observations they need from outer space. Each of the remaining speakers in this symposium is participating in this program. Other institutions cooperating in the NASA Astronomy Programs include the National Bureau of Standards, the Army Ballistic Missile Agency, the Massachusetts Institute of Technology, California Institute of Technology, Columbia University, the Universities of Rochester, Colorado, Arizona, New Mexico, and Chicago, Kitt Peak National Observatory, and NASA's Goddard Space Flight Center. In addition, much of the engineering and construction will be done by industrial contractors.

Space Telescopes and Components*

LYMAN SPITZER, JR.
Princeton University Observatory, Princeton, New Jersey
(Received March 24, 1960)

A brief analysis is given of some of the major problems involved in the design of a large satellite telescope for stellar observations. A 1000-kg structure is assumed, 2 m on a side, in orbit at an altitude of either 800 km or 36 000 km, with orbital periods of 101 min and 24 hr, respectively.

Stabilization during guiding requires countering the perturbing torques due to air drag, solar radiation pressure, the tidal force of the earth, and magnetic forces of ferromagnetic materials. The first three torques can be reduced by appropriate symmetry, and the last by use of iron with low permanent magnetization. A torque of 100 dyne cm should be adequate for stabilization. This torque can readily be produced by applying a rotating magnetic field to an "inertial sphere," consisting of an aluminum shell, positioned by a rapidly oscillating magnetic field. At 800 km the eddy currents in a sphere 40 cm in diameter, rotating in the earth's magnetic field, will transmit a torque as great as 100 dyne cm directly to the earth, and thus the sphere can continue to absorb a torque of this magnitude indefinitely. At an altitude of 36 000 km, the angular momentum accumulated by the sphere must be dumped in some way; jets of gas, and controlled magnetic and radiative torques provide possible means. To set the telescope, rotation of the entire satellite by as much as 180° in 6 min can be achieved either by an inertial sphere or by three separate wheels, one for each axis.

To sense the direction in which the telescope points, for control of setting, a number of techniques are possible. Coarse orientation can be obtained by simple measures of the light from the sun and the infrared radiation from the earth; measurement of the direction of the earth's magnetic field and use of gyroscopes present alternate possibilities. If observations can be limited to stars of the fifth magnitude or brighter, the automatic guidance system can accept all light within a circle ½ degree in radius, and the coarse orientation may suffice for initial acquisition, since the angle of the sun from the optical axis can easily be measured with considerable precision. For acquisition of fainter stars, the stars themselves must be used for fine orientation, either with televisio cameras and ground control, or by precise measures of angles fro a few bright stars. Once a program star or guide star has be acquired, automatic guidance with an accuracy better than second of arc would appear entirely possible.

Since storage batteries and electronic components are best ke at about 20°C, while photoelectric detectors should be cooled −80°C for low dark current, a two-chamber satellite seems desi able. The satellite rotates about the optical axis automatically keep the warm chamber facing the sun. Solar batteries produci a mean power of about 100 w are placed on this side. The oth side comes into equilibrium with the infrared radiation from t earth and with the heat leakage from the warm chamber; a ter perature between −65° and −95°C can be achieved. To mainta the focus and resolution of the optical system one may use fus silica mirrors, with a relative thermal expansion of less than 10 over this temperature range. For positioning the various optic elements, thermally compensated structures, using dissimil metals, may be used. An arrangement of concentric tubes promis to yield the necessary thermal homogeneity required. Altern tively, the mirrors and all supports could all be made of al minum, and conduction through sufficiently massive suppor relied upon for thermal homogeneity.

As an example of these concepts, a preliminary design is pr sented for a spectroscopic instrument, with a 24-in. mirror and number of phototubes for scanning a stellar spectrum with hi resolution. The over-all reliability is investigated, on the basis minimum failure rates for standard components. A mean life about a year is computed before accumulating failures render t instrument unusable. The design includes considerable redundan of separate systems. If each electronic component could be ma separately redundant, this mean life would be increased by order of magnitude. Because of failures not envisaged in t analysis a number of separate launchings would presumably required to yield a fully operating instrument.

THE possibility of placing an astronomical observatory in a satellite orbit poses an enormous challenge as well as an exciting opportunity. The research avenues opened up by a telescope above the atmosphere are certainly broad, but the engineering problems posed by the requirement of reliable operation in so novel an environment are also substantial. The present paper surveys briefly some of the basic problems that appear with a satellite telescope. Problems characteristic of satellites generally, including launching, power supply, data storage, telemetering, and ground control, are not treated here. Presumably by the time that a large telescope is placed in orbit, these problems will have been solved in connection with other satellite programs. However, a large telescope poses problems not encountered with other types of equipment, such as precise positioning and stabilization of the direction in which the telescope points, and the launching, alignment, and focusing of a precise a complex optical system under the environment conditions encountered in space.

In the first section these environmental characteristi are briefly discussed. Subsequent sections treat t problems of rotating and stabilizing the telesco during setting and guiding, respectively, and of sensi the orientation during these operations. Problems temperature control and of optical adjustment a also treated, and a preliminary quantitative analys of system reliability is given. A simple conceptu design of a satellite spectroscopic telescope is presente at the end of this paper. The emphasis here is primari on a stellar telescope. While some of the discussio especially on stabilization, is relevant also to a sol instrument, the specific problems of such an instrume have not been considered.

I. ENVIRONMENTAL CHARACTERISTICS

Any satellite is exposed to two radically differe environmental situations. First it is violently launche

* This work has been supported in part by the Air Force Cambridge Research Center, under a contract with Princeton University.

into orbit, and then during its free orbital motion it floats in a virtually force-free vacuum. The forces during launching are very large. In addition to a steady-state acceleration, typically between 10 and 30 g, there is also a very large vibration, producing alternating accelerations as great as 20 g over frequencies from a few cycles per second up to several kilocycles. This vibration poses a particularly serious problem, since it virtually requires that all free mechanical oscillations of the satellite and its equipment have resonant frequencies in the high kilocycle range. Such high rigidity requires much greater weight than is normal, in addition to much more careful design. In principle, it should be possible to reduce at least the high-frequency vibration by means of shock mounts, but the combination of high, steady acceleration together with the strong vibration poses serious practical problems in the design of shock mounting, and this approach has not been followed. Evidently the designing of a precise, high-resolution optical system that will still be in adjustment after such violent treatment as a satellite launching is not a simple task.

Once the satellite is in orbit the problem of structural strength disappears entirely. Because of weightlessness the problem of variable flexure, which becomes so difficult in large earthbound telescopes, is absent in space. Thus, in principle, much larger telescopes are theoretically possible in space than on the earth or the moon. One may visualize a very large telescope in space, with a diameter exceeding 400 inches, and a resolution better than 0.01 sec of arc. In the near future, however, we must probably consider a mirror not more than 60 inches in diameter; for telescopes of this size, weightlessness is not of decisive importance.

One problem associated with weightlessness is the absence of a large mass that can be used to absorb the reaction torques required in setting and guiding the telescope. Section II is largely devoted to a discussion of this problem.

Besides weightlessness, another characteristic of the environment in which a satellite moves is the high vacuum. It is this vacuum, of course, which is the main advantage of a satellite telescope, providing full transmission and perfect seeing over virtually the entire spectrum. This vacuum introduces engineering complexities. Thermal equilibrium is no longer dominated by convection; radiation and conduction are the only processes which occur. Radiation transmitted by the vacuum may have undesirable effects on the equipment; ultraviolet light and x rays may affect reflecting coatings. If moving parts are provided, lubrication of any bearing surfaces poses special problems. Bombardment by small meteors is also a problem, in principle, although measures on meteorites (Whipple and Fireman 1959) indicate that the erosion of the mirror surface should be less than 10^{-6} cm year^{-1}, and quite negligible during a year. Damage of delicate equipment by small meteors can in any case be virtually eliminated by the use of a protecting double skin around such equipment, as suggested by Whipple (1952).

A major and previously unexpected feature of a satellite's environment is the presence of trapped energetic particles in the Van Allen radiation belts. According to the recent survey by Van Allen (1959), the radiation extends from about 800 km to 30 000 km with electrons and energetic protons in the lower layer and electrons of lower energy in the outer layer. Even at latitudes as low as 400 km, considerable radiation may be present at intermediate and higher latitudes (Van Allen, McIlwain, and Ludwig 1959). Bombardment of a satellite generates x rays which may produce unwanted background noise in photoelectric detectors and in electronic systems generally. Shielding is possible, but requires additional weight. We shall assume here that any satellite is either just below the major Van Allen belts, at about 800-km altitude, or just outside, at about 36 000 km. These are logical orbits to consider, quite apart from considerations of trapped particles. A mean altitude of 800 km is about the lowest in which atmospheric drag is safely negligible even if the orbit is not exactly circular. At 36 000 km the period is about 24 hr, and if the orbit is nearly equatorial the satellite, with some adjustment, can remain always visible from a particular ground station.

The density at 800 km has been determined from the observed changes of satellite orbits. According to Harris and Jastrow (1959), the density at this altitude is about 10^{-16} g cm^{-3}. The pressure ρv^2 produced by motion of a satellite through gas at this density, ρ, with the circular velocity 7.5×10^5 cm sec^{-1} is equal to 5.6×10^{-5} dyne cm^{-2}. At 36 000 km the density is presumably down to its mean value for interplanetary space, about 10^{-21} g cm^{-3}, and is entirely negligible. These values are somewhat uncertain, and in any case fluctuations of about an order of magnitude may be anticipated.

Another important environmental characteristic is the radiation field that is present. The dominant source of heat is, of course, the sun, which produces a virtually constant flux of 1.35×10^6 ergs cm^{-2} sec^{-1} at the earth. About 95% of the solar energy is in wavelengths between 0.3 and 2.5μ. The sunlight reflected from the earth is somewhat less in magnitude. According to the discussion by Byers (1953) the mean albedo is 0.36, with wide variations depending on cloud coverage. The infrared radiation emitted from the earth is considerably less variable than the reflected light. The effective temperature of the radiating earth, corresponding to an albedo of 0.36, is 250°K; the corresponding intensity, I, of the emitted infrared radiation, peaked between 5μ and 20μ, is about 7×10^4 erg cm^{-2} sec^{-1} steradian^{-1}. About three-fourths of this radiation originates in the atmosphere, at and below the base of the stratosphere, with about one-fourth emitted directly from the earth's surface. Since

the mean emission from each latitude is apparently within about 5% of the average value, the earth on the average is a relatively uniform source in the infrared, although at equatorial latitudes fluctuations of I by as much as 20% may occur as a result of changes in cloud coverage (Byers 1953, Fig. 2).

Yet another characteristic of outer space is the presence of force fields which may produce torques in a satellite. These fields are of three types, radiation, gravitational, and magnetic. The radiation field from the sun already described yields a radiation pressure of 4.5×10^{-5} dyne cm^{-2}, about the same as the air drag at 800 km; a perfectly reflecting surface will experience twice this pressure, of course. Radiation from the earth produces a pressure which is about one-fourth of this, for a satellite at 800 km, and is entirely negligible at 36 000-km altitude. The inhomogeneity of the gravitational field, which produces tides on a fluid body, will produce torques on any body which is not spherically symmetric. These torques, which are considered in detail in Sec. III, are proportional to the inverse cube of r, the distance from the earth's center, and at 36 000-km altitude ($r=4.2\times10^9$ cm) are smaller than at 800 km ($r=7.2\times10^8$ cm) by a factor of 1/200. The primary dipole component of the earth's magnetic field also varies as r^3. According to McNish (1939) the magnetic moment of the earth's dipole field is 8.1×10^{25} cgs units. The corresponding field intensity at 800-km altitude is 0.44 gauss at the magnetic poles and half this value at the magnetic equator. At 36 000 km, the equatorial field is 1.1×10^{-3} gauss. During a magnetic storm these values may fluctuate by as much as 10^{-3} gauss.

From some aspects, the most important feature of a satellite's environment is its unsuitability for human life. Even if man could be safely launched into orbit and then returned, maintenance of a staff at a space station would very much increase the cost and complexity of the enterprise. Hence there are strong arguments for the use of unmanned equipment as much as possible. It may ultimately prove necessary, in order to ensure continuing operation of complex apparatus, to provide for human supervision, at least for ocasional replacement of faulty components. In the near future, however, the initial apparatus will most likely be unmanned.

II. ROTATION AND STABILIZATION OF A SATELLITE

In controlling the direction in which a satellite telescope points, three different problems may be distinguished. First, the rate of rotation, which is presumably large immediately after launching into orbit, must be reduced to a tolerable value. Second, a stellar telescope must be set to point at a desired region of the sky, and reset from time to time for different observational programs; for a solar telescope, of course, this resetting problem does not appear. Third, during each observation the orientation of the telescope must be held constant to whatever accuracy the observation requires.

The first problem may be regarded as part of the launching process, and need not be considered here. In fact, most of the initial reduction of angular momentum may take place before the telescope is separated from the final rocket stage. Jets of gas provide a possible method for getting rid of the initial angular momentum, but a number of other techniques have also been suggested.

In this section we consider the physical problems involved in setting and guiding the telescope, postponing to the next section the problems of attitude sensing; i.e., of determining the direction of the telescope's optical axis, for control of setting and guiding. We shall assume at the outset that the entire satellite is to be rotated during these operations. Rotating the telescope with respect to the rest of the satellite would involve large bearings, gear trains, etc., and would be relatively much more cumbersome than the methods discussed in the following paragraphs. Guiding by rotation of small auxiliary mirrors offers no advantages when all perturbations are of very low frequency, and would be complicated to control if the main telescope were slowly rotating. The first subsection below discusses the basic requirements for the rotational speed during setting and for the torque applied during guiding; subsequent subsections outline possible methods of meeting these requirements.

Torques Required

The torque which must be applied to a satellite when it is being set, or pointed, towards a particular region of the sky depends on the time available for this process. For a satellite at 800-km altitude, the time available for communication with a ground station in a single pass over the station is limited to about 7 min, if the maximum range of radio communication is assumed to be 1800 km; the satellite will be above the visible horizon for about 15 min, with a maximum range of about 3300 km. If the setting is to occur while the telescope is controlled from the ground, which is desirable from the standpoint of simplicity, the setting process should not require more than 7 min. For a satellite at 36 000 km, pointing could, in principle, take much longer, but at the corresponding loss of observing time. Since this requirement is not difficult to meet, we shall assume that the satellite can be rotated 180° in 7 min. With one minute for acceleration and another for deceleration, the required angular rotation rate is 0.6° sec^{-1}, or 1.0×10^{-2} radian sec^{-1}.

The torque required depends on I, the moment of inertia of the satellite. As a basis for computations we shall consider throughout this paper a satellite in the shape of a cube, 2 m on a side and 10^6 g in mass. For

uch a structure a value of 10^{10} g cm^2 for the three rincipal moments of inertia is reasonable. The value f $I\omega$ during pointing is then 10^8 g cm^2 sec^{-1}. The orque during the minute of acceleration is 1.7×10^6 yne cm.

Stabilization of the telescope during exposure, when he direction of the optical axis must remain constant o within the resolving power of the telescope, is omplicated by the presence of perturbing torques. hese can interfere seriously with guiding even though hey are several orders of magnitude less than the ormal gravitational torques on the earth's surface. Vhile a telescope on the earth is fairly well balanced, weight of 5 kg some 2 m away from the axis of otation will usually not interfere with setting or uiding. Such a torque amounts to 10^9 dyne cm, much reater than what is required for setting a satellite elescope. During guiding, even a vastly smaller torque ill lead to an angular rotation of the satellite that is uch too great. For example, a torque of only 10^3 yne cm will in 1 min accelerate a satellite with I equal o 10^{10} g cm^2 up to an angular velocity of 1.2 min of rc per minute of time. Even with a torque as low as dyne cm, the satellite will drift 3.6 sec in 10 min of ime. As we shall see, torques of at least 10 to 100 yne cm are to be expected, and it follows that active ontinuous guiding will be required in space exactly s on earth.

Perturbing torques can be produced by particle ombardment and by the three fields considered in the rst section, namely, radiation, gravitational, and agnetic. We consider each of these.

The torque due to solar radiation pressure is of articular importance as it is unaffected by increasing istance from the earth, hence this torque may be he chief perturbation on a satellite in a 24-hr orbit, t an altitude of 36 000 km. If we again take a face of he satellite to be a square, 2 m on a side, the total adiation pressure for perfect reflection at normal ncidence becomes 3.6 dyne. The torque is equal to his force multiplied by the distance between the enter of pressure and the center of gravity. If the atellite is kept symmetric, with the center of gravity t the center of pressure, this distance will vanish. n practice, the center of pressure will not always be n line with the center of gravity because of differences n the reflection and absorption properties of the ifferent sides. In addition to variation of optical roperties with angle of incidence, one side will have olar batteries, another may be highly reflecting, at east for visible light, while yet another may be highly bsorbing. Since the torque on each half of the satellite eparately cannot amount to more than 90 dyne cm, nd will usually be less, the total unbalanced torque ight be greater than 10 dyne cm but is most unlikely o exceed 50 dyne cm. The torque due to radiation rom the earth is limited to about one-fourth these alues.

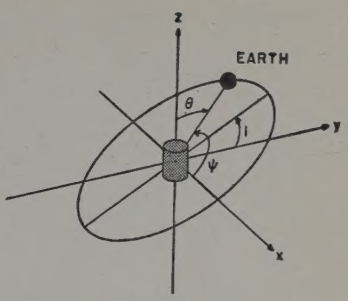

FIG. 1. Coordinate system relative to cylindrical satellite.

If the satellite is designed to minimize the torque due to radiation pressure, the torque due to particle bombardment will be small. The momentum transferred to the satellite by an air molecule is likely to be nearly independent of surface conditions and of the angle of incidence. At 800 km the pressure due to particle bombardment is about the same as solar radiation pressure, but the net torque can be readily kept below 5 dyne cm by making the satellite symmetrical within about 1 cm.

The gravitational or tidal torque on an orbiting satellite can be computed to a very high approximation from the three principal moments of inertia. The appropriate expressions have been derived by several authors, including Roberson and Tatistcheff (1956), Roberson (1958), and Nidey (1960). The higher-order torques, which vary as r^{-4}, and which have been considered by Nidey, are relatively extremely small. The formula for the main gravitational torque becomes very simple if two of the principal moments of inertia are equal, i.e., if the satellite is effectively cylindrical. If we take a coordinate system defined by the ellipsoid of inertia, and let $I_x=I_y$ be the two equal moments, then the potential energy, U, of orientation in the gravitational field of a point mass, M, at a distance r becomes

$$U=\frac{3GM}{2r^3}(I_x-I_z)\cos^2\theta, \qquad (1)$$

where θ is the angle between the z axis and the direction to the point mass.

For a satellite moving about the earth, θ changes in the course of the orbit, if the orientation of the satellite telescope is assumed fixed with respect to the stars. The geometry as seen from the satellite is indicated in Fig. 1. The center of the earth moves about the satellite in a circle inclined at an angle i with respect to the xy plane; thus i is the angle between the pole of the earth's apparent orbit and the z axis of the satellite. Since the ellipsoid of inertia is symmetrical around the z axis, we may choose the x axis to coincide with the direction of the earth when this crosses the xy plane. The position of the earth in its path is measured by the angle ψ between the x axis and the direction to the earth's center.

From simple trigonometry we then obtain

$$-L_x=\frac{3GM}{2r^3}(I_x-I_z)\sin 2i\sin^2\psi \tag{2}$$

$$-L_y=-\frac{3GM}{2r^3}(I_x-I_z)\sin^2 i\sin 2\psi \tag{3}$$

$$-L_z=0, \tag{4}$$

where L_x represents the torque around the x axis, etc. In a circular orbit r is constant, the mean value of $\sin 2\psi$ is zero, and there is no mean torque about the y axis. However, a mean torque exists about the x axis. If I_x and I_y are not equal, mean torques may appear about all three axes, in addition to a variety of periodic terms.

The magnitude of the torques involved is readily computed from the above equations. If, in accordance with the previous discussion, we let I_z equal 10^{10}, and assume that I_x and I_y are negligible, the mean torque for a satellite at 800-km altitude and with i equal to 45° is 8×10^3 dyne cm, a relatively large value. If the ellipsoid of inertia can be made spherical with an accuracy of about 1%, which should be possible, the mean torque can be reduced to about 100 dyne cm. To achieve higher symmetry involves problems of flexure during test, and differential thermal contraction in orbit, but one may hope that the principal moments might be made equal to one part in 10^3, yielding a mean torque of 10 dyne cm. As we have seen, for a satellite in a 24-hr orbit this gravitational torque is much less, amounting to 0.4 dyne cm if $(I_x-I_z)/I_x$ equals 10^{-2}.

The magnetic field of the earth will produce a torque on ferromagnetic materials, on electric currents, and on rotating conductors. The ferromagnetic torque can be readily computed in terms of the mean flux of induction, B, in the volume V of the material. Since the dipole moment per unit volume is $(\mathbf{B}-\mathbf{H})/4\pi$, we have

$$L=\frac{\mathbf{H}\cdot(\mathbf{B}-\mathbf{H})V}{4\pi}\approx\frac{HBV\sin\theta}{4\pi}, \tag{5}$$

provided B much exceeds H; θ is the angle between the two vectors, $\mathbf{H}$ and $\mathbf{B}$. In ordinary commercial iron the residual B may be from 1 to 100 gauss. If we take 100 gauss for B, let H equal 0.3 gauss, and consider that the satellite contains 10 kg of iron, with a volume of 1.3×10^3 cm^3, we find that for θ equal to 90° the value of L is 3×10^3 dyne cm, a relatively large value. Even in a 24-hr orbit, where H is less by two orders of magnitude, L will be appreciable if large amounts of magnetized iron are present.

A torque of order 10^3 dyne cm can very much complicate the guiding problem. It is possible that a satellite telescope can be built with less than a kilogram of ferromagnetic material, although motors, televisi cameras, and electronic circuits are generally design to use such materials.

The torque on a given amount of iron can be mi mized by reducing both B and θ. With some care can be reduced well below 100 gauss. To achieve t greatest possible reduction, one may use high permeable iron in a nearly spherical configuration. this case $\mathbf{B}$ will equal $3H$ in magnitude and will nearly parallel to $\mathbf{H}$. If the coercive force on t material is H_c, then with a slowly rotating field t component of $\mathbf{B}$ perpendicular to $\mathbf{H}$ is about H Wakefield (1959) has shown that the torque on a sol sphere is then given by

$$L=6HH_cV/4\pi^2. \tag{6}$$

Evidently $6H_c/\pi$ replaces $B\sin\theta$ in Eq. (5). Since H is 0.013 gauss for mumetal, L is reduced by more tha three orders of magnitude from the values compute above. If the sphere is hollow instead of solid, Eq. (6 is still approximately valid, provided that the iron unsaturated; V is then the volume enclosed by t sphere. Thus a hollow sphere could be used for magnet shielding of iron components that must be elongate or cannot be made highly permeable. One problem the use of mumetal, or of the alloys with even low H_c, is that H_c can be increased by mechanical strai such as may be experienced at launching. It is possibl however, that by these methods the perturbing ma netic torques on a satellite at 800 km may be kept belo 100 dyne cm.

The magnetic torque on a current, I, enclosing plane area, A, is given by the usual formula

$$L=(HIA/10)\sin\theta, \tag{7}$$

where θ is now the angle between $\mathbf{H}$ and the outwar normal to the plane. Unless a circuit is deliberatel designed to enclose a large area, L is easily kept belo 1 dyne cm for the circuits in a satellite telescope.

Finally we consider the torque produced on th satellite as a whole by the rotation of the magneti field. This effect is greatest for a polar orbit, in whic case $\mathbf{H}$ rotates with a period of half the orbital perio The torque on a spherical shell rotating in a uniform magnetic field is considered below. If we represent th satellite structure as an aluminum sphere of radius 1 cm and of thickness 1 cm, giving a weight of 340 kg then for H equal to 0.3 gauss and ω equal to $2\times10^-$ radians per sec, the torque found from Eq. (8) is 1 dyne cm. This result assumes that the resistivity, γ is 2.8×10^{-6} ohm, its value for Al at 20°C. Evidentl the eddy current drag on a rotating satellite at 800 km is appreciable but not very important. At 36 000 km the torque is less by some five orders of magnitude.

To summarize this discussion, the largest perturbin torque on a satellite at 36 000 km is due to solar radia tion pressure. This torque would be less than 10 dyn

m on a symmetrical satellite with all sides identical, ut may be as great as 50 dyne cm if different sides have ifferent optical properties. On a satellite at 800 km the idal and ferromagnetic torques can much exceed this adiative torque. The tidal torque on an asymmetrical atellite at this altitude can be in the range from 10^3 to 0^4 dyne cm. By appropriate symmetry this torque can e reduced by two to three orders of magnitude. The erromagnetic torque on 10 kg of iron magnetized at 00 gauss is also in the range from 10^3 to 10^4 dyne cm if he satellite is relatively close to the earth's surface. By educing both the amount of iron and its permanent nagnetization, by use of highly permeable materials in early spherical shapes, and perhaps by using some nagnetic shielding, it should be possible to reduce this nagnetic torque also by several orders of magnitude. Evidently, if these various torques can be reduced by he amounts anticipated, a torque of 100 dyne cm should e adequate for guidance.

Inertial Sphere

The simplest, most effective way to rotate a satellite n one direction is apparently to rotate an internal mass n the opposite direction. We consider here the use for his purpose of a spherical conducting shell, positioned y a high-frequency magnetic field, and subject to orques by another magnetic field rotating at lower requency. This configuration, which we shall call an "inertial sphere," has the advantage, during setting, hat only one large mass is needed, and the gyroscopic ffects that appear with several rotating wheels are bsent. During guiding, such a sphere has the advantage hat it is relatively frictionless; in addition, for a atellite at 800 km the angular momentum communi- ated to the sphere, when there is a steady perturbing orque, will be damped by eddy currents due to the arth's magnetic field. For a satellite at 36 000 km, or or one at 800 km subject to torques larger than 100 lyne cm, this sphere must be supplemented by other levices to dispose of the angular momentum. Even in his case, however, an inertial sphere may be useful as art of an attitude control system.

We consider first the angular acceleration of the nertial sphere, postponing until later the problem of ositioning. The torque on a rotating sphere in a uni- orm magnetic field may be analyzed by conventional lectromagnetic theory. For a thin spherical shell of adius a, thickness w, and resistivity η (in ohm cm) we ave (Smythe 1950)

$$L=\frac{2\pi w a^4 \omega H^2 \times 10^{-9}}{3\eta(1+4a^2\omega^2/9\delta^4)} \text{ dyne cm}, \tag{8}$$

where ω is the angular velocity, assumed perpendicular o $\mathbf{H}$, and δ is the skin depth, given in centimeters by the usual formula

$$\delta^2=\frac{\eta\times 10^9}{2\pi\omega}. \tag{9}$$

It follows that as ω is varied L has a maximum value L_m when δ^2 equals $2a\omega/3$, or when ω equals a value ω_m, given by

$$\omega_m=\frac{3\eta\times 10^9}{4\pi a w}. \tag{10}$$

From Eq. (8) we find that

$$L_m=\tfrac{1}{4}a^3H^2. \tag{11}$$

From the usual formula for the amount of inertia of the spherical shell, taken about a diameter as axis, we find that

$$I\omega_m=2a^3\rho\eta\times 10^9. \tag{12}$$

The power dissipated at any frequency is simply $L\omega$, since the rotational energy is dissipated in eddy currents. It is of interest that neither L_m nor $I\omega_m$ depends on the thickness or the mass of the sphere; however, as w and the mass decrease, ω_m increases and the power at maximum torque increases. These results may also be applied if the field is rotating with an angular velocity ω relative to the sphere.

From these equations we may determine the radius and other properties of an inertial sphere adequate for satellite pointing and guiding. The first condition is that the sphere can absorb an angular momentum of 10^8 g cm^2 sec^{-1}, which we have previously set as a requirement for rotating the telescope to a new direction in at most seven minutes. The acceleration is most simply carried out by a driving magnetic field, rotating at a fixed angular velocity, ω_d. To achieve a high torque, ω_d should not differ much from ω_m; we assume that it is somewhat greater. Evidently ω_s, the angular velocity of the inertial sphere relative to fixed axes, will not increase beyond ω_d. If we set the maximum design value of ω_s equal to ω_m, Eq. (12) may be used to determine a^3 if we equate $I\omega_m$ to 10^8. For an aluminum sphere at 20°C, η is 2.8×10^{-6}, and we find that a is 19 cm. To provide a slight margin of safety we round off a to 20 cm, giving $I\omega_m$ equal to 1.2×10^8.

We may next insert this value of a into Eq. (11) and determine the maximum torque that can be exerted on the sphere by the earth's magnetic field, which we again take to be 0.3 gauss. This value of L_m is 180 dyne cm. During guiding, if a constant perturbing torque acts on the satellite, an equal torque will be exerted on the sphere by means of a magnetic field H_d rotating at the angular frequency ω_d. An equal but opposite torque is then exerted on the sphere by the earth's field. Clearly this equilibrium is possible only if the torque is substantially less than L_m, and ω_s is therefore less than ω_m. If ω_s were equal to ω_m, there would be a danger that the torque exerted by the rotating field might exceed the

torque L_m, due to the earth's field, in which case the sphere would accelerate steadily until ω_s equaled ω_d, and all control would be lost. At ω equal to $\omega_m/3$, L is 0.6 L_m, or about 100 dyne cm, a practical upper limit. It is fortuitous, of course, that the same value of a satisfies the requirements both for guiding and for setting in the case of a satellite at 800-km altitude.

Since a diameter of 40 cm is not very large for a sphere in a satellite 200 cm across, L_m and $I\omega_m$ could both be increased by a moderate increase of a. In addition, $I\omega_m$ could be increased by increasing η, through the use of a suitable alloy of Al, at a cost either of increased power or increased mass.

The choice of thickness w is somewhat arbitrary, but determines the balance between mass and required power. If we take a thickness of 0.5 cm, and a mean radius of 20 cm, the mass is 6.8 kg, and ω_m is 67 sec^{-1}. The moment I of the sphere is 1.8×10^6 g cm^2. During setting, when ω_s equals ω_m, the maximum rotation rate is about 600 rpm, a rather leisurely rate for a sphere of this size; the stress in the aluminum is negligible even at substantially higher rates of rotation. The acceleration during the first minute of setting to a different star must produce a torque of 1.7×10^6 dyne cm. A driving field of about 30 gauss, rotating with an angular frequency of $4\omega_m/3$, or about 14 cycles per second, will produce the desired torque. The mean rate of increase of kinetic energy is about 6 w, which is about equal to the dissipation rate associated with eddy currents in the sphere. Additional ohmic dissipation will occur in the external coils; if the mass of these coils is about equal to that of the sphere, this external ohmic dissipation will also amount to some 6 w. If the thickness and mass of the sphere are doubled, and the frequency halved, the power required is reduced by a factor of t the magnitude of the rotating magnetic field remain unchanged.

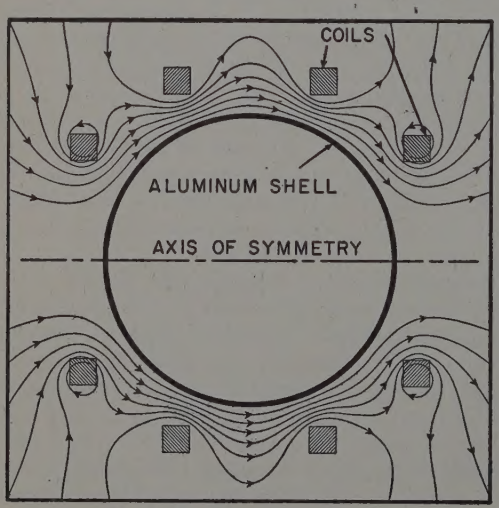

FIG. 2. Magnetic positioning field around inertial sphere. The magnetic field is inversely proportional both to the separation between adjacent lines of force and to distance from the axis of symmetry. The conductivity of the sphere is taken to be infinite for the rapidly varying positioning field.

During guiding, the sphere rotational velocity ω_s remain less than $\omega_m/3$, or 22 radians sec^{-1}, if the m torque remains below 100 dyne cm. A continu driving field of half a gauss (or an intermittent fiel correspondingly greater energy density), rotating ag at ω_d equal to $4\omega_m/3$, can transmit the desired torqu the sphere, which will then dump it into the eart magnetic field. The power dissipation rate will be ab 10^{-3} w, which is entirely trivial. The magnitude of applied torque produced by the rotating field depends ω_s, decreasing from its maximum value, L_m, when sphere rotates at $\omega_s/3$ in the same direction as the fi rotates, to 88% of L_m when the sphere rotates at $\omega_s/3$ the opposite direction. Also, if the rotation vector ω at an angle to ω_d, then the applied torque will no lon be parallel to ω_d. A detailed analysis by Hering (19 shows that the maximum torque that can appear ab an axis perpendicular to ω_d is about 3% of the tor applied in the direction ω_d, provided that ω_s is at m $\omega_m/3$ and ω_d equals $4\omega_m/3$.

Next we turn to the problem of positioning the sphe The basic concept here is to surround the sphere w a magnetic field alternating so rapidly that the lines force cannot penetrate the sphere. The amplitude the total flux in the positioning field is assumed c stant, corresponding to the assumption that this fiel driven by an alternating current of constant amplitu If the conductors producing the magnetic field located close to the sphere, then any motion of t sphere away from its designed equilibrium will co press the lines of force, producing restoring forces.

Figure 2 shows one possible arrangement, where t external coils have cylindrical symmetry about a co mon axis, which is also a diameter of the sphere in equilibrium position. The magnetic field is inverse proportional both to the distance between lines of for and to the axial distance. This plot was determined a resistance analogue board developed by Wakefi (1956). In this plot, the currents in adjacent coils a all equal and have all the same direction, giving t maximum field strength at the surface of the sphe Another possibility would be to use oppositely direct currents in adjacent coils, which would reduce somewh the inductance of the external circuit and might increa the stability of the sphere's position.

The required frequency of the positioning field m be computed from Eq. (9) for the skin effect. We requi that ω_p, the angular frequency of the positioning fiel be such that δ is half the thickness, w, of the sphere wa Then H just inside the sphere is less than its value ju outside by a factor 0.14, while the magnetic pressu outside is fifty times that inside. For an Al wall 20°C, and h equal to 0.5 cm, we find that ω_p is 1.8×1 giving a frequency f_p of about 300 cycles per second.

The magnitude of the field required for positioning e sphere is very small, because all perturbations are ry small. The worst perturbation, found during tting, occurs if the sphere is not at the center of avity of the satellite. To avoid setting up oscillations e frequency at which the sphere oscillates about its id-position must be appreciably shorter than the 60 c in which the angular acceleration of the satellite curs. Let us assume a period of 20 sec for the period, , of oscillation. Since the mass, M, of the sphere is 6.8 , the force constant, equal to $M(2\pi/P)^2$, must be 0 dyne cm^{-1}.

The relationship between the force constant and the agnetic field is rather involved, and must probably be etermined experimentally. To give an order of magnide result, however, we may consider the one-dimenonal problem, in which a conducting slab is confined etween two parallel conducting planes. Let X be the idth in equilibrium of the vacuum space between the ab and the conductor on each side, and let H_p be the uilibrium intensity of the magnetic field, assumed arallel to the plane surfaces, and with a constant flux n each side of the slab. When the slab is displaced by n amount x, the field on one side increases by the factor $/(X-x)$, while the other decreases by the correspondg factor $X/(X+x)$. Since the magnetic pressure is roportional to $H^2/8\pi$, the force constant K becomes

$$K=AH_p^2/2\pi X. \tag{13}$$

f we set A equal to the projected area of the sphere, .26×10^3 cm^2, and take 5 cm for X, the effective disance from the sphere wall to the outer conductors that estrict the positioning field, we find that the root-meanquare H_p is 4.1 gauss.

The power dissipated in eddy currents in the sphere ay also be determined from the slab approximation. n one side of the slab we have approximately

$$P=AH_p^2\eta\times 10^2/8\pi^2\delta. \tag{14}$$

f now we replace A by the total area of the sphere, nsertion of numerical values gives a total power issipation rate of about one watt. Even with some alowance for losses in the external coils producing the ositioning field, the total power should not exceed everal watts. Except when the satellite is being rotated, his power could certainly be reduced by at least an rder of magnitude.

Rotation of the sphere about the axis of symmetry n Fig. 2 does not produce any torque in the presence f the positioning field. Rotation of the sphere about ither of the two axes produces a torque. From Eq. (8) t may be shown that the ratio of this torque to that roduced by rotation in the earth's field is about equal o $2(\omega_m H_p/\omega_p H_e)^2$, or 1.5. This torque, which is easily ffset by the driving field, will be much diminished if T_p is reduced during guiding.

Some damping of the positional oscillations of the sphere would be desirable. Since the inductance of the positioning field depends strongly on the displacement of the sphere, such damping would in principle not be difficult to provide. It might be simplest to provide damping by ground control of additional field coils, using for sensing telemetered indications of the voltages across small measuring coils distributed around the sphere.

The properties of the inertial sphere tentatively derived in this discussion are summarized in Table I. On paper the performance seems satisfactory, with mass and power requirements relatively low. As compared with more conventional inertial wheels, apparently the only appreciable disadvantage of this type of system is that it does not lend itself to one particular technique discussed in the next section for precise setting on a star, since the number of revolutions about each axis cannot readily be counted with great accuracy. An additional disadvantage may be the complication required for stabilizing positional oscillations of the sphere. Problems of vibration must also be considered. The advantages of a nearly frictionless system with no gyroscopic problems during setting, and with one mass serving for rotation about any of three axes, may be rather important.

Other Methods of Attitude Control

While an inertial sphere has apparently a number of attractive features, the amount of angular momentum which it can dispose of is necessarily limited, and at 36 000-km altitude is essentially zero. Thus some addi-

Table I. Characteristics of Inertial Sphere.

General Properties	
Radius of aluminum shell	20 cm
Wall thickness	0.5 cm
Mass	6.8 kg
Moment of inertia	1.8×10^6 g cm^{-2}
Angular frequency at maximum torque, ω_m	67 radian sec^{-1}
Angular momentum at rotational frequency ω_m	1.2×10^8 g cm^2 sec^{-1}
Positioning Characteristics	
Intensity of positioning field, H_p	4 gauss
Angular frequency of positioning field, ω_p	1800 radian sec^{-1}
Power dissipation in positioning field	0.1 w
Period of positional oscillations	20 sec
Characteristics in Setting	
Intensity of driving field, H_d	30 gauss
Angular frequency of driving field, $\omega_d=4\omega_m/3$	88 radian sec^{-1}
Maximum rotation rate of sphere, ω_m	67 radian sec^{-1}
Duration of acceleration	1 min
Mean power dissipation during acceleration	6 w
Total power during acceleration, approximately	20 w
Characteristics in Guiding	
Intensity of driving field, H_d	0.5 gauss
Angular frequency of driving field, $\omega_d=4\omega_m/3$	88 radian sec^{-1}
Maximum rotation rate of sphere, $\omega_m/3$	22 radian sec^{-1}
Maximum steady torque in earth's field of 0.3 gauss, L_m	100 dyne cm

tional method for getting rid of angular momentum is required in a 24-hr orbit, and may even be needed at 800 km.

One possibility is the use of jets of gas. By the use of water vapor or some other convenient gas, an injection velocity of some 5×10^4 cm sec^{-1} is readily obtained. With an axial distance of a meter, a steady torque of 10^3 dyne cm can be offset for a year with a total mass ejection of only 6 kg. Since precise control of the gas ejection rate would be difficult, the use of jets would probably be limited to getting rid of the angular momentum stored in an inertial sphere or in rotating wheels. Jets could, in principle, also be used for setting, since only 20 g of gas would be needed to accelerate the satellite up to a rotation rate of 10^{-2} radians sec^{-1}, and another 20 g to decelerate. One such setting every day would require a mass of 14 kg during a year, which begins to be appreciable. While more settings might be required, a rotation rate appreciably less than 10^{-2} radians sec^{-1} might be tolerated. Reliable operation of gas flow valves for a year might be a problem.

Another method to dispose of angular momentum is to vary one of the external torques in a controlled way. We consider the different possibilities for a satellite at 36 000 km. The tidal torque is not very suitable for this purpose. Even a change of I_x by as much as 10% would introduce a torque of only 4 dyne cm, which is inadequate. Thus we are left with radiation pressure and magnetic forces as the two remaining possibilities. The magnetic field has the disadvantage that it produces no torque around any axis parallel to the magnetic field. Moreover, the field at this distance is both weak and variable.

Solar radiation pressure can also produce controlled torques by the use of moving rotating vanes. For these to produce controlled torques about any one of the three axes, and at any aspect of the telescope, a substantial number of moving parts would appear to be required. For guiding during an exposure an inertial sphere or its equivalent might still be required, and would in any case be helpful for setting.

Evidently, for a satellite in a 24-hr orbit, angular momentum could be disposed of by gas jets, by controlled magnetic torques, or by varying the radiation torque. For a satellite at 800-km altitude, the radiative torque is inadequate; the magnetic torque is much greater but might offer problems of control because of the rapid variation of the magnetic field around the orbit; however, gas jets could readily be used once a day or so if the perturbing torques exceeded 100 dyne cm.

III. SENSING FOR POINTING AND GUIDANCE

To point a satellite telescope in a particular direction by remote control and to keep it pointed correctly requires not only some method of controlled rotation but also a sensing mechanism to determine the actual direction of the optical axis. Two separate problems may be distinguished. First, there is the problem o setting the telescope to point in the proper directio within a certain tolerable area. The sensing proble here is to determine the orientation of the telescope i space to aid in setting. The second problem is keepin the telescope pointed in the desired direction durin guiding while photons from a certain object in the sk are collected. Both these problems are simplest, o course, for a solar telescope. The discussion here will b devoted to a stellar instrument. Since the problem o guiding during exposure is simplest, we discuss it firs

Guiding

With a telescope on earth an astronomer normall guides on starlight collected by the main telescope. Fo direct photography it is customary to use "guide stars outside the field being photographed. For spectroscopy the starlight reflected from the slit jaws may also b used.

Essentially the same method may be used for auto matic guiding on a satellite. A simple scheme, in prin ciple, is to use a reflecting pyramid with its apex pointe at the arriving photons. The light will then be reflecte to four photocells, and the relative amplitudes of th signals indicate in which direction the center of th stellar image is displaced from the apex of the pyramid With a suitable servo-system and a means for controlle rotation of the satellite, the stellar image can be kep accurately at the apex. If a guide star is not the prograr object, the sensing devices must somehow be moved t the proper position relative to the optical axis. Th mechanical problems involved and the electronic prob lems of signal detection and servo-system design ar interesting but not basic.

One problem associated with the design of the guid ance system is the range of angles over which the sensin elements receive a useful signal. This range determine the maximum angle at which a star can be kept withi the range of the guidance system and ultimately brough to rest at the proper position; this maximum angle w shall call the "guidance admission angle," and denot by γ. Evidently, when a telescope is reset to a differen star, the automatic guidance system will take over whe the star is within the guidance admission angle. From thi standpoint the admission angle should be as great a possible.

The size of the guidance admission angle is limited however, by unwanted light, since all photons within circle of radius equal to the admission angle are receive by the detector. The unwanted light may be divide into two types: (a) uniform radiation coming from th zodiacal light and faint stars, and (b) radiation varyin sharply with direction, as from a single star or a com pact group of stars. The uniform light has the sam effect as an increased noise level in the detector Individual stars have a more serious effect; the bes that can be expected is that the telescope will point t

TABLE II. Mean numbers of stars per square degree.

m	4	5	6	7	8	9	10
N_m	0.013	0.038	0.10	0.30	0.83	2.3	6.2
m	11	12	13	14	15	16	17
N_m	16	43	110	280	670	1500	3200

ıe brightest star in the field. A tendency for the tele-
:ope to point slightly away from the brightest star,
›wards the next brightest object, can be partly over-
ome if the sensitivity is made greatest near the center
f the field, and least near the outer edge. However, if
ı addition to the guide star several fainter stars are
resent, all on one side of the field of view, the telescope
ıay direct itself toward some intermediate point.

We consider these effects quantitatively. Let us
ssume that the guidance system will not operate
ffectively if any other star in the field of view is as
ıuch as one-tenth as bright as the guide star. Thus if
he magnitude of the guide star is m, there must be no
›ther stars of magnitude $m+2$ or less in the field of view
f the guidance system is to bring the guide star to the
›roper position. In addition, we also require that there
›e at most one star of magnitude about $m+3$, since two
uch stars would be one-eighth as bright as the guide
tar. Stars fainter than $m+3$ we shall ignore, since these
vill tend to be more uniformly distributed.

Let $P_m(\gamma)$ be the probability that there be no other
tars (except the guide star) within the admission angle
ıs bright as $m+2$ in magnitude, and at most one star
›f magnitude $m+3$. This probability can be readily
›omputed from the Poisson distribution law, if the
listribution of stars is assumed random. Let $p(m)$ be
he mean number of stars within a solid angle $\pi\gamma^2$, and
vith an apparent magnitude between $m-\frac{1}{2}$ and $m+\frac{1}{2}$.
Then we have

$$P_m(\gamma)=\{1+p(m+3)\}\exp-\sum_{m=0}^{3}p(m), \qquad (15)$$

where

$$p(m)=\pi\gamma^2N_m; \qquad (16)$$

with γ measured in degrees, N_m is the number of stars
›er square degree. Values of N_m, taken from Seares,
Van Rhijn, Joyner, and Richmond (1925), are given
in Table II; their values for galactic latitudes 0–10° are
ısed with m taken as the photographic magnitude.
Values of $P_m(\gamma)$ computed in this way are plotted in
Fig. 3 for values of γ between 1′ and 1°.

A correction to these probabilities must also be made
for double stars. According to Aitken (1935) about 5%
of all stars are visual doubles, with separations ranging
from a few seconds of arc for faint stars up to 40″ for
stars of about the second magnitude. For values of γ
greater than 1′ of arc, a simple automatic guidance
system will have difficulty acquiring either of the two
components. Thus the values of P_m in Fig. 3 should all
be reduced by about 5% for this effect.

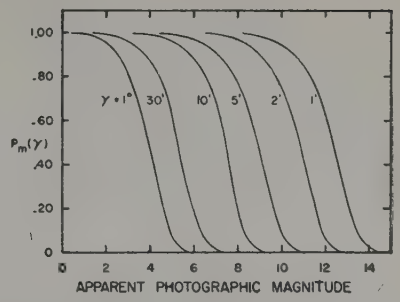

FIG. 3. Probability that guidance system will operate properly on a star of magnitude m. The angle γ is the admission angle of the guidance system.

The results in Fig. 3 are in any case very approximate. Since the guide star may initially be near the edge of the field of view, one should perhaps require that there be no interfering stars within a radius equal to 2γ. On the other hand, the assumption that the guidance system cannot function effectively on a guide star with another star one-tenth as bright within the field may be too conservative.

We must consider also the uniform light due to faint stars, diffuse galactic light, and zodiacal light. According to data presented by Roach and his colleagues (1954), integrated starlight and the zodiacal light are about equally important. In the galactic plane the brightness due to integrated starlight is between two and six stars of fifth magnitude (visual) per square degree, the exact value depending on galactic longitude; near the galactic poles the brightness is less by an order of magnitude. Similarly, the zodiacal light in the plane of ecliptic varies from about seven stars of the fifth magnitude (visual) per square degree at 45° from the sun to about 1.5 such stars per square degree near the Gegenschein; near the poles of the ecliptic the corresponding brightness is about 0.6. Within an admission angle of 30′ the general illumination may amount to as much as 10 stars of the fifth magnitude, but will usually be substantially less. Figure 3 indicates that with an admission angle of this size a fifth-magnitude star is about the faintest that can be observed because of interfering stars. The general illumination increases the noise to at most ten times the signal, which should be tolerable, especially since there are no high-frequency perturbations, and long integrating times may be used.

These results all refer to light in the visible portion of the spectrum. If light in the far ultraviolet is used for guidance, the picture is somewhat altered. With early-type stars a wider admission angle is possible, since most of the other stars will be of lower surface temperature, and will radiate little in the ultraviolet. The tendency of O and B stars to occur in clusters and associations is an effect in the opposite direction. The general illumination from starlight and diffuse light will also be less in the far ultraviolet.

The general conclusion may be drawn that for guiding

on a star as faint as the fifth magnitude a guidance admission angle, γ, in the general neighborhood of half a degree is probably adequate most of the time. If light in the far-ultraviolet part of spectrum is to be used for acquisition, a considerably greater value of γ might be employed. To acquire stars fainter than the twelfth magnitude, γ must be less than 1′ of arc, with at most a few seconds for the very faintest stars.

Acquisition

A much more difficult problem than guiding is that of pointing the telescope in the right direction initially, and thus to "acquire" the star in the automatic guidance system. A great variety of systems is possible. Some of the more important such systems will be considered briefly here.

On the earth, acquisition is normally carried out in two stages. First the telescope is set by use of the angles which the telescope axis makes with respect to the earth. Then visual inspection of the star field is used to determine the difference between the desired and the actual direction of the optical axis.

To an astronomer the most straightforward method for pointing a satellite would appear to be the use of roughly this same technique. First, the satellite can be pointed with reference to the angles between the optical axis and both the sun and the earth. Next, the star field can be viewed through a television camera and the telescope axis pointed in the direction desired. We discuss these two steps in more detail.

Since nothing in the satellite is fixed with respect to the earth and the sun, the angles between these bodies and the telescope cannot be read off circles in the manner customary on earth. However, the radiation from the sun provides a convenient means for measuring the angle to this body. The problem of measuring the angle between the telescope axis and the direction of the sun (which we shall here call the "sun angle") is simplified if the telescope is rotated about its axis s that one side, which we shall call the "sunny side," always faces the sun as closely as possible. Such a orientation is desirable in any case both for temperatur control and for efficient use of solar batteries. Then group of radiation detectors on the sunny side, pointe in various directions in the plane containing the tel scope axis and the sun, should be capable of measurin the sun angle to better than a degree. This measuremen cannot be made, of course, unless the satellite is i sunlight. However, a satellite at 800 km will be i darkness at most about one-third of the time.

The angle between the telescope axis and the eart can also be measured easily, although less precisely Actually it is simpler and more useful to measure different angle. If the optical axis of the telescope i along the x axis, and the sun is in the xz plane, it is bes to measure the angle of the earth (i.e., of its apparen center) about the z axis. This angle will be called th "earth angle." To measure the earth angle from satellite at 800 km we can use a series of radiatio detectors sensitive primarily to infrared light. Radiatio from 5 to 20 μ is emitted rather uniformly over the sur face of the earth, and a series of such detectors on th dark side of the satellite, pointed in different direction in the xy plane (see Fig. 4), might determine the eart angle with an accuracy of a few degrees. At 36 000 km this method is less useful, partly because of the dimin ished flux from the earth at this greater distance, and partly because of interference by the solar radiation when the solid angle of the earth is small, the sun wil illuminate most of the detectors that can see the eart if the earth is within 45° of the sun.

Other methods can be used to measure the eart angle. A small controllable telescope could scan th earth, determining the position of one or both horizons the hardware required for this technique seems rathe complicated. An alternate possibility is to measure th direction of the earth's magnetic field with respect t the satellite. Since the position of the satellite with respect to the earth is known, such a measuremen would provide an adequate substitute for the eart angle.

Alternatively, a system of gyroscopes could be used for coarse orientation. However, a system of this sort involving both moving parts and electronic circuits seems less reliable for long-period use than the simple radiation detectors required to measure the sun and earth angles.

Once the orientation of the satellite is roughly known, the second stage of acquisition can begin with the use of a television camera, transmitting the star field to an observer on the ground. The field of view required for the television camera will depend on the accuracy of the coarse preliminary orientation. Since a television camera has a resolution of at most a few hundred lines, this field of view should not be more than a hundred times wider

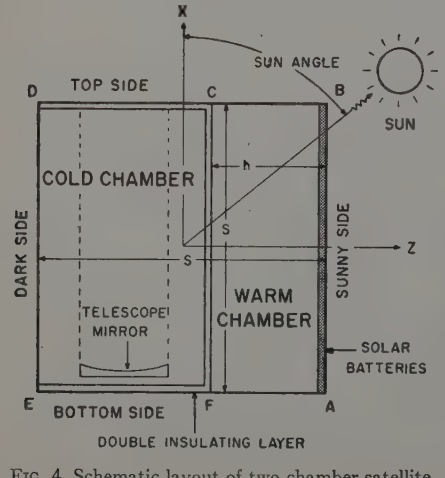

FIG. 4. Schematic layout of two-chamber satellite.

han the admission angle of the final guidance system. If his admission angle is one minute of arc, for example, he field of view of the television screen should not exceed a degree. If the probable error of the rough orientation exceeds the guidance admission angle, two television cameras are required. One may envisage a small wide-angle telescope, yielding a television picture some 10° on a side, and another television camera viewing a field of perhaps 0.5° through the main telescope. With the wide-angle picture including stars down to magnitude five or six, one might even be able to determine where the telescope was pointing by recognizing constellations, with only partial information from the coarse orientation system.

Evidently this system requires a ground observer as a link in the chain. For a satellite in a 24-hr orbit this is no problem, but for a close satellite this restriction means that the telescope can be set only on those occasions when it is in communication with a ground system. If the exposure time on a star is several hours, this limitation is not serious. With the existing network of stations, communication with a satellite is possible once every orbital period—about 100 min for a satellite at 800-km altitude. For a satellite in a polar orbit communication once every period is possible from a single station near one of the poles. For a spectroscopic satellite, designed to scan a stellar spectrum in the far-ultraviolet, an observation time of 12 to 24 hr is none too long for a single star, and for such a satellite a single command station anywhere on the earth (within the latitude range covered by the satellite) might suffice.

A wide variety of other sensing schemes, not using television cameras, are also possible. In view of the many components in a television camera and transmitter (see Sec. V), it seems wise not to place exclusive reliance on this technique. Here we describe three other possible methods for sensing the direction in which the telescope axis points.

The simplest method is to increase the accuracy of the coarse orientation, and increase the admission angle of the guidance system, so that no television camera is required. As one possibility, a guidance admission angle as great as 30 min can be used. As shown above, so large an admission angle restricts observation to relatively bright stars, of about fifth magnitude. However, for the first year or so of ultraviolet stellar observations this would not be a very serious restriction. An accuracy better than half a degree should be obtainable for the sun angle, but is more difficult for the earth angle; temporal variations of the infrared emissivity can produce errors of several degrees in the earth angle. With an error of this magnitude, some hunting along an arc centered at the sun will be required. As suggested by Code, the bright program star might be identified by its color index for visible light, which in principle can readily be measured. Alternatively, a number of photocells could view different fields along an arc of constant sun angle to aid in locating the program star.

If observations are to be made on stars fainter than the fifth magnitude, or on close doubles, a smaller guidance admission angle than 30′ is required, and observations of stars provide the best means for sensing the orientation of the telescope with sufficient accuracy to acquire the program star. One system of this type which does not use television has been proposed by Nidey (1959). A group of small telescopes, say six in number, are fastened rigidly together at the proper angles so that each points at some bright star when the whole group is properly oriented. Each telescope has its own sensing elements—photocells or photodiodes—and the error signals from all six are combined in a servo-system with inertial wheels or some other means for stabilization so that the group of telescopes is always maintained at some fixed orientation. The main telescope is then rotated mechanically to any desired position. For initial orientation of the group of small telescopes, coarse orientation by sun angle and earth angle or by a system of gyroscopes would presumably be required. The accuracy of the initial orientation need not be very high, however; because of the brightness of the six guide stars, the admission angles could be as great as a degree. This system would presumably provide guidance with an accuracy of a second of arc or better. If more precise guidance were needed, final guidance could be provided either on the program star or on adjacent stars, with an accuracy limited only by the resolution of the main telescope, and with an admission angle of at most several seconds of arc.

This system has several important advantages. It promises positive positioning of the telescope at all times with great accuracy. For a close satellite this yields two substantial advantages. Firstly, when the program star is occulted by the earth, guidance is not lost; this problem is discussed in the subsection immediately below. Secondly, if programing of star settings is desired, so that the telescope can be pointed to a different star when not in communication with the ground, this system can be used for this purpose, since in principle the main telescope can be set with very high accuracy relative to the group of guiding telescopes.

The chief disadvantage of this system is its mechanical complexity. The small telescopes get in the way of the main instrument, for some directions of pointing. In the compact structure required for launching into orbit these difficulties are substantial, and may occasionally require resetting each of the small telescopes from one bright star to another. For a satellite at 800 km, about six telescopes are needed because of occultation of stars by the earth; the associated complexity seems undesirable. At 36 000-km altitude, however, occultation is unimportant, the number of telescopes can be reduced to two, and the system becomes considerably simpler and more promising.

Yet another possibility would be to control with precision the rotation of the telescope from one star to the next. As with the system of stellar guidance, this

method presupposes an initial setting on a bright star. To measure precisely the orientation of the satellite around the optical axis the sun or another star could be used. The angular rotation of the telescope would be reduced to a very low value, either with a separate inertial sphere or some other method. Then the satellite could be rotated very precisely with three inertial wheels, counting the number of revolutions about each of the three axes. The accuracy available in this way is limited primarily by the drift of the telescope as a result of torques during the setting time. With a torque of 100 dyne cm, a moment of inertia of 10^{10} g cm^2, and a setting time of 7 min, this drift amounts to about 3 min of arc, giving a lower limit of several minutes of arc for the guidance admission angle. About the same limit is found from thermal changes in the moments of inertia of the satellite and of the inertial wheels. To achieve this accuracy for a rotation of 180° would require measuring the number of revolutions of the inertial wheels to one part in about 10^4; this accuracy can readily be achieved by counting individual rotations, but would be much more difficult to obtain with an inertial sphere only, whose rotation rate would presumably be determined by measurements of induced voltages or currents. With 1% accuracy for angular velocity measures of an inertial sphere, the telescope could be rotated 30° with an accuracy of about half a degree. Alternatively, the amount of rotation during setting could be measured precisely with a separate gyroscopic system, again at the cost of substantial complexity.

In summary, we have seen that coarse orientation, presumably using the radiation from the sun and the earth (or the earth's magnetic field) is a virtual necessity for any satellite. The sun angle and earth angle may not be required for each setting on a new star but are apparently required at least initially for a simple if rough orientation in space. If the guidance admission angle can be taken as great as half a degree, with restriction of the observing program to single stars of magnitude five or brighter, no further sensing mechanism is required provided some hunting along an arc of constant sun angle can be tolerated. If an admission angle of at most a few minutes is desired, the stars are most conveniently used for the sensing during the final stages of acquisition. Three possibilities for using stellar positions are: (a) television cameras viewing the star field around the program star; (b) several small telescopes guiding continuously on relatively bright stars; (c) initial setting on a bright star, with subsequent precisely measured rotation to the position of a program star. The choice between these different techniques must presumably be based in part on the scientific program planned and in part on considerations of reliability. To provide redundance, some combination of these techniques may be desirable.

Occultation

A special problem, which is discussed separately here, is the problem of occultation of a program star by the earth. For a satellite at 36 000-km altitude this problem is quite unimportant; occultation is rare, and in any case the satellite is in continual communication with the ground. For a satellite at 800 km, however, occultation of most program stars will occur once each orbit, for a time interval ranging up to 35 min. If pointing and acquisition are carried out only when the satellite is in communication with the ground, the telescope can usually not be reset on a different object during this time, and observing time is lost. More seriously, the program star may be difficult to reacquire when the star re-emerges from behind the earth.

The amount the telescope axis drifts during occultation depends, of course, on the perturbing torque. Let us suppose that when the star disappears, all guidance ceases; the driving current for the inertial sphere, or any similar controlled source of torque, is turned off, and the telescope drifts freely. With a torque of 100 dyne cm and the usual value of 10^{10} for the moment of inertia, the total angle of drift in 30 min is about one degree. This calculation assumes that the rate of drift is initially zero. Actually, this assumption may not be valid. Shortly before the star is occulted its apparent position in the sky will start to change because of refraction in the atmosphere. This effect may be reduced either by a long time constant in the servo-system, or by a suitable choice of wavelengths for guiding. Evidently if the perturbing torque were as low as 10 dyne cm, the star might well be within the guidance admission angle after occultation was over, and hence be reacquired. With a torque of 100 dyne cm automatic reacquisition seems difficult.

Guidance may be retained during acquisition either by use of gyroscopes or by reliance on other stars. Apparently one of the simplest schemes is to use a star nearly opposite in the sky to the program star. Such an "anti-star" will obviously not be occulted when the program star is behind the earth. Moreover, if the direction to the anti-star makes an angle of 1° to the optical axis, rotation about the direction to the anti-star during occultation will not be too critical for reacquisition; a rotation of 1° about this axis will move the program star only 1 min of arc away from its desired position.

One may visualize a small telescope, with some 15 cm aperture, and with its axis parallel to that of the main telescope. A sensing element could then be moved, on control from the ground, to any position within a circle 1° in radius. The maximum error of positioning should be somewhat less than the guidance admission angle. With a telescope of this aperture the photon count from a 9th magnitude star should be several thousand per second, ample for guiding with a time constant of several seconds. There will usually be a number of stars

of this magnitude or brighter in a circle 1° in radius. This provision for guiding on an anti-star, during occultation of a program star, may not be required if the perturbing torques are small or if the satellite is in communication with a ground station once every orbital period. Without it, however, the net observing time might be significantly reduced, especially if communication with the ground occurs only once every 12 or 24 hours.

IV. PROBLEMS OF TEMPERATURE CONTROL

While conditions in space are relatively constant, the temperature of a satellite telescope, observing stars from an orbit near the earth, will be constantly changing. When the satellite moves into the earth's shadow, the temperature of at least the outer parts of the satellite will drop rapidly. As the telescope points from one star to another the portions of the satellite illuminated by the earth and the sun will change and the mean temperatures will alter. Maintaining resolution and focus of a precise high-resolution optical instrument, despite these thermal variations, is a substantial problem. In principle, the temperature might be maintained nearly constant by appropriate thermostatic control with temperature sensing elements, heater wires, and a suitable servo-system. Active elements of this sort, however, are liable to failure, and the same objective can apparently be obtained by entirely passive methods. Hence we shall assume no active heating (or cooling) elements on the satellite.

On a spectroscopic satellite the problem is complicated by the requirement that at least some of the photocells be kept at a relatively low temperature, in the neighborhood of −80°C or less, to reduce the background current. Dry-ice temperatures are probably not necessary for detectors at wavelengths as short as 1800 A, since such energetic photons can eject photoelectrons from surfaces with a high work function, but for the important wavelength range from 2500 to 3000 A, presently known detectors show an appreciable dark current at room temperature; this dark current can be reduced by several orders of magnitude by cooling to −80°C.

In principle this cooling can readily be produced in space by shielding the equipment from solar radiation, and allowing it to radiate to space and the earth. Since solar batteries, storage batteries, transistors, and other equipment are best operated at about room temperature, we are led to a two-chamber satellite, as shown in Fig. 4. The satellite is again taken to be a cube, for simplicity, with a height S. The x axis is taken to be parallel to the optical axis of the telescope. The satellite is assumed oriented around the x axis so that the sun lies in the xz plane; the z axis is taken to be perpendicular to the side AB containing the solar batteries. The temperature of the warm chamber is determined primarily by solar radiation; that of the cold chamber, by radiation from the earth and heat leakage through the insulating layer separating the two chambers. Evidently this geometry is suitable only for a stellar telescope. Problems of temperature control for a solar instrument are not discussed here.

We treat below the equilibrium temperatures of the two chambers, and the variation of these temperatures. Finally we discuss how a telescope may be designed so as to function effectively in the temperature environment anticipated.

Temperature of the Warm Chamber

Considering first the average temperature for a particular telescope orientation, we start with the basic principle that the temperature adjusts itself so that the outgoing thermal radiation equals the absorbed heat from the sun. For a black plane surface, oriented normally to the solar radiation and radiating on both sides, T is 60°C (333°K). If the angle between the sunlight and the absorbing plane (the sun angle in Fig. 4) is only 45°, however, the absolute temperature is less by $2^{-\frac{1}{6}}$, or a factor 0.917, giving a drop of 28° below the temperature for normal incidence.

As shown by Gast (1956) the radiation reflected and emitted by the earth will increase these temperatures by about 20° for a satellite at an altitude of 800 km. However, such a satellite will be in the earth's shadow for 36 min each orbit, amounting to 36% of the time, if the sun is in the orbital plane, and the resulting reduction of solar heat influx reduces the mean temperature by about 30°. Thus for a black plate at 800 km, the mean temperature is about 10° less than for one at 36 000 km.

If we assume that the solar batteries behave as black absorbers at all wavelengths, the satellite shown in Fig. 4 corresponds roughly to the flat plate in the simple calculation. Energy is absorbed on the face AB and radiated both from AB and from the sides BC and EF, as well as from the corresponding areas on the xz planes, which we shall call the "twilight sides." We assume that these lateral areas have the same optical properties as the solar batteries. If the ratio h/S is 0.25, the total radiating area is the same as for the flat plate at normal incidence, and the temperature is also the same.

Since temperatures as great as 60°C are rather high for storage batteries and other equipment, it is desirable to increase the radiating area by increasing h. Moreover, if h/S is increased to 0.4, the variation of T with sun angle is much reduced by the absorption of sunlight on the top or bottom sides of the satellite. As the sun angle changes from 90° to 45° (or 135°), T changes over a range of only about 8° with this value of h/S. The actual temperature reached will depend on the detailed optical properties of the surfaces involved; to some extent these properties may be controlled.

We discuss next the variability of temperature. If a thin slab of thickness w, and specific heat c per gram

cools by radiation from one side, with no radiation incident on it, it is readily seen that

$$\frac{T}{T_0}=\left\{1+\frac{3(1-R)\sigma T_0^3 t}{\rho w c}\right\}^{-\frac{1}{3}}, \qquad (17)$$

where σ is the usual radiation constant, R the reflectivity, and T_0 the temperature at the time t is equal to zero. Inserting numerical values, we find that for a black aluminum sheet 1 cm in thickness, and for T_0 equal to 300°, T/T_0 falls to 0.89 in 35 min; here ρ and c equal 2.7 g cm^{-3} and 8.8×10^6 ergs g^{-1} deg^{-1} (0.21 cal g^{-1} deg^{-1}). Such a sheet 2 m on a side would weigh 100 kg. Thus the temperature of even such a relatively massive sheet will drop almost 40° during passage through the earth's shadow.

If w is small, the temperature of the skin will evidently be close to its equilibrium value most of the time. The radiation field inside the warm chamber will then show fluctuations similar to those found for the solar radiation absorbed. Any silvered (or aluminized) object of appreciable mass will have a long thermal time constant, and will come to an equilibrium temperature nearly equal to the mean value computed above for the warm chamber as a whole. Hence we see that temperature fluctuations of the material making up the sunny side of the satellite do not affect the mean temperature of silvered objects within the warm chamber. Large differences of temperature between the skin of the satellite and some of the structural members may create large thermal stresses, which must be considered in the design.

We conclude that in a satellite at 36 000-km altitude, the temperature of the warm chamber can probably be kept within a few degrees of a design value in the general neighborhood of room temperature, for sun angles between 45° and 135°. For a satellite at 800 km the mean temperature depends on whether or not the satellite orbit passes through the earth's shadow, the range of possible temperatures amounting to 30°. Variations of temperature with sun angle can be made small by a proper choice of h/S. During passage of the satellite through the earth's shadow, the skin temperature may drop sharply, but this change will not produce marked thermal fluctuations within silvered materials in the warm chamber.

Temperature of the Cold Chamber

The cold chamber receives heat leaking through from the warm chamber and infrared radiation from the earth reaching the dark side. Heat is radiated primarily from the dark side, which we assume black in the infrared. The equilibrium temperature reached can be made low, in the neighbourhood of 160° to 200°K.

We discuss first the leakage of heat through the double insulating layer. This layer is composed of two metal plates with the inner surfaces silvered, as in a thermos bottle. The heat flow due to radiation can be made very small. Let us suppose that the outer surfaces of the two metal sheets making up the layer are painted black in the infrared. Then each plate will be at the temperature of the chamber which it bounds. Let R be the reflection coefficient of the silvered surfaces in the infrared, and T_w, T_c be the temperatures of the warm and cold chambers, respectively. Then the heat flux radiated by the warm silvered surface is less than that from a black body by the factor $1-R$. Since R is nearly unity, most of the emitted radiation will be reflected back from the cold silvered side, and will be reflected back and forth many times, gradually being absorbed equally in the two plates. Thus the power absorbed in the cold plate, radiated from the warm plate, is reduced by another factor 2.

The net heat loss or leakage flux, F_L, to the cold plate per cm^2, is given by

$$F_L=0.5\sigma(1-R)\{T_w^4-T_c^4\}, \qquad (18)$$

where σ is the usual radiation constant. Since T_w is about five times T_c^4, we may neglect this latter quantity in the computations. For a silvered (or aluminized) surface R is about 0.98 in the infrared. If T_w is 300°K, F_L is 4.6×10^3 ergs cm^{-2} sec^{-1}, less than 1% of the solar flux on the sunny side. In addition to the radiation heat leak, there will also be a conductive heat flow through the various structural elements connecting the two chambers. In principle this can be made even less than F_L by the use of appropriate ceramic spacers.

In a satellite at 36 000 km, the heat flux from the earth is not much greater than the leakage flux. The equilibrium value of T_c under these conditions is in the neighborhood of 110°K. This value is probably lower than desirable. Any higher value, almost up to T_w, can be achieved by increasing F_L, simply by decreasing the effective value of R in the insulating layer and by increasing the infrared reflectivity of the cold side. Since T_w is constant to within 2%, T_c should also be constant to within the same accuracy, or about 4°K.

When a satellite is at 800-km altitude the flux of energy from the earth is substantial, and becomes the dominant heat source for the cold chamber. The intensities of the sunlight reflected from the earth and of the infrared radiation emitted from the earth and its atmosphere have been discussed in Sec. I. To get rid of the variability associated with light reflected by the earth we shall assume that the dark side of the satellite is painted to reflect 90% of the reflected sunlight—visible and near infrared—and is black in the infrared. For a first approximation we may then neglect the heat input to the dark side from this earth-reflected sunlight, and consider only the absorption of the infrared radiation from the earth. We also neglect temporal and spatial variations of the earth's infrared emissivity. With these simplifying assumptions we may now compute the mean energy input, evaluating first the flux from the

rth at any point in the satellite's orbit, and then veraging over the orbit.

To carry out this average, we introduce two systems spherical coordinates. One system is essentially enith angle θ and azimuth ϕ measured by an observer n the dark side of the satellite. We take ϕ to be zero or the great circle intersecting the horizon (the xy lane) in the direction of the x axis. The other system, esignated by Θ, Φ is centered at the apparent center f the earth; we take Φ equal to zero for the great circle assing through the zenith. The zenith angle of the arth's center we denote by θ_E. We denote by I the ntensity per unit solid angle of the infrared radiation rom the earth, which, as we have seen in Sec. I, equals $\times 10^4$ ergs cm^{-2} sec^{-1} steradian. The flux on the dark ide is then given by

$$F = I \int\int \cos\theta \sin\Theta d\Theta d\Phi, \tag{19}$$

ntegrated over that portion of the earth above the orizon. Evidently

$$\cos\theta = \cos\Theta \cos\theta_E + \sin\Theta \sin\theta_E \cos\Phi. \tag{20}$$

The limits of integration in Eq. (19) are those for which Eq. (20) gives a positive value for $\cos\theta$, subject to the condition that θ be less than χ, the apparent angular radius of the earth.

Equation (19) may be integrated analytically when θ_E is less than χ (i.e., when all the earth is visible from he dark side), giving a variation of F proportional to $\cos\theta_E$. Numerical integration of the equation for other values has been carried out numerically by R. Härm, ielding the values in Table III. The value of χ is the pparent angular radius of the infrared layer as seen rom the satellite. We may take this layer to be at an ffective height of 10 km. On this assumption the values f χ corresponding to altitudes of 400, 800, and 1200 km bove the earth's surface are 70.5°, 62.8°, and 57.5°,

TABLE III. Heat radiation from earth at various altitudes.

θ_E or i	$F(\theta_E)/I$			$\bar{F}(i)/I$		
	400 km	800 km	1200 km	400 km	800 km	1200 km
0	2.792	2.485	2.235	0.916	0.690	0.550
10	2.749	2.447	2.201	0.921	0.694	0.556
20	2.623	2.335	2.100	0.934	0.711	0.578
30	2.431	2.152	1.935	0.956	0.740	0.610
40	2.207	1.924	1.717	0.985	0.776	0.652
50	1.960	1.676	1.476	1.021	0.823	0.703
60	1.696	1.418	1.228	1.057	0.868	0.746
70	1.431	1.163	0.991	1.094	0.910	0.788
80	1.168	0.918	0.758	1.118	0.937	0.814
90	0.916	0.690	0.550	1.127	0.946	0.823
100	0.683	0.486	0.370			
110	0.476	0.313	0.223			
120	0.302	0.170	0.112			
130	0.165	0.079	0.040			
140	0.069	0.021	0.005			
150	0.015	0.001	0.000			
160	0.000	0.000	0.000			

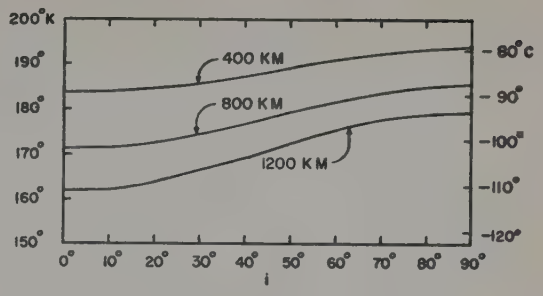

FIG. 5. Temperature of cold chamber. The angle i is the inclination of the dark side of the satellite relative to the plane of the satellite's orbit. The heat influx averaged over an orbital period has been set equal to σT^4.

respectively. Clearly, $F(\theta_E)$ vanishes when θ_E is 160° or more, since then none of the earth is visible from the dark side of the satellite.

Next we average $F(\theta_E)$ over an orbit, assuming that the orbit is circular, and that hence χ, the apparent radius of the earth, is constant over the orbit. We have

$$\bar{F}(i) = \frac{1}{\pi} \int_{-\pi/2}^{+\pi/2} F(\theta_E) d\psi, \tag{21}$$

where

$$\cos\theta_E = \sin\psi \sin i. \tag{22}$$

The angles i and ψ are identical to those shown in Fig. 1. Thus, i is the inclination of the earth's apparent orbit relative to the plane of the dark side (the xy plane in Figs. 1 and 4). When i vanishes, θ_E remains constant at 90°, and $\bar{F}$ equals $F(90)$. Values of $\bar{F}(i)/I$ are also listed in Table III. For i greater than 90°, $\bar{F}(i)$ equals $\bar{F}(180-i)$. The mean value of $\bar{F}(i)/\pi I$, integrated over all solid angles, equals the fraction of the sky filled by the earth, or $\sin^2\chi/2$.

The equilibrium temperature of the cold chamber at which the emitted flux σT_c^4 equals $\bar{F}$ may readily be computed from the values in Table III and the value of I cited above, yielding the values shown in Fig. 5. Evidently the total range of temperature at 800 km is 14° or about 10% of the absolute temperature. For some orbits, however, not all this range is available. If, for example, the pole of the orbit is either directly at the sun or 90° away, the total range of i is only 45°, if the sun angle is restricted to the range from 45° to 135°. The range of variation of temperature is then only 7°. In any case, this variability could be reduced if the twilight sides of the cold chamber were also made reflecting and absorbing. As we shall see below, however, the inhomogeneity of radiation produced by this modification may offset the gain. Additional variation of mean temperature will be introduced if the orbit is elliptical. For example, if perigee is at 600 km and apogee at 1200, the mean temperature will vary by some 10° depending on whether the earth is at apogee or at perigee when it passes over the dark side. Finally, variations of the

infrared intensity, I, with position on the earth and with time will also produce some variability of T. For example, for a satellite in an equatorial orbit, the equilibrium temperature of the cold chamber could fluctuate over a range of 20° if the cloud coverage varied over the extreme range from zero to 100%.

The mean temperatures shown in Fig. 5 must be increased for leakage from the hot side. Since the values of $\bar{F}$ are about ten times the value of F_L computed from Eq. (18), these temperatures must be increased by 2.5% or 5°. This value can be reduced if the outer surfaces of the double insulating layer are silvered, and may readily be increased if higher temperatures are desired for the cold chamber. Another increase in T of about this order will be produced by absorption of reflected sunlight from the earth.

Lastly, we consider the variability of temperature during each orbital period. If there is only one radiating surface such variation will be immaterial; if all components within the dark chamber are silvered, the mean intensity of radiation inside the cold chamber will be the same everywhere in the chamber and equal to $\bar{F}/\pi$ computed above. If absorbing surfaces were also included on the two twilight sides, this automatic homogeneity would disappear, and different parts of the cold chamber would be subject to different radiation fields. This effect might offset the greater constancy of the mean radiation field with changing i provided by the additional absorbing surfaces. In any case the main telescope and any finding telescope require holes in the top surface of the satellite, and these holes will absorb radiation from the earth and emit radiation to space. While such holes are likely to have a total area substantially smaller than that of the absorbing dark side, they introduce an inhomogeneity in the internal radiation field, especially in the vicinity of such critical elements as the secondary mirror. If it were important that all components have the same equilibrium temperature for each orientation of the satellite, these critical components could doubtless be shielded from radiation coming in through such holes.

To summarize this section, we have seen that in a satellite at 36 000-km altitude the temperature of the cold chamber can be maintained constant at about any design value, within a few degrees, by suitable treatment of the insulating layer and the dark side. In a satellite at 800 km the mean radiation temperature during an orbit varies with different directions in which the telescope is pointed; with the heat leak from the warm side reduced to a minimum this mean temperature ranges from about −80°C to about −95°C. With a somewhat greater heat leak provided and with some allowance for design uncertainties, the temperature of the cold chamber should stay safely within a range from −65° to −95°C.

Maintenance of Optical Resolution

With mean temperature changing from day to da by perhaps as much as 15°, as the direction of the tel scope changes, considerable design effort is required t ensure the highest possible resolution for a satelli telescope. Two problems must be solved. First, th figure of each optical element must not be impaired b thermal inhomogeneities. Second, the relative positio of the different optical elements and detectors must b correct.

The first problem is very much eased by the relativel low rate of heat exchange by radiation alone. In terrestial telescope the outer layer of a mirror com rapidly to thermal equilibrium with the surroundin air, as a result of conduction, and the inner layers com to equilibrium with the outer layers very slowly, ov periods of several hours. A mirror in a vacuum will co only by radiation, provided the supports are mad nearly nonconducting, and, if all surfaces are aluminize the rate of radiation in the far infrared will be reduce by a factor 50. For any solid body we may define a external time constant, τ_e, as the time required f radiation from the surface to reduce the temperatu differential by $1/e$, assuming infinite thermal condu tivity within the body. Evidently τ_e is simply the exce heat of the body divided by the rate of radiation fro the surface. For a plane slab of thickness w, radiatin from one side only, we have

$$\tau_e = c\rho w/4\sigma(1-R)T^3, \qquad (2$$

where c is the specific heat, ρ the density, R the refle tivity in the infrared, and σ the radiation constan Equation (23) must be modified if the temperatu differences are an appreciable fraction of T [see E (17)]. For an aluminized or silvered surface R is abo 0.98 in the far infrared, and at 200°K τ_e/w is abo 6×10^5 sec cm^{-1} for either aluminum or quartz. Th for a quartz disc 5 cm thick, the external time consta is about a month, while for an aluminum sheet 0.5 c thick τ_e is about three days. If radiation is lost fro both surfaces, these times are reduced by one-half.

The time required to reach thermal equilibrium i ternally, through atomic conduction, is much less. F a slab of thickness w cooling in the lowest mode, wi one surface kept at a fixed temperature, and with n heat loss from the other surface, the internal time co stant, τ_i, is given by

$$\tau_i = 4c\rho w^2/\pi^2 K, \qquad (2$$

where K is the coefficient of thermal conductivity a other symbols have the same meaning as above. F an aluminum slab 0.5 cm thick τ_i is 0.12 sec. For quartz disk 5 cm thick, τ_i is 32 min, enormously le than the value of τ_e computed above. Even for a 10-c thickness τ_i is only 2 hr. Evidently τ_e could be safe reduced by one order of magnitude, by the use of more radiating surface on one side, for example, a

fill exceed τ_i by a large factor. We conclude that thermal inhomogeneity in the optical elements is not likely to be a serious problem.

The second problem, that of positioning, is more difficult to solve. If the full resolving power is desired in the ultraviolet, the accuracy of positioning required is very great. For example, with an $f/3$ primary the diameter of the extra-focal image equals the diameter of the diffraction image at 2000 A (to the first minimum) at a distance of 4×10^{-4} cm away from the focal plane. Evidently with a focal length of some 2 m the distance from the primary mirror to a detector or a secondary mirror must be correct to one part in 10^6.

One method of solving this problem is continually to refocus the telescope automatically. In principle this would not be difficult, at least during observations on a relatively bright star. In practice, however, the hardware required is relatively complex, and another potential source of failure. We shall again confine attention to several passive methods.

One simple approach, suggested by Meinel, is to use one type of metal both for the optical elements and for all support and positioning elements. The entire structure would then expand and contract together. The feasibility and long-term dimensional stability of metal mirrors is now under investigation at the National Observatory at Kitt Peak. Another problem associated with this concept is the temperature uniformity required for the structure as a whole. With aluminum, for which the expansion coefficient is 2×10^{-5} per degree C, the temperatures of all components must be the same to within 0.05°C. To maintain this homogeneity by thermal conduction over a structure 2 m long, if the radiation temperature changes by as much as 15°, and if mirrors and structural supports tend to cool at quite different rates, requires rather massive structural elements, with an aluminum wall thickness of at least 5 cm. However, if all elements have virtually the same external time constant τ_e, with thermal conductivity between elements reducing an otherwise small thermal differential, the amount of conducting material required would be substantially less.

Another approach is to use material with a very low coefficient of expansion. Pyroceram has essentially a zero coefficient of expansion at room temperature, and would be ideal if the telescope were to be maintained at this temperature. Fused silica has zero coefficient of expansion at −80°C, as shown in Fig. 6, and varies in length by at most one part in 10^6 over a range of 30°, from −95° to −65°C. Evidently this is an ideal material for optical elements in a satellite telescope.

A structural material with similar properties would be desirable for positioning the optical elements. Invar is probably not suitable because of its ferromagnetism, which would considerably complicate the guidance problem. One is tempted to consider quartz rods for positioning all the optical elements with respect to each other. The launching stresses probably make it unwise to use such a fragile material so extensively.

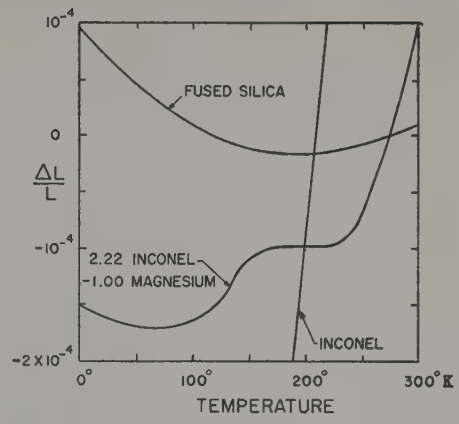

FIG. 6. Coefficients of thermal expansion.

Another possibility is to use different metals, cancelling out the differing coefficients of expansion as in a familiar compensated pendulum. The chief difficulty of such schemes is maintaining the different metals at the same temperature to the required accuracy of 0.05°. It appears that this problem can be solved by a concept developed by Rogerson, who suggests using concentric tubes of suitably chosen materials, as shown in Fig. 7. The basic idea is to use two metals with coefficients of expansion differing by about a factor 2. Then with two tubes of the less expansive metal and one tube of the more expansive, a system can be achieved with a very low net expansion and high thermal homogeneity. As shown in Fig. 7, ball bearings between the tubes provide some rigidity while still permitting relative motion.

The particular example of a Rogerson tube shown in Fig. 7 utilizes inconel and magnesium. The net expansion coefficient, when oppositely combined in the ratio 2.22 to 1, is shown in Fig. 6, computed from data given in a summary by Lacquer (1952). Evidently the total change of length of this combination in the range from −65° to −95°C is about one in 10^6. Actually, inconel is mildly ferromagnetic at low temperatures, with a Curie point of −40°C. Inconel X, with a permeability of 1.003 at room temperature and a Curie point of

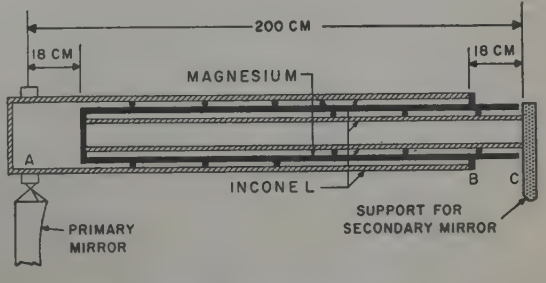

FIG. 7. Thermally compensated support tube.

−173°C, is preferable; the thermal expansion of Inconel X is about the same as for inconel at high temperatures, and presumably also for low temperatures. Other combinations are also possible, including, for example, a combination of inconel and aluminum in the ratio of 1.73 to 1, with a tube length somewhat greater than the separation between primary and secondary.

To assure the proper temperature homogeneity, the outer surface of the tube structure in Fig. 7 is silvered or aluminized. The outer surface of the magnesium tube is also reflecting between B and C, but is made black in the infrared between A and B. Any end plates and other structural elements are silvered or aluminized, but all other surfaces of the three tubes are black in the infrared. Since the innermost tube is entirely surrounded by the magnesium tube, which from a thermal standpoint is surrounded by the outer inconel tube, all three tubes should have almost exactly the same temperature in equilibrium. If the outer radiation temperature drops by 15°, temperature differences as great as 0.15° may appear between tubes; however, by choice of the relative thicknesses of the tubes and of the infrared reflectivities of the various surfaces, the temperature of the magnesium tube can be kept equal to the mean temperature of the two inconel tubes to better than the required value of 0.05°C. Evidently any thermally compensated optical system, like an all-metal system, requires careful study before it can be relied upon.

This preliminary survey would appear to indicate that either an all-metal system, of a combination of quartz optics and thermally compensated supports offers promise of satisfactory performance under the changing conditions anticipated at 800 km. For a satellite telescope at 36 000-km altitude the variability of temperature is less by an order of magnitude, and probably either system could provide the required optical resolution at all times.

V. RELIABILITY

The greatest single problem in the design of any satellite is to ensure that the equipment will operate after it is placed in orbit. This problem is particularly acute for a satellite telescope, which should preferably operate for many months, if not years.

In the long run this problem may require that repairs and modifications be possible in orbit. Perhaps a maintenance team could come up to the satellite occasionally to check all components and make any repairs or changes that seem required. Another possibility might be to provide means for working on the equipment by remote control. The techniques that have been devised for remote manipulation of radioactive materials could perhaps be adopted for remote repairs of equipment on a satellite. If two mechanical hands and a television screen can be provided in a satellite, one can visualize two sets of such equipment, so that one can be used to repair the other.

Until repairs in orbit are possible, the design of equi ment must take into account the probability that a component may fail. Clearly, the more components th are required for the functioning of a satellite the great the probability that the satellite system will fail operate properly. Hence there is a very urgent argume for simplicity in all satellite design work. In additio some components are more likely to fail than othe and should be avoided as far as possible. To increase t reliability of the satellite, redundance should be reli upon as much as possible; i.e., additional componen and systems should be provided so that the failure any one element will not prevent the satellite syste from functioning as planned.

A preliminary quantitative evaluation of these effec has been developed by Hufnagel (1959), whose trea ment we shall follow here. Any such analysis must based on the probability of failure for each type unit—resistors, vacuum tubes, transistors, capacito and the like. Such a probability may be measured the fraction of units of a given type which fail in a u interval of time, when a large number of such units a being tested. This failure rate will be relatively hi initially, as units which are defective because of man facturing errors, damage in shipment, etc., fail operate. After a short time, however, the failure ra may be assumed to drop to a lower value, and to rema nearly constant for a substantial time. The failure ra may rise again if the units wear out physically; t time to wear out may be called the "longevity." W consider times which are long compared to the failu time of initially defective units, but short compared the longevity. The assumption of a constant failure ra is then likely to be a reasonable first approximation.

The failure rate for each type of unit evidently d pends on how the unit is used. Thus the failure rate o resistor can be decreased by a factor three if the pow dissipation rate is reduced to less than 20% of the rat value. Even if each type of unit is used with the utmo care, however, there is still an appreciable failure ra While the available data are not very complete, cru estimates can be made of these minimum failure rat for different types of units. These estimates, compil by Hufnagel, are given in Table IV. It may be not that the value given for capacitors is for a power dissip tion rate at most 10% of the rated value.

TABLE IV. Minimum failure rates of various components.

Unit	Failure Rate
High-Speed motors (5000–10 000 rpm)	2×10^{-1} year^{-1}
Vacuum Tubes	1×10^{-1}
Low-Speed motors (below 1000 rpm)	1×10^{-2}
Transistors	3×10^{-3}
Resistors	1×10^{-3}
Semiconductor Diodes	4×10^{-4}
Capacitors	1×10^{-4}
Connectors	1×10^{-4}

We assume that in any satellite system defective units have been eliminated by a relatively brief test period. Then the failure rate may be set equal to a constant value, α, and the fraction of each type of unit that will be operating after a time t will be simply $\exp(-\alpha t)$. If there are N separate units, then the probability $P_N(t)$ that all components will still be operating after a time t is given by the product of the probabilities that each component will be operating; hence we have

$$P_N(t)=e^{-N\alpha t}. \tag{25}$$

More generally, if a system contains N_i components of type i, each with a failure rate α_i, and if the failure of any one component will lead to a failure of the system, we have for α_s, the system failure rate,

$$\alpha_s=\Sigma_i N_i\alpha_i. \tag{26}$$

In a typical electronic system each transistor is normally accompanied by about half a dozen other elements (resistors, capacitors, etc.) and a dozen connectors. If as the mean failure rate for each of the six additional components we take 10^{-3} year^{-1}, the value for resistors, we obtain about 10^{-2} year^{-1} per transistor for α_s. Thus in a system with 100 transistors the failure rate is about 1 year^{-1}. If 90% reliability is desired, the time of operation must not exceed about a month. In the normal television camera, with some 50 transistors, the failure rate will be about 0.5 year^{-1}.

Evidently the system failure rate can be much reduced if redundant elements are used. If two separate systems are provided, the probability $P_1(t)$ that at least one is operating is given by

$$P_1(t)=1-\{1-e^{-\alpha_s t}\}^2, \tag{27}$$

where α_s is again given by Eq. (26). For small $\alpha_s t$, the probability of failure, $1-P_1(t)$, is much decreased by the redundance. The mean life of the system is increased by only 50%, however. Alternatively, each component in the system could be made separately redundant, so that a double failure of a single component would be required for system failure. The system failure probability under this condition, which we denote by $P_2(t)$, is

$$P_2(t)=\prod_i[1-\{1-e^{-\alpha_i t}\}^2]\approx\prod_i[1-\alpha_i^2t^2], \tag{28}$$

since we are considering times such that $\alpha_i t$ is small. If there are N_j components of each type j, $P_2(t)$ is approximately given by

$$P_2(t)=\exp-\Sigma_j N_j\alpha_j^2t^2. \tag{29}$$

If the system is made up of N components with all about the same failure rate, the mean life is now increased by a factor of order $N^{\frac{1}{2}}$ as a result of the assumed redundance. In a system with a thousand or more components, the increase in reliability would be very large indeed.

In most practical situations, however, it is difficult to make each separate component redundant without some switching arrangement. For example, it is not usually possible to put passive circuit elements in series or parallel in such a way that the performance of the circuit will be unimpaired by one element either shorting out or going open circuit. Switching circuits introduce new possibilities of failure, and in complex systems may much reduce the advantages of great redundance.

For any specific system the failure rate can be estimated from the above equations. It should be emphasized again that these are all minimum rates, and represent the best that can be hoped for with present components. Mechanical failures during the launching are not taken into account in Table IV. Human errors are also possible, especially during the final testing and adjustment of the equipment; their probability presumably increases with increasing equipment complexity, but cannot be evaluated quantitatively. Subject to these reservations, a satellite telescope system with several motors and several thousand electronic parts, including transmitters, data storage equipment, and a limited amount of program control, together with considerable redundance of separate subsystems, can have a theoretical mean life of about a year before failures prevent any useful operation.

VI. LAYOUT

To illustrate some of the general principles discussed in the preceding sections a possible design of a satellite telescope will be discussed here. One preliminary design of this sort has been worked out by the Perkin-Elmer Corporation for the Princeton University Observatory. The general features of this design are shown in Fig.8; some of the details are discussed below.

We have already seen that the general shape of a satellite should be highly symmetrical, in order to reduce as much as possible the perturbing torques due to radiation pressure, atmospheric particles, and the earth's gravitational field. To fit the satellite into the cylindrical structure of the launching rocket, the cubical

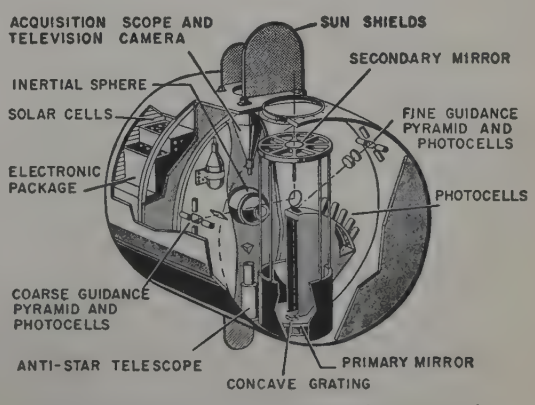

FIG. 8. Conceptual design of proposed spectroscopic satellite telescope.

configuration discussed previously is here replaced by a cylinder 2.1 m in diameter, and 1.8 m in length. With these proportions the three principal moments of inertia would all be equal if the satellite were a cylinder of uniform density. The telescope mirror is assumed to be 60 cm in diameter, or 24 in.

Most effective use of the solar battery cells is obtained if the sunny side is taken to be one end of the cylinder. The optical axis of the telescope is then along a diameter of the cylinder. The warm side, containing electronic packages, is then at one end of the cylinder as shown in the figure, separated from the cold side by the double insulating layer shown by the shaded wall.

An inertial sphere, shown encircled by several positioning coils, is placed at the center of the cylinder. Placing the sphere at the center of gravity minimizes the possibility of exciting positional oscillations of the sphere, and also reduces the coupling between such oscillations and small rotations of the satellite as a whole. The telescope is then placed at an end of the cylinder, next to the dark side. In the figure a structural wall is shown separating the telescope from the other half of the cold chamber.

Since the telescope is designed for ultraviolet spectroscopic work entirely, definition is required only on the axis. Hence the instrument envisaged in this design is a relatively conventional $f/3$ cassegrain, with an $f/20$ secondary forming an image at the entrance slit of the spectrograph. For a multipurpose telescope a better arrangement would be that proposed by Meinel, placing the secondary beyond the primary focus to yield a Gregorian system, with a wide flat field. A variety of different focal positions would be provided at various places in the focal plane, with perhaps an image tube placed at the center, and slits for various spectrographs, with differing resolutions and differing wavelength regions, placed around the periphery. Grazing-incidence mirrors could be used to deflect the light away from the optical axis and thus to provide more space for the spectrographic and detecting equipment. The use of various fixed focal positions, one for each type of observation, is a more reliable arrangement than converting the main focus from one type of observation to another.

The primary mirror is shown in the figure as a sandwich type, with two quartz disks spaced apart by quartz tubes. This type of construction, designed to reduce weight, has been successfully used for small pyroceram mirrors, and may be feasible in quartz. It is also possible that a simple quartz disk, one or two inches in thickness, might be used, since structural rigidity in orbit is no consideration, and various methods can be used to support a simple disk during grinding and testing.

The spectrograph is of conventional Rowland type, with photocells positioned around the Rowland circle. To ensure that the instrument remains in constant focus, R. Scott of Perkin-Elmer has suggested that two quartz sectors be used as the structural elements, with entrance slit, grating, and exit slits all positioned wit respect to these sectors. In observations on a single sta two of the phototubes (signal tubes) would be set a particular wavelengths for a minute or so, the numb of photon pulses during this interval stored on a tap recorder, and the signal tubes then moved to a ne position. The two fixed phototubes would serve a monitors, and the ratio of photon counts in a signal tub and in a monitor tube, all corrected for dark coun would be the primary datum of observation. This tech nique has been used in the visible by Rogerson, Spitze and Bahng (1959). Programs of research on interstella matter could be carried out with such an instrumen have been discussed by Spitzer and Zabriskie (1959).

A pair of signal tubes and a corresponding pair o monitors are shown in Fig. 8 on the assumption tha one pair would be sensitive in the wavelength regio 800 to 1600 A, while another would be sensitive fro 1600 to 3200 A. The fifth phototube would receive th zero-order spectrum, useful in the initial focusing o the telescope, and in analyzing the performance of th instrument.

It is assumed that rough information on the orienta tion of the satellite would be obtained by measures o the sun angle (angle from the sun to the optical, or z axis) and of the earth angle (azimuthal angle of th earth around the cylinder, or z, axis). In addition th satellite would be oriented around the optical axis t keep the sun in the xz plane. The necessary sensin elements are not shown. To aid in the acquisition, separate wide-angle telescope is shown, with a fiel roughly 10° across, feeding a television camera.

The guidance system is composed of two parts, coarse guidance pyramid with a field of about 30′ of arc and a fine guidance pyramid with a field of about 0.2 this latter pyramid might well enclose the slit jaws, bu is shown separately in the figure. Thus the guidanc admission angle is about 15′; if the acquisition televisio camera fails, a star of sixth magnitude or brighter migh still be acquired, perhaps with some hunting. On th other hand, the combination of the fine and coars guidance systems can be made to yield a system wit a marked peak of sensitivity close to the optical axis so that the brightest star within the guidance admissio angle will be placed exactly on the slit of the spectro graph, if the other stars in the field are not too bright For settings on fainter stars, by direct control from th ground, a separate television camera is shown, viewin the field of the coarse guidance system; the coars guidance pyramid and detectors would presumably b inactive when such direct settings were made.

To reacquire stars after occultation by the earth, a anti-star telescope is shown in Fig. 8. If the perturbin torques can be held below 30 dyne cm, the drift durin occultation is less than the 15′ guidance admission angle and the anti-star telescope is not needed, provide observation is restricted to stars of about the sixth

magnitude or brighter. As with the other telescopes, this instrument has a sun shield to keep sunlight out for sun angles between 45° and 135°.

The electrical power delivered by the solar battery cells is determined by the total area, the sun angle and the fraction of time illuminated. If we take an area of 3×10^4 cm², a minimum sun angle of 45°, and illumination 65% of the time, we obtain an average electric power source of about 100 w. The conversion efficiency assumed in this calculation is 5% of the incident solar flux. This power supply is apparently adequate both for the steady power drain and for the intermittent peak power required for several transmitters, television cameras, etc.; these operate for brief intervals several times a day during communication with the ground. Evidently storage batteries will be required for this peak load. The total weight of this satellite instrument should not exceed a couple of tons.

One characteristic of a satellite telescope of this type is the highly integrated nature of the design. In particular the design of the guidance system depends intimately on the magnitude of the perturbing torques, including such engineering details as the degree of static and dynamic symmetry possible, and the amount of ferromagnetic materials on board the satellite. The temperature stability required for the optical system demands careful attention to the conduction and radiation properties of all parts of the satellite, especially of the cold chamber, including, for example, sources of dissipation within this chamber. One may hope that with sufficient attention to all details, with adequate preflight testing and with a sufficient number of separate satellites launched, a powerful telescope above the earth's atmosphere may become an operating reality, yielding the revolutionary advances in astronomy that we expect.

REFERENCES

Aitken, R. G. 1935, *The Binary Stars* (McGraw-Hill Book Company, Inc., New York), Chap. X.

Byers, H. R. 1953, *The Earth as a Planet*, edited by G. P. Kuiper, (University of Chicago Press, Chicago, Illinois), Chap. 7.

Gast, P. R. 1956, *Scientific Uses of Earth Satellites*, edited by J. A. Van Allen (University of Michigan Press), Chap. 9.

Harris, I. and Jastrow, R. 1959, *Planetary and Space Sci.* **1**, 20.

Hering, K. 1959, Unpublished manuscript, Perkin-Elmer Corporation.

Hufnagel, R. 1959, Unpublished manuscript, Perkin-Elmer Corporation.

Lacquer, H. L. 1952, U. S. Atomic Energy Commission Rept., AECD-3706 (Los Alamos Scientific Laboratory).

McNish, A. G. 1939, *Terrestrial Magnetism and Electricity* edited by J. A. Fleming (McGraw-Hill Book Company, Inc., New York), Chap. VII.

Nidey, R. 1959, (unpublished).

Nidey, R. 1960, *J. Am. Rocket Soc.* (to be published).

Roach, F. E., Pettit, H. B., Tandberg-Hanssen, E., and Davis, D. N. 1954, *Astrophys. J.* **119**, 253.

Roberson, R. E. and Tatistcheff, D. 1956, *J. Franklin Inst.* **262**, 209.

Roberson, R. E. 1958, *J. Franklin Inst.* **265**, 13.

Rogerson, J. B., Spitzer, L. and Bahng, J. 1959, *Astrophys. J.*, **130**, 991.

Seares, F. H., Van Rhijn, P. J., Joyner, M. C., and Richmond, M. L. 1925, *Astrophys. J.*, **62**, 320.

Smythe, W. R. 1950, *Static and Dynamic Electricity* (McGraw-Hill Book Company, Inc., New York), 2nd ed., Chap. XI, p. 417.

Spitzer, L. and Zabriskie, F. 1959, *Publs. Astron. Soc. Pacific* **71**, 412.

Van Allen, J. A. 1959, *J. Geophys. Research* **64**, 1683.

Van Allen, J. A., McIlwain, C. E., and Ludwig, G. H. 1959, *J. Geophys. Research* **64**, 271.

Wakefield, K. E. 1956, U. S. Atomic Energy Commission Rept., NYO-7313 (Project Matterhorn PM-S-23).

Wakefield, K. E. 1959 (unpublished).

Whipple, F. L. 1952, *Physics and Medicine of Upper Atmosphere*, edited by C. S. White and O. O. Benson, Jr. (University of New Mexico Press), Chap. 10.

Whipple, F. L. and Fireman, E. L. 1959, *Nature* **183**, 1315.

Recent Experiments from Rockets and Satellites

HERBERT FRIEDMAN
U. S. Naval Research Laboratory, Washington 25, D. C.
(Received March 24, 1960)

During 1959, rocket experiments succeeded in advancing several areas of ultraviolet and x-ray astronomy. The solar disk was photographed in Lyman-α with a resolution of better than one minute of arc. Spectrograms were obtained down to wavelengths below the He I and He II resonance lines. Solar x-ray emission coincident with visible flares was mapped from 60 A down to 0.2 A. For the first time a small optical telescope was used for the study of ultraviolet emissions in the night sky. It demonstrated the feasibility of ultraviolet color mapping of the stars and has given us some new clues to the nature of the ultraviolet nebulosities surrounding the early stars.

SOLAR DISK PHOTOGRAPHY

SPECTROHELIOGRAMS in *Hα* and *Ca* K are the best optical indices of solar activity. The *Hα* and *Ca* K plage formations have characteristically different appearances related to the solar levels in which the emissions are excited. Lyman-α (1216 A) and the *He* resonance lines (584 and 304 A) arise in the higher levels of the chromosphere. Solar disk photographs in these emission lines would greatly advance our understanding of the structures of the chromosphere and the inner corona. It appears from a variety of data, that the chromosphere is not a spherically homogeneous shell, but rather a columnar structure of hot and cold regions. If the resolution of the ultraviolet pictures were comparable to that of the *Ca* K line pictures taken from the ground, detailed comparisons could be made, which could perhaps reveal the temperature variations in the hot and cold regions and the temperature dependence on height.

J. D. Purcell, D. M. Packer, and R. Tousey (1959) of NRL obtained a photograph of the solar disk in Lyman-α from an Aerobee rocket on March 13, 1959, with a resolution of better than one minute of arc. Earlier attempts by W. A. Rense and his colleagues (Miller *et al.* 1956) at the University of Colorado using lithium fluoride optics had shown that great improvement in camera speed was necessary in order to obtain pictures with significant detail. The NRL camera employed mirror optics and utilized recently developed techniques for producing highly reflecting surfaces. Satisfactory exposures were made in 1/50 of a second and the limiting resolution obtained could be attributed entirely to the movement of the pointing control within the short interval of exposure.

The NRL camera (Fig. 1) consisted of two concave mirror diffraction gratings ruled with 600 lines per inch. The first grating produced a series of dispersed images of the sun in Lyman-α and other solar wavelengths nearby. A diaphragm placed in the focal plane blocked the adjoining wavelengths and passed the Lyman-α image through an aperture to the second ruled grating. The secondary dispersing system further purified the transmitted image of extraneous wavelengths and focused the final image of the monochromatic disk on photographic film. In the laboratory the camera was capable of producing an image with a resolution of 2 seconds of arc. Figure 2 is a reproduction of the disk photograph made from the rocket. It is clear that most of the Lyman-α emission comes from plage formations. There is a detailed correlation between this picture and simultaneous photographs made from the ground in *Ca* K and *Hα*. The Lyman-α picture shows a grosser plage structure and much greater contrast than the *Ca* K picture. It is well established that the fraction

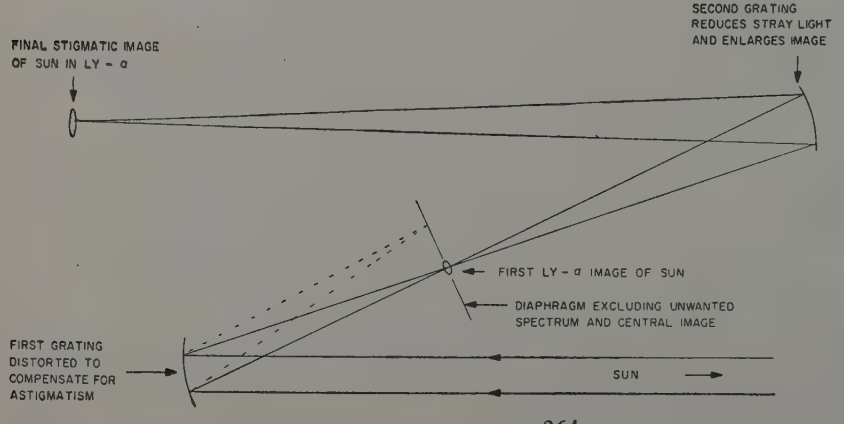

FIG. 1. Camera used to obtain pictures of the sun in the Lyman-α line (Purcell and Tousey, NRL).

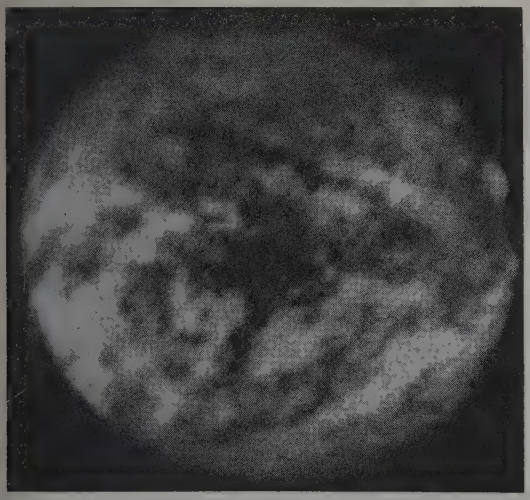

FIG. 2. Lyman-α Disk Photograph (Packer, Purcell, Tousey and Hunter, NRL).

the solar surface covered by *Ca* plages reaches a maximum at sunspot maximum and nearly vanishes at sunspot minimum. We may expect Lyman-α plages to follow a similar cycle which would correspond to a large variation in solar Lyman-α flux between minimum and maximum.

The problem of photographing the disk in shorter ultraviolet wavelengths, including the He resonance lines, is primarily one of improving reflectivity. Research efforts in this direction are being made by Haas at Fort Belvoir and Tousey at NRL. In the Lyman-α camera, one grating was coated with *Al* plus MgF_2 (reflectance = 80%) and the other with *ZnS* (reflectance = 31%). It is also possible to resort to scanning techniques, utilizing a wobbling mirror and a narrow band photodetector at its focus. The mirror movement traces out a raster scan at the detector, which can transmit the TV-type picture information to ground via telemetry.

In some of the earliest efforts to measure solar Lyman-α use was made of the thermoluminescent $CaSO_4$:*Mn* phosphor, which has a long wavelength excitation cutoff at 1350 A. In combination with a lithium fluoride filter, this phosphor would respond to a band of solar radiation comprised almost entirely of Lyman-α. The phosphor can be used to replace the photographic film in the focal plane of a mirror telescope. After exposure in the rocket and subsequent recovery, the phosphor can be heated to thermoluminescense in visible light. The glowing image can then be recorded on photographic film. Consideration is being given to this type of imaging in future rocket experiments.

THE SOLAR ULTRAVIOLET SPECTRUM

New information about the solar spectrum in the extreme ultraviolet has been obtained by three independent groups of researchers at the Naval Research Laboratory, the University of Colorado, and the Air Force Cambridge Research Center. The following is a brief summary of their results:

1. The Naval Research Laboratory—J. D. Purcell, D. M. Packer, and R. Tousey. A successful spectrograph experiment was performed with an Aerobee-Hi rocket 13 March 1959. The instrument was a normal incidence 40-cm radius, 600 line/mm tripartite replica diffraction grating blazed for 1000 A and was directed at the sun by a biaxial pointing control. Twenty exposures were made with times varying from $\frac{1}{2}$ to 60 sec. A 30-sec exposure covered the altitude range 194.6 to 198 km over the peak of the flight. The slit width was 15 μ, dispersion 40 A/mm, setting the resolving power to about 0.6 A.

The photospheric continuum (Fig. 3) is visible down to 1550 A where it merges with the stray light background. Fraunhofer lines are clearly present above 1750 A. Nearly 100 emission lines, about 60 of which had not been previously observed, have been identified in the spectrogram. Among the new lines identified thus far are those produced by *Mg* X, *O* II, *O* III, *O* IV; *Ne* I, *Ne* III; *Si* I, *Si* II; *S* I and *C* I. At least eight lines of the Lyman series of hydrogen are present. The series ends at a fairly abrupt rise in background density marking the edge of the Lyman continuum which begins at 910 A and extends to shorter wavelengths. Lyman-γ is missing. It appears that the atmosphere at 200 km is still optically thick to Lyman-γ and that the absorber is molecular nitrogen. This behavior is consistent with an atmospheric model intermediate between those deduced from rockets and those deduced from satellites.

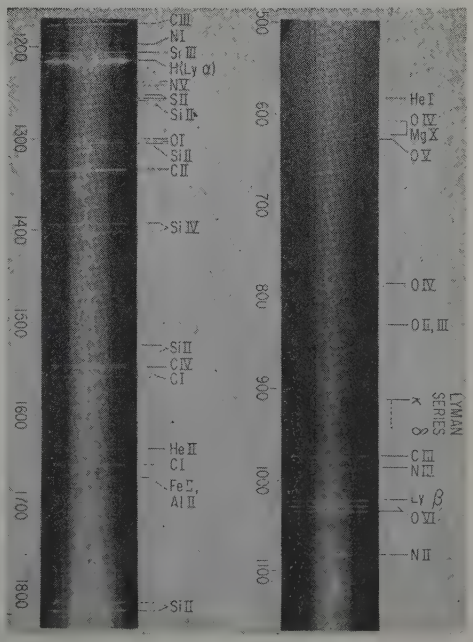

FIG. 3. Solar spectrogram (Packer, Purcell, and Tousey, NRL).

TABLE I.

Date	Altitude (km)	Solar zenith angle	Flux ergs cm^{-2} sec^{-1}
June 4, 1958	212	80°	0·81
June 4, 1958	140	80°	0·04
March 30, 1959	195	60°	0·42
March 30, 1959	175	60°	0·21

The Lyman continuum can be followed down to about 820 A, but at shorter wavelengths the background seems to be entirely due to stray light. The shortest wavelength appearing in the spectrum is *He* I, 584 A. The *Ne* VIII doublet (E_i=207.3 ev) falls at 770.5 and 880.2 A *Mg* X appears very weakly at 609.9 and 624.9 A (E_i=327.9 ev). The intensities have been compared with Lyman-α. Tentative values are as follows: Lyman-β =1/60 Lyman-α; the helium continuum is comparable in total intensity to Lyman-β; *He* I=1/20 Lyman-β.

2. W. A. Rense and T. Violett, University of Colorado. To photograph the spectrum below 1000 A, W. A. Rense has used a grazing incidence spectrograph which provides much greater speed than the normal incidence geometry. As of the spring of 1959, he had obtained four spectrograms on two flights that showed the *He* II 304 A resonance line. His estimated intensities are given in Table I. Rense believes that there was still considerable air absorption at the peak of each flight and that the flux above the atmosphere would have been much higher than that reaching the rocket. He estimates that the intensity of *He* II 304 A is comparable to or greater than the intensity of Lyman-α when extrapolated to above the atmosphere.

The most recent paper published by Rense and Violett (1959) lists spectrum lines down to 83.9 A. In the previously described NRL spectrogram, 50 lines are clearly present and are identified between 1216 and 550 A. The University of Colorado group lists 50 unidentified lines in the same range, which do not appear in the NRL spectrogram. An additional 50 lines in the University of Colorado spectrogram are identified—about 25 of these are not present in the NRL spectrogram and 25 of the NRL lines are not listed in the Colorado spectrogram. There appear to be major discrepancies in the results reported by the two laboratories. A serious problem in the use of grazing incidence spectrographs is that the intensity of stray light at short wavelengths is almost great enough to blot out the spectrum lines. In their article Rense and Violett assign estimated intensities to all the observed lines. If added up as listed, the total flux of ultraviolet radiation below 1000 A would exceed 500 ergs cm^{-2} sec^{-1}. This seems improbably high. Rense in a private communication estimates that the true value may be closer to 10 erg cm^{-2} sec^{-1}. Past theoretical attempts to explain the ionospheric production by this portion of the solar spectrum have required intensities of the order of 0 to 0.7 erg cm^{-2} sec^{-1}.

3. H. Hinteregger—U. S. Air Force Cambridge R search Center. Data on the intensity of the solar *H* 304 A emission line and its absorption by the upp atmosphere were obtained by H. Hinteregger on Marc 12, 1959. The rocket-borne spectrograph used a 2- radius concave grating mounted for grazing incidenc at an angle of about 86 deg. Intensities were measure by a photomultiplier tube having an extended cathod surface almost totally insensitive to wavelengths longe than 1500 A, but highly efficient at shorter wavelengths The portion of the Rowland circle normally covered b photographic film was instead scanned by an ex slit cut in a continuous steel belt. The belt was drive along the Rowland circle so that the spectrum wa scanned repeatedly from 1300 A to 250 A. Radiatio emerging at any slit position in this wavelength rang was received on the cathode of the multiplier tube an counting rates were telemetered to ground.

From 140 km to the peak altitude of 210 km, 1 wavelength scans were recorded. Each scan clearl showed the *He* 304 A line so that it was possible to plo the intensity vs altitude. No other spectrum line c comparable importance was detected below 1000 A. Th rocket was flown in the morning with the sun at 58 de from the zenith. The maximum rate of absorption oc curred at 180 to 185 km and the intensity was estimate to be 0.28 erg cm^{-2} sec^{-1} extrapolated to the top of th atmosphere.

It is to be hoped that future rocket spectroscop experiments will provide spectrograms more suitable fo quantitative densitometry and the evaluation of energ fluxes and that the disagreements between various ex perimenters will soon be resolved.

THE PROFILE OF SOLAR LYMAN-α

J. D. Purcell and R. Tousey (1959) of NRL hav described a high resolution profile of solar Lyman- photographed in an Aerobee-Hi rocket flown on July 2 1959. The spectrograph employed a 50-cm radius 120 line/mm diffraction grating in the 13th order. Th dispersion was 2.6 mm/A. Overlapping orders and stra light were effectively eliminated by use of a simila grating as a predisperser. The optical system was stig matic so that the spectrum line corresponded to point in a narrow slice diametrically crossing the sun. Nin successful exposures were made with times varyin between 4 sec and 120 sec at altitudes from 92 km t 197 km. The solar zenith angle was 69 deg. Figure 4 i a spectrogram and its microphotometer tracing obtaine with a 30-sec exposure covering the altitude regio 134 km to 163 km.

The emission line has a half-maximum width of th order of 1 A with wings extending about an angstro on either side of center. The center of the line shows broad depression leaving two maxima separated b

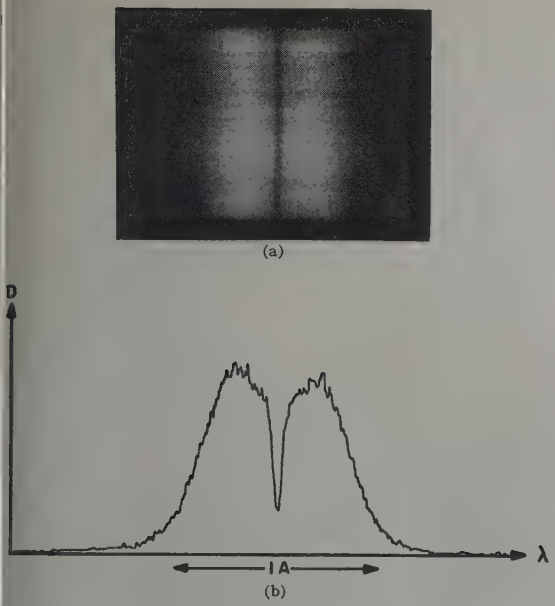

FIG. 4. Lyman-α Profile (Purcell and Tousey, NRL).

approximately 0.4 A. The broad absorption is most likely produced in the solar atmosphere. In its general features, the profile resembles the *Ca* H and K lines and the *Mg* II doublet. In the center of the broad weak reversal is a deep narrow central absorption core. It is believed that this narrow core can be attributed to absorption by geocoronal hydrogen.

THE NIGHT SKY LYMAN–α GLOW

Attempts to measure Lyman-α from the night sky have shown that the earth's shadow is filled with a diffuse glow (Kupperian *et al.* 1959). It is generally agreed that this glow arises from the scattering of solar Lyman-α by neutral hydrogen, but it is not clear as to how much of the hydrogen is telluric in origin and how much is interplanetary. A model distribution based on interplanetary hydrogen requires about 0.2 atom per cc distributed in a layer about 1 a.u. thick at the distance of the earth's orbit. F. S. Johnson (1960) has shown that a geocoronal hydrogen model can be constructed which also fits the experimentally observed Lyman-α glow, if the optical depth of the hydrogen between 120 km and 10 earth radii is nearly unity.

Several other experimental observations must be fitted into a theory of the source of the Lyman-α glow. The rocket experiment (Kupperian *et al.* 1959), measured an albedo of 42% when looking back at the terrestrial atmosphere from heights greater than 120 km. If this outward flux is Lyman-α backscattered from cold hydrogen below 120 km, the incident radiation from the night sky must have a narrow profile to account for the high percentage of the albedo. Johnson has argued that if the hydrogen atoms scattering Lyman-α were located in interplanetary space, then the earth's velocity relative to a stationary interplanetary distribution would introduce a large Doppler shift. The shift corresponding to the 30 km/sec orbital velocity, would reduce the scattering by hydrogen at the 100-km level, where the mean thermal velocity is about 2 km/sec, to a very small percentage. Brandt and Chamberlain (1960) have argued that the backscattered radiation is not resonantly scattered, but can be interpreted as an air glow excited in some other way, i.e., particle bombardment. It is also possible that interplanetary hydrogen at one a.u. has an orbital motion comparable to that of the planets. This would minimize the Doppler shift argument of Johnson.

The solar Lyman-α profile measured by Purcell and Tousey seems to indicate the existence of neutral hydrogen in the terrestrial atmosphere. The temperature derived from the width of the absorption core is less than 2100°K and the equivalent width of the core decreases by almost 50% between the altitudes of 97 km and 200 km. From the measured equivalent width of the core, Purcell, Tousey, and Mange calculated the neutral hydrogen content to be 5×10^{12} atoms per square-centimeter column in the slant path between the rocket and the sun. This would reduce to 2×10^{12} per square centimeter for a vertical column, if most of the hydrogen is located near the earth. This is significantly less than required in Johnson's geocoronal model.

It is planned to conduct measurements of the overhead brightness of the Lyman-α glow in high flying rockets. Although the measurements already made show very little change with altitude between 120 and 200 km, this height range is not great enough to really prove or disprove the geocoronal theory. Instrumentation has been prepared for a flight to 1500 km in a Javelin rocket and, if successful, the results should provide a better basis for determining the hydrogen distribution.

ULTRAVIOLET RADIATION FROM CELESTIAL SOURCES

The only published observations of the ultraviolet emissions of celestial sources consist of two rocket experiments (Kupperian *et al.* 1959; Kupperian *et al.* 1958) performed by the Naval Research Laboratory in 1955 and 1957. The second experiment revealed bright ultraviolet nebulosities against which the hot stars were not detectable. Although many different theoretical attempts have been made none provide a satisfactory explanation of the nebulosities. A new rocket experiment performed by E. T. Byram, T. A. Chubb, and H. Friedman of NRL in November, 1959, although only partially analyzed at this time, clearly distinguishes stars as well as nebulosities in the same ultraviolet band. It is possible to reconcile the various experimental results if it is assumed that the nebulosities consist of Lyman-Alpha radiation broadened by several angstroms. The ability to detect stars then depends on whether or not the short

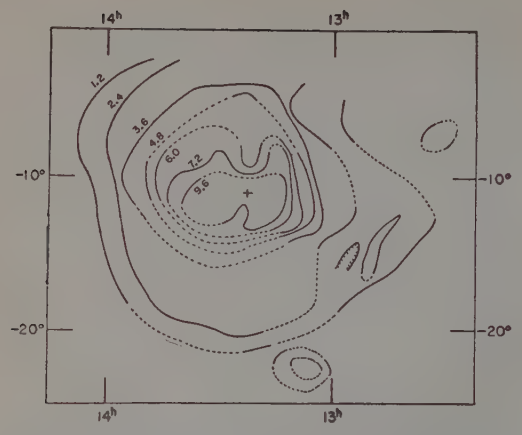

FIG. 5. Isotopes of surface brightness for nebula around α Virginis in units of 10^{-4} ergs/cm²/sec for nominal spectral range 1225–1350 A. (Kupperian *et al.* 1958).

wavelength threshold of the photo-detectors includes the reddened Lyman-Alpha emission.

The first experiment (NRL Aerobee 25) was in the nature of a crude survey with a 20-degree field of view and revealed strong emission in a band (1225–1350 A) from the Puppis Vela region and several weaker sources in the Milky Way. The follow-up experiment (NRL Aerobee 31) in 1957 refined the collimation by placing bundles of nickel tubing 0.03 in. in diameter and 0.6-in. long in front of the photon counter detectors, thereby producing a circular field of view about 3 deg in diameter at half maximum. With this improvement in geometrical definition, a rough mapping of most of the visible portion of the sky was accomplished. Whereas the earlier experiment could only indicate that the radiations originated in the directions of the hot 'stars,' Regulus, Gamma-Velorum, and Zeta Puppis, the higher resolution of the 1957 experiment showed that the sources are actually broad nebular emission regions surrounding blue stars. The stars themselves were not apparent against the very bright nebular background. In additi to the emission nebulosity identified with Orion a Puppis Vela in the galactic plane, isolated patches nebulosity were observed at high galactic latitudes, t most interesting being a roughly circular region abo 20 to 25 deg in diameter, surrounding Spica, the hotte star in the region of Virgo (Fig. 5). Observations of t same sources in a band including Lyman-α (1100–1350 were defeated by the presence of the bright Lyman glow covering the entire sky.

The most recent experiment (Aerobee NRL 30) was the nature of a preliminary test of components plann for a more elaborate experiment in 1960. For the fi time, a small telescope was employed in rocket a tronomy. It consisted of a 4-in. parabolic mirror mount off axis as shown in Fig. 6, the focused image bei reflected by a small plane mirror to a photodetect mounted in the side of the telescope tube. The field view was restricted by an aperture at the focus to 1 square degrees. The scan of the sky was accomplish by the spin and precession of the rocket. The signa telemetered to ground by the detector showed at lea seven stars which appeared to be individual poi sources and a comparable number of nebulous patch Because of the smaller field of view there was a propo tionate reduction in the number of stars scanned by t spinning telescope and the rocket motion was not favorable as in Aerobee NRL 31.

An example of what appears in the telemetered reco to be emission from a point source is shown in Fig. The source has an apparent size equal to the angul aperture of the telescope. Figure 8 shows a scan what we believe to be a region of nebulosity in Orio The telemetering system was the PPM-type in whi 312 data points are recorded per second. At the r rate of the rocket, only three data points were record per degree of scan. Point stars showed up in only o roll since the precession angle changed by several d grees per roll. A nebular region such as shown in Fig. could be identified in successive rolls, even though t direction in which the telescope pointed changed

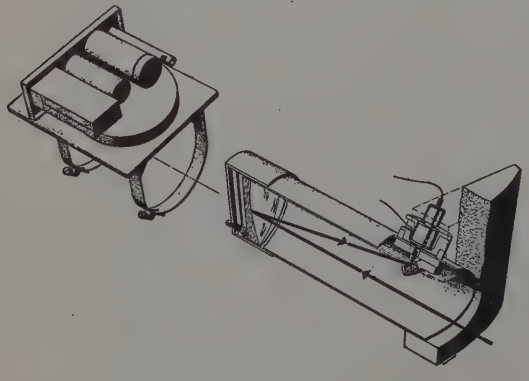

FIG. 6. Telescope instrumentation used in November 1959. Detector used with telescope was an ion chamber with a CaF_2 crystal window and filled with a NO, Co_2 mixture. The chamber was operated at a gas gain of about 5000.

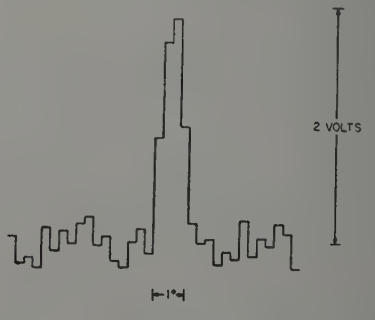

FIG. 7. Reproduction of a point source telemetering response seen by the telescope instrumentation of Fig. 3. The point da of PPM telemetering have been replaced by horizontal line se ments. The variations in background signal are limited in amp tude and are manifestations of electrometer noise.

5.5 degrees. At the present time, the identifications of the observed sources are only tentative. An accurate solution of the rocket aspect problem is being determined by correlation of visible light photometer signals with the known positions of bright stars.

The maximum intensities observed in the latest experiment were comparable to those observed in 1957, but the total flux from the nebular region in Orion is very much weaker and the area of the nebulosity appears considerably reduced. The band width of the detector, which was an ion chamber with a gas gain of about 1000, was again defined by the cutoff of calcium fluoride presumed to be 1225 A, and the nitric oxide ionization threshold at 1350 A. It would appear therefore that the latest results are in direct contradiction to the earlier observations of the brightness of the nebulosities and the absence of detectable stars in the same band width.

In attempting to reconcile the apparently conflicting data we have found evidence that offers a possible answer to the dilemma. We believe that in the Aerobee NRL 31 experiment the observed nebulosity was Lyman-α sufficiently broadened to the red so that it could pass through a cold calcium fluoride filter. The stellar emission seen in the newer data, we believe to be radiation from the stellar continuum detected through a relatively warm calcium fluoride window with a cutoff at a wavelength too long to pass the reddened portion of nebular Lyman-α. To understand the experimental problem, refer to Fig. 9, which shows that the transmission of calcium fluoride at its short wavelength limit is strongly temperature dependent (Knudson and Kupperian 1957). Between 0°C and 30°C, the cutoff is shifted about 10 A. If the entire broadening of nebular Lyman-α to the red is only a matter of a few angstroms, it is possible for a filter at 0°C to pass a large portion of the nebular emission and for a filter at 30°C to almost completely exclude it. At the time the experiments were performed, the critical importance of the temperature of the calcium fluoride was not realized and no effort was made to record it in the rocket. The flight showing nebulosity was made in March when the night time temperature at White Sands Missile Range was quite

FIG. 8. Reproduction of telemetered data during telescope scan through Orion nebulosity.

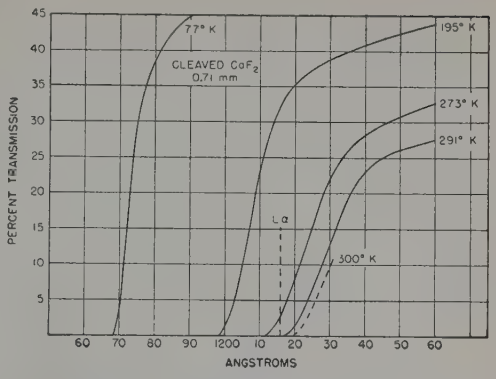

FIG. 9. Temperature dependence of CaF_2 far-ultraviolet transmission. (Knudson and Kupperian 1957).

low. The photon counter used in that experiment was mounted on the skin of the rocket exposed to ambient temperatures several hours before launching. In the telescope experiment flown in November of this year, the entire instrumentation section was heated by infrared lamps up to the time of launching. No measurement of temperature at the telescope position was made and it is only possible to say that the temperature was probably somewhere between 20 and 30°C. If we assume that the suspected condition leading to cold calcium fluoride in one flight and warm calcium fluoride in the other actually existed, then it would appear that the observed nebulosities are reddened Lyman-α.

A preliminary estimate of the nebulosity in the Orion region from Aerobee NRL 30 indicates that the total flux observed is perhaps two orders of magnitude less than the flux observed from the same source by Aerobee NRL 31. This may mean that the major part of the nebular emission falls within a few Angstroms of the central wavelength of Lyman-α.

Theoretically, it appears possible to explain the observed nebulosity if it is Lyman-α and to account for the star signals as stellar continuum emission. The true situation can only be determined by further experiments. We plan to utilize the temperature dependent characteristics of calcium fluoride transmission to provide the necessary wavelength discrimination in our next series of experiments. By controlling and measuring the temperature of a set of calcium fluoride filters used in combination with detectors having lithium fluoride windows (1100–1350 A), it should be possible to shift the cutoff from 1215.7 A to longer wavelengths with a high degree of accuracy.

Attempts to explain the observed nebulosity in terms of a continuum emission between 1225 and 1350 A have considered the ordinary optical processes of excitation by stellar radiation, the two-photon emission of continuum radiation from hydrogen excited to the $2S$ state, atomic recombination processes involving S, Si, and C, and charge-transfer processes within the nebular plasma leading to continuum radiation or emission in the

Lyman bands of molecular hydrogen. All of these processes fail by orders of magnitude to explain the observed fluxes.

The total power radiated from Spica at wavelengths shorter than the Lyman limit should be 10^{37} erg/sec if it is assumed that Spica radiates like a blackbody at a temperature of 32 000°K. The power radiated in the observed nebulosity (Aerobee NRL 31) was also about 10^{37} erg/sec. Since most of the stellar energy radiated at wavelengths less than 912 A would be converted to Lyman-α in the nebula, the supply of Lyman-α from the nebula may be sufficient to account for the flux observed in the rocket experiments. If, however, the observed radiation was Lyman-α broadened only a few angstroms, the average efficiency of the photon counters working near the threshold of transmission of calcium fluoride would have been considerably less than in the middle of the wavelength range 1250–1350 A. The computed incident flux of nebular radiation would have to be increased accordingly.

Assuming that stellar radiation converted to Lyman-α in the nebula is sufficient to supply the observed nebular flux, it is still necessary to explain the process by which so much of the Lyman-α emission is spread to the red. The Doppler width for a 10 000-degree nebular plasma is only a few hundredths of an angstrom and the cross section for scattering at $\Delta\lambda = 1$ A measured from the center of Lyman-α would be less than 10^{-24} cm^{-2}. The cross section for radiation damping at $\Delta\lambda = 1$ A is 3.3×10^{-20} cm^{-2} and falls off as $(1/\Delta\lambda)^2$. Aller (1959) has pointed out that in the direction of Orion, the total number of neutral hydrogen atoms per square-centimeter column indicated by 21-cm radiation measurements is about 10^{21} and that the Lyman-α emission line would be black for a width of 7 A about the central wavelength. Radiation damping alone could therefore account for a crowding of Lyman-α into the wings of the line in the case of Orion. In the case of Spica, the observed nebulosity had a radius of 17 parsecs. With an average density, $n_H \sim 3$ cm^{-3}, the total number per square centimeter column in the direction of the star would be 1.7×10^{20} and the core of Lyman-α would be black for about 1.5 A from the center. If n_H were as high as 10, the line would be black for about 3 A from the center.

Another possible explanation for the observed flux may be corpuscular emission from the star. It has been suggested by Fesenkov (1949) and Masevitch (1949) that early stars evolve along the main sequence by continuous ejection of protons. Su-Shu Huang (1958) and Struve (1958) have proposed high-energy particle emission from stars to explain the extra luminosity of secondary components of some double-lined spectroscopic binaries. The process has been compared to the excitation of the terrestrial atmosphere in auroral displays by solar protons. Shklovsky (1959) has attempted to explain the rocket observations of ultraviolet nebulosity by assuming that a star such as Spica is a strong emitter of protons at velocities exceeding 1000 km/sec. As a result of charge transfer processes in the ground and in excited states and, in addition, excitation and ionization due to collisions, the fast corpuscles lose energy mainly in the form of Lyman-α quanta with strong Doppler displacements. An additional source of Doppler-shifted Lyman-α is the scattering of Lyman-α in the nebula by fast particles that have been neutralized. Using the available data on cross sections for the various processes and making reasonable assumptions about the density of particles in the nebula, Shklovsky can explain the presence of Lyman-α Doppler shifted from 20 to 75 A. He further proposes that the rate of stellar energy loss due to particle emission is about five times the observed ultraviolet luminosity. This corresponds to a loss of 5×10^{-6} solar masses per year. Although Shklovsky's treatment is aimed at explaining a nebulosity consisting of Lyman-α Doppler shifted as much as 75 A, similar considerations would apply if the Doppler shift were only a few angstroms, and the stellar power dissipated in fast particle emission would be correspondingly smaller.

SATELLITES

The primary contributions of satellite experiments in 1959 were to our knowledge of the Van Allen radiation belts. Vanguard III and Explorer VII carried ion chambers intended as radiation detectors for x rays and Lyman-α. The x-ray ion chambers had windows of beryllium, 0.005-in. thick, which were transparent to electrons of energies greater than 150 kev. In planning the experiments, lower orbits were specified and it was not anticipated that the electron fluxes would cause serious interference below 400 miles. Unfortunately for the solar x-ray and Lyman-α measurements, the Van Allen belt radiation swamped the detectors most of the time even at perigee altitudes (as low as 322 miles in Vanguard III). The experiments have proven fruitful therefore only to the extent that they have mapped the soft electron borders of the Van Allen belts. To conduct solar photometry experiments in future satellites, it will be necessary to protect ion chamber detectors from soft electron fluxes by means of magnetic deflection.

CONCLUSION

In every area of rocket astronomy discussed in the foregoing substantial progress is being made and opportunities exist for important new developments. The detection of wavelengths as short as 80 A indicates that it may soon be possible to photograph the solar x-ray line spectrum to its short wavelength limit. The high resolution profile of Lyman-α is only the first step in the direction of still higher resolution solar spectroscopy. Instrumentation employing echelle techniques is scheduled to fly in 1960 with the expectation of an order of

nagnitude greater resolution. Considering the few at-empts that have been made to study the ultraviolet missions from the night sky, it is not surprising that here is considerable uncertainty about the measure-nents and their interpretation, but it is also remarkable ow much useful information has been derived from uch simple measurements. 1960 should witness some najor advances in ultraviolet astronomy.

Studies of solar flare activity have been carried as ar as seems justified with rocket techniques. Future xperiments most definitely require the use of satellites. Preliminary rocket surveys of the night sky for x-ray missions have yielded negative results. Here too, it ppears that the longer observation time provided by satellite will be essential to any future attempts at -ray astronomy.

REFERENCES

Aller, L. H., 1959, *Publs. Astron. Soc. Pacific* **71**, 324.
Brandt, J. C., and Chamberlain, J. W. 1959, *Astrophys. J.* **130**, 670.
Fesenkov, V. G., 1949, *Soviet Astron. A. J.* **26**, 67.
Huang, Su-Shu, 1958, *Publs. Astron. Soc. Pacific* **70**, 473.
Johnson, F. S., 1960, *J. Geophys. Research* **65**, 577.
Knudson, A. R., and Kupperian, Jr., J. E., 1957, *J. Opt. Soc. Am.* **47**, 440.
Kupperian, J. E., Jr., Bryam, E. T., Chubb, T. A., and Friedman, H., 1959, *Planetary and Space Sci.* **1**, 3.
Kupperian, J. E., Jr., Milligan, J. E., Bogges, III, A., 1958, *Astrophys. J.* **128**, 453.
Masevitch, A. G., 1949, *Soviet Astron. A. J.* **26**, 207.
Miller, S. C. Jr., Mercure, R., and Rense, W. A., 1956, *Astrophys. J.* **124**, 580.
Purcell, J. D., Packer, D. M., and Tousey, R., 1959, *Nature* **184**, 8.
Purcell J. D., and Tousey, R., Paper presented at 104th Meeting *AAS*, December 1959.
Rense, W. A., and Violett, T., 1959, *Astrophys. J.* **130**, 954.
Shklovsky, I. S., 1959, *Soviet Astron. A. J.* **36**, 579.
Struve, O., 1958, *Publs. Astron. Soc. Pacific*, **70**, 5.

Controlled Experiments in Celestial Mechanics

G. M. Clemence
U. S. Naval Observatory, Washington, D. C.
(Received March 24, 1960)

Experiments are described for measuring a possible dependence of the earth's gravitational field on its orbital velocity, a secular change in the constant of gravitation, the constants of the orbit of the earth, the mass of the moon, and the mechanical ellipticity of the moon.

THE fundamental concept in celestial mechanics is gravitation. Isaac Newton thought of it as a force. Einstein thought of it as a geometrical property. Observations show that Einstein's concept is more fruitful than Newton's but it is not certain that Einstein's word is the final one on the subject, especially as attempts to unify general relativity with quantum mechanics have not been successful. In any case, increases in the precision of observations have usually been followed by reformation of fundamental concepts, and there is no reason to suppose that gravitational phenomena are an exception to the rule. Speaking more particularly, all that we know of gravitation is that the inverse-square law requires a small correction, which is given within the errors of observation by the well-known relativistic correction to the motion of the apsides.

Hitherto we have been limited to the observation of such celestial bodies as we found ready made at our disposal, and equally important, we have been limited on the observational side to observing the angle between two objects (for the zenith distance is only a convenient intermediate step to such a result). We have hardly begun to explore the possibilities of accomplishments with artificial celestial bodies in gravitational fields where no natural bodies exist, nor of exploiting measurements of range and velocity, which have been brought within practical possibility by radar techniques. The useful possibilities in these two directions are enormous, being limited only by the proviso that the bodies observed must be outside the range where they are afflicted by atmospheric drag. The intimate connection between atmospheric drag and the solar radiation is now well known, and it is of such a character as to render worthless for our attention all the artificial satellites thus far created.

We do not yet know the limiting distance beyond which the atmospheric drag is unimportant. It is clear that it must be beyond any existing satellite, but whether the perigee distance must be greater than 1000 miles or greater than 10 000 is not yet certain. All that is certain is that perigee distances much smaller than 1000 miles will cease to be interesting as soon as larger ones exist. The requirement for most problems in celestial mechanics is that the resisting medium should absorb less than one part in a hundred million of the energy of the satellite in a year.

The two most important questions relating to gravitation itself that I have thought of are: (1) is the earth's active gravitational potential a function of its velocity and (2) does the constant of gravitation vary secularly with the time? Very little observational evidence o either of these questions exists.

The first question can best be investigated by ob serving the period of revolution of a satellite throug several revolutions of its primary around the sun. Wha is to be looked for is an annual variation in the perio of revolution of the satellite, in phase with the orbita velocity of the earth, or in the opposite phase. The orde of magnitude that it is desirable to measure is a par in ten thousand million, which is just within the rang of precision of the best astrometric measurements a optical wavelengths, and which also should be attain able by radar-ranging.

For the second fundamental problem (the possibl secular variation of the constant of gravitation) existin techniques of observation will suffice. The problem con cerns the scale of time; the constant of gravitatio has the dimensions of an acceleration, and the questio is whether the scale of gravitational time is such as t hold the "constant" really constant. Several theoreti cians have thought not, in other words, the scale o time given by an atomic clock differs from the one t which we are all accustomed. E. A. Milne was led t the concept of two scales of time in a very simple an fundamental way: by considering how two observer on different particles in space might synchronize thei clocks by the exchange of light signals, first on the sup position that the observers are relatively stationary an second on the supposition that they are receding uni formly from each other. It turns out that if the clock are synchronized by very simple rules, then one tim scale has a logarithmic ratio to the other, such that a some moment identified with the creation of the uni verse, one clock reads zero while the other reads minu infinity, in other words that the age of the universe i infinite in one scale and, say, ten thousand million year in the other. It may not be strictly necessary to identif the two hypothetical scales of time with gravitional tim and atomic time, but it is natural to do so, since onl these two have been found in nature; in any case a comparison of the two natural scales is of interest.

Until now, the only gravitational clock good enoug for the purpose, and that runs fast enough to be ob served with the necessary precision, is the moon. A world-wide program of lunar observations has been i progress for about two years with this comparison as

ne of its principal objects. But there are two objections the moon as a clock. In the first place the theory of ne motion is barely adequate; W. J. Eckert has been orking on it, with some interruptions, for more than years, and while that is not a long time for the conruction of a good lunar theory, we should not be idle hile we are waiting for him to finish it. In the second lace, and more importantly, the moon revolves more owly than a nearer satellite, and it appears that the ale of gravitational time can be established as well om a suitable satellite as from the moon in about onenth of the time, that is to say, in one year instead of n. Such a satellite should be far enough from the earth make the departures of the earth's field from an llipsoid negligible, and near enough to have a good ngular velocity, say between 1000 and 10 000 miles.

Since we cannot be certain that atmospheric drag is nperceptible, even at a distance of 10 000 miles, the xperiment must be planned in such a way as to make s elimination possible. The most promising method ppears to be to launch two satellites from the same ocket, in orbits as nearly identical as possible. The atellites should be identical in all respects, except that ne should be more massive than the other by, say, a actor of ten. The drag, if it is perceptible, can then be neasured differentially, and thus taken into account.

A problem slightly less fundamental than the two I ave mentioned is the test of general relativity by oberving how fast a clock will run in a satellite as comared with one on the ground, commonly referred to s the gravitational red shift. Since plans for that exeriment are already well advanced I may be excused om discussing it. I also leave aside the relativity effect n the motion of the apsides, which is so well tested y the inner planets that it is no longer of primary nterest, and in any case may eventually be obtained s a by-product of other experiments.

Having disposed of the two most fundamental probms of celestial mechanics, we come next to the system f astronomical constants, about 20 in number, inluding the solar parallax, the constant of aberration, ne mechanical ellipticity of the earth, the ratios of the nasses of the earth, moon, and sun, and the mechanical llipticity of the moon. I mention only the ones the alues of which are most in need of improvement. The xperiments that have been made in this field with atural bodies, and those that may be made with artiial ones, are far too numerous to describe here. I nention only a few that seemingly cannot be accomlished with the new techniques of observation only, ut that actually require new celestial bodies. I thereore pass over the solar parallax; Brouwer and Lilley ave recently proposed to determine it by observing ne annual change in the radial velocity of hydrogen louds, and very promising experiments are in progress at Paris, using measurements of the radial velocity of Venus at optical wavelengths. Until the results are known it would be a waste of money to create an artificial planet for this purpose.

An artificial planet would be, however, of very great interest for other purposes. It should be possible easily to measure its distance by radar-ranging with enough precision to give the constants of the orbit of the earth to at least two more significant figures, making it the most precisely known of planetary orbits, whereas until now it has been among the most difficult to determine. The most direct method is by direct observations of the sun, but such observations have errors more than ten times as great as good observations of a minor planet. In principle, the orbit of the earth can be determined by observing any planet, but in practice it is found that observations of Venus and Mars, which are geometrically the most suitable, are affected by errors nearly as great as in the case of solar observations, whereas the minor planets are either too far from the earth or near it for too short a time. Also, by observing the monthly variation in the distance of the artificial planet, the mass of the moon would be determined with considerably greater precision than by existing techniques. Probably of all methods of determining the mass of the moon, this is the best.

Among the constants on which the motion of the moon depends, the most troublesome is the mechanical ellipticity of the moon itself, which affects the motion of the perigee perceptibly. In principle it could be determined from the observed motion of the perigee by subtracting from it all other effects, but in practice the other effects are so numerous that an independent determination is much to be preferred. What is required is a sub-satellite of the moon; the rotation of the apsides of its orbit will measure the moon's mechanical ellipticity. Since a body is not likely to remain in a sub-lunar orbit for many years, in consequence of the large terrestrial and solar perturbations, it must be observed with the highest precision, and as frequently as possible. Both radar-ranging and angular optical measurements should be employed. Besides the mechanical ellipticity of the moon, we should also get the mass of the moon with good precision.

It is not necessary to have separate experiments for getting the mass of the earth, nor for the constant of aberration, because these can be derived from the other constants I have mentioned. Also, the mechanical ellipticity of the earth will eventually be determined to five figures as a by-product of other experiments.

The ideas mentioned here are not exclusively, nor even mostly, my own, but have been developed in numerous conversations with others, particularly D. Brouwer, R. H. Dicke, M. Schwarzschild, L. J. Spitzer, and B. Strömgren.

Solar Experiments*

LEO GOLDBERG
The Observatory, University of Michigan, Ann Arbor, Michigan
(Received March 24, 1960)

Owing to the well-known negative temperature gradient in the solar atmosphere, the solar chromosphere and corona emit strongly in the far-ultraviolet and x-ray regions of the spectrum, as has already been revealed by observations from rockets. The highly energetic events connected with solar flares also result in strong emissions at very short wavelengths. Hence, solar experiments from satellites will have high priority in the astronomy space program.

Design work has been begun on the development of solar instrumentation to be flown in a series of vehicles with progressively larger payloads. The first experiment is being designed for a vehicle that can carry instruments up to a weight of about 100 lb and that will be stabilized with a pointing accuracy of a few minutes of arc. Two scanning spectrometers will be employed, one covering the spectral region from 1600 to 500 A and the other from 600 to 75 A. The resolving power would be about 1 A, and the spectrometers would have a combined weight of about 45 lb. It is also hoped that some type of x-ray imaging device will b flown in the first vehicle.

Plans are also being developed for the installation of a sma solar observatory with a variety of instruments totaling abo 600 or 700 lb, exclusive of stabilization gear, power supply an storage, etc. The instruments would include a high-dispersio spectrometer operating in the region from 3000 to 75 A, one o more spectroheliometers to register images of the sun in Lyman- and other monochromatic radiations, an x-ray telescope an spectrometer, and equipment for the observation of low-frequenc radio emission from the sun.

Finally, it is pointed out that a number of important problem in solar physics can be solved better by observations from balloon rather than from satellites. These include studies of the hydro dynamic and magnetic properties of the solar photosphere, an observation of the infrared solar spectrum.

THE sun is an object of very high priority for observation from satellites and space probes. Its great luminosity makes it relatively easy to observe both because the problems of pointing accuracy and guiding are simpler and because the requirements for detector sensitivity are much less stringent than for any other object in the sky. Although many important solar problems can be solved by observations from balloons, satellites and rockets are absolutely indispensable for the observation of far ultraviolet and x radiation, which in turn are the key to a correct understanding both of the chromosphere and corona and of the processes that occur within them. Thus far, it has not been possible to deduce an unambiguous model of the solar chromosphere from ground-based observations alone. Numerous attempts have been made to construct models that satisfy either optical data or radio data and in some cases both. Some of the models are homogeneous, while others attempt to distinguish between the so-called hot and cool regions. One point is very clear, and that is that no two models are in agreement. Probably the only statements on which all students of the chromosphere would agree is (1) that the chromosphere is made up of regions of high and low temperature, which in the low chromosphere are perhaps as different as 30 000° and 5000°, and (2) that the temperature gradient in the chromosphere is negative and that within its confines the temperature of the solar atmosphere somehow increases from its value of about 4500°K at the top of the photosphere to the order of magnitude of one million degrees in the corona.

The importance of extra-terrestrial observation as a means for investigating the structure of the sun's outer layers has already been strikingly demonstrated b means of the photographs of the ultraviolet solar spec trum obtained from rockets by Tousey and his collabo rators at the Naval Research Laboratory and by Rens and his associates at the University of Colorado. Th latter has achieved an ultraviolet limit of 80 A. Th photographs reveal that the continuous spectrum radi ated by the solar photosphere diminishes very rapidl in intensity with decreasing ultraviolet wavelength, a would be expected from a blackbody with a temperatur of about 5000°K, and that below λ1700 the spectrum co sists almost entirely of emission lines radiated by th solar chromosphere. Apart from the fact that the oc currence of lines of highly-ionized elements is evidenc of very high temperature, the spectrum displays a re markable range in level of ionization, as evidenced b the occurrence of multiple stages of ionization. For ex ample, carbon is represented by its neutral atom an also by the singly- and doubly-ionized forms, all of the giving lines of about equal intensity. The same is tru of nitrogen, and in the spectral region between 150 and 1050 A oxygen is represented by every stage ionization through *O* VI. The occurrence of multiple io ization stages is obviously a consequence of the stee negative temperature gradient in the chromosphere an the lower corona. In these regions of the solar atmo sphere, the range of physical conditions is so great tha every stage of ionization can find a level at which co ditions for its occurrence are favorable. It goes witho saying that the detailed analysis of the ultraviolet spe trum, particularly when center-to-limb intensity mea urements are available, will go a long way towar clearing up existing ambiguities in the chromospher temperature gradient.

Since the temperature of the chromosphere increas

* Supported in part by Contract NASw-55 with the National Aeronautics and Space Administration.

ith height, and since the removal of electrons from toms shifts the spectrum towards shorter wavelengths, follows that at shorter and shorter wavelengths in he ultraviolet solar spectrum, the radiation comes from igher and higher levels in the chromosphere. Eventu-lly, a point in the spectrum is reached at which the mission begins to be predominantly of coronal origin. ust as there is a transition between the spectrum of the hotosphere and that of the chromosphere at around 1700, so there is a similar transition, although not so harply defined, between the chromospheric and coronal pectra in the vicinity between about 100 and 500 A. rom the observation of forbidden lines in the visible egions of the spectrum, it is known that metallic atoms uch as iron, calcium, and nickel are very highly ionized n the corona. The resonance lines corresponding to hese forbidden lines occur chiefly in the spectral re-ion below 50 A. Friedman and his co-workers at NRL ave recorded the emission of x rays from the sun down o wavelengths as short as nearly $\frac{1}{10}$th of an angstrom. ery little is known about either the place or mechanism f origin of solar x rays, except that they are frequently reatly enhanced at the times of solar flares and hence t least a strong component must be connected with olar activity. Up to the present, no type of imaging evice for x rays has been used on the sun. I consider hat the development of such a device, an x-ray tele-cope, and its establishment in a satellite with suitable etectors, is one of the most challenging of the many olar satellite experiments that can be designed. Such device would add a whole new dimension to solar re-earch, whereas most of the other experiments that can e proposed represent extensions of existing techniques.

The importance of carrying out solar investigations rom satellites needs no further elaboration and there-ore I shall now turn to some of the specific forms that hese investigations will take. It should be emphasized hat in spite of the great novelty associated with ob-erving the sun from a satellite, the methods we em-loy will be largely extensions of classical procedures, t least in the beginning. That is to say, we shall be mploying rather conventional methods to obtain spec-ra, intensities, line profiles, spectroheliograms, etc.

The first solar experiments with satellites are neces-arily rather primitive, and, in fact, are not at all as ophisticated as those already carried out with rockets. his is because the rockets have been equipped with wo-axis sun followers, whereas the Sputniks, Van-uards, and Explorers have had no attitude control hatsoever. The only solar experiments that are feasible rom such vehicles are those in which solar radiation in ather broad wavelength bands is monitored on a fairly ontinuous basis. In experiments already attempted, yman-α and x rays have generally been the radiations tudied. As simple as this type of experiment is, it would ive extremely valuable information on the ultraviolet mission of solar flares if it could be carried out system-tically for a period of from several months to a year.

Experiments comparable in sophistication to those which have already been flown in rockets are planned in connection with the so-called orbiting solar observatory program of NASA. This program will make use of a 300-lb satellite launched by a Thor-Delta rocket. The vehicle will be stabilized with a pointing accuracy of a few minutes of arc, and can carry astronomical instruments up to a total weight of between 50 and 100 lb. As Dr. Roman has reported, three groups are preparing experiments for this vehicle, the Goddard Space Flight Center of the NASA, the University of Colorado, and the University of Michigan.

At the University of Michigan, Dr. Liller and I have been studying the feasibility of equipping the Thor-Delta satellite with two scanning spectrometers, one covering the spectral region from 1600 to 500 A and the other from 600 to 75 A. The resolving power would be about 1 A and the spectrometers would have a combined weight of about 45 lb. The detailed designs of the scanning spectrometers have not yet been carried out, but our preliminary studies have revealed a number of problem areas. Most of the problems arise on account of the lifetime of the experiment, which we hope would be about one year. The jamming of detectors by the Van Allen radiation is also a matter of great concern, and in fact, all solar ultraviolet experiments from satellites to date have failed because of this reason.

The desired long lifetime of the experiment and the Van Allen radiation prevent the adaptation of already successful rocket experiments for satellite use. For example, H. E. Hinteregger of the Air Force Cambridge Research Center has developed a scanning monochromator which at first glance would appear to be ideally suited to satellite application. The monochromator is used at grazing incidence and the solar ultraviolet intensities are telemetered directly to ground from the rocket. Automatic wavelength scanning is achieved by the motion of a continuous steel tape with four equidistant slits along the Rowland circle of the concave grating. The receiver is a photomultiplier manufactured by the Bendix Research Laboratories. The sensitive element is a large tungsten cathode, which has a high photoelectric yield throughout the far ultraviolet, but has practically no sensitivity to longer wavelengths. It is therefore free of the usual kind of scattered light. The major source of noise comes from charged particles in the environment. This instrument has been flown successfully in an Aerobee rocket, and accurate measurements carried out of the intensity of the solar He^{+} line at 304 A.

Unfortunately, it is not at all obvious that the scanning method would work in a vacuum, since there are severe lubrication problems connected with the motion of the steel tape and of the driving motor. Reports on the performance of motors operated for long periods of time in vacuum tanks are conflicting. There are some reports that motor bearings wear out completely within a few days, whereas others insist that

motors have been operated in vacuum for many months without signs of obvious bearing damage. The loads under which the bearings operate are probably of crucial importance here, and it may well be that bearing lubrication will not be a problem in the gravity-free environment of a satellite.

We have also been studying the problem of achieving good optical focusing in the face of the extremes of temperature to which the spectrometers will be subjected during any one revolution of the satellite. We are considering two solutions, which represent more or less limiting cases. The entire system can be built of materials like invar and quartz with the idea of keeping focal distances fixed under all conditions. The other solution is to use metallic mirrors throughout, thus making it possible for the apparatus to come quickly to temperature equilibrium.

One of the most difficult problems of all will be that of establishing and maintaining an accurate intensity calibration at all wavelengths in the spectrum. This problem assumes great importance because the degree of variability of the ultraviolet solar spectrum will be one of the most interesting questions to be explored during the lifetime of the scanning spectrometer. There is no doubt whatever, from spectroheliograms made in visible light, that emission from the chromosphere is variable, and the variations in intensity should be greatly amplified in the ultraviolet. I am referring, of course, to variations other than those associated with catastrophic disturbances such as solar flares. However, if the response of the spectrometer to radiation varies with time, investigation of the variability of the ultraviolet solar radiation would be difficult or impossible. Unfortunately, very little information is available on the extent to which the components will age in the satellite environment nor as to the effects of the aging. For example, what effect will prolonged exposure to ultraviolet radiation have on the reflecting properties of thin, evaporated films? It may be that we shall have to expect the calibration of the system to change with time and merely to recalibrate it at regular intervals by sending up duplicate equipments in rockets.

In addition to the two scanning spectrometers, we hope also to include an experimental version of an x-ray telescope, provided one can be developed in time and that its weight is not prohibitive. The pointing accuracy of the Thor-Delta vehicle will be between one and five minutes of arc. The engineering design of the vehicle has not yet been completed and therefore it is not known whether the solar telescope will be pointable to any given part of the solar disk. We feel that this capability is extremely important, even if it means sacrificing some part of the instrument payload, since without it quantitative measurements would be almost impossible.

Aside from its own merits, the Thor-Delta program presents a valuable opportunity to try out many of the instrumental techniques that will be employed with the large stabilized platform in the NASA orbiting astronomical observatories program. If the engineering predictions are fulfilled, the Agena B rocket will launch into orbit about 600 or 700 lb of instruments, exclusive of stabilization gear, power supply and storage, etc. This payload is so large that one can begin to think in terms of not merely one or two experiments, but of a variety of instruments comprising a fairly complete solar observatory. We have made some preliminary studies of the instrumentation that might go into such a large vehicle and have reached some tentative conclusions although no final decisions have yet been made.

First, the heart of the solar observatory would be a high-dispersion spectrometer operating in the region from 3000 to 75 A. Actually, this range would be covered by three separate spectrometers with coverages between 3000 and 1500 A, 1600 and 500 A, and 600 and 75 A. The resolving power of the spectrometer would of course be different in the different spectral regions, but in general it would be between 50 000 and 100 000. It is anticipated that the solar telescope will have a pointing accuracy of one second of arc or better and that the direction of pointing can be controlled by an observer on the ground, who would be guiding directly on a televised image of the sun. Our hope is to develop a system whereby the observer can select any desired region of the spectrum for scanning, and any portion of the sun's disk or corona for analysis.

The combined weight of the three spectrometers would be about 250 lb. A second major installation in the satellite would be one or more spectroheliometers designed to register images of the sun in Lyman-α and other monochromatic radiations on the photosensitive surface of a vidicon tube. The most interesting lines to use for this purpose, other than Lyman-α, are, of course, the neutral and ionized resonance lines of helium at 584 A and at 304 A, respectively. If the angular resolution of the spectroheliograms were as small as two seconds of arc, we could probably expect important advances in our knowledge of the structure of the chromosphere, particularly as regards its nonhomogeneity. If, as the evidence suggests, there are large temperature fluctuations in the chromosphere, the spectroheliograms made in different lines should exhibit great differences in their intensity patterns, especially when they are also compared with spectroheliograms made simultaneously from the ground in low-excitation lines. It is very probable that such angular resolution could be obtained by the use of photographic film, processed automatically in the satellite, and scanned electronically. It is not known, however, whether the photographic film could be adequately shielded against the Van Allen radiation. Therefore, it will probably be necessary to employ direct scanning techniques, with their currently lower resolving power, but with some hope that the resolving power will be considerably improved within the next two years. We are also assigning very high priority to the instal-

ion in the orbiting observatory of an x-ray telescope d x-ray spectrometer, provided that such equipment n be developed during the next two years.

The orbiting observatory should also include equip- ent for the observation of radio emission from the n and at present the most important experiment of is kind that can be visualized would be the extension the dynamic radio spectra of solar bursts to very w frequencies on the order of one megacycle. Designs r such equipment are being studied by Professor Had- ck at the University of Michigan, and it is our hope at the radio and optical equipment can be flown to- ther in the same vehicle. A number of other projects e under consideration for inclusion in the orbiting ob- rvatory, such as the measurement of the ultraviolet id infrared spectral energy distribution and the solar nstant, the use of a coronagraph to observe the spec- um of the corona in the wavelength range between 00 A and 3000 A, and others.

Although satellites and other space vehicles can con- ibute uniquely to the solution of the problems of the romosphere and corona, it is well to point out that any other problems in solar physics can be solved bet- r by other means. For example, satellites should prob- ly not be used to investigate problems connected pri- arily with the photosphere of the sun. Most of the diation from this region of the solar atmosphere falls the visible, and it is difficult at present to see how servations in the inaccessible ultraviolet can con- ibute much to the solution of unsolved problems of ie photosphere. The most important of these unsolved roblems are (1) the physical structure of both the ighest and the lowest layers of the photosphere, and 2) the hydrodynamic and magnetic properties of the hotospheric layers. The greatest obstacle in the way f a solution to these problems is not the ultraviolet bsorptivity of the earth's atmosphere, but its turbu- nce, which until recently has prevented observations t the extreme limb of the sun and has masked the true haracter of motions in the solar photosphere. It seems ery likely that for these and other problems of the hotosphere the techniques of balloon astronomy will e much more useful than those of satellites. It is to be oped that in the near future the technique of direct hotography pioneered by Schwarzschild will be sup- lemented by high-resolution spectrograms that will re- veal the local Doppler shifts associated with the small- scale granulation.

It is also doubtful whether satellite techniques can be very useful in the improvement of solar abundances. It is generally agreed that uncertainties in the Boltz- mann factor represent a major source of error in the determination of abundances from absorption lines with lower excitation potentials of several volts. It is assumed that much more accurate results could be obtained by use of the resonance lines which, for some of the most abundant elements in the solar atmosphere, occur in the far ultraviolet. It is true that the presence of several elements, which have not yet been revealed in the vis- ible spectrum, may be established by ultraviolet obser- vations, but it is extremely doubtful that the abun- dances of very many elements will be substantially re- fined by the measurement of ultraviolet lines. The reason is that there are very few lines in the Fraunhofer spectrum below $\lambda 3000$ which are not badly blended and since the continuous background is not well defined, it is usually impossible to measure equivalent widths. The existence of a continuous background in the visible spectrum is extremely important for abundance deter- minations, because the continuous spectrum is formed by hydrogen, and hence the measurement of a line in- tensity relative to the continuous background yields the abundance of the atom relative to that of hydrogen. In the far ultraviolet, the so-called continuous background is formed by the overlapping wings of neighboring ab- sorption lines and hence intensity measurements are difficult to interpret in terms of chemical abundances.

Finally, I would not assign very high priority at this time to observation of the infrared solar spectrum. The earth's atmosphere cuts out large regions of the infrared solar spectrum, including virtually all radiation from 24 μ to 1 mm wavelength. The loss of these spectral regions is a serious one for solar physics, but not all of the blame can be placed on the earth's atmosphere be- cause there already exist a number of relatively trans- parent windows, notably the one at 10 μ, through which observations are limited not by the atmosphere but by the insensitivity of existing detectors. Furthermore, an enormous increase in infrared transparency can be secured from balloons, which fly above the water vapor, and hence I would definitely assign second priority to elab- orate satellite-borne infrared experiments.

Stellar Astronomy from a Space Vehicle

ARTHUR D. CODE
Washburn Observatory, University of Wisconsin, Madison, Wisconsin
(Received March 24, 1960)

Space research in stellar astronomy will initially concentrate on observations in the vacuum ultraviolet and x-ray region. Future observations will be substantially aided by a series of general sky surveys in the ultraviolet both by rocket flights and satellite observations. This paper describes some of the stellar observations that might prove most profitable in the light of current astrophysical knowledge. The topics discussed fall under the following headings: A. Ultraviolet and infrared survey studies, B. Stellar energy distribution, C. Stellar spectroscopy, D. Interstellar medium, E. Extragalactic studies, and F. High resolution studies.

I. INTRODUCTION

THE opportunity to carry out astrophysical investigations throughout the entire electromagnetic spectrum, through the use of space vehicles, cannot fail to have a tremendous impact on the future course of stellar astronomy. The possibility of realizing the full resolving power of astronomical telescopes and conducting observations freed of the bright sky background contributed by scattered light and permanent aurorae is also of great significance.

The relation between various energy units and some of the available detectors is illustrated in Fig. 1, throughout the electromagnetic spectrum. The terrestrial atmospheric absorption is indicated schematically. The bulk of astronomical observations have necessarily been restricted to the radio window extending from a few meters to about 1 cm, and to the optical window from about 1 μ to $\frac{1}{3}$ μ. It may be noted that the optical window falls in the energy range corresponding to the energy maximum of the G and F type stars. This region also represents energies in the range between 1 and 10 ev. This means that many of the atomic transitions fall within this optical window. By no means do all the atomic transitions occur in this region and in particular the resonance lines of many important elements such as hydrogen and helium are to be found in the far ultraviolet. Conversely, the majority of molecular transitions occur in the far infrared, along with the radiation from cool bodies such as the late-type stars, planets, and interstellar dust. Most of the radiation from the early-type A, B, and O stars is emitted in the far ultraviolet and the details of their energy distribution will provide crucial data on their atmospheric structure.

The preceding discussion has revolved about the limitations imposed upon terrestrial astronomy by the atmospheric absorption. The effects produced by the differential refraction of the earth's atmosphere, however, are familiar to all astronomers. With a telescope of 36-in. aperture the diffraction would place approximately 99% of the stellar radiation within a radius of 0.2 second of arc; rarely is the seeing good enough to concentrate this radiation within a disk of 1 second of arc radius. The seeing scintillation blurs photographic details, produces light loss at the entrance slit of a spec trograph, reduces photometric accuracy, and sets a limi on the precision of astrometric measurements.

The limiting magnitude observable with a given in strument is set by the brightness of the sky backgroun and its variation with time. The fluctuation in the nigh sky background due both to effects of seeing and vari ations in the permanent aurorae increases the back ground noise by a factor of the order of three over th pure statistical noise to be expected. The sky brightnes itself is probably greater by a factor of two than th average brightness above the terrestrial atmosphere.

It may be anticipated that many of the fundamenta problems that will confront astronomers in the nea future will not be found on any current list of researc programs. Nevertheless it is wise to review some of th current problems that can be pursued from space tele scopes. The following outline reviews some of thes problems in the field of stellar astronomy.

II. SURVEY OF PROMISING AREAS OF RESEARCH

A. Ultraviolet and Infrared Survey Studies

Current astrophysics asks many questions, the res lution of which, it is believed, may be found by obse vations in the previously inaccessible regions of th electromagnetic spectrum. The opening up of this fron tier presents a challenge to look not only for the ex pected but also for the totally new and unexpected To date, astronomers have just barely had a glimpse o the sky in the far ultraviolet. We do not know just wha is to be found. Thus the first steps should necessarily b of the nature of a survey. What are the brightest object in far ultraviolet or infrared? We may guess, but it i only a guess. What is the total radiation density? Ho opaque is the interstellar medium? What are the mos prominent spectral features? Can we see the corona emission from other stars? What do the galaxies loo like? In short, just what does the astronomical univers look like from above the terrestrial atmosphere?

It would therefore be exceedingly important to pro duce an analogue of the BD and HD catalogues for th ultraviolet. Not only will these surveys guide future in

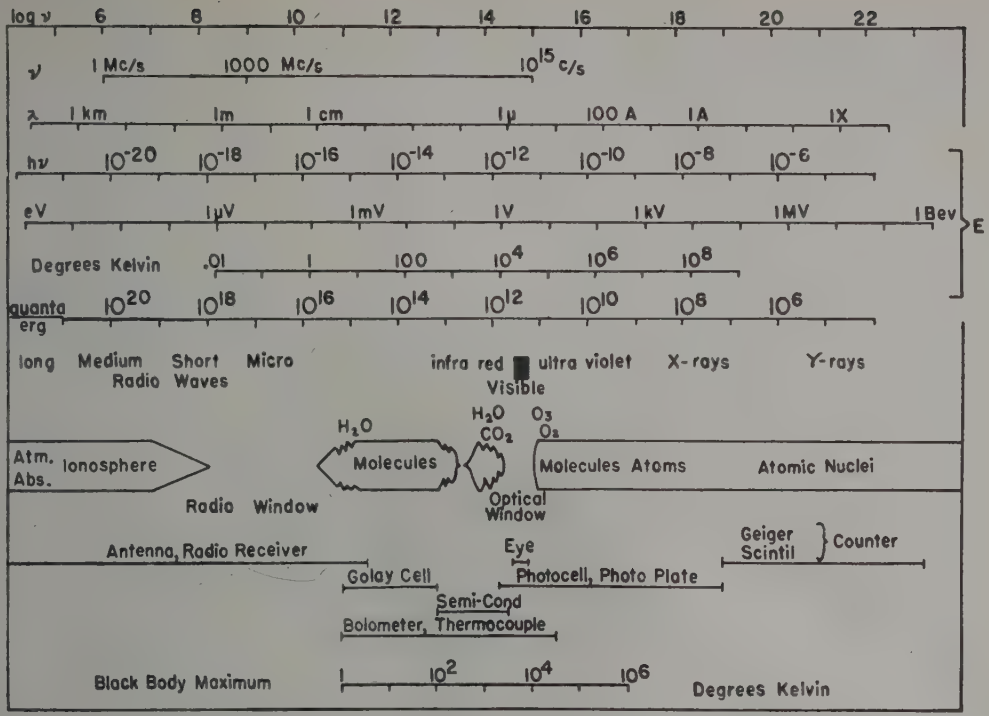

FIG. 1. Relation of energy units and detectors as a function of frequency.

restigations but they will themselves provide answers o some of our immediate problems.

Liller has discussed the precepts for initial sky surveys Astronomical Experiments proposed for earth sate-ites, University of Michigan) which provide an ade-quate basis for any such program. He selects the follow-ng wavelength regions with the priority ratings to be given them in parentheses, λ2700 (A), λ2100 (B), λ1600 (B), λ1300 (A), λ1216 (B), λ800 (B), λ10–100, and λ1–10 (A), and discusses the reasons for choosing these spectral regions.

To this list should be added the x-ray and γ-ray spectrum below 1 A. Infrared surveys should also prove valuable. The energy maximum of the coolest stars falls n the infrared; presumably so does the contribution rom the galactic bulge. In any event, to reiterate, we lo not know what we shall find. This is the basic philos-ophy of a survey program of this nature.

B. Stellar Energy Distribution

Theoretical studies of the structure of stellar atmos-pheres have met with considerable success despite the oversimplification of the problem. Simple model atmos-pheres in radiative equilibrium in which the effects of convective transport and line blanketing have been allowed for, in only a cursory manner adequately account for the energy distribution in the continuum of F and early G stars. The source of continuous opacity in the spectral region from about 3000 A longward appears to be accounted for and, while other sources of opacity may play a role in the ultraviolet, the energy in this region is small for these stars and thus has little effect on the atmospheric structure. Model atmosphere calculations provide the basis for theoretical discussions of the line spectrum and it is from these studies that our knowledge of the chemical abundances of the elements comes.

Figure 2 shows the energy distributions calculated by the method of model atmospheres for a main sequence G0 star and a B0 star. The energy scale is normalized to the energy incident per square centimeter per second per unit frequency interval above the terrestrial atmosphere for stars of visual magnitude V=0. Observations for the star β Comae, G0 V, are indicated by the filled circles and have been corrected from measurements for the effect of line blanketing. The star υ Orionis, B0 V, is compared with the model by the open circles which incorporate a small correction for interstellar reddening. While both sets of observations appear to be reasonably represented by the model atmosphere the bulk of the energy for the hotter star lies to the shortward of the atmospheric cutoff at 3000 A, thus measurements of the energy distribution in the photographic and visual give very small leverage on the problem. Figure 3 shows an extension of these model atmosphere energy curves to the ultraviolet. The usual atmospheric window is indicated by the vertical dashed lines. The energy in the visual corresponds to approx-

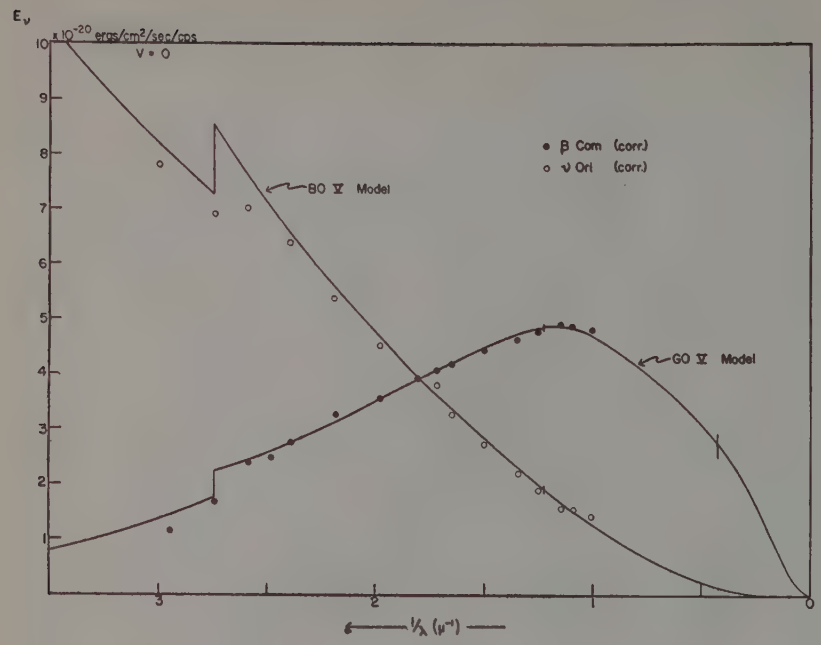

FIG. 2. Spectral energy distribution for main sequence B0 and G0 stars.

imately 1000 photons per A per sec per sq cm and while the energy per unit frequency interval at the maximum of the B star near 1000 A is 10 times as great, the number of photons is only twice as large. This implies that the number of recorded events for an ultraviolet detector is not significantly increased.

Do the model atmospheres that have been constructed for the hotter OB and A stars adequately represent the atmospheric structure of these objects? The early Naval Research Laboratory results suggest that in the B stars the energy at λ1300 A may be much less than that predicted on the basis of model calculations. Moreover, early A stars behave in the photographic region in a manner that is difficult to explain quantitatively. It may be that an important contribution to the opacity in the ultraviolet has been neglected, or that the effect of line blanketing modifies the temperature distribution and the emergent flux considerably. Any process that redistributes only a very small fraction of the flux near the energy maximum into the observable longwavelength tail of the energy curve will profoundly influence the distribution in this region. The Lyman lines of neutral hydrogen are very strong in the cooler stars, but as pointed out above, the flux is small in the ultraviolet and the influence of the Lyman lines negligible. In the hottest stars the Lyman lines are probably nearly as weak as the Balmer lines and their influence on the continuous spectrum may not be too important. However, the convergence of the Lyman lines and the Lyman continuum would be expected to produce a significant effect. In the late B and early A stars the hydrogen lines are strong and, moreover, occur in the region of the energy maximum. Here the effect of the line blanketing may seriously distort the continuum in the photographic and visual region. A program to extend the energy distribution of stars into the ultraviolet will elucidate these problems. It is expected that the Lyman absorption 912 A will be so great that virtually no radiation will appear shortward of the series limit. What radiation remains should be effectively chopped off at the series limit for *He* I at 504 A. Line blanketing and convergence of the Lyman lines will, however, cut the intensity down well before the limit at 912 A. Some of this energy will reappear shortward of the limit as well as in the longer wavelength region. Thus observations shortward of 900 A would be desirable. Such observa-

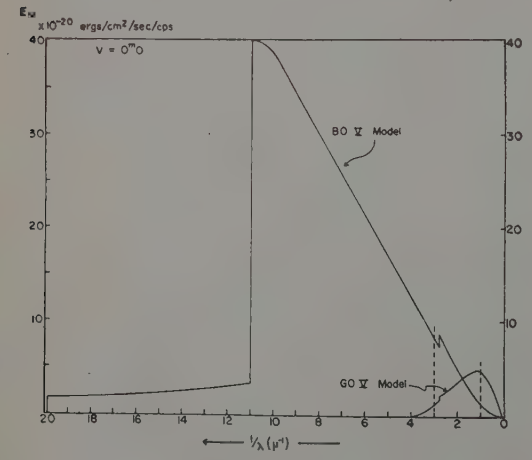

FIG. 3. Far-ultraviolet spectral energy distribution for main sequence B0 and G0 stars.

ons are complicated by the fact, to be discussed below, hat the opacity of interstellar hydrogen and helium for ven the closest star may be so great that essentially o stellar radiation will penetrate between approxiately 10 A and 912 A. Even so, or because of this rediction, measurements should be attempted in this ectral region.

C. Stellar Spectroscopy

The resonance lines of hydrogen, helium, carbon, oxyen, nitrogen, and other elements occur in the ultraiolet while important molecular lines appear in the frared. Abundance determinations from ground-state ransitions are the most reliable and many other imortant conclusions may be drawn from the study of hese lines. We can predict the intensities to be expected or these lines and lists for identification have been made y a number of investigators.

The low dispersion spectral surveys will provide inormation on what spectral features actually are presnt; however, analysis of these lines will require detailed tudies star by star. A number of the lines will be suffiiently strong so that only moderate resolution will be equired, in particular the Lyman lines. Aller has conidered the expected profiles for Lyman-α and for the *Mg* II doublet at λ2796 and 2803. The core of the Lyman line is probably saturated for all spectral types, owever, near the line center the intensities would be listorted by the interstellar absorption in any case. The ving grows by electron collision rather than natural damping or ion collision as one goes progressively to otter stars with greater electron pressures. Aller estinates the width at half intensity for a G star to be less han 30 A to increase to a maximum of the order of 140 A in early A stars and then to weaken due to ionization on going to hotter stars.

Line profiles of the wings of the Lyman lines and of he resonance lines of such elements as *NI* λ1200,*OI* λ1302, *CI* λ1657, *SiI* λ2515, and others will provide vital data on chemical composition, particularly in ts relation to stellar evolution and thermonuclear processes.

In the x-ray region many lines from highly ionized atoms should appear. In fact, such observations will be primarily of coronal emission. Studies of emission line stars and peculiar stars in which normal processes are often displayed in a highly exaggerated form will make fascinating studies. The opportunity to check on line emissions believed to be responsible for the fluorescent excitation of levels from which some emission lines in the photographic region originate is possible. In addition new fluorescence lines may be found. Mechanisms responsible for depopulating states may be examined. In short, both classical stellar spectroscopy and fascinating new discoveries await the exploration of the ultraviolet spectrum.

In the cool stars we may expect to find molecular absorptions of H_2O, CO_2, and others in the infrared. New detectors, such as solid state devices, are offering promise that we shall be able to observe stellar radiation into the far infrared and not have to depend solely upon heat-sensitive detectors and their accompanying high noise levels.

D. Interstellar Medium

1. Interstellar Radiation Field Density: Estimates of the degree of ionization of interstellar gas, temperature of dust grains, and other properties of the interstellar medium are based upon calculations of the expected radiation density. This depends upon extrapolating stellar radiation and interstellar absorption into the ultraviolet. Clearly a more direct way would be to measure the radiation field. This would require a relatively simple photometer. The space vehicle would not, of course, be imbedded in the interstellar medium but rather the interplanetary medium and effects originating within the solar system would have to be allowed for. This would appear possible, however. The cosmic ray flux would also be a logical part of such an investigation. Particular attention should be paid to the integrated radiation in the neighborhood of various atomic series limits.

2. Law of Interstellar Reddening: An extension of the interstellar reddening curve would be a natural byproduct of the investigation of measurements of stellar energy distribution. Figure 4 shows the form of the average interstellar reddening curve adapted from the work of Whitford. The heavy line represents the observed curve while the extrapolation is based upon Van de Hulst's discussion of possible scattering particles. Figure 5 shows an extension of this curve further into the ultraviolet. The position of Lα is indicated by the vertical line and at 912 A the interstellar medium becomes opaque due to hydrogen absorption.

The observing technique would be basically the same as that applied in the photographic and visual. An ex-

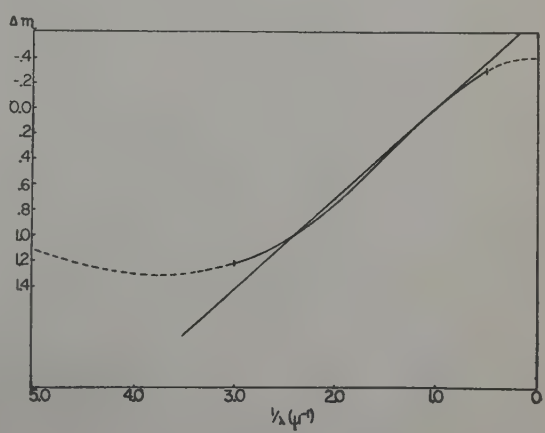

FIG. 4. Interstellar reddening curve.

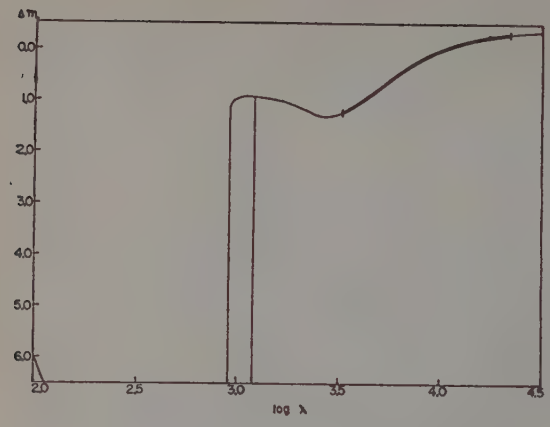

FIG. 5. Ultraviolet extension of interstellar reddening curve.

tension to the infrared would yield an accurate determination of the ratio of total absorption to selective absorption. In the near ultraviolet the present reddening curve is seen to begin to level off. The variation of reddening in the ultraviolet will yield information on the size distribution and refractive index of the interstellar particles which in turn bears on the formation of grains. With the wide base line in wavelength there are other methods that may be employed to establish this curve. The observation of emission lines in Be stars or nebulae would serve this purpose.

Two examples of familiar transitions occurring in diffuse nebulae that could be used to define points on the reddening curve are shown in Figs. 6(a) and 6(b). The relative intensities of the lines in the [O III] transition shown in Fig. 6(a) are known from quantum mechanical data and therefore permit a determination of the interstellar reddening over the base line extending from 5007 A to 2322 A. In the case of the permitted *O* III lines excited by the 303.8 A line of ionized helium the number of quanta appearing in the ultraviolet line 2836 A is equal to that in the observed 3759 A transition. There are a number of other cases similar to these, but of course the studies of emission lines from diffuse nebulae and planetary nebulae in the ultraviolet are of interest in their own right, a feature that we now turn to.

3. Emission Nebulae: Studies of line ratios in emission nebulae will make it possible to determine more accurate and extensive abundances and to make estimates of the electron density and temperature that are less subject to the uncertainties introduced by differences in chemical composition. Certain line ratios may make it possible to determine the relative contributions of radiative and collisional excitation. Figure 7 represents a synthetic spectrum in the ultraviolet for a planetary nebula such as NGC 7027. All line strengths were computed by T. Daub assuming a temperature of 10 000°K and using cross sections computed or interpolated by Seaton for most lines and estimates due to Osterbrock for others.

The examination of the γ-ray and cosmic-ray flu from nebulae that are nonthermal radio sources provide a check on such mechanisms as synchrotron radiatio and cosmic ray particle acceleration.

Investigations of the continuous spectra can assist i specifying the nature of the excitation. A suspected ex citing star may be verified. Emission in the Lyman line will be difficult or impossible to observe due to the gen eral interstellar hydrogen absorption. However, som radiation will appear in two-photon emission rather tha in Lα and the continuum measures along with th Balmer lines would be a measure of the Lyman lin strength. The emission nebulae are essentially enhance regions of the interstellar medium to which we shal now direct attention.

4. Interstellar Lines: The resonance lines of *H*, *He*, *O*, *N*, *C*, and other elements of interstellar origin wil appear in absorption superimposed on stellar spectra Studies analogous to the interstellar calcium and sodium investigations can be carried out as well as abundanc determinations of interstellar material. This is particu larly important because in the normal observable regio

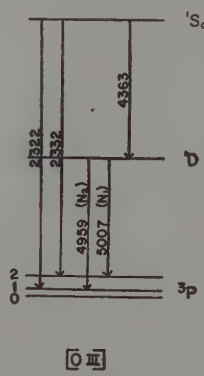

FIG. 6. Nebular transitions useful in defining points in the reddening curve.

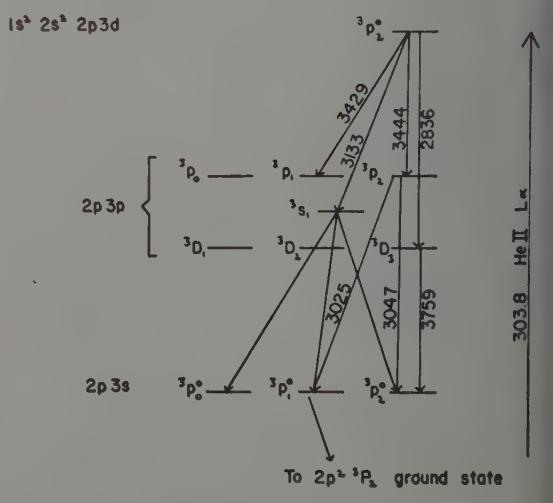

O III FLUORESCENCE

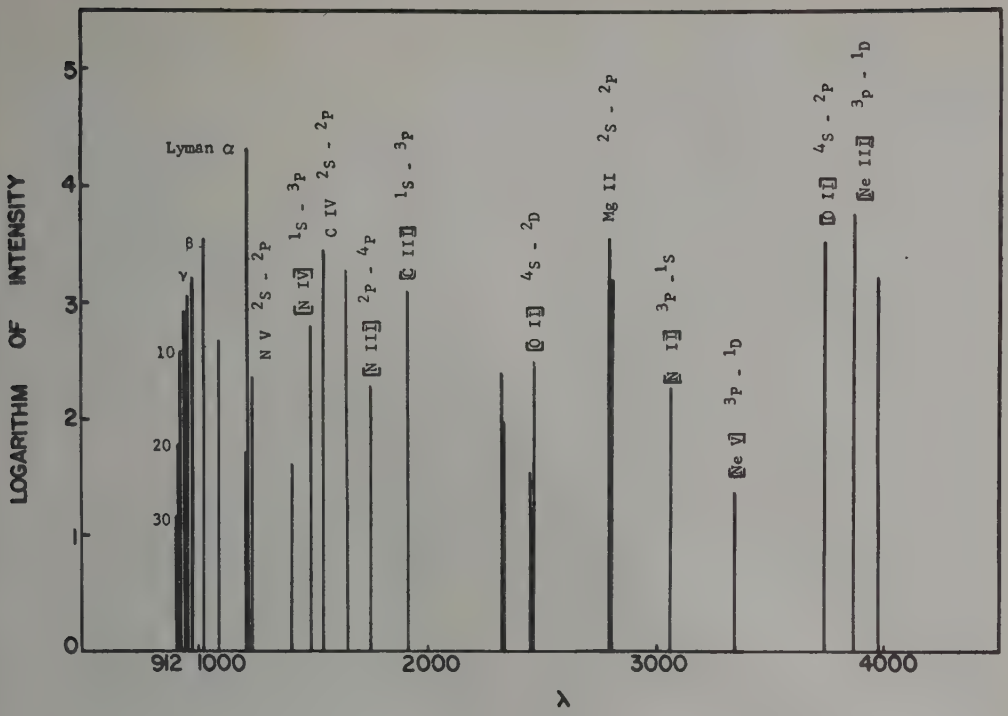

FIG. 7. Expected ultraviolet spectrum of a planetary nebula.

ne limitation on the number of different elements that nay be observed is a serious limitation on our under-tanding of the interstellar medium. The possibility of bserving neutral hydrogen is particularly exciting. If nis can be done, observations similar to the 21-cm radio bservations could be carried out with high spacial reso-ution. Distance criteria would be provided on the basis f the stars in which the absorption lines are observed. 'he difficulties alluded to the above, of making any neasurements in the Lyman lines, require more exten-ive discussion. Aller and Osterbrock and Spitzer have onsidered the problem.

Hydrogen is about 10^5 to 10^6 times as abundant as odium; furthermore, *HI* is less ionized than *NaI* under ll conditions. Thus *HI* is more abundant than *NaI* by factor of 10^6 or 10^7 in interstellar space. Interstellar *laI* lines are observed in suitable stars at 500 to 1000 arsecs, hence interstellar *HI* lines would be observed n distances of 5×10^{-5} to 10^{-3} parsecs, that is, they vould be strong in all stars. The optical depth in the enter of the line would average 10^9 per kiloparsec. Aller stimates that in the direction of the Orion Nebula the ne is totally black over a width of about 7 A.

The situation is, however, not too discouraging. Measurements of the equivalent widths and of the vings of the Lyman interstellar lines will yield velocity eterminations and abundance measurements although he accuracy would be low. For nearby stars the small cale structure of the interstellar hydrogen may be studied. The extent to which the material is concentrated in clouds should be assessable. We may in fact be able to see out in some directions.

Molecular hydrogen has several lines arising from the absolute ground state in the region between 1200 to 1300 A. There is a fair chance that one or more of these members of the Lyman bands would be resolved from stellar lines at some spectral type. This would give a measure of H_2 in interstellar space which is not only descriptive data pertinent to galactic structure but bears on the catalytic properties of interstellar grains. Thus if we find it too difficult to observe neutral hydrogen, we may at least hope to see H_2. Molecular hydrogen also gives rise to transitions in the infrared. In an *HI* region the rotational lines from the ground state of H_2 occurring at 28.1 μ, 16.9 μ, and 12.0 μ should be present. Other lines appearing in the infrared are the ionic lines of *C* II and *Si* II, atomic lines of *O* I and rotational lines of *CH*, *NH*, and *OH*.

For an optically thin *H* II region it is problematical whether or not observations at Lyman-α would be significantly better than $H\alpha$ measurements even if the intervening absorption permitted Lyman-α emission measurements. For an optically thick *H* II region (Strömgren sphere) it is possible that emission wings might be observed beyond the absorption line in some cases. It may well be, however, that the absorption of Lyman-α by H_2 or *O* I and re-emission by resonance fluorescence will occur near the boundary of an *H* II

region. Thus the boundaries of *H* II regions may be delineated by emission rings in H_2 or *O* I.

In any event, the study of the interstellar medium in the far ultraviolet will be fascinating and productive.

E. Extragalactic Studies

The high hydrogen opacity of a galaxy means that Lyman-α photons will be scattered throughout the system. The energy may be lost by dust absorption or by two-photon emission. The latter will however be ineffective over galactic dimensions at a density of the order of one atom per cubic centimeter. Thus in directions in which the interstellar grains are ineffective Lα radiation should probably escape from a galaxy.

The Lyman-α emission from extragalactic nebulae with red shifts greater than 1000 km/sec will be free of any galactic Lyman absorption. Radio observations suggest that the neutral hydrogen may form an extensive halo about a galaxy. The extent of galactic systems not only in Lyman emission but also in integrated light at different wavelengths will be valuable. The lower sky brightness from a space vehicle should make it possible to observe extragalactic systems to greater distances. The shift of the energy maximum may be followed out into the infrared. Red shift measurements in L-α may be extended to distances beyond the present range of terrestrial telescopes. The γ-ray emission from bright radio sources such as Cygnus A would provide information on the nonthermal mechanism responsible for the radio emission. Detection of γ-ray radiation in the region of the neutral π-meson decay range would lend credence to the speculation that a collision of a galaxy, predominately matter, with an antimatter galaxy, is responsible for some bright sources. The intergalactic medium is subject to more stringent examination. Within a cluster of galaxies the Lyman emission between galaxies may be observed. A general prevailing medium of neutral hydrogen throughout extragalactic space would produce a shallow absorption line extending from 1213 A on to the velocity shift of the galaxy observed.

Baum has proposed a simple cosmological experiment involving the measurement of integrated sky radiation at several wavelengths. The problem is related to the classic paradox of Olber's, which asks essentially why is not the sky a surface of uniform brightness equal to the average surface brightness of stellar photospheres. The measurement of this extragalactic light narrows down the acceptable cosmological models considerably. This extragalactic component must, of course, be separated from the galactic light, zodiacal light and light scattered by the solar nebulae.

F. High Resolution Studies

Many more experiments could be added to this revie among which are those utilizing the full resolution th a telescope is capable of with an accompanying increa in astrometric accuracy and several magnitudes gain minimum detectable signal. Accurate parallaxes ar proper motions are highly desirable for subdwarfs, whi dwarfs, SS Cygni stars, and other selected objects. Clo astrometric binaries which are now simply spectroscop binaries become observable. These programs provi basic data on stellar luminosities, masses and radii. fact, some stars may be resolved as disks. Accura measurements of the Einstein shift may be made.

Some time in the future it may become practic to make observations from space vehicles several astr nomical units from the earth, thus extending the ba line for parallax measures.

These programs are, however, of a somewhat mo difficult technological class and are probably to be i cluded in a later generation experiment.

G. Stellar Experiments

Within the auspices of N.A.S.A., the working grou on orbiting astronomical observatories is planning undertake some of the studies outlined above throug the participation of other groups. Briefly the stellar e periments planned are as follows:

The survey programs to be undertaken by the Smit sonian Institution are described in a separate prese tation. The Goddard Space Lab is carrying out a numb of rocket flights designed to provide basic reconnai sance data on energy distributions and spectral detail It is their intention to extend this program to a satelli telescope. The Princeton group is planning a telescop capable of making high resolution spectroscopic studi of bright stars designed for investigations of both stell and interstellar line profiles. The University of Wisco sin plans to carry out spectrophotometric investigatio of low resolution in order to study stellar energy distr bution and emission line intensities of diffuse and plan tary nebulas.

Longer range plans are being undertaken by A.U.R.A directed toward a versatile precision telescope of larg aperture placed in a twenty-four hour orbit. Such a instrument would be capable of carrying out some of th more difficult and advanced research problems and mos likely following up the new and unexpected encountere in our first probes in extraterrestrial astronomy.

Proposed Stellar and Interstellar Survey

FRED L. WHIPPLE AND ROBERT J. DAVIS
Smithsonian Astrophysical Observatory, Cambridge, Massachusetts

Previous planning for the design, construction and operation of n astronomical telescope in a satellite orbit was presented by iembers of the Smithsonian Astrophysical and Harvard College bservatories (R. J. Davis, R. E. McCrosky, F. L. Whipple, and . A. Whitney *Astron. J.* **64**, 50 1959). Further elaboration of iese plans is presented, including possible systems for measuring right-line radiation of the interstellar medium and obtaining slit-ss spectra of stars, as well as a broad survey of the entire sky in iree colors between 1000 and 3000 A. With the support of the Tational Aeronautics and Space Administration the design pro-ram is under way at the Smithsonian Astrophysical Observatory. lans are also developing for an Aerobee rocket firing in late 1960 r early 1961 in which a TV image-tube system covered by a nulticolor mosaic filter can produce a preliminary shallow survey of both nebulosity and bright stars over a strip of the sky some 150° by 4°. Since the rocket will be neither precisely stabilized nor controlled at high altitudes, the exact position of the observational strip can only be approximated. Direct image photographs of stars and nebulosity, however, will be available in spectral regions from below Lyman-alpha to approximately 2000 A.

The Westinghouse Electric Corporation has undertaken the development of special materials for TV image tubes sensitive to spectral regions in the far uv. The precise spectral regions in which the rocket and satellite experiments will be conducted depend upon these developments.

The astrophysical significance is discussed of the proposed experiments in the regions of Lyman-alpha and above for stars and interstellar material.

FOR several years now, the Smithsonian Astrophysical Observatory has been defining the objectives nd planning the instrumentation and experiments for satellite telescope. The primary purpose of this project ill be to survey above the earth's atmosphere the ltraviolet radiation from the stars. Both the project nd the orbiting telescope are named "Celescope."

During this time, we have been in consultation with Dr. William A. Baum, of the Mount Wilson and Palo-nar observatories, who is interested in doing sky pho-ometry over a few square degrees at a time in the arious regions of the far ultraviolet. Since the two pro-rams seem to coordinate rather nicely, our relationship as been mutually beneficial.

The planning program for our first Celescope has been nderway for about two years, initially under the sole uspices of the Smithsonian Astrophysical Observatory, ut since last summer with the support of the National eronautics and Space Administration as a phase of heir Orbiting Astronomical Observatories project. We ave made considerable progress toward determining he task and drafting the basic design of this first atellite telescope. Our plans include provisions for a eries of preliminary rocket flights to test the various omponents and units of the Celescope. Already we are ompleting the design and beginning the manufacture f a payload assembly for the first of these test flights, n Aerobee-Hi rocket to be launched within the next ear.

As we have said before (Davis, McCrosky, Whipple, nd Whitney 1959; Davis, Whipple, and Whitney 1959; Davis 1959), the broad purpose of our Celescope survey s to map the ultraviolet radiation field of the entire elestial sphere by means of three-color television tech-niques. At the same time, we plan to obtain spectro-copic information about the brighter stars and other liscrete sources of ultraviolet radiation; a slitless spec-roscope will feed into a fourth television camera. To achieve these aims, we must first solve several fundamental problems in theoretical and applied physics; specifically, these involve a search for optical filters, reflecting surfaces, spectral dispersing materials or components, and photosensitive surfaces suitable for a survey in the far ultraviolet. We propose to outline here the progress that we have already made toward solving these problems, and to pose some of the questions that remain to be answered.

The models that have been computed for stellar atmospheres indicate that most of the radiation from the hotter stars occurs at wavelengths too short to penetrate to the lower atmosphere of the earth. In order to test these theoretical computations, we must therefore make our observations at heights above 100 km where the ultraviolet and x-ray radiations can be detected. And since balloons cannot attain such altitudes, we must operate our instruments from rockets or artificial satellites. We favor the latter for a complete survey of the celestial sphere, particularly as satellites permit us easily to transcend the 100-km limit. We are now contemplating orbits at approximately 800 km.

Although we expect that most of the observational data furnished by the Celescope will be from the hotter stars, these data will constitute a mere fraction of the astrophysically interesting results. Ultraviolet spectra of the sun, taken during the past several years from rockets (Aboud, Behring, and Rense 1959; Violett and Rense 1959), indicate that exciting discoveries await us in observing the cooler stars. We should also be able to learn a good deal about the extensive bright nebulosities detected by the Naval Research Laboratories rocket observations of radiation between 1230 and 1350 A (Kupperian, Boggess, and Milligan 1958); although the nebulosities obliterated any stellar images that might otherwise have been observable during those rocket flights, the increased angular resolution that our television techniques will give us should enable us to find any stars present. These and many other problems in

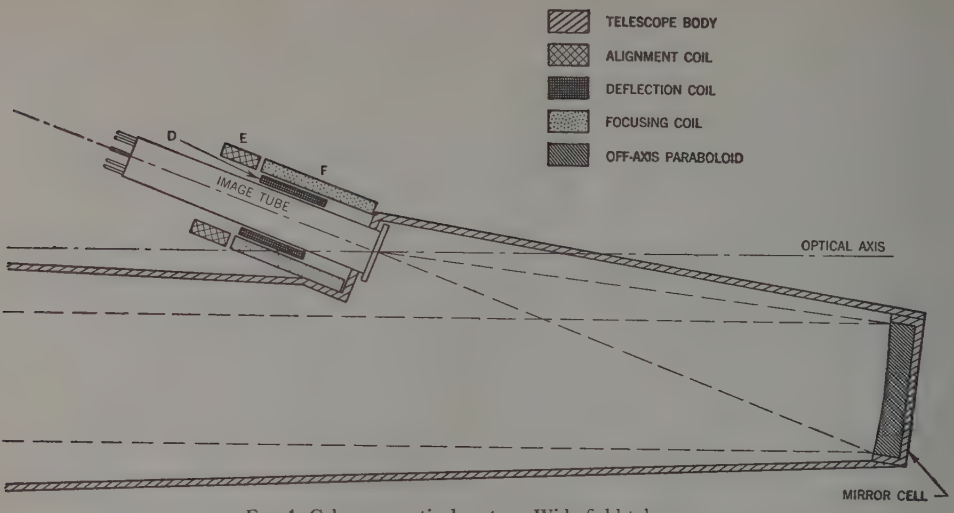

FIG. 1. Celescope optical system. Wide field telescope.

astrophysics can be successfully investigated by means of a satellite telescope.

In order for it to be most useful, our survey should be done quickly and reliably, and should map out the work for the later, more sophisticated experiments. We have emphasized optical and mechanical simplicity in the design of the Celescope. Therefore, when our allocation of useful payload was increased, we diversified our experiment rather than enlarged it.

Our prime optical system is an off-axis reflecting telescope of 8-in. aperture and 24-in. focal length. This extremely simple optical system is illustrated schematically in Fig. 1. There are no secondary optical elements except those in the slitless spectroscope.

Among the important reasons for our choosing a single-element reflecting system were that the few substances that are transparent in the ultraviolet show extremely low transmissivity, and that reflecting substances show low reflectivity to wavelengths shorter than 1400 A. Large achromatic lenses for the extrem ultraviolet would not be practical, both because suit able materials of correct optical properties are lackin and because those few types of crystals that are trans parent to ultraviolet radiations are commercially avail able only in small sizes. And a nonachromatic lens o reasonable thickness would at best transmit less tha 1% of the incident radiation below 1050 A.

On the other hand, coatings for mirrors are availabl that will reflect at normal incidence as much as 30% o the radiation down to 1000 A (Hass and Tousey 1959) Figure 2 shows the reflectivities, at normal incidence of various metals. We plan at present to use the alum inum film overcoated with magnesium flouride, as de veloped by Hass and Tousey (1959); this appears t be the best reflecting surface available for our spectra region.

We have not yet completed the design of the dis persing element of our slitless spectroscope. We are no

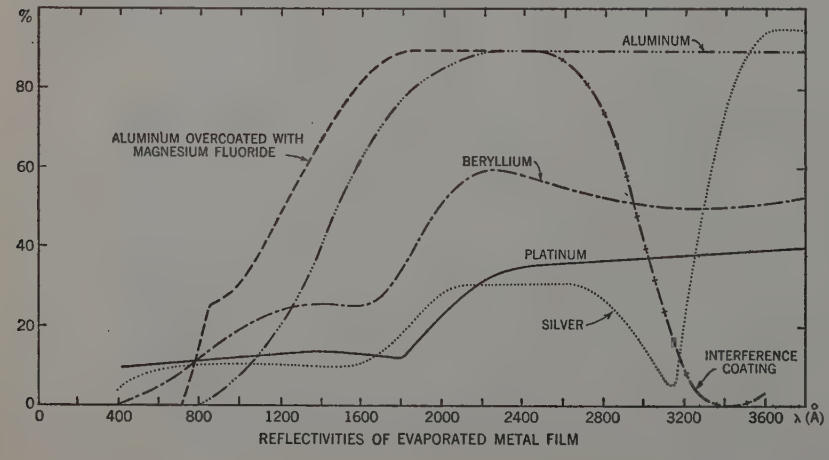

FIG. 2. Reflectivites of various surface materials in the ultraviolet.

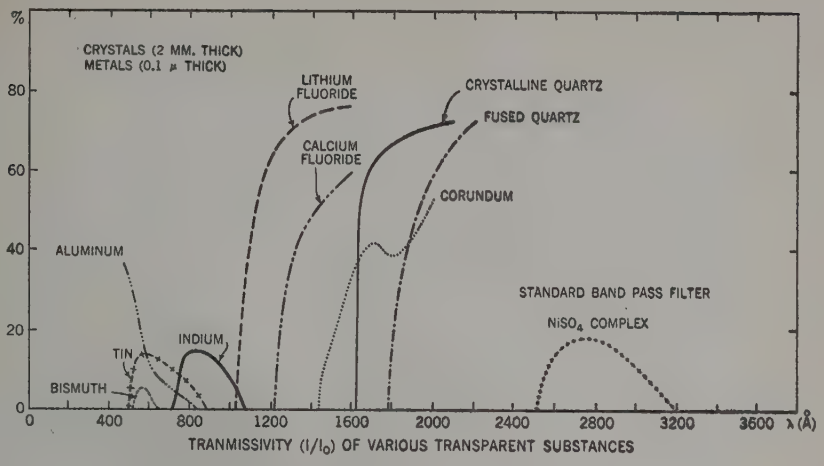

FIG. 3. Transmissivities of various substances in the ultraviolet.

weighing the merits of objective prisms made of lithium fluoride, and of various designs of objective gratings. Our goal is to obtain slitless spectra of A0 and hotter stars of the 5th magnitude or fainter, with 20 A resolution between 1100 A and 3000 A.

To keep our optical and mechanical systems simple, we have had to make our over-all electronic system complex. Our proposed satellite experiment requires four separate television systems, each with its own optics, to convert the image information into electrical signals for transmission to the ground stations: three of these constitute the multicolor ultraviolet television system, while the fourth is for the slitless spectroscope.

Our requirements for sensitivity and spectral response are unusually severe: each system must be capable of detecting A0 stars of 10th magnitude or fainter, and should have a response outside its spectral range of not more than 10^{-4} times its peak response. As a goal to aim for, we have selected three spectral ranges: from 1230 to 1600 A, from 1600 to 2200 A, and from 2200 to 3000 A.

Another, and very severe, requirement for the television system is that it be as simple and reliable as possible. This apparently rules out the use of image orthicon and similar tubes, and leaves us with a choice of image-dissector, vidicon, or intensifier-vidicon types. In July, 1959, the Westinghouse Electric Corporation undertook at its research laboratories in Pittsburgh a program aimed at solving the many problems involved in the development of a television tube sensitive to ultraviolet, or the "Uvicon" as they have termed it. The Laboratories are developing various photosensitive surfaces for both vidicon and ebicon tubes, the latter being a type of intensifier vidicon developed by Westinghouse. They expect to produce soon the first prototype uvicons.

One of the reasons necessitating our support of this uvicon program is the evident lack of commercial and military applications of these tubes. In recent years, much of the well-financed research in television systems has been devoted to the development of image tubes sensitive to infrared and visible light, but none to tubes meeting our needs.

In order to attain the necessary bandpass characteristics for the spectral sensitivities of our system, we must couple the short-wavelength cutoff properties of transparent crystals (see Fig. 3) with the long-wavelength cutoff properties of photosensitive substances (see Fig. 4). The development program at Westinghouse has been mainly concerned with problems involving the latter properties, since those of the former have been more thoroughly studied and show fewer complexities. Figure 3 illustrates the short-wavelength cutoff properties of several transparent crystalline substances. Both vidicons and ebicons require a transparent window to support their photosensitive surfaces. It is evident from Fig. 4 that we cannot, by means of the techniques to be used in the first Celescope, study radiations below 1050 A, since that is the cutoff wavelength of lithium fluoride and no other known crystalline substance is transparent below 1200 A. Disregarding for the moment the possibility of using very thin metallic filters, we see that purely optical bandpass filters below the nickel-sulphate transmission near 2900 A are at present unavailable to us.

Most standard television image tubes have a resolving power of 500 lines. With our system, such a tube would give a practical resolving power of approximately 30 seconds of arc. In the Celescope the usual television scan rate of 30 frames per second of time will be reduced to one frame per second in order to reduce the video bandwidth to approximately 200 kc, with a corresponding reduction in the transmitted bandwidth.

Since the exposure time need not be equal to the scan time, exposures of 10 sec are contemplated. The power requirements are perhaps no more severe than an average of 5 to 10 w. Approximately 5% of the total time that the satellite is in orbit will be available for obser-

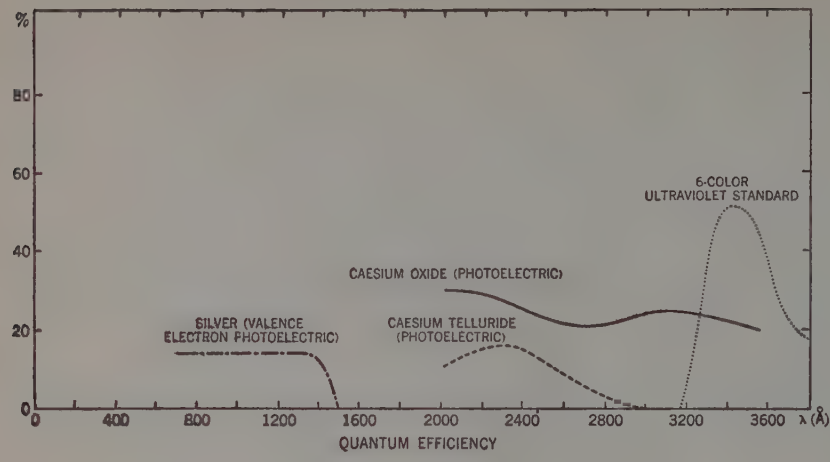

FIG. 4. Quantum efficiency of the photoelectric effect for various materials.

vation if a network of two coordinated receiving stations is located in North America, one station on the east coast and the other on the west coast. Power supplies consisting of solar batteries or isotope power-packs appear to be quite practical for operation over a period of a year or more.

Data analysis will be made directly from magnetic tapes rather than from photographs. The analysis will be accomplished by means of high-speed digital computers. We foresee an accuracy of 0.2 magnitude over a range of 10 magnitudes.

Details of technical operation, stabilization, orientation, command systems, and related problems need not be discussed here, as they are already adequately treated elsewhere (see references and other papers in this issue of the Astronomical Journal). It should perhaps be pointed out, however, that the restrictions on orientation and pointing stability are relatively broad: approximately 10 seconds of arc per second of time for angular motion, and 10 minutes of arc in pointing precision.

As must already be evident, our astrophysical program of research in the ultraviolet requires a parallel program of laboratory research. We must study intensively the properties of optical and photosensitive materials under different physical conditions in order to uncover such important phenomena as the recently discovered fact that the short-wavelength cutoff of calcium fluoride is dependent on temperature (Knudson and Kupperian 1957). More work must be done on the methods of determining the spectral distribution of photons from the energy spectrum of emitted photoelectrons (Hinteregger 1956). More work must be done on deterioration of the transmissivity of crystals (Gordon 1959); specifically, we must ascertain the effects of aging upon our various optical components, both in the humid atmosphere prior to launching, and in the radiation-riddled near-vacuum of space. As yet, there is no definite knowledge concerning the properties of space, of stars, and of interstellar matter in the region near Lyman-alpha; the few rocket observations bearing on this prob lem are incomplete and conflicting.

We hope that our preliminary rocket flights will pro vide us with basic quantitative information that wil indicate the kind of results we can expect from th Celescope. We are now working on the construction o the payload for the Aerobee-Hi rocket which will carry to an altitude of approximately 270 km a conventionally timed image-tube system with suitable filters for the fa ultraviolet. Our total payload, which will probably b between 100 and 150 lb, will include an optical systen of 3-in. aperture and 12-in. focal length, giving a 4-de square field; the overall design of this system is th same as that illustrated in Fig. 1. The orientation o this rocket optical system will be only partially con trolled; we expect to maintain the axial rotation speed at less than 15 degrees of arc per second of time, s that the system will cover a small circle of the sky and provide observations of a strip 4 degrees of arc in width and 200 degrees of arc in length during a total obser vation time of approximately 300 sec. The approximate position of this strip is indicated in Fig. 5, which also shows by means of five-pointed stars those objects which Davis (1956) calculated would be brighter than 2nd magnitude at 1250 A.

As indicated in Fig. 6, the five filters of this rocket payload will be used in a compact system placed directly in front of the image-tube surface. During the course of the observations, any cosmic source of radiations in the spectral ranges of these filters and at off-axis distance of not more than 1 degree of arc will be registered through most of the filters. We expect that approximately 50 stars should be bright enough to register in this experiment, and that even so simple a system as filters should give us considerable information about the ultraviolet distribution of light in the hot stars.

As Aller (1959) has pointed out, interstellar space is probably essentially opaque to radiations from 916 A down to approximately 30 A. Thus, there are both astrophysical and engineering reasons for limiting our

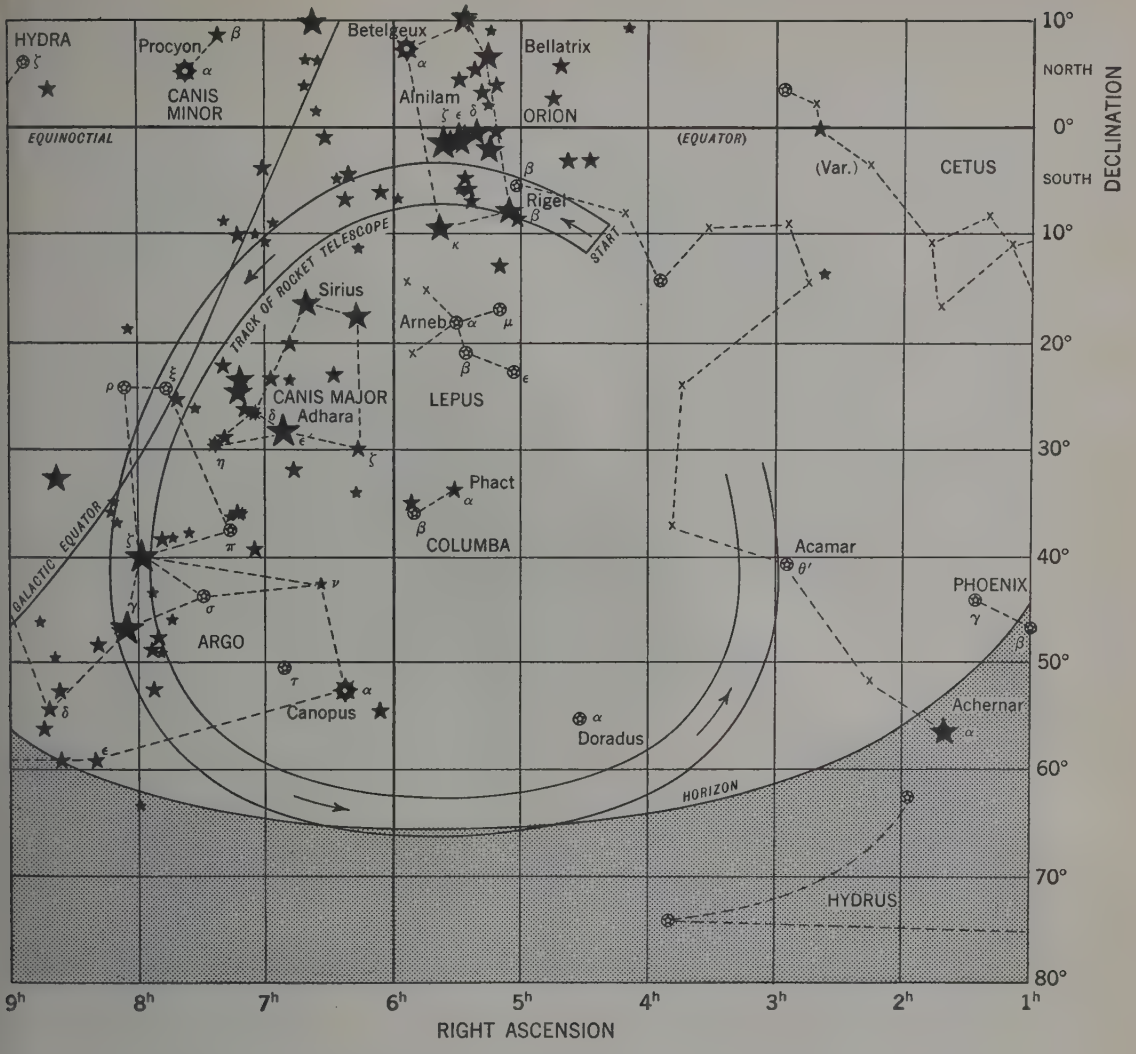

FIG. 5. Planned track of optical axis of Aerobee-Hi prototype Celescope.

first Celescope to the spectral regions above 1000 A. However, we do plan to investigate the transition region between 1000 A and 100 A in some of our preliminary rocket experiments; possibly we will use techniques employing the thin metallic filters the transmissivities of which are indicated in Fig. 3 (see also Walker, Rustgi, and Weissler 1959). We are doing so because to plan a nonsolar satellite experiment for this region would be inadvisable until after we have the results of such preliminary rocket observations; these observations will take the form of long-exposure slit spectra of low resolution on such nearby stars as Sirius, Regulus, Spica, and Gamma Velorum.

Looking ahead to the study of soft x rays from space, we can now very profitably make a serious approach to the problems involved in focusing and detecting radiation below 100 A. Dr. Albert V. Baez of the Celescope staff has commenced such a study. Earlier (Kirkpatrick and Baez 1948), he studied various means of forming optical images of x-ray sources; one method employed two spherical mirrors at grazing incidence. Giacconi and Rossi (1960) have also considered the use of grazing incidence to collect soft x rays into a spectroscope slit or into a nonimaging detector. However, since these devices rely on geometrical optics at grazing incidence, they suffer severely from the lack of appreciable angular field when optical speed is significant.

Dr. Baez is now investigating the x-ray focusing properties of zone plate systems that are either unsupported or are supported on lithium-fluoride surfaces. In order to confirm the diffraction focusing properties expected for such a device, he has already tested a self-supporting

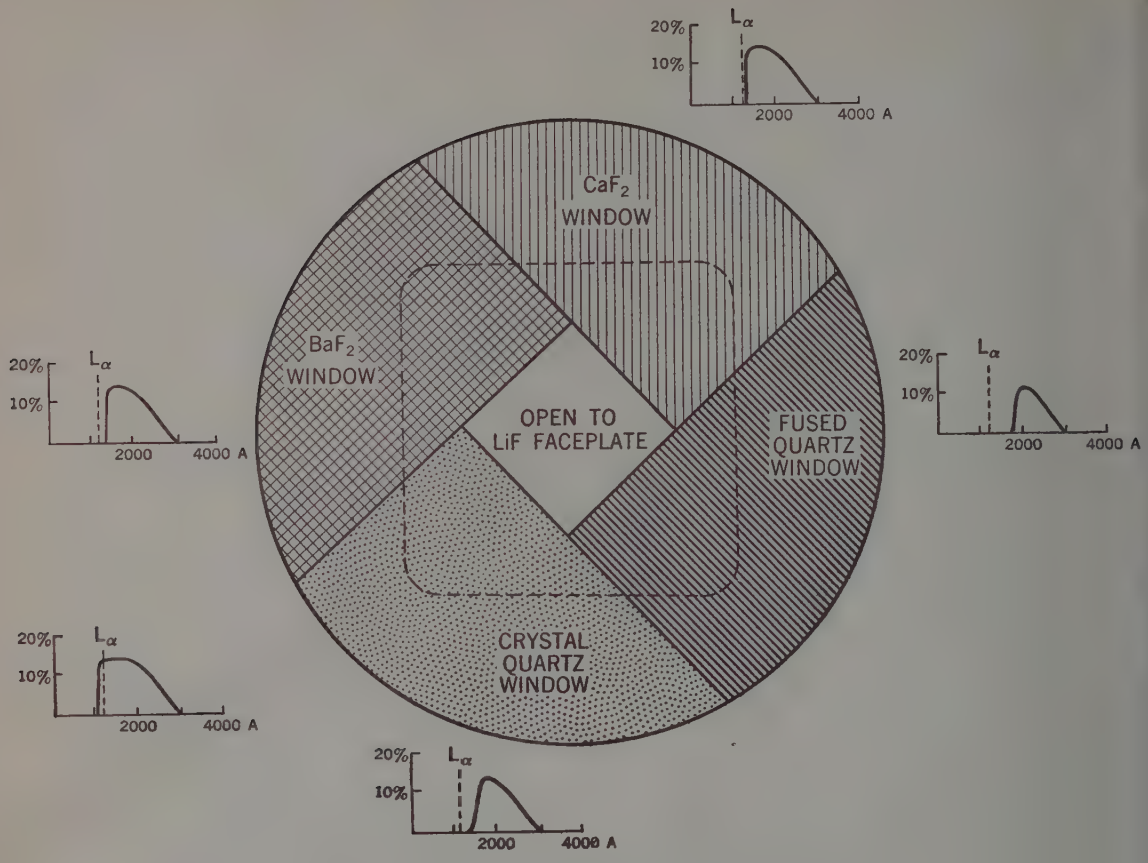

FIG. 6. Optical filter for Aerobee-Hi prototype Celescope.

plate approximately 3 mm in diameter, having 38 zones. The zone plate provides an appreciable field of image formation, and tremendous advantage over truncated or Fresnel-type paraboloidal surface (Giacconi and Rossi 1960). Dr. Baez is now planning similar zone plates of both shorter and longer focal length, as well as some with more zones. Our program includes an attempt to detect and measure x rays from stellar and interstellar sources, possibility as an Aerobee experiment subsequent to our first ultraviolet-imaging experiments with rockets.

REFERENCES

Aboud, A., Behring, W. E., and Rense, W. A. 1959, *Astrophys. J.* **130**, 381.

Aller, L. H. 1959, *Publs. Astron. Soc. Pacific* **71**, 324.

Davis, R. J. 1956, *Scientific Uses of Earth Satellites*, edited by Van Allen (University of Michigan Press, Ann Arbor, Michigan), p. 157.

——. 1959, Paper presented at the Semi-Annual Meeting, Am. Rocket Soc., San Diego, Calif., 8–11 June; A. R. S. Preprint.

Davis, R. J., McCrosky, R. E., Whipple, F. L., and Whitney, C. A. 1959, *Astron. J.* **64**, 50.

Davis, R. J., Whipple, F. L., and Whitney, C. A. 1959, *Astronautical Sci. Rev.* **1**, 9.

Giacconi, R., and Rossi, B. 1960, *J. Geophys. Research* **65**, 773.

Gordon, R. B. 1959, *Am. Sci.* **47**, 361.

Hass, G., and Tousey, R. 1959, *J. Op. Soc. Am.* **49**, 593.

Hinteregger, H. E. 1956, *Scientific Uses of Earth Satellites*, edited by Van Allen (University of Michigan Press, Ann Arbor, Michigan), p. 166.

Kirkpatrick, P., and Baez, A. V. 1948, *J. Opt. Soc. Am.* **38**, 766.

Knudson, A. R., and Kupperian, J. E., Jr. 1957, *J. Opt. Soc. Am.* **47**, 440.

Kupperian, J. E., Jr., Boggess, A., III, and Milligan, J. E. 1958, *Astrophys. J.* **128**, 453.

Violett, T., and Rense, W. A. 1959, *Astrophys. J.* **130**, 954.

Walker, W. C., Rustgi, O. P., and Weissler, G. L. 1959, *J. Opt. Soc. Am.* **49**, 471.

The Motion of an Artificial Satellite in the Vicinity of the Critical Inclination

GEN-ICHIRO HORI
Yale University Observatory, New Haven, Connecticut

(Received December 23, 1959)

The motion of an artificial satellite near the critical inclination is studied by the method of canonical transformation. The solution, valid to the order of the square root of the coefficient of the second harmonic of the earth's potential, gives three different types of motion of the perigee: circulation, libration, and the transition type.

1. INTRODUCTION

THERE being no method which leads to a closed solution of the problem of the motion of an artificial satellite, as in most of the problems in celestial mechanics, several solutions by successive approximations have been published. These solutions, such as that of Brouwer (1959), Garfinkel (1959), and Kozai (1959), become inapplicable for the long-period terms at the critical inclination $\cos^{-1}1/(5)^{\frac{1}{2}}$.

This difficulty of the small divisor may suggest that the physical character of the earth's potential prevents our obtaining the same form of the solution throughout the whole range of the inclination.

It is shown that, as in similar situations in other dynamical problems, the difficulty is avoided by developing the solution not in powers of the small parameter itself but in powers of the square root of it.

Both the second and the fourth harmonics of the earth's potential are taken into account because the contributions of the latter are comparable to those of the former in the discussion of the long-period terms. The importance of the ratio of the two parameters, or more precisely, that between the coefficient of the fourth harmonic and the square of the coefficient of the second harmonic, was pointed out by Garfinkel (1959).

Since the problem of the critical inclination concerns the long-period and the secular terms only, the solution can begin after the transformation performed by Brouwer (1959) to eliminate the short-period terms. The method used in this paper is a further adaptation of the principle developed originally by von Zeipel (1916), on which Brouwer's method is also based. By the elimination of the short-period terms the problem has been reduced to a system of one degree of freedom. From a purely mathematical point of view, the problem may be considered to have been solved completely, for we can eliminate the time from the equations of motion and we have the energy integral, this resulting from the fact that the Hamiltonian does not contain the time explicitly. However, it is of interest to get the solution in a more practical form, that is, the explicit functions of the time to supplement the short-period terms already given by Brouwer.

A detailed discussion of the solution valid only as far as of the order of the square root of the parameter of the second harmonic of the earth's potential is given here, though further refinement of the solution may be possible without any theoretical difficulties.

2. THE EQUATIONS OF MOTION

The earth's potential is written as

$$U=\frac{\mu}{r}+\frac{\mu k_2}{r^3}(1-3\sin^2\beta)+\frac{\mu k_4}{r^5}(1-10\sin^2\beta+\frac{35}{3}\sin^4\beta). \quad (1)$$

The equatorial plane of the earth is taken as the reference plane, and β is the declination; $\mu=k^2M$ where M is the mass of the earth and k the Gaussian constant.

An alternative form for U is

$$U=\frac{\mu}{r}+\frac{\mu A_2}{r^3}P_2(\sin\beta)+\frac{\mu A_4}{r^5}P_4(\sin\beta),$$

where P_2,P_4 are the Legendre polynomials. The relations between k and A are

$$A_2=-2k_2 \quad \text{and} \quad A_4=+\frac{8}{3}k_4. \quad (2)$$

The equations of motion in the Delaunay variables are

$$dL/dt=\partial F/\partial l, \quad dl/dt=-(\partial F/\partial L),$$
$$dG/dt=\partial F/\partial g, \quad dg/dt=-(\partial F/\partial G),$$
$$dH/dt=\partial F/\partial h, \quad dh/dt=-(\partial F/\partial H),$$

with the Hamiltonian

$$F=\frac{\mu^2}{2L^2}+\frac{\mu^4k_2}{L^6}\left[\left(-\frac{1}{2}+\frac{3}{2}\frac{H^2}{G^2}\right)\frac{a^3}{r^3}+\left(\frac{3}{2}-\frac{3}{2}\frac{H^2}{G^2}\right)\frac{a^3}{r^3}\cos(2g+2f)\right]$$
$$+\frac{\mu^6k_4}{L^{10}}\left[\left(\frac{3}{8}-\frac{15}{4}\frac{H^2}{G^2}+\frac{35}{8}\frac{H^4}{G^4}\right)\frac{a^5}{r^5}+\left(-\frac{5}{6}+\frac{20}{3}\frac{H^2}{G^2}-\frac{35}{6}\frac{H^4}{G^4}\right)\frac{a^5}{r^5}\cos(2g+2f)\right.$$
$$\left.+\left(\frac{35}{24}-\frac{35}{12}\frac{H^2}{G^2}+\frac{35}{24}\frac{H^4}{G^4}\right)\frac{a^5}{r^5}\cos(4g+4f)\right], \quad (3)$$

where f is the true anomaly. The Delaunay variables are related to Kepler's elements in the following way:

$L=(\mu a)^{\frac{1}{2}}$, l=mean anomaly,

$G=L(1-e^2)^{\frac{1}{2}}$, g=argument of the perigee,

$H=G\cos I$, h=longitude of the ascending node.

Because of the assumed rotational symmetry of the earth, the variable h does not enter into the Hamiltonian F. The elimination of the short-period terms leads to a new Hamiltonian F^* which does not contain the variables h and l. The new equations of motion are, after this process, of the form

$$dG'/dt=\partial F^*/\partial g', \quad dg'/dt=-(\partial F^*/\partial G'),$$

a system of one degree of freedom. In these equations the prime indicates that the short-period terms have been eliminated, and F^* is a function of the primed variables, though H' is equal to H. For simplicity we shall remove the primes and the asterisks in the following discussion. The fundamental equations of motion are then

$$dG/dt=\partial F/\partial g, \quad dg/dt=-(\partial F/\partial G), \tag{4}$$

with the new Hamiltonian $F=F_0+F_1+F_2$, where

$$F_0=\frac{\mu^2}{2L^2},$$

$$F_1=\frac{\mu^4k_2}{L^3G^3}\left(-\frac{1}{2}+\frac{3}{2}\frac{H^2}{G^2}\right), \tag{5}$$

$$\begin{aligned}F_2=&\frac{\mu^6k_2^2}{L^5G^5}\left\{\frac{15}{32}-\frac{9}{16}\frac{k_4}{k_2^2}-\left(\frac{27}{16}-\frac{45}{8}\frac{k_4}{k_2^2}\right)\frac{H^2}{G^2}\right.\\&+\left(\frac{15}{32}-\frac{105}{16}\frac{k_4}{k_2^2}\right)\frac{H^4}{G^4}+\frac{3}{8}\frac{L}{G}\left(1-6\frac{H^2}{G^2}+9\frac{H^4}{G^4}\right)\\&-\frac{L^2}{G^2}\left[\frac{15}{32}-\frac{15}{16}\frac{k_4}{k_2^2}-\left(\frac{15}{16}-\frac{75}{8}\frac{k_4}{k_2^2}\right)\frac{H^2}{G^2}\right.\\&\left.\left.-\left(\frac{105}{32}+\frac{175}{16}\frac{k_4}{k_2^2}\right)\frac{H^4}{G^4}\right]\right\}\\&+\frac{\mu^6k_2^2}{L^5G^5}\left(1-\frac{L^2}{G^2}\right)\left[-\frac{3}{16}\left(1-16\frac{H^2}{G^2}+15\frac{H^4}{G^4}\right)\right.\\&\left.+\frac{5}{8}\frac{k_4}{k_2^2}\left(1-8\frac{H^2}{G^2}+7\frac{H^4}{G^4}\right)\right]\cos 2g.\end{aligned} \tag{6}$$

The subscripts of F represent the order of the quantities, k_2 being considered of the first order. In the discussion I shall use the notation

$$\begin{aligned}F_2&=F_{2s}+F_{2p}\\&=F_{2s}+Q_2\cos 2g.\end{aligned} \tag{7}$$

3. THE CANONICAL TRANSFORMATION

Consider a canonical transformation from the variables L, G, H, l, g, h to L, G', H, l', g', h' with the determining function

$$S=Ll+G'g+Hh+S_n(L,G',H,g), \tag{8}$$

and let a new Hamiltonian be

$$F^*=F_0^*+F_1^*+F_2^*,$$

which is sufficient for obtaining the secular terms in g as far as the second order. The relation

$$F(L,G,H,g)=F^*(L,G',H) \tag{9}$$

leads to

$$\begin{aligned}&F_0+F_1+F_1'\frac{\partial S_n}{\partial g}+\tfrac{1}{2}F_1''\left(\frac{\partial S_n}{\partial g}\right)^2\\&\quad+\tfrac{1}{6}F_1'''\left(\frac{\partial S_n}{\partial g}\right)^3+\cdots+F_2+F_2'\frac{\partial S_n}{\partial g}\\&\quad+\tfrac{1}{2}F_2''\left(\frac{\partial S_n}{\partial g}\right)^2+\cdots=F_0^*+F_1^*+F_2^*,\end{aligned} \tag{10}$$

where the F are to be considered functions of the new variables and the primes on F stand for the derivatives with respect to G'.

In the usual procedure, available in the case when F_1' is not near zero, S_n is developed in powers of k_2 as

$$S_n=S_1+S_2+\cdots, \tag{11}$$

S_1 being determined by the relation

$$F_1'\frac{\partial S_1}{\partial g}+Q_2\cos 2g=0, \tag{12}$$

and S_2 by

$$F_1'\frac{\partial S_2}{\partial g}+\tfrac{1}{2}F_1''\left[\left(\frac{\partial S_1}{\partial g}\right)^2-\left(\frac{\partial S_1}{\partial g}\right)_s^2\right]+F_2'\frac{\partial S_1}{\partial g}=0,$$

and so forth, with the new Hamiltonian

$$\begin{aligned}F_0^*&=F_0(L),\\F_1^*&=F_1(L,G',H),\\F_2^*&=F_{2s}(L,G',H),\\F_3^*&=\tfrac{1}{2}F_1''\left(\frac{\partial S_1}{\partial g}\right)_s^2.\end{aligned} \tag{13}$$

When F_1' is near zero, however, the equation that determines the first approximation of S_n should contain the term $\frac{1}{2}F_1''(\partial S_n/\partial g)^2$ and may be written as

$$F_1'\frac{\partial S_n}{\partial g}+\tfrac{1}{2}F_1''\left(\frac{\partial S_n}{\partial g}\right)^2+Q_2\cos 2g=0, \tag{14}$$

with the new Hamiltonian (13), provided that F_1'' does not vanish when F_1' vanishes, which condition is satisfied in the present case. Then S_n begins with $S_{\frac{1}{2}}$ and, formally, may have the form

$$S_n=S_{\frac{1}{2}}+S_1+\cdots. \tag{15}$$

Equations (14) and (13) are, however, not a unique set for determining $S_{\frac{1}{2}}$ and the new Hamiltonian. This ambiguity comes from the fact that the equation determining $S_{\frac{1}{2}}$ is a quadratic one and that the general principle requiring $S_{\frac{1}{2}}$ to be purely periodic in g loses its meaning.

As an alternative principle we consider the energy integral of the equations of motion, Eqs. (4),

$$F=F_0+F_1+F_{2s}+Q_2\cos 2g=C, \tag{16}$$

and we require that $S_{\frac{1}{2}}$ give the solution that contains the stable equilibrium solution. Equations (4) and (16) give the stable equilibrium solution $g=\text{const}$, $G=\text{const}$ by

$$\frac{dG}{dt}=\frac{\partial F}{\partial g}=-2Q_2\sin 2g=0,$$

$$\frac{dg}{dt}=-\frac{\partial F}{\partial G}=-(F_1'+F_{2s}'+Q_2'\cos 2g)=0.$$

The conditions $\partial F/\partial g=0$, $\partial F/\partial G=0$ can be satisfied only if $g=0$, π, or $\pi/2$. Since the coefficient Q_2 is positive, the function $F(G,g)$ has an absolute minimum at $g=\pi/2$, which corresponds to a stable equilibrium solution. For $g=0$ or π there is an unstable equilibrium, associated with an asymptotic solution. Therefore, for stable equilibrium

$$g=\frac{\pi}{2}, \tag{17}$$

$$\frac{\partial}{\partial G}(F_0+F_1+F_{2s}-Q_2)=0. \tag{18}$$

Let the set of equations that determines $S_{\frac{1}{2}}$ and the new Hamiltonian be

$$(F_1'+F_{2s}'-Q_2')\frac{\partial S_{\frac{1}{2}}}{\partial g}+\tfrac{1}{2}F_1''\left(\frac{\partial S_{\frac{1}{2}}}{\partial g}\right)^2+2Q_2\cos^2 g=0, \tag{19}$$

and

$$\begin{aligned} F_0^*&=F_0(L),\\ F_1^*&=F_1(L,G',H),\\ F_2^*&=F_{2s}(L,G',H)-Q_2(L,G',H). \end{aligned} \tag{20}$$

Equation (19) leads to the solution

$$\frac{\partial S_{\frac{1}{2}}}{\partial g}=-\frac{F_1'+F_{2s}'-Q_2'}{F_1''}\pm\left[\left(\frac{F_1'+F_{2s}'-Q_2'}{F_1''}\right)^2-\frac{4Q_2}{F_1''}\cos^2 g\right]^{\frac{1}{2}} \tag{21}$$

or, putting

$$g^*=g-\frac{\pi}{2}, \tag{22}$$

$$\frac{\partial S_{\frac{1}{2}}}{\partial g^*}=-\frac{F_1'+F_{2s}'-Q_2'}{F_1''}\pm\left[\left(\frac{F_1'+F_{2s}'-Q_2'}{F_1''}\right)^2-\frac{4Q_2}{F_1''}\sin^2 g^*\right]^{\frac{1}{2}}. \tag{23}$$

We also have

$$\frac{dg^*}{dt}=-\frac{\partial F^*}{\partial G'}=-(F_1'+F_{2s}'-Q_2'). \tag{24}$$

It is clear that the solution [Eqs. (23) and (24)] gives a stable equilibrium when $F_1'+F_{2s}'-Q_2'$ vanishes.

After determining $S_{\frac{1}{2}}$ by Eq. (19), the equation to determine the next term of S_n, say S_1, is

$$F_1'\frac{\partial S_1}{\partial g}+\tfrac{1}{2}F_1''\cdot 2\frac{\partial S_{\frac{1}{2}}}{\partial g}\frac{\partial S_1}{\partial g}+\tfrac{1}{6}F_1'''\left(\frac{\partial S_{\frac{1}{2}}}{\partial g}\right)^3+2Q_2'\cos^2 g\cdot\frac{\partial S_{\frac{1}{2}}}{\partial g}=0,$$

or

$$\left(F_1'+F_1''\frac{\partial S_{\frac{1}{2}}}{\partial g}\right)\frac{\partial S_{\frac{1}{2}}}{\partial g}+\tfrac{1}{6}F_1'''\left(\frac{\partial S_{\frac{1}{2}}}{\partial g}\right)^3+2Q_2'\cos^2 g\cdot\frac{\partial S_{\frac{1}{2}}}{\partial g}=0;$$

we may develop S_n in powers of $k_2^{\frac{1}{2}}$ as

$$S_n=S_{\frac{1}{2}}+S_1+\cdots,$$

at least formally.

4. THE CONTRIBUTION OF THE FOURTH HARMONIC

The contribution of the fourth harmonic of the earth's potential is shown by the terms having the factor k_4/k_2^2 in expression (6) of F_2. It is clear that, when k_4 is of the order k_2^2, this contribution is comparable with that of the second harmonic. For the earth we have, according to O'Keefe, Eckels, and Squires (1959)

$$k_2=5.4\times 10^{-4} \quad \text{and} \quad k_4=6.4\times 10^{-7}, \tag{25}$$

and, therefore,

$$k_4/k_2^2=2.2. \tag{26}$$

It is noticed here that the expressions (6) and (7) lead to

$$Q_2=\frac{\mu^6 k_2^2}{L^5G^5}\cdot\frac{3}{4}\left(1-\frac{L^2}{G^2}\right)\left(1-\frac{H^2}{G^2}\right)\left(1-5\frac{H^2}{G^2}\right) \tag{27}$$

if we assume the relation

$$k_4/k_2^2=3/2. \tag{28}$$

Equation (12) then takes the form

$$\frac{3}{2}\frac{\mu^4k_2}{L^3G'^4}\frac{\partial S_1}{\partial g}+\frac{\mu^6k_2^2}{L^5G'^5}\cdot\frac{3}{4}\left(1-\frac{L^2}{G'^2}\right)\left(1-\frac{H^2}{G'^2}\right)\cos 2g=0 \tag{29}$$

after division by the factor $1-5H^2/G'^2$, and this equation is valid even in the critical inclination case. In other words, for this particular potential there is no critical inclination. The relation (28) is equivalent to

$$A_4/A_2^2=1. \tag{30}$$

For this particular potential, with additional terms,

$$U=-\frac{\mu}{r}\left[1+\sum_{n=1}^{\infty}\frac{A_2^n}{r^{2n}}P_{2n}(\sin\beta)\right];$$

the exact solution has been obtained by Vinti (1959) so that the disappearance of the critical inclination is quite natural. It may be said that all the problems of the motions of artificial satellites arise from the difference between the relations (26) and (28). It may also be said that the critical inclination with the associated presence of the small divisor is due to the physical character of the earth's potential; it cannot be removed by any method.

5. DETERMINATION OF $S_{\frac{1}{2}}$

The expression (23) yields $\partial S_{\frac{1}{2}}/\partial g$ or, equivalently $\partial S_{\frac{1}{2}}/\partial g^*$, in the form,

$$\frac{\partial S_{\frac{1}{2}}}{\partial g^*}=A\pm[A^2-B\sin^2g^*]^{\frac{1}{2}}, \tag{31}$$

where

$$A=-\frac{F_1'+F_{2s}'-Q_2'}{F_1''} \tag{32}$$

and

$$B=\frac{4Q_2}{F_1''}=-\frac{1}{8}\frac{\mu^2k_2}{L^2}\left(1-\frac{L^2}{G'^2}\right)\left[1-16\frac{H^2}{G'^2}+15\frac{H^4}{G'^4}+\frac{5}{8}\frac{k_4}{k_2^2}\left(1-8\frac{H^2}{G'^2}+7\frac{H^4}{G'^4}\right)\right]\left(1-\frac{15}{2}\frac{H^2}{G'^2}\right)^{-1}.$$

The last expression is reduced to

$$B=-\frac{2}{5}\frac{\mu^2k_2}{L^2}\left(1-\frac{L^2}{G'^2}\right)\left(1-\frac{2}{3}\frac{k_4}{k_2^2}\right),$$

by the substitution of $H^2/G'^2=1/5$, and hence

$$B>0 \quad \text{when} \quad k_4/k_2^2>3/2,$$
$$B<0 \quad \text{when} \quad k_4/k_2^2<3/2.$$

Thus B is positive at the critical inclination for the earth's potential. It is also noticed that $B>0$ means $Q_2>0$ because F_1'' is positive in this case.

Caution is necessary with regard to the double sign appearing in the expression for $\partial S_{\frac{1}{2}}/\partial g^*$. The double sign should be interpreted as

$$\pm(A^2-B\sin^2g^*)^{\frac{1}{2}}=\begin{cases}-A[1-(B/A^2)\sin^2g^*]^{\frac{1}{2}} & \text{when} \quad A^2\geqq B,\\ \text{two-valued function} & \text{when} \quad A^2<B.\end{cases} \tag{34}$$

The upper form, the case $A^2\geqq B$, includes the special case $B=0$. Then S should lead to the identical transformation because g does not enter into the Hamiltonian F. The lower form, the case $A^2<B$, corresponds to a libration. For simplicity, however, we shall use the upper notation in both cases in the following discussion.

Introducing k by the relation

$$k=(B/A^2)^{\frac{1}{2}}, \tag{35}$$

we have

$$\frac{\partial S_{\frac{1}{2}}}{\partial g^*}=A-A(1-k^2\sin^2g^*)^{\frac{1}{2}}. \tag{36}$$

k takes values from 0 to ∞ for all the combinations of the possible values of A and B except the case when A and B vanish simultaneously. The case $k=\infty$ corresponds to the stable equilibrium solution. The integration of Eq. (36) leads to

$$S_{\frac{1}{2}}=Ag^*-A\int_0^{g^*}(1-k^2\sin^2g^*)^{\frac{1}{2}}dg^*. \tag{37}$$

When k is greater than unity, the integrand of this expression is a two-valued function, and $S_{\frac{1}{2}}$ itself becomes a multivalued function, to be discussed later.

Equation (37), differentiated with respect to G', is

$$\frac{\partial S_{\frac{1}{2}}}{\partial G'}=A'g^*-\left(A'-\frac{A}{2B}B'\right)\mathbf{F}(k,g^*)-\frac{A}{2B}B'\mathbf{E}(k,g^*), \tag{38}$$

where

$$\mathbf{F}(k,g^*)=\begin{cases}F(k,g^*) & \text{for} \quad k\leqq 1,\\ \displaystyle\int_0^{g^*}\left[\pm\frac{1}{(1-k^2\sin^2g^*)^{\frac{1}{2}}}\right]dg^* & \text{for} \quad k>1;\end{cases} \tag{39}$$

$$\mathbf{E}(k,g^*)=\begin{cases}E(k,g^*) & \text{for} \quad k\leqq 1,\\ \displaystyle\int_0^{g^*}[\pm(1-k^2\sin^2g^*)^{\frac{1}{2}}]dg^* & \text{for} \quad k>1.\end{cases} \tag{40}$$

$F(k,g^*)$ and $E(k,g^*)$ are the elliptic integrals of the first and second kinds, respectively, and the double signs attached to the integrands in the expressions (39) and (40) are to show explicitly the multivalued character of the integrals.

6. THE SOLUTION

The solution of the equations of motion Eqs. (4) has now been obtained in the following forms:

$G'=\text{const},$

$$g^{*\prime}=\left(-\frac{\partial F^*}{\partial G'}\right)t+g_0^{*\prime} \quad (g_0^{*\prime}:\text{const}), \tag{41}$$

and

$$\begin{aligned} G&=G'+\frac{\partial S_{\frac{1}{2}}}{\partial g}\\ &=G'+A-A(1-k^2\sin^2 g^*)^{\frac{1}{2}}, \end{aligned} \tag{42}$$

$$\begin{aligned} g^*&=g^{*\prime}-\frac{\partial S_{\frac{1}{2}}}{\partial G'}\\ &=g^{*\prime}-\frac{\partial A}{\partial G'}g^*+\left(\frac{\partial A}{\partial G'}-\frac{A}{2B}\frac{\partial B}{\partial G'}\right)\mathbf{F}(k,g^*)\\ &\quad+\frac{A}{2B}\frac{\partial B}{\partial G'}\mathbf{E}(k,g^*), \end{aligned}$$

or

$$\begin{aligned} g^{*\prime}&=\left(1+\frac{\partial A}{\partial G'}\right)g^*-\left(\frac{\partial A}{\partial G'}-\frac{A}{2B}\frac{\partial B}{\partial G'}\right)\mathbf{F}(k,g^*)\\ &\quad-\frac{A}{2B}\frac{\partial B}{\partial G'}\mathbf{E}(k,g^*). \end{aligned} \tag{43}$$

Equation (43) is the implicit expression for g^* as a function of $g^{*\prime}$, that is, a linear function of the time.

The variables l and h are obtained by the relations:

$$\begin{aligned} l'&=l+\frac{\partial S_{\frac{1}{2}}}{\partial L}\\ &=l+\frac{\partial A}{\partial L}g^*-\left(\frac{\partial A}{\partial L}-\frac{A}{2B}\frac{\partial B}{\partial L}\right)\mathbf{F}(k,g^*)\\ &\quad-\frac{A}{2B}\frac{\partial B}{\partial L}\mathbf{E}(k,g^*) \end{aligned} \tag{44}$$

$$\begin{aligned} h'&=h+\frac{\partial S_{\frac{1}{2}}}{\partial H}\\ &=h+\frac{\partial A}{\partial H}g^*-\left(\frac{\partial A}{\partial H}-\frac{A}{2B}\frac{\partial B}{\partial H}\right)\mathbf{F}(k,g^*)\\ &\quad-\frac{A}{2B}\frac{\partial B}{\partial H}\mathbf{E}(k,g^*), \end{aligned} \tag{45}$$

and

$$l'=\left(-\frac{\partial F^*}{\partial L}\right)t+l_0' \quad (l_0':\text{const}), \tag{46}$$

$$h'=\left(-\frac{\partial F^*}{\partial H}\right)t+h_0' \quad (h_0':\text{const}). \tag{47}$$

L and H are, of course, already given as constants; G' and $g_0^{*\prime}(=g_0'-\pi/2)$ are the two integration constants for the equations of motion Eqs. (4), and the six integration constants for the whole problem are L, G', H, l_0', $g_0^{*\prime}$, and h_0'.

7. THE EVALUATION OF THE FUNCTIONS $\mathbf{F}(k,g^*)$ AND $\mathbf{E}(k,g^*)$

Consider the integrals

$$\int_0^\theta \frac{d\theta}{(1-k^2\sin^2\theta)^{\frac{1}{2}}}$$

and

$$\int_0^\theta (1-k^2\sin^2\theta)^{\frac{1}{2}}d\theta\left(k>1,\ 0\leqq|\theta|\leqq\sin^{-1}\frac{1}{k}\leqq\frac{\pi}{2}\right).$$

It is easy to see that these integrals may be expressed as standard elliptic integrals by the change of variable from θ to u defined by

$$\tan\theta=\frac{\cos u}{(k^2-1)^{\frac{1}{2}}}. \tag{48}$$

The results are:

$$\int_0^\theta \frac{d\theta}{(1-k^2\sin^2\theta)^{\frac{1}{2}}}=\frac{1}{k}\left[F\left(\frac{1}{k},\frac{\pi}{2}\right)-F\left(\frac{1}{k},u\right)\right], \tag{49}$$

$$\begin{aligned} \int_0^\theta (1-k^2\sin^2\theta)^{\frac{1}{2}}d\theta&=\frac{k^2-1}{\kappa}\left[F\left(\frac{1}{k},u\right)-F\left(\frac{1}{k},\frac{\pi}{2}\right)\right]\\ &\quad+k\left[E\left(\frac{1}{k},\frac{\pi}{2}\right)-E\left(\frac{1}{k},u\right)\right]\\ &\quad+\tan\theta(1-k^2\sin^2\theta)^{\frac{1}{2}}. \end{aligned} \tag{50}$$

Now consider the functions $\mathbf{F}(k,\theta)$ and $\mathbf{E}(k,\theta)$. When k is less than or equal to unity, these functions reduce to the standard elliptic integrals $F(k,\theta)$ and $E(k,\theta)$, respectively, degenerating for $k=1$ to the elementary functions:

$$\begin{aligned} F(1,\theta)&=\ln\tan\left(\frac{\pi}{4}+\frac{\theta}{2}\right)\\ E(1,\theta)&=\sin\theta \end{aligned} \qquad \text{for} -\frac{\pi}{2}\leqq\theta\leqq\frac{\pi}{2}. \tag{51}$$

When k is greater than unity, on the other hand, $\mathbf{F}(k,\theta)$ and $\mathbf{E}(k,\theta)$ are multivalued functions having the following expressions:

$$\begin{aligned} &\mathbf{F}(k,\theta)=\mathfrak{F},\ -\mathfrak{F}\pm2\mathbf{F},\ \mathfrak{F}\pm4\mathbf{F},\ -\mathfrak{F}\pm6\mathbf{F},\cdots,\\ &\mathbf{E}(k,\theta)=\mathcal{E},\ -\mathcal{E}\pm2\mathbf{E},\ \mathcal{E}\pm3\mathbf{E},\ -\mathcal{E}\pm6\mathbf{E},\cdots, \end{aligned} \tag{52}$$

where

$$\mathfrak{F}\equiv\mathfrak{F}(k,\theta)=\int_0^\theta \frac{d\theta}{(1-k^2\sin^2\theta)^{\frac{1}{2}}}(-\varphi\leqq\theta\leqq\varphi), \tag{53}$$

$$\mathbf{F}\equiv\mathbf{F}(k)=\int_0^\varphi \frac{d\theta}{(1-k^2\sin^2\theta)^{\frac{1}{2}}}, \tag{54}$$

TABLE I. The elliptic integrals $\mathbf{F}(k,x)$ and $\mathbf{E}(k,x)$.

$\mathbf{F}(k,x)$, $0 \leqq k \leqq \sqrt{2}$

k \ x	0°	10°	20°	30°	40°	50°	60°	70°	80°	90°
0.0	0.000	0.175	0.349	0.524	0.698	0.873	1.047	1.222	1.396	1.571
0.1	0.000	0.175	0.349	0.524	0.699	0.874	1.049	1.224	1.399	1.575
0.2	0.000	0.175	0.349	0.525	0.700	0.877	1.053	1.231	1.409	1.587
0.3	0.000	0.175	0.350	0.526	0.703	0.881	1.062	1.243	1.425	1.608
0.4	0.000	0.175	0.350	0.527	0.707	0.889	1.073	1.261	1.450	1.640
0.5	0.000	0.175	0.351	0.529	0.712	0.898	1.090	1.285	1.485	1.686
0.6	0.000	0.175	0.352	0.532	0.718	0.911	1.111	1.319	1.533	1.751
0.7	0.000	0.175	0.353	0.535	0.726	0.927	1.140	1.366	1.603	1.846
0.8	0.000	0.175	0.354	0.539	0.736	0.948	1.179	1.432	1.707	1.995
0.9	0.000	0.175	0.355	0.544	0.748	0.975	1.233	1.536	1.888	2.281
1.0	0.000	0.175	0.356	0.549	0.763	1.011	1.317	1.735	2.436	
1.1	0.000	0.176	0.358	0.556	0.780	1.061	1.479			
1.2	0.000	0.176	0.359	0.562	0.805	1.144				
1.3	0.000	0.176	0.362	0.571	0.838	1.383				
1.4	0.000	0.176	0.364	0.582	0.885					
$\sqrt{2}$	0.000	0.176	0.365	0.584	0.893					

$\mathbf{E}(k,x)$, $0 \leqq k \leqq \sqrt{2}$

0.0	0.000	0.175	0.349	0.524	0.698	0.873	1.047	1.222	1.396	1.571
0.1	0.000	0.175	0.349	0.523	0.698	0.872	1.046	1.219	1.393	1.567
0.2	0.000	0.174	0.349	0.523	0.696	0.869	1.041	1.213	1.384	1.555
0.3	0.000	0.174	0.348	0.522	0.693	0.864	1.033	1.201	1.368	1.535
0.4	0.000	0.174	0.348	0.520	0.690	0.857	1.022	1.185	1.346	1.506
0.5	0.000	0.174	0.347	0.518	0.685	0.848	1.008	1.163	1.316	1.467
0.6	0.000	0.174	0.347	0.515	0.679	0.837	0.989	1.136	1.278	1.418
0.7	0.000	0.174	0.346	0.512	0.672	0.824	0.967	1.102	1.230	1.356
0.8	0.000	0.174	0.345	0.509	0.664	0.808	0.939	1.060	1.171	1.276
0.9	0.000	0.174	0.343	0.505	0.654	0.789	0.906	1.008	1.094	1.172
1.0	0.000	0.174	0.342	0.500	0.643	0.766	0.866	0.940	0.985	1.000
1.1	0.000	0.174	0.341	0.495	0.631	0.740	0.815			
1.2	0.000	0.174	0.339	0.490	0.616	0.707				
1.3	0.000	0.173	0.338	0.483	0.598	0.663				
1.4	0.000	0.173	0.335	0.475	0.578					
$\sqrt{2}$	0.000	0.173	0.335	0.474	0.575					

and

$$\mathcal{E}=\mathcal{E}(k,\theta)=\int_0^\theta (1-k^2\sin^2\theta)^{\frac{1}{2}}d\theta (-\varphi\leqq\theta\leqq\varphi), \quad (55)$$

$$\mathbf{E}=\mathbf{E}(k)=\int_0^\varphi (1-k^2\sin^2\theta)^{\frac{1}{2}}d\theta. \quad (56)$$

It is understood that in these expressions

$$\varphi=\sin^{-1}\frac{1}{k}<\frac{\pi}{2}. \quad (57)$$

Thus $\mathfrak{F}$, $\mathbf{F}$, $\mathcal{E}$, $\mathbf{E}$ are evaluated by the formulas (49) and (50) when the values of θ and k are given. Table I and Fig. 1 show the general character of these functions in the range $0\leqq k\leqq\sqrt{2}$.

8. THE MEAN MOTIONS OF THE VARIABLES $g^{*\prime}$, $l^\prime$, $h^\prime$

The mean motions of $g^{*\prime}$ or $g^\prime$ are obtained by Eq. (41) combined with the Hamiltonian (20), and those for $l^\prime$ and $h^\prime$ by Eqs. (46) and (47), respectively, by essentially similar procedures.

Defining λ and ϵ by

$$\lambda=k_4/k_2^2, \quad (58)$$

$$\epsilon=1-5(H^2/G'^2), \quad (59)$$

we may write the Hamiltonian as

$$F^*=F_0^*+F_1^*+F_2^*,$$

with

$$F_0^*=\frac{\mu^2}{2L^2},$$

$$F_1^*=\frac{\mu^4k_2}{L^3G'^3}\left(-\frac{1}{2}+\frac{3}{2}\frac{H^2}{G'^2}\right), \quad (60)$$

$$F_2^*=\frac{\mu^6k_2^2}{L^5G'^5}\left\{\frac{21}{32}-\frac{19}{16}\lambda+\left(-\frac{75}{16}+\frac{85}{8}\lambda\right)\frac{H^2}{G'^2}\right.$$
$$+\left(\frac{105}{32}-\frac{175}{16}\lambda\right)\frac{H^4}{G'^4}+\frac{3}{8}\frac{L}{G'}\left(1-6\frac{H^2}{G'^2}+9\frac{H^4}{G'^4}\right)$$
$$\left.+\frac{L^2}{G'^2}\left[-\frac{21}{32}+\frac{25}{16}\lambda+\left(\frac{63}{16}-\frac{115}{8}\lambda\right)\frac{H^2}{G'^2}\right.\right.$$
$$\left.\left.+\left(\frac{15}{32}+\frac{245}{16}\lambda\right)\frac{H^4}{G'^4}\right]\right\}. \quad (61)$$

In the vicinity of the critical inclination, where

$$\epsilon\lesssim O(k_2)^{\frac{1}{3}}, \quad (62)$$

there results

$$\frac{dg^{*\prime}}{dt}=-\frac{3}{2}\frac{\mu^4k_2}{L^3G'^4}\epsilon+\frac{3}{10}\frac{\mu^6k_2^2}{L^5G'^6}\times\left[-7+\frac{50}{3}\lambda+\frac{L^2}{G'^2}\left(9-\frac{82}{3}\lambda\right)\right], \quad (63)$$

$$\frac{dl'}{dt}=\frac{\mu^2}{L^3}-\frac{3}{5}\frac{\mu^4k_2}{L^4G'^3}(1+\tfrac{3}{2}\epsilon)+\frac{3}{20}\frac{\mu^6k_2^2}{L^6G'^5}\times\left[-5+\frac{50}{3}\lambda+\frac{8}{5}\frac{L}{G'}+\frac{L^2}{G'^2}(3-14\lambda)\right], \quad (64)$$

$$\frac{dh'}{dt}=-\frac{3(5)^{\frac{1}{2}}}{5}\frac{\mu^4k_2}{L^3G'^4}\left(1-\frac{\epsilon}{2}-\frac{\epsilon^2}{8}\right)+\frac{3(5)^{\frac{1}{2}}}{20}\frac{\mu^6k_2^2}{L^5G'^6}\times\left[-9+\frac{50}{3}\lambda-\frac{12}{5}\frac{L}{G'}+\frac{L^2}{G'^2}(11-22\lambda)\right]. \quad (65)$$

These expressions are valid as far as the order k_2^2, but, of course, are different from those obtained by Brouwer (1959) for the noncritical case. Moreover $g^{*\prime}$, l', and h' are not the secular parts of the corresponding variables g^*, l, and h, inasmuch as $\partial S_{\frac{1}{2}}/\partial g$ is not purely periodic in g, as shown in Sec. 3.

The mean motion of $g^{*\prime}$ is about ϵ times slower than the mean motions of h' and $l'-\mu^2/L^3$ in the critical inclination case. The value of G' which will give $dg^{*\prime}/dt=0$ corresponds to a stable equilibrium.

In the expression for the node, we adopted the positive value of H/G', assuming that the motion of the satellite is direct. For the other variables the sense of the motion has no effect.

TABLE Ia. Supplementary table for maximum values of x.

	$x_{\max}$	$\mathbf{F}(k)$	$\mathbf{E}(k)$
$k=1.1$	65°.38	2.111	0.833
$k=1.2$	56°.44	1.723	0.736
$k=1.3$	50°.28	1.493	0.664
$k=1.4$	49°.59	1.331	0.606
$k=\sqrt{2}$	45°.00	1.311	0.599

9. THE SOLUTION INCLUDING THE LONG-PERIOD TERMS

After $g^{*\prime}$, l', h' have been obtained as linear functions of the time, g^*, l, and h, which include the secular and

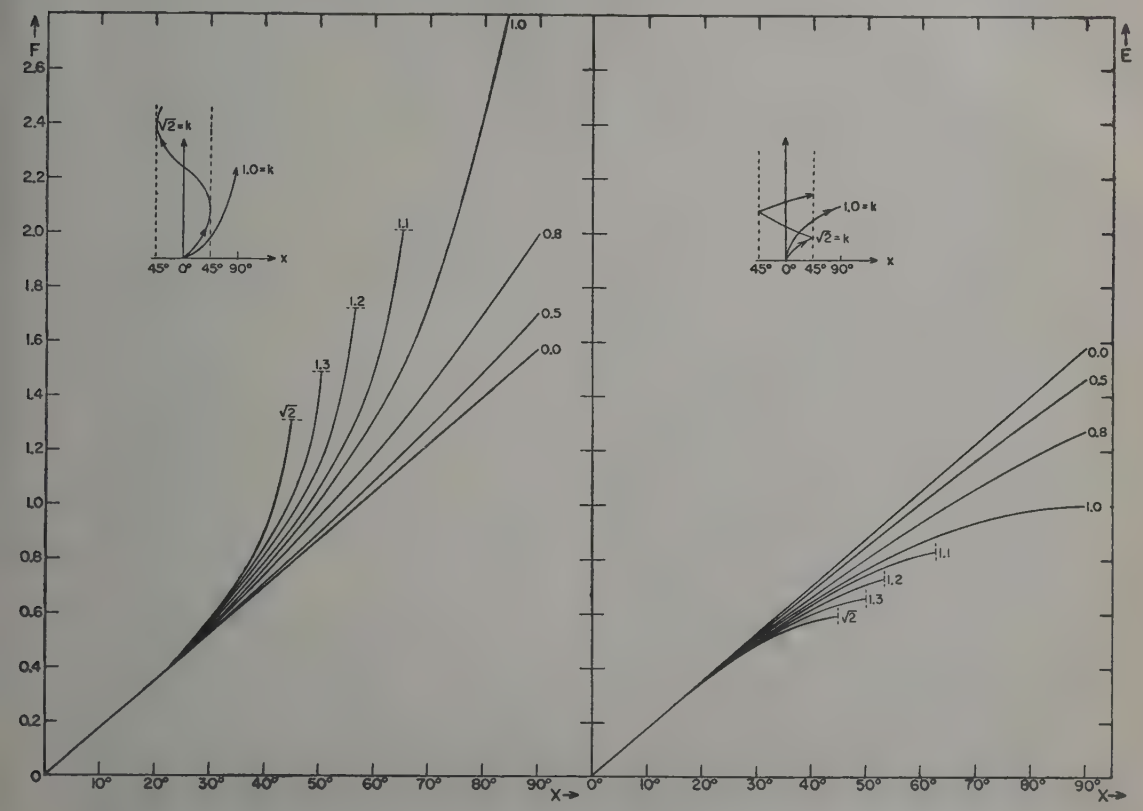

FIG. 1. The functions $E(k,x)$ and $F(k,x)$ with k as the parameter. For $k\leqq 1$, they reduce to the standard elliptic integrals $E(k,x)$ and $F(k,x)$ respectively; for $k>1$, they are the inverse of periodic functions.

the long-period terms, are obtained from Eqs. (43), (44), and (45), respectively. The quantities A, B, and their derivatives with respect to G', L, H will now be expressed as functions of L, G', H. In the vicinity of the critical inclination:

$$A=-\frac{G'}{2}\epsilon(1+3\epsilon)+\frac{G'}{10}\frac{\mu^2k_2}{L^2G'^2}\times\left[-7+\frac{50}{3}\lambda+\frac{L^2}{G'^2}\left(9-\frac{82}{3}\lambda\right)\right], \quad (66)$$

$$B=\frac{2}{5}\frac{\mu^2k_2}{L^2}\left(1-\frac{L^2}{G'^2}\right)\left[1-\frac{2}{3}\lambda-\frac{5}{4}\left(1-\frac{26}{15}\lambda\right)\epsilon\right], \quad (67)$$

$$\frac{\partial A}{\partial G'}=-1-\frac{11}{2}\epsilon+O(k_2), \quad (68)$$

$$\frac{\partial B}{\partial G'}=\frac{G'}{15}\frac{\mu^2k_2}{L^2G'^2}\left[21+2\lambda-\frac{L^2}{G'^2}(9+10\lambda)\right], \quad (69)$$

$$\frac{\partial A}{\partial L}=0+O(k_2), \quad (70)$$

$$\frac{\partial B}{\partial L}=-\frac{4}{5}\frac{\mu^2k_2}{L^3}(1-\tfrac{2}{3}\lambda), \quad (71)$$

$$\frac{\partial A}{\partial H}=\frac{G'}{H}(1+5\epsilon)+O(k_2), \quad (72)$$

$$\frac{\partial B}{\partial H}=-\frac{H}{15}\frac{\mu^2k_2}{L^2H^2}\left(1-\frac{L^2}{G'^2}\right)(21+2\lambda),$$
$$k=(B/A^2)^{\frac{1}{2}}. \quad (73)$$

These expressions suffice to give the solution as far as the order $(k_2)^{\frac{1}{2}}$. It is noticed that B, which includes the factor $1-L^2/G'^2$, does not produce a small divisor in the right-hand members of expressions (43), (44), and (45), as $e\to 0$ because of the following relation:

$$\lim_{B\to 0}\frac{1}{B}[F(k,g^*)-E(k,g^*)]$$
$$=\frac{1}{A^2}\lim_{k2\to 0}\frac{1}{k^2}[F(k,g^*)-E(k,g^*)]$$
$$=\frac{1}{A^2}(\tfrac{1}{2}g^*-\tfrac{1}{4}\sin 2g^*). \quad (74)$$

Formulas (43), (44), and (45), combined with formulas (63), (64), (65) for the primed variables, and with formulas (66), $\cdots$, (73), and (35) for the coefficients of g^*, $\mathbf{F}(k,g^*)$, $\mathbf{E}(k,g^*)$ in the expressions (43), (44), and (45) and for k, together with the value of λ are sufficient to calculate the motions of the perigee, the mean anomaly, and the node when the constants L, G', H are given. Formula (42) gives the motion of G. The integrals $\mathbf{F}(k,g^*)$, $\mathbf{E}(k,g^*)$ are evaluated by formulas (39), (40), (49), (50), and (52). Of course, the variable g^* should be obtained first from Eq. (43).

The characteristic features of the motion of the satellite depend on the value of k, especially for the motion of the perigee. The equation for g^*, Eq. (43), is quite different in its nature from the equations for l, h. It is essentially an implicit equation for g^* as a function of $g^{*\prime}$, which is a linear function of the time, as is easily seen from the fact that the coefficient of g^* in the right-hand member of Eq. (43) is of the order of $(k_2)^{\frac{1}{2}}$, while that for $\mathbf{F}(k,g^*)$ is of finite order. It is seen from the nature of the integrals $\mathbf{F}(k,g^*)$ and $\mathbf{E}(k,g^*)$ that when k is less than unity the motion of the perigee is expressed as a sum of a linear motion and a periodic motion; when $k>1$ the motion becomes a libration about the point $g^*=0$, or $g=\pi/2$, the amplitude and the period of the libration depending on the value of $k(1<k<\infty)$. The case $k=\infty$ corresponds to the stable equilibrium solution, and $k=1$ is the transition case; the motion is asymptotic with g approaching the value $\pm\pi/2$ counted from the libration point. There is no libration in the motion of the node, and, of course, none in that of the mean anomaly. It is also to be noticed that the terms containing g^*, $\mathbf{F}(k,g^*)$, $\mathbf{E}(k,g^*)$ in the right-hand members of the expressions (44) and (45) for the motions of the mean anomaly and the node, respectively, contribute something to the secular parts of the corresponding variables, though the main parts of them are contained in l' and h'. These contributions are found to be of the order of $g^{*\prime}$.

We shall discuss the basic equation, Eq. (43), in some detail.

Case I: $k=0$.

This occurs when $B=0$ or $1-L^2/G'^2=0$. With the help of the relation (74), we have

$$g^{*\prime}=\left(1+\frac{1}{4A}\frac{\partial B}{\partial G'}\right)g^*-\frac{1}{8A}\frac{\partial B}{\partial G'}\sin 2g^*, \quad (75)$$

and the quantity $1/A\cdot\partial B/\partial G'$ is of the order $(k_2)^{\frac{1}{2}}$ when $\epsilon\sim O(k_2)^{\frac{1}{2}}$, or finite when ϵ vanishes at the critical inclination.

Case II: $k=1$.

This occurs when $A^2=B$. With the help of relation (51), we have

$$g^{*\prime}=\left(1+\frac{\partial A}{\partial G'}\right)g^*-\left(\frac{\partial A}{\partial G'}-\frac{1}{2A}\frac{\partial B}{\partial G'}\right)\times\ln\tan\left(\frac{\pi}{4}+\frac{g^*}{2}\right)-\frac{1}{2A}\frac{\partial B}{\partial G'}\sin g^*, \quad (76)$$

where the coefficient of g^* is of the order ϵ and that of $\ln \tan(\pi/4+g^*/2)$ finite, while that of $\sin g^*$ of the order ϵ or finite according as ϵ is of the order $(k_2)^{\frac{1}{2}}$ or zero. Thus the asymptotic character of g^* as a function of $g^{*\prime}$, which is a linear function of the time, is clear; g^* is bounded in the range $\pm\pi/2$.

Case III: $k=\infty$.

This occurs when $A=0$, and corresponds to the stable equilibrium solution. Then $dg^{*\prime}/dt=0$, since relations (32) and (41) yield

$$dg^{*\prime}/dt=F_1''A.$$

Therefore $g^{*\prime}$ is a constant, say $g_0^{*\prime}$. While the integrals $\mathbf{F}(k,g^*)$, $\mathbf{E}(k,g^*)$ require g^* to be zero, Eq. (43) itself becomes $g_0^{*\prime}=0$. The solution is then $g^*=0$, or $g=\pi/2$. Also we have $l=l'$, $h=h'$, and $G=G'$. In other words, the motions of the mean anomaly and the node contain no long-period terms and G becomes constant satisfying the relation $A(G)=0$.

The foregoing three cases are the only ones where the solutions are expressed by elementary functions. We can see, however, the general character of the solution, neglecting the terms containing g^* and $\mathbf{E}(k,g^*)$ in Eq. (43) and putting $\partial A/\partial G'=1$, as justified by the relations (67), (68), and (69) when ϵ is not so close to zero. Then

$$g^{*\prime}=\mathbf{F}(k,g^*),$$

and there results

$g^*=\mathrm{am}(k,g^{*\prime})$, when $k<1$.
$g^*=$purely periodic function of $g^{*\prime}$, when $k>1$.

In the latter case, the period and the amplitude of this periodic function of $g^{*\prime}$ is $4\mathbf{F}$ and $\sin^{-1}(1/k)$, respectively, where $\mathbf{F}$ is given by expression (54). When we consider the remaining terms, the period becomes

$$4\left[-\left(\frac{\partial A}{\partial G'}-\frac{A}{2B}\frac{\partial B}{\partial G'}\right)\mathbf{F}-\frac{A}{2B}\frac{\partial B}{\partial G'}\mathbf{E}\right],$$

though the amplitude does not change. It is easily seen that g^* as a function of $g^{*\prime}$, or the time, has a secular part when $k<1$.

10. ENERGY INTEGRAL

The expression (16) is the energy integral of the equations of motion, Eqs. (4), and the solution for G, Eq. (42), is just the same relation as the energy integral, though the former is only approximately valid. A graphical representation of the energy integral will aid the discussion. Taking the abscissa as g axis and ordinate as F axis, we get a graphical representation of relation (16); G is taken as a parameter. Figure 2 may serve

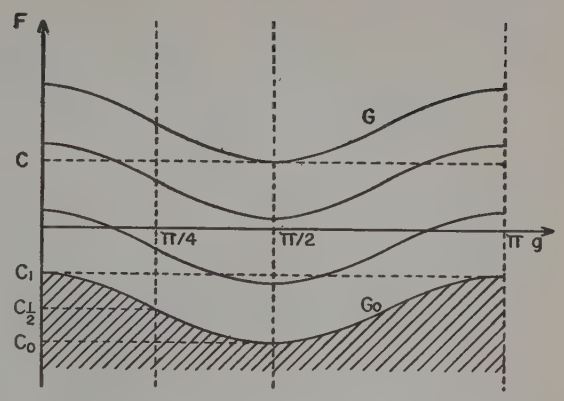

FIG. 2. The function $F(G,g)=F_0+F_1(G)+F_{2s}(G)+Q_2(G)\cos 2g$ with G as parameter. When C is given, $F=C$ represents an implicit relation between G and g: C_0 corresponds to the stable equilibrium; C_1 to the unstable equilibrium and asymptotic orbit. Libration case for $C_0<C<C_1$; circulation case for $C>C_1$.

for a qualitative discussion: we observe that Q_2 is positive in the vicinity of the critical inclination for the earth's potential, and that F has a minimum, which occurs when $g=\pi/2$ and the parameter G satisfies the condition $F_1'(G)+F_{2s}'(G)-Q_2'(G)=0$. This latter holds at the exact critical inclination where $F_1'(G)=0$.

The value C_0 in Fig. 2 corresponds to the stable equilibrium, and C_1 to the asymptotic case $k=1$; the case $k=\sqrt{2}$ corresponds to $C_{\frac{1}{2}}$ where the amplitude of the libration is $\pi/4$. When $C>C_1$, the motion becomes circulatory, corresponding to the case $k<1$.

The relation between G′ and C is given by

$$\begin{aligned} C&=F_0^*+F_1^*(G')+F_2^*(G') \\ &=F_0+F_1(G')+F_{2s}(G')-Q_2(G'), \end{aligned} \tag{77}$$

where F_0 is a function of L only and is considered a constant. It is easy to find graphically the value of G' when a value of C is given: when C is given we can find the curve which takes the value C in the point $g=\pi/2$, then the corresponding value of the parameter G is just the value of G'.

In the present paper one method of successive approximation is presented: the solution is of analytical character, but only an approximation. As an alternate method, we may solve the problem numerically by integrating the equations of motion, Eqs. (4), which are reduced to a differential equation of the first order with the help of the energy integral. Today with high-speed calculators readily available, this numerical approach has obvious practical merits.

ACKNOWLEDGMENTS

The author would like to express his hearty thanks to Dr. Dirk Brouwer, who suggested this problem and who has given many useful suggestions and much

encouragement in the course of the work, and also to Dr. Boris Garfinkel for valuable comments on a draft of the manuscript. The work has been supported by a contract with the Air Force Cambridge Research Center.

REFERENCES

Brouwer, D. 1959, *Astron. J.* **64**, 378.
Garfinkel, B. 1959, *Astron. J.* **64**, 353.
Kozai, Y. 1959, *Astron. J.* **64**, 367.
von Zeipel, H. 1916, *Arkiv Mat. Astr. Fys.* **11**, No. 1.
Vinti, J. P. 1959, *J. Research Nat. Bur. Standards* **63B**, 105.

THE ASTRONOMICAL JOURNAL VOLUME 65, NUMBER 5 JUNE, 1960

An Extrapolation Formula for Stepping the Calculation of the Orbit of an Artificial Satellite Several Revolutions Ahead at a Time

DAVID MACE AND L. H. THOMAS
Service Bureau Corporation, New York and Watson Scientific Computing Laboratory, New York

(Received February 12, 1960)

A method of solving the equations of motion of an artificial satellite has been developed in which not every successive revolution is computed; we extrapolate ahead several revolutions from each computed revolution. If it is allowable to extrapolate five revolutions, for example, the work of computing is reduced almost by a factor of five. This method was applied to a typical satellite orbit computation and was found to provide predictable accuracy.

1. INTRODUCTION

WE are concerned with integration of the equations of motion of an artificial satellite over many periods of revolution. If successive revolutions are closely similar, so that, for example, successive nodes are close together, we may extrapolate without loss of accuracy as many revolutions as will make the step from node to node of computed revolutions about the same as the step needed in step by step integration of one revolution. The systematic scheme for extrapolation discussed in this paper then affords a considerable saving of computing time over a method requiring the computation of every revolution. This method may be regarded as a simple case of that given earlier by one of us (Thomas 1958) and is similar to that of Taratynova (1958).

2. THE EQUATIONS OF MOTION

Take a right-hand rectangular Cartesian coordinate system $C(x,y,z)$ with origin at the center of the earth, z axis in the direction of the earth's North pole, and x axis in the plane of the earth's equator towards the vernal equinox. (Fig. 1.) We shall consider the direction of these axes as fixed.

We regard the earth as an ellipsoid of revolution with approximate gravitational potential at external points

$$\varphi=\frac{E}{r}+\frac{Eb^2}{r^3}\tfrac{1}{3}(\tfrac{1}{2}m-\epsilon)(3\cos^2\theta-1),$$

in terms of geocentric distance r and co-latitude θ. E is the earth's constant, b the mean radius of the earth, m the ratio of centrifugal force at the equator to mean gravity, and ϵ the ellipticity of the earth. Moments of the earth's mass higher than the second are neglected in this paper.

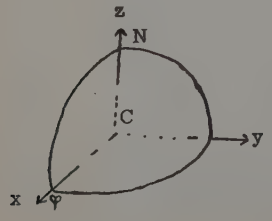

FIG. 1. Coordinates.

The retardation of the satellite due to drag is assumed to be

$$C_D\frac{A}{M}\rho v^2,$$

in terms of its speed v. C_D is the drag coefficient of the satellite, A its cross-section area, M its mass. ρ is atmospheric density. We choose for the atmospheric density an exponentially decreasing function of altitude

$$\rho_0 e^{-c(r-R)},$$

in terms of the excess of r over a base value R at which atmospheric density is ρ_0. c is the constant of exponential decrease.

The differential equations of motion are then

$$\ddot{x}=-\frac{E_x}{r^3}\left[1+k\frac{(x^2+y^2-4z^2)}{r^4}\right]-[\rho_0' e^{-c(r-R)}v]\dot{x}$$

$$\ddot{y}=-\frac{E_y}{r^3}\left[1+k\frac{(x^2+y^2-4z^2)}{r^4}\right]-[\rho_0' e^{-c(r-R)}v]\dot{y}$$

$$\ddot{z}=-\frac{E_z}{r^3}\left[1+k\frac{(3x^2+3y^2-2z^2)}{r^4}\right]-[\rho_0' e^{-c(r-R)}v]\dot{z},$$

here

$$r^2=x^2+y^2+z^2$$

$$v^2=\dot{x}^2+\dot{y}^2+\dot{z}^2.$$

The dots indicate time differentiation, and E, k, ρ_0', c, and R are constants.

For the purpose of testing our method of integration, we regard these equations as exact, and adopt values of the constants as follows: By using values $\epsilon=0.00335$ and $m=0.00347$ with $b=6.3711\times10^3$ km, $k=b^2(\frac{1}{2}m-\epsilon)=6.5554\times10^4$ km^2, while E is 3.9861×10^5 km^3/sec^2. Adopting the value $c=0.01$/km, and taking $R=b$, we assume arbitrarily $\rho_0'=C_DA\rho_0/M=2.7\times10^{-5}$/km, which makes the drag retardation at perigee in the orbit we shall compute comparable with the effect of the earth's asymmetry.

3. THE COMPARISON INTEGRATION

We took the foregoing equations with initial values $x=7200$ km, $y=0$, $z=0$; $\dot{x}=0$, $\dot{y}=6.1$ km/sec, $\dot{z}=6.1$ km/sec, so that we started with perigee at the ascending node, and an inclination of $\pi/4$. This speed leads to an apogee of 12 000 km.

The equations of motion were integrated using the Cowell formula

$$x(t_{n+1})=\delta t^2\left(\nabla^{-2}+\frac{1}{12}\nabla^0+\frac{1}{12}\nabla^1+\frac{19}{240}\nabla^2+\frac{3}{40}\nabla^3+\frac{836}{12\,096}\nabla^4+\frac{275}{4032}\nabla^4+\frac{33\,953}{518\,400}\nabla^6+\cdots\right)\ddot{x}(t_n)$$

for x, and similar expressions for the y and z coordinates, where ∇ is the usual backwards difference operator,

$$[\nabla f(t_n)=f(t_n)-f(t_{n-1}),\quad \nabla^2 f(t_n)=f(t_n)-2f(t_{n-1})+f(t_{n-2}),\text{ etc.},].$$

We obtain a series of coordinates and summations and differences of the acceleration components at equal intervals of time δt. A typical table for the z coordinate at times $t_1,t_2,t_3,\cdots$ is arranged as in Fig. 2. Velocity

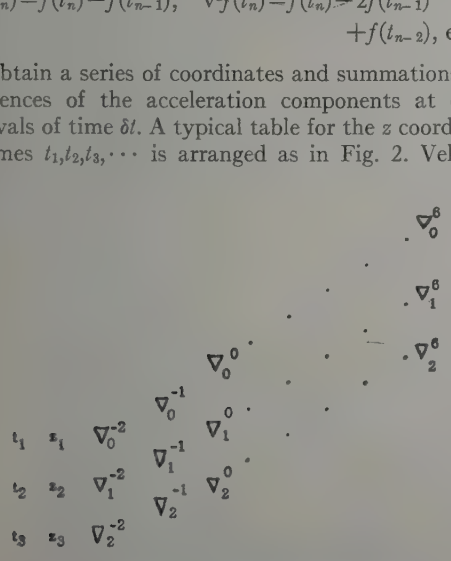

FIG. 2. Difference in the Cowell integration.

components for computing the drag are given by the formula

$$\dot{x}(t_{n+1})=\delta t\left(\nabla^{-1}+\frac{1}{2}\nabla^0+\frac{5}{12}\nabla^1+\cdots\right)\ddot{x}(t_n)$$

for $\dot{x}$, and similar expressions for $\dot{y}$ and $\dot{z}$. Values of $\ddot{x}(t_{n+1})$, $\ddot{y}(t_{n+1})$, and $\ddot{z}(t_{n+1})$, are then found from the equations of motion and new lines of the difference tables computed. The whole process is conveniently started with given values of x, y, z, $\dot{x}$, $\dot{y}$, and $\dot{z}$, by a successive approximation scheme over several successive time steps backwards and forwards.

Sixth differences of the acceleration components were used in the main difference tables as indicated in Fig. 2, and the integration was extended over 25 000 steps at a time interval of 1 min, covering about 150 complete revolutions at 160 steps/revolution. Only the first term of the formula was used to approximate the velocity components. The inclusion of further terms would not alter the general results of this paper. Ten decimal digits were kept in the accelerations, leading to 12 in the second summations, and in the values of the coordinates. These were rounded to ten digits and the accelerations were then computed and again rounded to ten digits, so that the final rounding contributed nearly all the error, giving a root mean square rounding error of $(1/12)^{\frac{1}{2}}$ in the right-hand place.

For the Cowell integration formula, Brouwer (1937) gives an expression for the root mean square rounding error in the semi-major axis $(1/\sqrt{3}\mu)n^{\frac{1}{2}}$ where n is the total number of steps and μ is the mean motion in radians per step. For the apogee this should be multiplied by $[(7-3e)(1+e)/2]^{\frac{1}{2}}$. We calculate from this that the root mean square error to be expected in the x coordinate after 1 revolution is 368 in the right-hand place.

Times near each successive descending node making the second sum of $\ddot{z}$ vanish ($\dot{z}<0$) were found by inverse interpolation using nine differences, and then the corresponding values of the second summations of $\ddot{x}$ and $\ddot{y}$ were found (Table I). The table of values of the second summation of $\ddot{x}$ for successive descending nodes was differenced until differences became irregular. The root mean square deviation from its mean of the first column of fluctuating differences, namely the third difference of the change in a revolution, divided by the root mean square of the corresponding binomial coefficients, $(20)^{\frac{1}{2}}$, gave 397, agreeing with the expected random integration error after 1 revolution.

Examination of the values of the second summations of $\ddot{x}$ and $\ddot{y}$ for the successive descending nodes shows that they change by only about one-tenth as much as in the step used in the Cowell integration and that they vary quite smoothly. We should therefore expect to be able to extrapolate about ten revolutions ahead at a time.

TABLE I. Second summations of acceleration components interpolated to the descending node.

Node	$\nabla^{-2}\ddot{x}$	$\nabla^{-2}\ddot{y}$
0	−134077976869	+ 2069940998
1	133735289678	2520546073
2	133391479167	2969471074
3	133046556723	3416713125
4	132700533639	3862268303
5	132353420496	4306133289
6	132005229411	4748305041
7	131655970775	5188780198
8	131305656519	5627555924
9	130954296522	6064629276
10	130601902932	6499997128
11	130248486429	6933657562
12	129894056534	7365607226
13	129538626436	7795843722
14	129182204634	8224364425
15	128824802246	8651166726
16	128466430283	9076248986
17	128107099157	9499608422
18	127746819617	9921243025
19	127385601002	10341150937
20	127023454194	10759329705

4. THE EXTRAPOLATION FORMULA

We seek a modification of the Adams-Bashforth formula for integration ahead that replaces the differences of the derivative by differences at a large interval of differences at a small interval.

The forward difference operator Δ is given in terms of the backward difference operator ∇ by $\Delta=\nabla/(1-\nabla)$, and the backward difference operator is connected with the differentiating operator D by

$$\nabla=1-e^{-D}.$$

Combining these formulas, we obtain

$$\Delta=\frac{\nabla}{(1-\nabla)}\frac{1}{\{-\log(1-\nabla)\}}D$$

$$=\left\{1+\frac{1}{2}\nabla+\frac{5}{12}\nabla^2+\frac{3}{8}\nabla^3+\frac{251}{720}\nabla^4+\cdots\right\}D,$$

the Adams formula giving the forward difference in terms of backward differences of the derivative.

In like manner, if $\bar{\Delta}$ is the forward difference operator at $1/n$th the step,

$$1-\nabla=(1+\bar{\Delta})^{-n},$$

and

$$\Delta=\frac{\nabla}{(1-\nabla)}\frac{1}{\{(1-\nabla)^{-1/n}-1\}}\bar{\Delta}$$

$$=\left\{1+\frac{1}{2}\left(1-\frac{1}{n}\right)\nabla+\frac{1}{12}\left(5-\frac{6}{n}+\frac{1}{n^2}\right)\nabla^2\right.$$

$$+\frac{1}{8}\left(3-\frac{4}{n}+\frac{1}{n^2}\right)\nabla^3+\frac{1}{720}\left(251-\frac{360}{n}+\frac{110}{n^2}\right.$$

$$\left.\left.-\frac{0}{n^3}-\frac{1}{n^4}\right)\nabla^4+\cdots\right\}n\bar{\Delta}$$

giving the forward difference in terms of backwa differences of the forward difference at a subinterv as indicated in Fig. 3. In particular, for $n=5$,

$$\Delta=(1+0.4\nabla+0.32\nabla^2+0.28\nabla^3+0.25472\nabla^4+\cdots)5\bar{\Delta}.$$

These formulas may be put in Lagrangian form, f any specified number of differences, just as the Cow and Adams-Bashforth formulas may. In particula stopping at the fourth difference, the last formula ma be written

$$f_{25}-f_{20}=11.2736\bar{\Delta}f_{20}-14.4944\bar{\Delta}f_{15}+13.4416\bar{\Delta}f_{10}$$
$$-6.4944\bar{\Delta}f_5+1.2736\bar{\Delta}f$$

The sum of these coefficients is five, as it should b for $n=5$.

5. THE METHOD OF INTEGRATION

We may use the foregoing formula to extrapolat ahead to descending node 25 any variable known a descending nodes 0, 1; 5, 6; 10, 11; 15, 16; and 20, 21 To define the orbit we need six values, which ar conveniently taken to be the first and second sum mations of each of the three components of acceleration since these are held with the greatest number of digits From these values we may, by successive approxi mation, find consistent accelerations and backwar differences to start a short step Cowell integratio (Cowell and Crommelin 1910) for 1 revolution, so a to obtain values at descending node 26, when th process may be repeated.

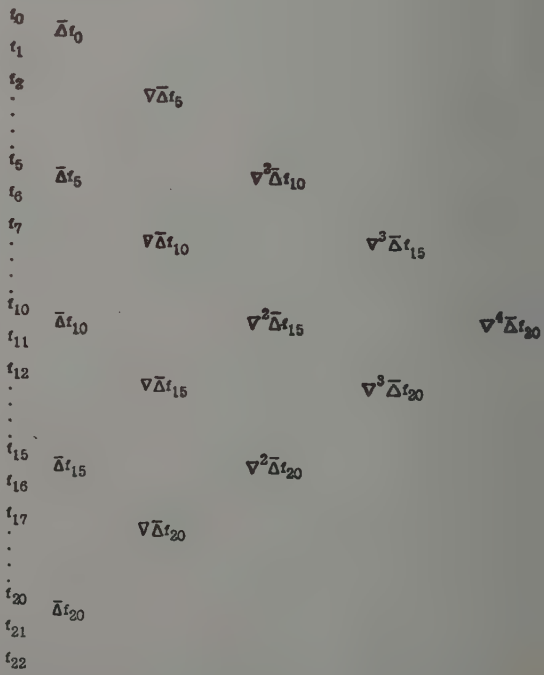

FIG 3. Table of differences for extrapolation ahead.

Our method, taken through an entire cycle, requires then the following successive calculations:

1. A Cowell formula short step integration for a single revolution.
2. An inverse interpolation to calculate the time of node crossing.
3. Direct interpolations to calculate second and first summations corresponding to the node.
4. Extrapolation ahead n revolutions of the second and first summations.
5. Successive approximations to obtain initial differences for the next short step integration.

A successive approximation scheme backwards and forwards in time from some given starting point may be used to start the whole scheme; it is not necessary to have computed 21 revolutions at a short interval. Other methods of integrating single revolutions may replace the Cowell method. Fiducial places other than the node may be used, such as apogee or perigee.

6. AGREEMENT WITH THE COMPARISON INTEGRATION

This process was carried out starting with the values for descending nodes 0, 1; 5, 6; 10, 11; 15, 16; 20, 21; given by the comparison integration, values being found for nodes 25, 30, 35, 40, $\cdots$, by the new method, (Table II) in which the last two digits have been discarded. We see that the new values of x differ from the comparison values by $+6\,800$; $-2\,200$; $+12\,300$; $\cdots$ in the last digit for nodes 25, 30, 35 $\cdots$. This is just about what would be expected. The sum of squares of the coefficients in the formula for extrapolation ahead is 560. Taking the square root, we get 24 as a factor to multiply the errors of 397 in the originally integrated coordinates. Thus a root mean square error of 9 530 would be expected in the first extrapolated coordinate.

In a long integration the mean square errors in successive extrapolations due to the error from a particular revolution partly cancel, leaving 25 (or in general n^2) instead of 560; this leads, in this case, to a total random error of $2\,000(N)^{\frac{1}{2}}$ after $5N$ revolutions.

TABLE II. Comparison of old and new values of x.

Node	Comparison value	New value	Difference
25	−1251916409	−1251916477	+ 68
26	1248241012	1248241083	+ 71
30	1233454603	1233454581	− 22
31	1229737273	1229737256	− 17
35	1214787870	1214787993	+123
36	1211030966	1211031101	+135
40	1195927833	1195927984	+151
41	1192133630	1192133795	+165
45	1176885669	1176885966	+297
46	1173056329	1173056627	+298
50	1157672049	1157672202	+153
51	1153809658	1153809825	+167
55	1138297158	1138297670	+512
56	1134403689	1134404222	+533
60	1118770678	1118771108	+430
61	1114848007	1114848446	+439
65	1099101773	1099102232	+459
66	1095151675	1095152148	+932
70	1079299077	1079299794	+717
71	1075323204	1075323950	+746

This could be improved only by integrating more exactly round the single revolutions. Note that the random error of the comparison integration is expected to be $800(N)^{\frac{1}{2}}$ after $5N$ revolutions, and keeping one more decimal digit would improve the new computation to this.

The actual total error increases steadily by 10 000 per 5 revolutions. Examination shows that the last column of differences retained in the extrapolations was irregular and that the previous column contributed about 10 000 per step. Here again improvement would require keeping more digits.

REFERENCES

Brouwer, D. 1937, *Astron. J.* **46**, 16.

Cowell, P. H. and Crommelin, A. C. D. *Greenwich Observations for 1909 Appendix* (Neill and Company, Ltd., Bellevue, England). 1910.

Thomas, L. H., 1958, *Astron. J.* **63**, 459.

Taratynova, G. P., 1958, "The motion of an artificial earth satellite in the non-central gravitational field of the earth when atmospheric resistance is taken into account," *The Russian Literature of Satellites*, Part 1, p. 74, (International Physical Index, Inc., New York). (The Runge-Kutta formula is applied to extrapolate many revolutions, treating each revolution as a differential step.)

Quantitative Tests of the Lick Observatory 120-Inch Mirror*

N. U. Mayall and S. Vasilevskis
Lick Observatory, University of California
(Received March 8, 1960)

A description and numerical example are given of the method developed for quantitative tests during the figuring of the Lick Observatory 120-in. mirror. The method represents a generalization of the Hartmann test in which the image pattern is measured in both the radial and tangential directions. Combination of the radial and tangential profiles, by imposition of closure and intersection conditions, permits the construction of a contour map and yields a complete evaluation of the concentration of light in the image. All the tests were made on stars with the telescope operated under regular observing conditions. In the most favorable test, the mirror concentrated the light as follows: 70, 95, and 97% within image diameters of 25, 50, and 100 μ, or 0.34, 0.68, and 1.35 seconds of arc, respectively. Depending on how the data are interpreted, the Hartmann constant ranges from 0.10 to 0.17 for this test.

I. INTRODUCTION

THE testing of the 120-in. mirror in the telescope was begun in July 1957, at a rather early stage of figuring the mirror by D. O. Hendrix assisted by H. R. Cowan. Knife-edge tests were made by Hendrix, and quantitative tests with a Hartmann screen were carried out by the authors. Mrs. Delia Herbig and A. G. A. Balz, J. Gibson, and A. R. Klemola took part in the measurement and reduction of the test plates.

For figuring a mirror the most convenient information is that about the actual shape of the surface, i.e., its linear departures from an ideal paraboloid. These data are particularly important for large and correspondingly flexible mirrors, where local irregularities may appreciably exceed the usual more regular zonal or astigmatic errors of small mirrors. The actual form of the surface was the primary goal of the quantitative tests from the very beginning, and for this purpose the original Hartmann (1904) method was considerably modified and refined as the testing proceeded.

In the initial stages the Hartmann plates were measured in the customary way along the radii, and radial profiles of the surface were obtained. Since the central part of the mirror is obscured by the observer's cage, the radial profiles could not be started from the center, and it was therefore assumed that the innermost unobscured zone of the mirror was at the same level and could serve as the common zero reference for all radial profiles. It soon became evident, however, that this assumption was not valid because of an appreciable astigmatism, and particularly because of local irregularities in any zone, including the innermost. After a number of trials and modifications in the fall of 1957, a method was finally worked out for deriving tangential profiles, i.e., those of concentric circular sections of the surface. From tangential and radial profiles combined, a complete contour map of the surface was obtained. This paper is a report on this method and its application.

The progress of the figuring has been reported elsewhere by Shane (1958) and by Whitford (1959).

II. HARTMANN SCREEN AND PHOTOGRAPHS

The Hartmann screen, or diaphragm, used to obtain the test plates is shown mounted on the telescope in Plate I, and the pattern of holes with respect to the mirror and its ribbed structure is shown in the composite photograph reproduced in Plate II. As may be seen in the illustration, the pattern of holes bears no regular relationship to the mirror rib structure, although the final tests indicated that a close relationship would have been more useful. All the test plates were taken at the

PLATE I. Hartmann diaphragm mounted at upper end of 120-in. reflector.

* *Lick Observatory Bulletin* No. 567.

ime focus with the simple apparatus illustrated in late III; in nearly every test, knife-edge photographs so were made with the 35-mm film camera and knife ige shown in Plate IV.

In making the Hartmann photographs, an average ocus was first visually located with the knife edge, hich was then replaced by the box shown positioned y the two knurled-headed pins in Plate III. This box as two slots for the exposures taken inside and outside ne focus; spectrograph plate holders for size $2\frac{1}{8}$- and $\frac{1}{4}$-in. plates were used. These slots are separated by in. and they locate the plate 2 in. inside and outside ne knife-edge focus to an accuracy of a few thousandths f an inch. For large zenith-distance photographs, when tmospheric dispersion would unduly elongate the nages, a filter could be placed in the beam by the slide hown in the illustration.

The Hartmann screen was constructed of sheet alumium, and considerable care was taken to locate accuately the positions of the holes. The usual instrument-hop method of scribe marks on bluing, a radius bar, ividers, and a long straight edge gave an accuracy of t least 1/64 in. for the hole centers, as judged by subequent measurement of the holes. At the time such recision seemed too extreme, but early in the testing he advantages of this accurate Hartmann screen beame apparent, and it was used as the primary standard n the comparison of the computed and measured hole attern. The latter consists of $2\frac{3}{8}$-in.-diam holes drilled in. apart on 32 radii that are spaced 11°.25 in position ngle. Holes on successive radii are staggered so that heir central distances change by 1.50 in. between adacent radii. The outermost holes are 57.25 in. from the enter, and, although there are eight, seven, or six holes

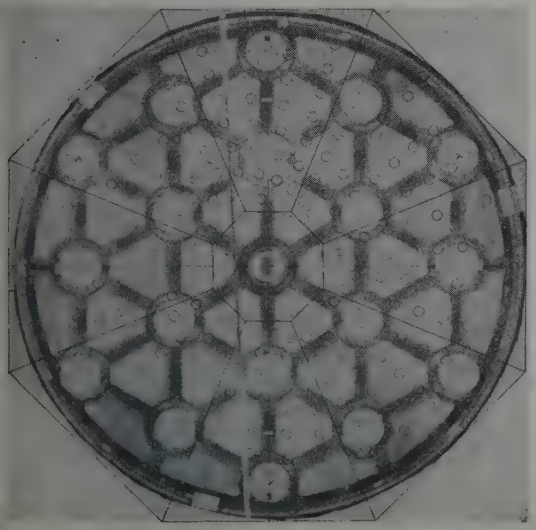

PLATE II. Composite photograph showing relationship of Hartmann-hole pattern with respect to ribbed-back structure of 20-in. mirror.

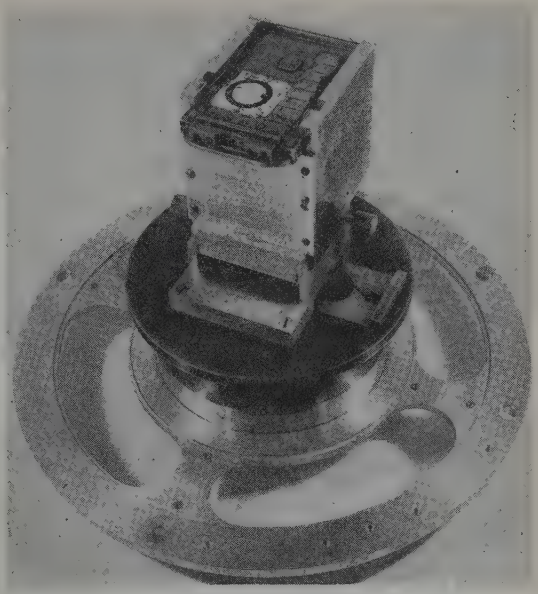

PLATE III. Plate-holder box and filter slide used to expose Hartmann test plates.

depending on the radius, usually images from only six or seven were measured because of interference from the observer's cage in the center of the telescope.

A Hartmann test ordinarily consisted of a pair of plates, each having an inside- and outside-focus exposure. The observer's cage was rotated by 120° to 180° between the two plates, in order to uncover enough holes in the screen to provide a symmetrical pattern by combination of measurements from the two plates, as described more fully in the following. Depending upon which images were better, either the inside- or outside-

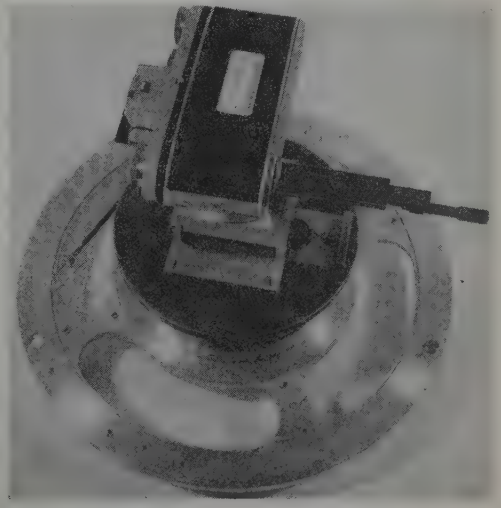

PLATE IV. 35-mm film camera and knife edge used to take knife-edge photographs.

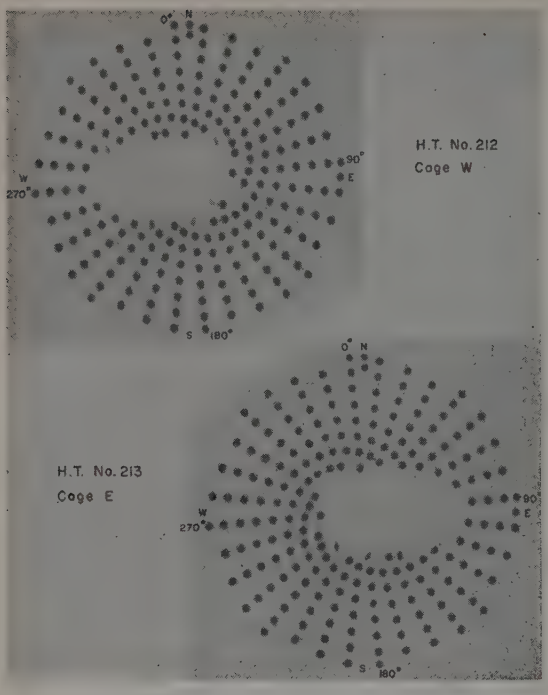

PLATE V. Reproductions of Hartmann-screen images measured on test plates taken January 3, 1959.

focus pattern was measured. Plate V is a reproduction of the January 3, 1959 plate-pair, on which the extrafocal patterns were measured. On many of these plates, the images of the eight outermost holes show radial tails, inward for inside the focus and outward for outside. These are due to the round-beveled edge of the mirror; to reduce the systematic effect, if any, on the measurements of such elongated images, these eight holes were diaphragmed to a smaller diameter for the last tests. Also, some of the images of interior holes were affected by the prime focus webs supporting the observer's cage, and by the ropes used to raise and lower the screen. None of these obstructions, however, proved to be serious in the measurement and reduction of the plates. The mirror usually was sufficiently smooth, and a large enough number of images was measured, to allow filling the gaps by interpolation.

Since nearly all the tests were made with the telescope pointed within 10° of the zenith, atmospheric dispersion had a negligible effect on the images. Thus it was possible to use an ordinary blue-sensitive emulsion for most of the plates. The exposures ordinarily ranged from 1 to 3 min, for Kodak IIa0 emulsion and for average to good seeing, as follows:

Exposure (min)	1	2	3
m_{pg}	2.9	3.7	4.1.

In poor seeing, these exposures were increased by 25 to 50%, but the image quality and measurement accuracy decreased so much under poor conditions that su testing was done only as an act of desperation.

III. METHOD

The principle of deriving profiles of the mirror surfa is shown in Fig. 1. Let SM be a ray, parallel to the op cal axis, which falls upon the mirror at M. If the mirr were a paraboloid, the reflected ray $M\sigma$ would pa through the focus; actually, an element $A'B'$ of t mirror is inclined by ϵ with respect to the element A of the ideal paraboloid, and the reflected ray will pier the focal surface at a distance $\delta=2f\epsilon$ from the focu Over a distance l of the element $A'B'$ the profile of t mirror will depart by $z=l\epsilon$ with respect to the ide paraboloid. Both relationships give

$$z=l\delta/2f. \qquad (1$$

The profile is obtained by summation of departures (of elements along a line; the determination of δ is d scribed as follows.

The distance between two adjacent holes of the sam radius on the Hartmann screen, 6 in., was assumed as basic element in the construction of the profiles. The for $f=600$ in., Eq. (1) may be written

$$z=\delta/200. \qquad (1$$

Thus, in order to detect a departure of $z=0.1\,\lambda=0.05$ from the paraboloid over a distance of 6 in., it is suf cient to determine δ with an accuracy of $10\,\mu$. Th formulas for determination of δ may be developed a follows:

In Fig. 2, C is the center of the Hartmann pattern o an extrafocal photograph, M is the center of rotation the plate carriage in the measuring engine, i.e., the origi of measured coordinates if they are obtained from dire and reverse measurements. If C is on the optical axi then the collimation error is zero, and H is the image of Hartmann-screen hole. In the presence of a collimatio

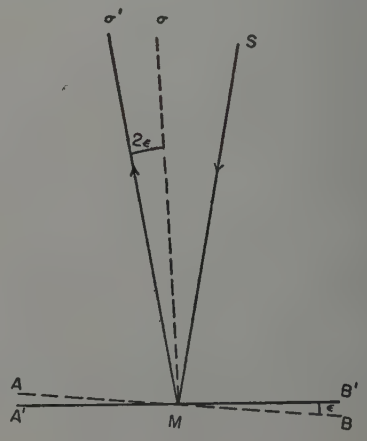

FIG. 1. Geometry and notation used for mirror element.

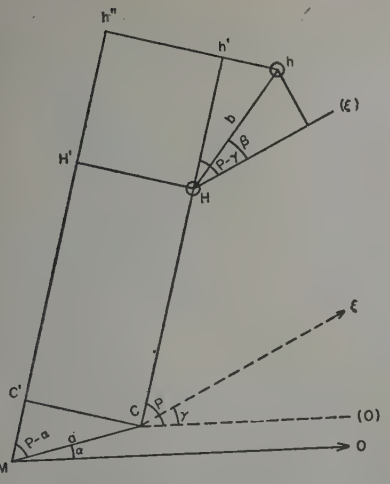

FIG. 2. Geometry and notation used in generalization of Hartmann method.

rror the image is at h; ξ is the direction from the optical xis towards C. The position angle P may be measured om an arbitrary direction MO; in testing the 120-in. irror, it was counted from a zeropoint 6° west of the orth point on the mirror. In this nomenclature, the adial r, and tangential t, displacements of h can be xpressed as

$$\begin{aligned} r &= Mh'' = CH + MC' + Hh' \\ &= (\rho + \sigma\rho) + a\cos(P-\alpha) + b\cos(P-\gamma-\beta), \\ t &= -hh'' = -CC' - hh' + \omega\rho \\ &= \omega\rho - a\sin(P-\alpha) - b\sin(P-\gamma-\beta), \end{aligned} \tag{2}$$

where the quantities in the above formulas are as ollows: ρ is the distance of the image of the hole from he center C of the Hartmann pattern on an extrafocal late. For rays parallel to the axis of a paraboloid, may be precomputed from

$$\rho = Rd/f + R^3 d/4f^3 + \cdots, \tag{3}$$

where R is the distance of a hole in the screen from its enter, f is the focal length of the paraboloid, and d is he distance of the plate from the focal plane. A table f ρ for the various holes was computed for this series f tests, and small variations in f and d were taken into ccount by introducing a scale correction, $\sigma\rho$. P is the osition angle of a hole; if the images chosen for orienta- ion are displaced due to errors in the mirror, an orienta- ion error ω will affect the tangential measurements by $\omega\rho$; a and α are polar components of the error of center- ng in the measuring engine; they may be transformed nto rectangular ones by

$$x = a\cos\alpha, \quad y = a\sin\alpha. \tag{4}$$

γ, β and b depend on the error of collimation. If X, Y are the rectangular coordinates of a hole of the Hart- mann screen, and X, as well as ξ in Fig. 2, is in the plane defined by the optical axis and the image of the star, then the linear displacement of the image of the hole is (Plummer 1898)

$$\Delta\xi = c(3X^2 + Y^2)/4f^2, \quad \Delta\eta = cXY/2f^2, \tag{5}$$

where c is the distance from the optical axis to the image of the star, i.e., to the center C. If R is the distance of the hole from the center on the screen, then

$$X = R\cos(P-\gamma), \quad Y = R\sin(P-\gamma). \tag{6}$$

In addition,

$$\Delta\xi = b\cos\beta, \quad \Delta\eta = b\sin\beta. \tag{7}$$

Combining Eqs. (5)–(7), and denoting

$$3R^2/4f^2 = \varphi, \quad u = c\cos\gamma, \quad v = c\sin\gamma, \tag{8}$$

we may write the last terms in Eq. (2) as

$$\begin{aligned} b\cos(P-\gamma-\beta) &= \varphi(u\cos P + v\sin P), \\ b\sin(P-\gamma-\beta) &= \frac{\varphi}{3}(v\cos P - u\sin P), \end{aligned} \tag{9}$$

where u and v are the rectangular components of the collimation error.

With the aid of Eqs. (4) and (9) the relationships, Eq. (2), may be transformed into

$$\begin{aligned} x\cos P + y\sin P + u\varphi\cos P \\ + v\varphi\sin P + \sigma\rho = r - \rho = \Delta r, \\ -x\sin P + y\cos P - u\frac{\varphi}{3}\sin P + v\frac{\varphi}{3}\cos P + \omega\rho = t. \end{aligned} \tag{10}$$

Radial and tangential measurements of each hole give the two equations, Eqs. (10), with six unknowns x, y, u, v, σ, and ω which may be found by a least squares solution from measurements of all the holes. The normal equations are much simplified by the symmetrical pattern of the screen. If weights ρ, proportional to the areas of zones represented by each hole, are assigned to Eq. (10), then the normal equations are:

$$\begin{aligned} [\rho]x + \frac{2}{3}[\varphi\rho]u &= [\Delta r\rho\cos P] - [t\rho\sin P], \\ \frac{2}{3}[\varphi\rho]x + \frac{5}{9}[\varphi^2\rho]u &= [\Delta r\varphi\rho\cos P] - \frac{1}{3}[t\varphi\rho\sin P], \\ [\rho]y + \frac{2}{3}[\varphi\rho]v &= [\Delta r\rho\sin P] + [t\rho\cos P], \\ \frac{2}{3}[\varphi\rho]y + \frac{5}{9}[\varphi^2\rho]v &= [\Delta r\varphi\rho\sin P] + \frac{1}{3}[t\varphi\rho\cos P], \\ [\rho^3]\sigma &= [\Delta r\rho^2], \\ [\rho^3]\omega &= [t\rho^2]. \end{aligned} \tag{11}$$

The coefficients on the left-hand side of Eqs. (11) may be computed for a series of tests, if for all tests measurements of the same set of holes are used in the solution. In the initial stages of figuring, every other radius was measured, but later, in 1958–1959, six holes were used on all 32 radii of the screen.

The solution of Eqs. (11) gives a best-fitting paraboloid to the mirror surface under the condition that the sum of squares of deflections of rays from the focus is a minimum. The computed values of the unknowns, inserted into Eq. (10) for each hole, then give the positions of corresponding images if they were formed by an ideal mirror; comparison of these computed positions, Δr_c and t_c, with the measured ones, Δr and t, give the radial and tangential components of deflections, which are proportional to the slopes of the actual surface with reference to an ideal paraboloid. It should be emphasized that only a sampling of the surface is obtained, and that assumptions have to be made regarding the surface between the holes. The simplest assumption is that the slope remains constant halfway towards the next hole in every direction. Thus, by successive summation of Eq. (1), profiles are obtained; usually, however, a smooth line is drawn instead of a trapezoidal profile. Whenever it was necessary, the knife-edge photographs were used for qualitative interpolation between the holes.

If both radial and tangential measurements are made, there are available two kinds of indication of reliability of the profiles obtained. First, each tangential profile has a point of intersection with every radial one, and vice versa; consequently, agreement between profiles at the intersections permits one to evaluate the accuracy of the results. Second, the closures of the tangential profiles serve as an additional check on measurement, on computation, and on the smoothness of the mirror, because large local nonrandom irregularities may give large closure errors. In the early stages of figuring, the departures from these conditions were much larger than later, when the surface became more regular.

It should be mentioned that this method does not require the measurement of plates taken on both sides of the focus; either of them will give the same result by reversing the signs of δ. The principle of the method is a comparison of the measured Hartmann pattern with that computed for an ideal paraboloid. The only requirement is that the holes in the screen should be placed with a sufficiently high precision, or that the errors of the screen should be known. To estimate the tolerance, we differentiate the first part of Eq. (3), which gives

$$\Delta\rho = d\Delta R/f, \tag{12}$$

or, for $f=600$ in. and $d=2$ in.,

$$\Delta\rho = \Delta R/300. \tag{12'}$$

The holes were placed radially and tangentially with an accuracy of at least 1/64 in. = 0.4 mm, which radially corresponds to $\sim 1\,\mu$. This accuracy is more than sufficient, as inspection of Eq. (1′) shows that a 1-μ error δ corresponds to a surface accuracy of $\sim 0.001\,\lambda$. One radius, however, as Hendrix discovered in the process of testing, was systematically displaced tangentially by a small angle. Thus the tangential measurements on this radius were corrected, by amounts ranging from 4 to 26 μ.

Finally, this method may be considerably simplified if only radial profiles are required. In this case formulas (10) and (11) may be rewritten

$$x\cos P + y\sin P + u\varphi\cos P + v\varphi\sin P + \sigma\rho = \Delta r, \tag{10}$$

and

$$\begin{aligned} [\rho]x + [\rho\varphi]u &= [\Delta r\rho\cos P], \\ [\rho\varphi]x + [\rho\varphi^2]u &= [\Delta r\rho\varphi\cos P], \\ [\rho]y + [\rho\varphi]v &= [\Delta r\rho\sin P], \\ [\rho\varphi]y + [\rho\varphi^2]v &= [\Delta r\rho\varphi\sin P], \\ [\rho^3]\sigma &= [\Delta r\rho^2]. \end{aligned} \tag{11}$$

These formulas may be generally used if there is evidence, or reason to believe, that tangential profiles are flat. In testing the 120-in. mirror, when the figuring between tests was such that its effect on the surface could be determined from comparison of radial profiles only, these simplified formulas were used. Also, if the mirror is collimated with a sufficient precision before testing, formulas (11) or (11′) become extremely simple because $u=v=0$.

IV. NUMERICAL EXAMPLE

The test of January 3, 1959, will be described in some detail as an example of the use of this method. Since the obscuration of the mirror by the oval-shaped observer's cage is unsymmetric with respect to the optical axis, each test measurements were made on two plates taken with opposite directions of the cage. The figures for covered holes on one plate were then filled from measurements of images of the corresponding holes on the other plate; measurements of common holes were used for this reduction. Since images from only a few inner holes on a few radii were missing, and since the weight of these inner holes is small, results from each of the two plates may be considered as independent; hence measurements from each were separately reduced. Comparison of the deflections obtained for corresponding images on each plate provided a good check on all the measurements and computations. After this check was made, means of the two deflections for each hole were formed and used to obtain the profiles.

Each plate was measured with a separate Gaertner single-screw engine having graduated circles for setting of position angles to 0°.01. Measurements in the radial direction of the pattern were made in the usual manner by successive settings on images of a diameter aligned horizontally parallel to the screw. In the tangential

TABLE I. Radial deflections and profiles.

Radius	P	Hole	D	R	r	Δr	Δr_c	δ_r	$\bar{\delta}_r$	$\Sigma \bar{\delta}_r$
8	90°	1	19.620	29.115	9.495	+205	+15	−190	−188	−180
		2	20.016	28.726	8.710	+ 14	+ 6	− 8	− 6	+ 8
		3	20.509	28.234	7.725	− 6	− 1	+ 5	+ 2	+ 14
		4	21.006	27.735	6.729	− 13	− 7	+ 6	+ 6	+ 12
		5	...	...	5.727	− 14	−12	+ 2	+ 6	+ 6
		6	...	...	4.705	+ 6	−16	− 22	− 18	+ 18
		7	...	...	3.718	− 9	−18	− 9	− 4	+ 22
24	270°	7	22.521	26.214	3.693	+ 16	+ 4	− 12	− 12	+ 38
		6	22.021	26.719	4.698	+ 13	− 2	− 15	− 15	+ 26
		5	21.511	27.223	5.712	+ 1	−10	− 11	− 11	+ 11
		4	20.999	27.737	6.738	− 22	−19	+ 3	+ 4	+ 4
		3	20.496	28.246	7.750	− 31	−29	+ 2	+ 6	+ 10
		2	19.983	28.755	8.772	− 48	−40	+ 8	+ 8	+ 18
		1	19.513	29.225	9.712	− 12	−51	− 39	− 44	− 26

direction, settings were made on images of a diameter aligned approximately perpendicular to the screw. Two images of the same two holes were used for orientation of both plates, and the plates were rotated by 11°.25 between succesive diameters. An error in position angle rotation ΔP enters directly into the tangential measurements, and its effect is

$$\Delta t = \rho \Delta P. \tag{13}$$

Since the maximum value of ρ was less than 5 mm, an error of 0°.01 in rotation produces an error $\Delta t < 1\,\mu$, which is negligible.

Table I shows radial measurements and computed deflections for one diameter ($E-W$). The first column gives the identification numbers for radii; they were numbered from 0 through 31. Next follows the position angle P, measured from N towards E, and then the identification numbers for holes, counted from outside towards the center. Although seven holes on each, except the shortest, radius were measured, only six were used in the least-squares solution. On long diameters, as in Table I, measurements for the outer holes were not used in forming the normal equations; on short diameters all six holes were used, and on intermediate diameters, the inner holes were omitted. This selection was made in order to avoid occasional image irregularities near the edge of the mirror and grazing-beam distortions due to the observer's cage.

D and R in Table I are the actual measurements in millimeters in the direct and reverse positions of the plate. $R-D=r$ is the measured distance, as defined by Eqs. (2) and (10); it is left in units of 0.5 mm in order to avoid a division of each difference by two. Holes five, six, and seven on radius eight are obscured by the cage; hence, the corresponding values for r are filled in from measurements from the other plate.

Then follows $\Delta r = \rho - r$; the difference is taken in the opposite sense as compared with Eq. (10), because the plate was taken outside the focus—Eq. (10) was derived for a plate inside the focus. In this and the remaining columns the units are 0.5 μ.

The next column gives Δr_c, the computed value of Δr; its computation will be shown later. Then follow radial deflections $\delta_r = \Delta r_c - \Delta r$; they are positive when the actual normal is inclined towards the optical axis, with reference to the normal of the ideal paraboloid. Then comes $\bar{\delta}_r$, the mean of the deflections obtained from both plates, and, finally, $\sum \bar{\delta}_r$, which is the radial profile referred to an arbitrary zero level indicated by the horizontal line.

In accordance with the foregoing definition of the sign of δ_r, deflections have to be added with their corresponding signs when summed outward, or, the signs must be changed, if the summation is done towards the center of the mirror. Usually the zero level of a profile was chosen so as to make most of the profile positive; large negative values ordinarily were left to indicate a sharply turned-down edge. The horizontal lines indicate not only the arbitrary zero level, but also the change of direction of summation. Since the units are 0.5 μ, 200 units in $\sum \bar{\delta}_r$ correspond to 1 λ (5000 A) in the profile, as can be found from Eq. (1′).

Table II shows tangential measurements for the same

TABLE II. Tangential deflections.

Radius	P	Hole	D	R	t	t_c	δ_t	$\bar{\delta}_t$
8	90°	1	0.362	0.393	+31	+18	−13	−14
		2	0.361	0.393	+32	+21	−11	−10
		3	0.368	0.382	+14	+24	+10	+ 8
		4	0.367	0.391	+24	+26	+ 2	+ 2
		5	...	...	+14	+27	+13	+16
		6	...	...	+41	+28	−13	− 8
		7	...	...	+46	+29	−17	−10
24	270°	7	0.396	0.362	−34	−21	+13	+13
		6	0.386	0.369	−17	−18	− 1	− 2
		5	0.383	0.376	− 7	−15	− 8	−10
		4	0.382	0.374	− 8	−12	− 4	−14
		3	0.385	0.366	−19	− 8	+11	+ 6
		2	0.381	0.370	−11	− 3	+ 8	+ 3
		1	0.383	0.378	− 5	+ 2	+ 7	+ 8

TABLE III. Mean tangential deflections and profiles.

Radius \ Zone	1	1A	1B	1C $\bar{\delta}_t$	1C $\Sigma\delta_t$	2	2A	2B	2C $\bar{\delta}_t$	2C $\Sigma\delta_t$	3	3A	3B	Corr. $\Sigma\delta_t$ 1C 1.759	Corr. $\Sigma\delta_t$ 2C 1.56
0	−12			(− 3)	+49	0			(−12)	+53	−16			+86	+83
1		−10		(−11)	38		−12		(−12)	40		−13		67	63
2			+11	(+ 8)	46			0	(− 1)	38			− 4	81	59
3				−18	28				+ 4	41				49	64
4	+ 6			(−12)	16	−18			(− 4)	36	0			28	56
5		−12		(− 2)	14		+ 7		(− 4)	31		−16		25	48
6			− 8	(− 8)	6			−10	(− 8)	22			− 2	11	34
7				+ 3	9				+ 4	25				16	39
8	−14			(−11)	− 2	−10			(+ 4)	28	+ 8			−4	44
9		+40		(+35)	+33		+30		(+24)	51		+18		+58	80
10			+12	(+10)	43			+ 5	(+ 6)	56			+11	76	88
11				+ 6	49				+ 5	60				86	94
12	0			(− 4)	45	− 6			(− 8)	51	− 8			79	80
13		−32		(−39)	6		−46		(−48)	2		−50		11	3
14			−18	(−17)	−11*			−13	(−13)	−12*			−14	−19	−19
15				+ 5	+ 5				+ 5	+ 4				+9	+6
16	−14			(− 4)	1	0			(+ 4)	7	+ 6			2	11
17		+41		(+33)	34		+25		(+26)	32		+26		60	50
18			+ 5	(+ 8)	42			+16	(+14)	45			+10	74	70
19				+ 7	49				+ 8	52				86	81
20	− 9			(+ 8)	57	+14			(+11)	62	+10			100	97
21		− 7		(− 4)	53		− 2		(+ 2)	63		+ 5		93	98
22			+ 8	(+ 5)	58			− 5	(− 5)	57			− 6	102	89
23				−11	47				− 8	48				83	75
24	+ 8			(+ 4)	51	+ 3			(+ 5)	52	+ 6			90	81
25		− 6		(− 6)	45		− 7		(− 8)	43		− 8		79	67
26			− 2	(+ 2)	47			+14	(+12)	54			+ 7	83	84
27				+24	71				+ 4	57				125	89
28	+24			(+ 8)	79	+ 2			(+ 6)	62	+ 8			139	97
29		− 3		(0)	79		+ 2		(0)	61		− 1		139	95
30			−11	(− 9)	70			− 2	(− 5)	55			−14	123	86
31				−18	52				+12	66				91	103
		Closure		−11					+20						
		Corr.		0					−32						
		* Adj. Closure		−11					−12						

diameter as given in Table I, and the column headings are self-explanatory. The sign of δ_t has been chosen so that tangential deflections are positive when the normal is inclined away from the direction of motion when going along the tangential profile clockwise as seen from above the mirror, i.e., *NESW*.

Tangential profiles were computed on a separate sheet, part of which is shown in Table III. As previously mentioned, the screen holes are staggered so that on adjacent radii they are closer to the center by 1.50 in., and this pattern repeats itself every four radii. The zones of the holes of the shortest radii were chosen for the tangential profiles; these radii have only six holes each. Derivation of only two profiles is illustrated in Table III. Each column contains the mean deflections $\bar{\delta}_t$ from both plates. To make use of all radii, the deflections corresponding to the zones chosen were obtained by horizontal interpolation; these deflections are given in parentheses. A Hartmann screen with no staggering of the holes would have been more convenient for the method developed here.

The sums of all the deflections for the two zones is given at the bottom of the completely-filled columns; they are the closure errors of the zones. If this error i larger than 16 units, a multiple of 32 is added to o subtracted from it, so as to have the final closure bette than 16 units (8 μ). The added or subtracted multipl is distributed equally to each deflection in the process o summation, which yields the profiles in the secon columns under zones 1C and 2C. The arbitrary zer levels are indicated by the lines near the middle of th columns.

Since the tangential summation is done over curvi linear intervals of $l_t = 2\pi R/32$, then if R is the radius o the zone, the figures for profiles have to be multiplie by a factor $l_t/6 = \pi R/96$ in order to obtain the sam vertical scale as that for radial profiles integrated ove intervals of 6 in. These factors and the profiles wit adjusted scale are given in the two last columns o Table III.

Before the plots of the profiles are shown and dis cussed, we describe briefly the computation of Δr_c an t_c. Formulas (11) were used for this purpose, and th numerical results are shown in Table IV. In order t have more convenient values of the coefficients in th least-squares solution, ρ and φ have been replaced by

$=\rho/10$ and $\varphi_1=100\,\varphi$. When these quantities ρ_1 and φ_1 are used in Eq. (10), the values for Δr_c and t_c are obtained by inserting into Eq. (10) the figures for x, y, u, v, σ, and ω, given in Table IV. To calculate the collimation error, c, from Eq. (8), however, the values of u and v in Table IV have to be multiplied by 100/2 in order to obtain the correction in millimeters. Thus, in the test of January 3, 1959, the most probable position of the optical axis, with respect to the Hartmann pattern center, was distant by $[(4.2)^2+(3.65)^2]^{\frac{1}{2}}=5.6$ mm in position angle $\tan^{-1}(3.65/4.2)=42°$.

Figures 3 and 4 show the radial and tangential profiles, respectively. Originally, each of the profiles was drawn in broken line, with reference to an arbitrary zero level; these levels are indicated by the short horizontal lines crossing the vertical center line for radial profiles, and at the beginning of the tangential profiles. The next step is to find a common zero level for all the radial and tangential profiles, and, finally, to reconcile them so that, at any intersection, the radial and tangential profiles cross at the same level.

Table V shows the adjustment of levels for two of the six zones; the units, as before, are 0.5 μ. Columns under T give the elevation of tangential profiles above arbitrary levels at each crossing with a radial profile; these elevations were read from Fig. 4 at the vertical marks for radii. The columns under R give the same information for the radial profiles; these elevations were read from Fig. 4 at each tangential profile marked there. $T-R$ is the difference between the arbitrary zero levels of the radial profiles and the corresponding tangential ones. The mean differences, $\langle T-R\rangle_{\text{av}}$, at the bottom of corresponding columns, give the difference between the mean level of all the radial profiles and the level of the particular tangential profile. Since each tangential profile has a different level, a common level was chosen so as to have all the profiles above this level. The figure for this level is shown as *Adopted* under $\langle T-R\rangle_{\text{av}}$; then $\Delta=Adopted-Mean$ is the difference between the original arbitrary level of a tangential profile and the new adopted one, which is common for all the profiles. This common zero reference is shown by a horizontal line under each profile in Fig. 4.

The next column, $T-R+\Delta$, is the difference between the original levels of the radial profiles and the adopted common one. In the absence of errors of measurement and of irregularities of the mirror surface, these differences would be the same for a particular radius at every tangential profile. Since this is not the case, the mean, $\langle T-R+\Delta\rangle_{\text{av}}$, was formed for each radius. It is given in the last column of Table V. This mean then was used to draw the horizontal lines of the common zero level in Fig. 3.

In order to reconcile the profiles at all intersections, the elevations of the tangential ones were read from the adopted common level in Fig. 4 for each radius, and were marked as crosses in Fig. 3. Then the final radial profiles were drawn as solid lines halfway between these markings and the original profiles. These final profiles then were transferred to the tangential ones, and they are shown as solid lines in Fig. 4. Comparison of the broken- and solid-line profiles shows that the profile adjustments are small or inappreciable fractions of the errors of the optical surface. Also, in one respect the averaging process is advantageous; by making the mirror seem smoother, it may help to prevent overcorrection during figuring.

The adjustment of levels and reconciliation of profiles serves as a good additional check for reliability of the test, but the procedure is necessary only when a contour map of the mirror is to be made. At the later stages of figuring, contours were drawn at intervals of 0.2 λ, as may be seen in Fig. 5. Points defining each contour were read from the tangential and radial profiles, and the contour map then always was compared with knife-edge photographs taken by cutting the beam from eight different directions. These two ways of appraising the mirror surface provided a complete picture of its figure.

TABLE IV. Solution of normal equations.

	$[\Delta r\rho_1\cos P]$	$+0.424$
	$[t\rho_1\sin P]$	$+1.197$
$A_1=[\Delta r\rho_1\cos P]-[t\rho_1\sin P]$		-0.773
	$[\Delta r\varphi_1\rho_1\cos P]$	$+0.285$
$[t\varphi_1\rho_1\sin P]=+0.395$	$\frac{1}{2}[t\varphi_1\rho_1\sin P]$	$+0.132$
$A_2=[\Delta r\varphi_1\rho_1\cos P]-\frac{1}{2}[t\varphi_1\rho_1\sin P]$		$+0.153$
	$[\Delta r\rho_1\sin P]$	$+0.553$
	$[t\rho_1\cos P]$	-0.503
$B_1=[\Delta r\rho_1\sin P]+[t\rho_1\cos P]$		$+0.050$
	$[\Delta r\varphi_1\rho_1\sin P]$	$+0.360$
$[t\varphi_1\rho_1\cos P]=-0.120$	$\frac{1}{2}[t\varphi_1\rho_1\cos P]$	-0.040
$B_2=[\Delta r\varphi_1\rho_1\sin P]+\frac{1}{2}[t\varphi_1\rho_1\cos P]$		$+0.320$

$$x=\frac{12.887A_1-33.121A_2}{533.875}=-0.028$$

$$y=\frac{12.887B_1-33.121B_2}{533.875}=-0.019$$

$$u=\frac{126.552A_2-33.121A_1}{533.875}=+0.084$$

$$v=\frac{126.552B_2-33.121B_1}{533.875}=+0.073$$

$$\sigma=\frac{[\Delta r\rho_1^2]}{66.447}=\frac{-1.234}{66.447}=-0.019$$

$$\omega=\frac{[t\rho_1^2]}{66.447}=\frac{+0.683}{66.447}=+0.010$$

V. ASTIGMATISM

The customary formulas for determination of astigmatism were modified so as to make use of numbers already obtained in the process of deriving the profiles. If a radius R on the screen is reproduced as r on the extrafocal plate at a distance d from the focus, then, to a first approximation of relation (3),

$$d=f\cdot r/R. \qquad (14)$$

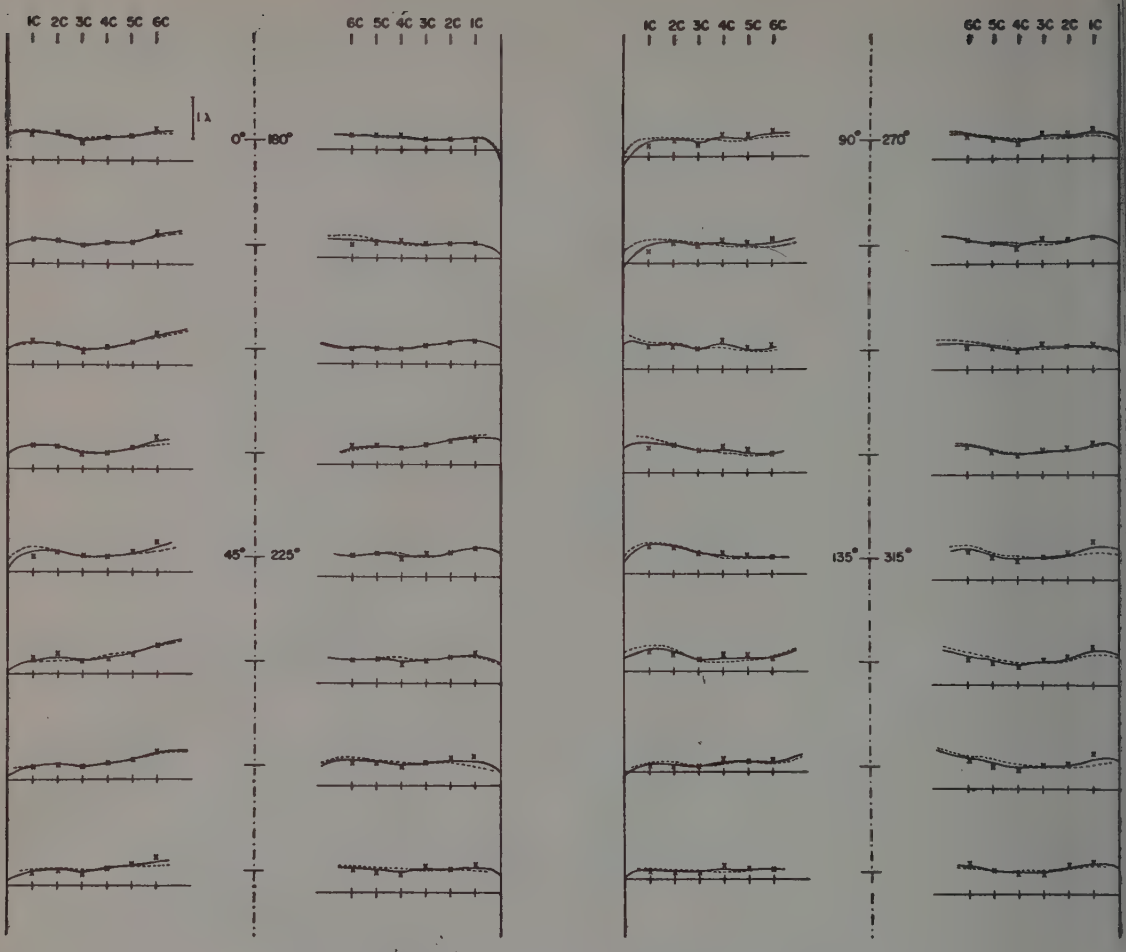

FIG. 3. Radial profiles from Hartmann test of January 3, 1959.

In the presence of astigmatism, d, f, and r are variable with orientation of R, and an increment in d is equal to that in f for a fixed position of the plate. Then differentiation of Eq. (14) gives

$$(1-r/R)\Delta f = f\cdot\Delta r/R. \tag{15}$$

For $d=2$ in. and $f=600$ in., $r/R=d/f=0.003$, and since Δf due to astigmatism is small, Eq. (15) may be rewritten

$$\Delta f = f\cdot\Delta r/R. \tag{15'}$$

The measured r's in Table I are affected by centering and collimation errors, as mentioned earlier. If measurements for pairs of two symmetrical holes of a diameter are combined, the centering and collimation errors are eliminated, as may be seen from the trigonometrical terms in Eq. (10). Since the scale effect is small and does not depend on the direction of a diameter, it may be neglected in the determination of astigmatism. Also, since an increment in r is equal to that in Δr, the latter may be used from Table I.

Errors of zones and local irregularities may give different foci for different pairs of holes of the same diameter; therefore, the mean of all values of Δr for each diameter was computed. Since the holes are staggered on consecutive diameters, errors of zones will produce different computed foci for different diameters even in the absence of astigmatism, and hence the mean focus for a common zone was computed from sums formed as follows:

Diameter	Adjusted sum, $\sum \Delta r'$
$0^{\circ}.00+n45^{\circ}$	$\Delta r_1/4+\sum_2^6 \Delta r_i+3\Delta r_7/4,$
$11^{\circ}.25+n45^{\circ}$	$\Delta r_1/2+\sum_2^6 \Delta r_i+\Delta r_7/2,$
$22^{\circ}.50+n45^{\circ}$	$3\Delta r_1/4+\sum_2^6 \Delta r_i+\Delta r_7/4,$
$33^{\circ}.75+n45^{\circ}$	$\sum_2^6 \Delta r_i.$

(16)

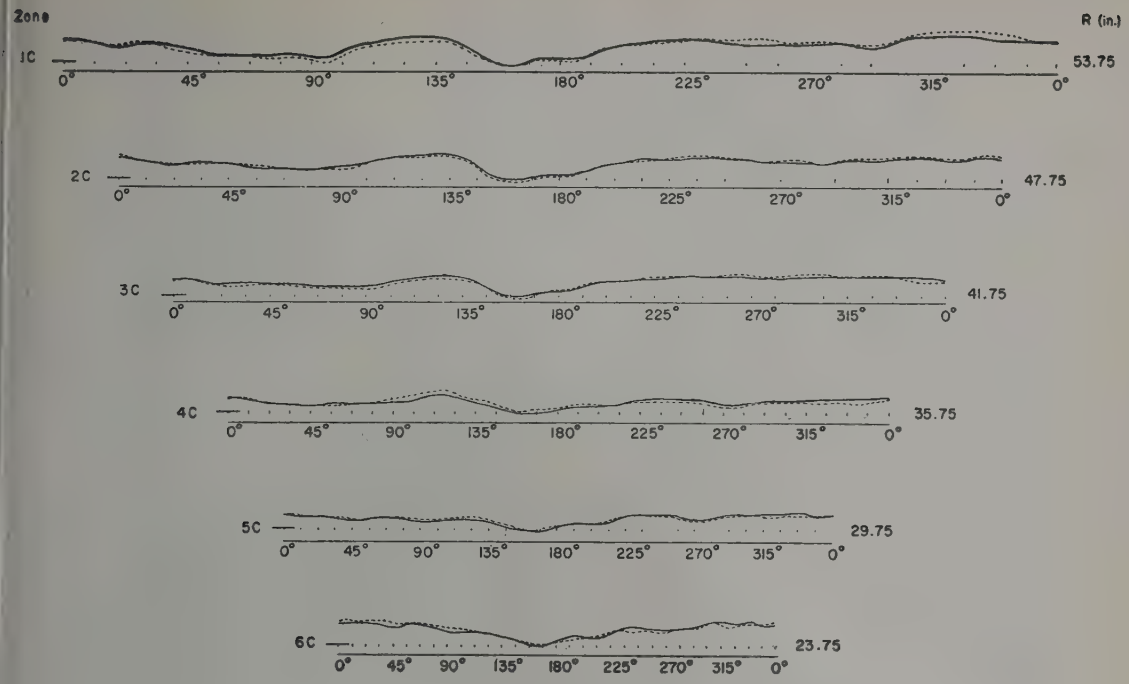

FIG. 4. Tangential profiles from Hartmann test of January 3, 1959.

TABLE V. Adjustment of levels.

Radius \ Zone	1C				2C				
	T	R	$T-R$	$T-R+\Delta$	T	R	$T-R$	$T-R+\Delta$	$\langle T-R+\Delta\rangle_{av}$
0	+90	+40	+50	+91	+100	+15	+85	+120	102
1	75	20	55	96	70	10	60	95	98
2	70	20	50	91	60	20	40	75	79
3	70	35	35	76	60	35	25	60	78
4	40	50	−10	31	60	30	30	65	72
5	25	0	+25	66	55	5	50	85	61
6	20	0	20	61	40	10	30	65	68
7	10	5	5	46	35	10	25	60	71
8	10	10	0	41	40	15	25	60	72
9	20	30	−10	31	60	30	30	65	79
10	55	45	+10	51	85	35	50	85	88
11	80	80	0	41	90	50	40	75	84
12	90	75	15	56	90	65	25	60	74
13	50	80	−30	11	45	60	−15	20	44
14	−10	20	−30	11	− 15	20	−35	0	23
15	− 5	15	−20	21	− 5	10	−15	20	31
16	+ 5	15	−10	31	+ 10	5	+ 5	40	42
17	35	5	+30	71	30	10	20	55	57
18	70	45	25	66	60	40	20	55	68
19	80	90	−10	31	75	70	5	40	52
20	95	45	+50	91	90	20	70	105	93
21	100	15	85	126	100	15	85	120	105
22	100	− 5	105	146	90	15	75	110	98
23	95	0	95	136	80	5	75	110	101
24	90	+20	70	111	80	10	70	105	88
25	85	35	50	91	75	10	65	100	90
26	75	5	70	111	75	10	65	100	95
27	105	35	70	111	90	15	75	110	100
28	135	25	110	151	90	10	80	115	102
29	140	35	105	146	100	10	90	125	105
30	130	15	115	156	90	0	90	125	104
31	110	30	80	121	95	15	80	115	103
		$\Sigma(T-R)$	1205	2517		$\Sigma(T-R)$	1420	2540	2527
		$\langle T-R\rangle_{av}$	38			$\langle T-R\rangle_{av}$	44		
		Adopted	79						
		Δ = *Adopted* − *Mean*	41			Δ	35		

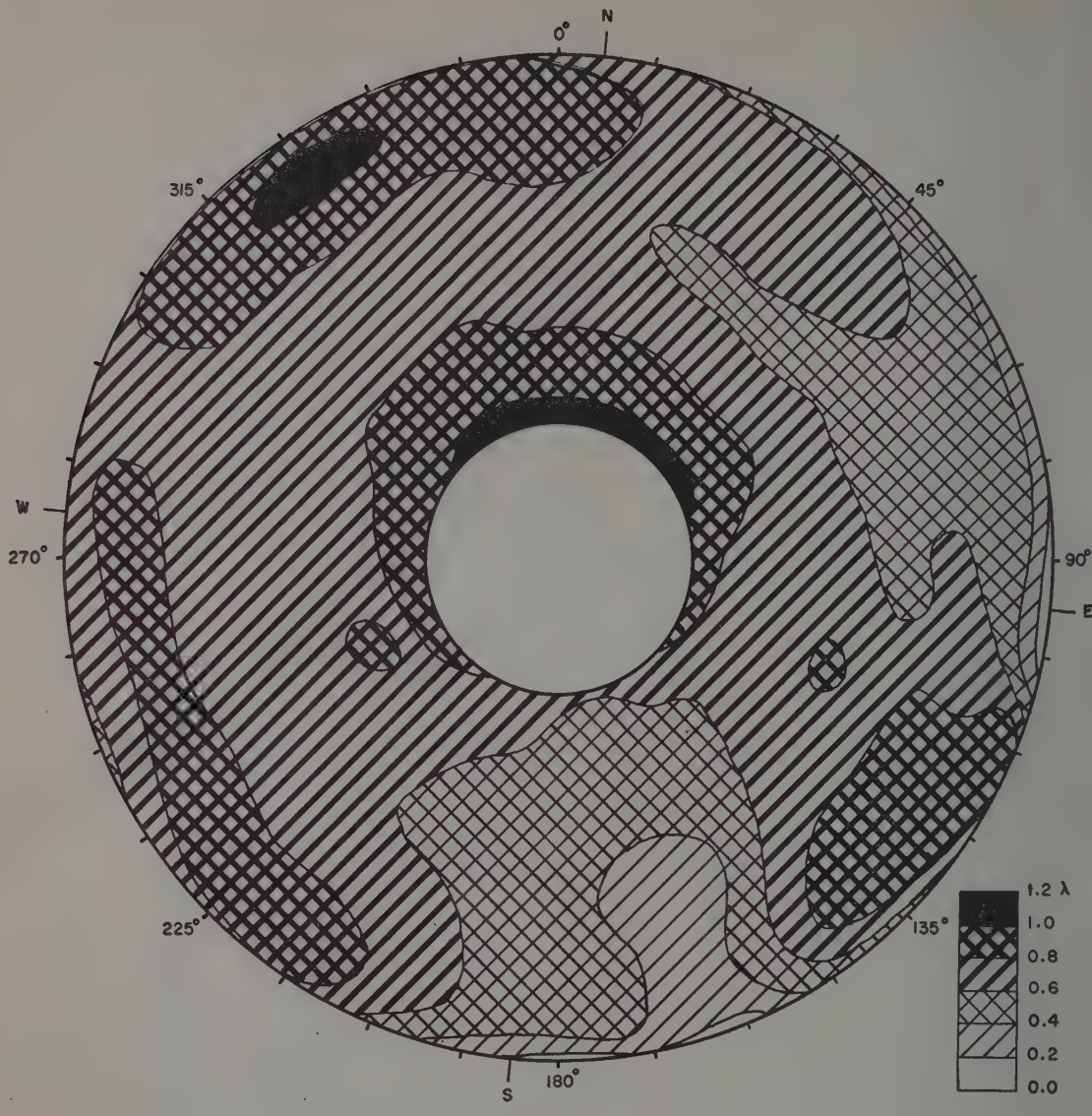

FIG. 5. Contour map, interval 0.2 λ, of optical figure of 120-in. mirror from test of January 3, 1959.

Then the astigmatism Δf was computed from

$$s=(\sum \Delta r'_P+\sum \Delta r'_{P+180°})/2\sum R,$$
$$\Delta f=(s-\bar{s})f, \qquad (17)$$

where the first formula contains in parentheses the sum formed according to Eq. (16) over the entire diameter, $\sum R$ is computed by following the same rule, $\bar{s}$ is the mean of values of s for all the diameters, and Δf is the departure of the focus of a particular diameter from the mean focus for all the diameters. The astigmatism Δf is plotted in thousandths of an inch in Fig. 6 for a few tests. It should be mentioned that astigmatism also may be computed from the radial deflections δ_r, but the method described was preferred because, since it is inc pendent of the least-squares solution, it served as additional check on the figure of the mirror represent by the profiles and contour map.

On August 12, 1957, the first determination of ast matism was made; it is shown in Fig. 6. This ast matism, with minor changes, persisted until October 2 in spite of one figuring period every week, on the av age. Since the shortest focus was along the $N-S$ dia eter, a local figuring was done in the N and S regions the mirror, and the next test, on November 2, shows t effect of this figuring. Although the focus along $N-$ became longer, the astigmatism elsewhere did n

ange appreciably in amount or character. No signifi-nt improvement was achieved by the next figuring, as own by the test of November 9.

The November 9, 1957 test was the first one when the ethod described here was used and a contour map was ade. The contour map showed quantitatively the regularities responsible for astigmatism, and the avail-bility of this information coincided with a considerable eduction in the astigmatism, as shown by the test of ovember 16. After that date there occurred only small nd irregular local fluctuations of the focus, and they id not reach the amount characteristic before Novem-er 16. The curve of January 3, 1959 in Fig. 6 is repre-ntative of the present astigmatism of the mirror.

VI. CONCENTRATION OF LIGHT AND HARTMANN CONSTANT

The information given by the testing as described bove is primarily useful in the process of figuring a irror. Although this information may also be used for decision on completion of the figuring, the distribution nd concentration of light in the image and the value f the Hartmann constant may better serve this purpose. s a graphical means of displaying this information, ne may construct a "scatter diagram" of the radial nd tangential deflections, as shown in Fig. 7 for the st of January 3, 1959. This plot indicates how well ght from some 200 points on the mirror falls within arious diameters. The same data may also be used to valuate the more quantitatively the concentration of ght, as follows: Total deflections δ given by

$$\delta = (\delta_r^2 + \delta_t^2)^{\frac{1}{2}}, \tag{18}$$

ere computed and grouped according to their size; ntervals of five units, i.e., of 2.5 μ were used for the roups. Since the amount of light represented by δ is roportional to ρ, for each δ in a group the corresponding was listed, and then $\sum \rho$ for each group was computed. his sum represents the relative amount of light falling ithin each zone of the image, and the percentage of ght for each zone or a circle can easily be computed. able VI gives the Hartmann constants and the per-ntage of light within image diameter of 25, 50, and 00 μ for some of the later tests. The selection of these nage diameters, and the calculation of the light con-ntration from radial deflections only, was suggested y I. S. Bowen's (1950) report on the final tests of the 00-in. mirror of the Hale Telescope.

If the amount of light within the various zones is ivided by the area of these zones, the distribution of ntensity within the image is obtained, and this dis-ution is shown in Fig. 8 for the test of January 3, 1959. he numbers for relative intensity are represented by ne histogram; the solid-line curve shows the smooth rn of intensity within the focal image. The intensity rops to one-half the maximum at a distance of 8 μ om the center.

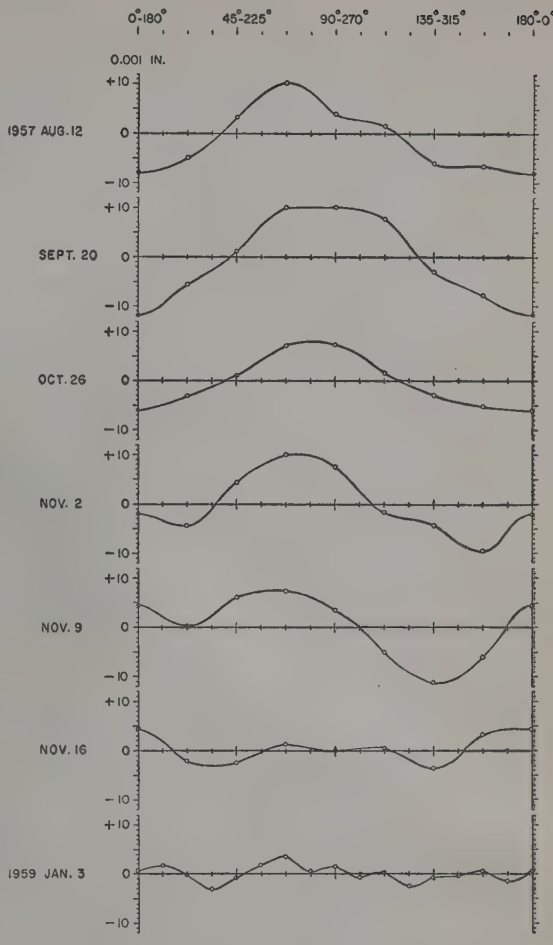

FIG. 6. Mean astigmatism curves for some representative dates.

The broken-line curve shows the intensity of light for a star one magnitude fainter than that represented by the solid line. Disregarding the seeing, we assume that for this fainter star the threshold of a photographic emulsion is reached at half the maximum intensity, i.e., the effective light forming the image is confined within the diameter of approximately 16 μ. Figure 7 shows that, for a star one magnitude brighter, the radius of the effective-light circle increases by less than 4 μ. From many investigations by Ross (1924), it follows that the minimum turbidity constant, i.e., the increase of the radius for double exposure, is of the order of 10 μ. For a Schwarzschild reciprocity exponent of $p=0.8$, the minimum increase for one stellar magnitude will be of the order of 15 μ, which is much larger than that due to the imperfect concentration of light by the mirror, in the test described. Seeing, of course, has an additional effect on the growth of the image, independent of the mirror figure.

If the concentration of light and distribution of intensity within the image are determined, the Hartmann

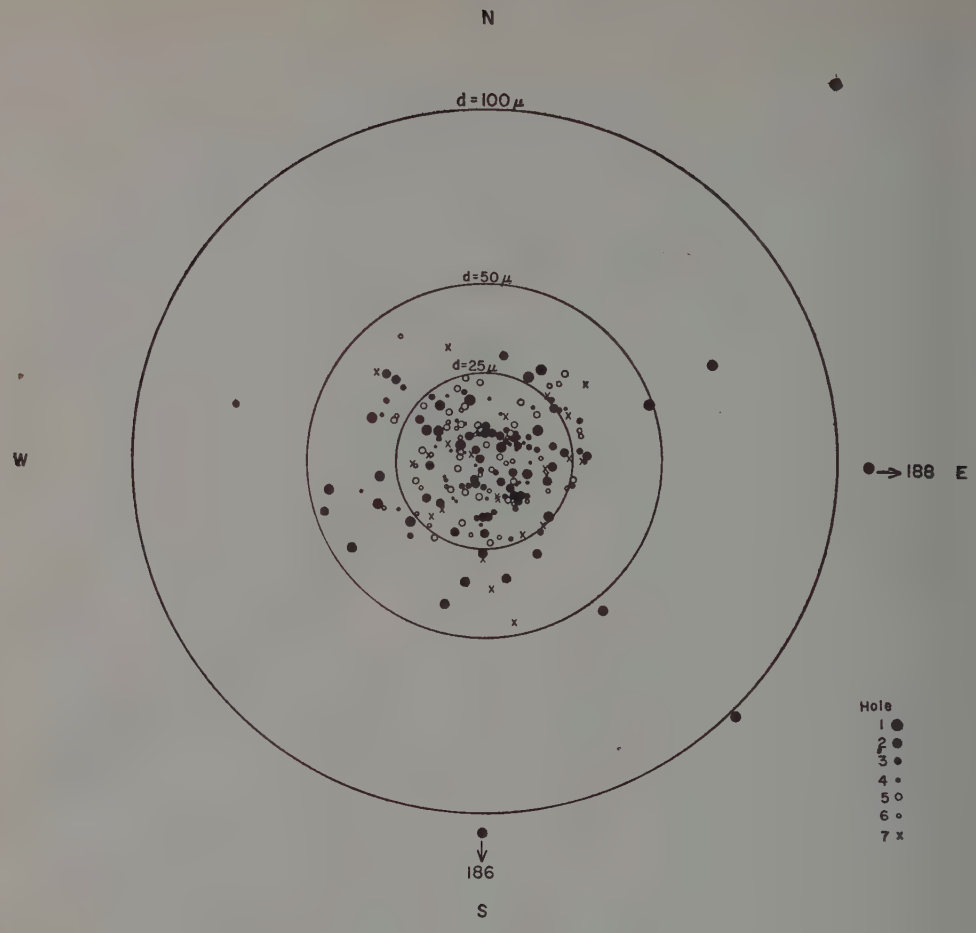

FIG. 7. Scatter diagram, in the focus, of light rays from nearly 200 Hartmann-hole areas on the 120-in. mirror for the test of January 3, 1959.

constant does not add much to this information. It was computed, however, as a traditional indicator of image quality. According to Hartmann's (1904) definition

$$T = 100\,000 \sum rd/F_0 \sum r, \qquad (19)$$

where d is the distance between images of two symmetri cal holes at radius r, on a plate in the mean focus F The same formula may be rewritten, for quantitie denoted and obtained in the process of testing describe

TABLE VI. Hartmann constants and concentration of light.

Date	Hartmann constant: Full deflections, All holes	Hartmann constant: Full deflections, Outer eight omitted	Hartmann constant: Radial only, All holes	Hartmann constant: Radial only, Outer eight omitted	Percentage of light within circle of diameter (100 μ = 1.35 sec. of arc): Full deflections, 25 μ	Full deflections, 50 μ	Full deflections, 100 μ	Radial only, 25 μ	Radial only, 50 μ	Radial only, 100 μ
1958 Aug 4	0.28	0.22	0.19	0.15	39	82	93	61	87	95
12	0.25	0.19	0.18	0.14	42	84	94	61	89	95
19	0.25	0.20	0.19	0.16	40	79	96	52	86	97
26	0.24	0.20	0.20	0.16	43	86	94	59	88	94
Nov 4	0.20	0.15	0.16	0.11	59	89	96	73	90	96
Dec 13	0.15	0.13	0.12	0.10	66	95	99	78	96	99
1959 Jan 3	0.15	0.12	0.12	0.09	70	95	97	81	96	97
May 4	0.17	0.16	0.12	0.11	48	93	99	73	96	99
9	0.18	0.17	0.12	0.10	53	92	99	76	97	99
29	0.17	0.15	0.12	0.11	56	94	99	75	97	99
June 2	0.17	0.16	0.11	0.10	53	93	99	79	96	99
14	0.17	0.16	0.12	0.10	56	95	99	76	98	99

e, as

$$T = 200\,000 \sum \rho\delta / f \sum \rho. \qquad (19')$$

ce $f = 600 \times 25\,400\ \mu$ and δ is in units of $0.5\ \mu$, we have

$$T = 0.00656 \sum \rho\delta / \sum \rho. \qquad (19'')$$

This formula was used for the computation of the rtmann constants given in Table VI. For some nths during 1958 the edge of the mirror was turned wn, and the Hartmann constant was significantly aller if the eight outer holes were omitted in the com- tation. As Table VI shows, the difference between e results for the two cases gradually decreased and ally became insignificant.

When the Hartmann constant was computed only m the radial deflections, Table VI shows that the ngential deflections, as components of total deflec- ns, have an appreciable effect on spreading the light the image. This effect may be present in every large irror, where local irregularities may be caused by homogeneous and flexible glass, and especially by local mperature distortions in the case of ribbed mirrors.

Table VI shows that the best figure of the mirror is presented by the test of January 3, 1959. No more guring was done until the second part of May, and all ie changes in the surface of the mirror through May 9 ere caused by variable temperature conditions. Some tutious local figuring was resumed after May 9, but it on became evident that the limits of improvement of ie surface were well within those of changes due to ormal variations in temperature. Therefore, after the

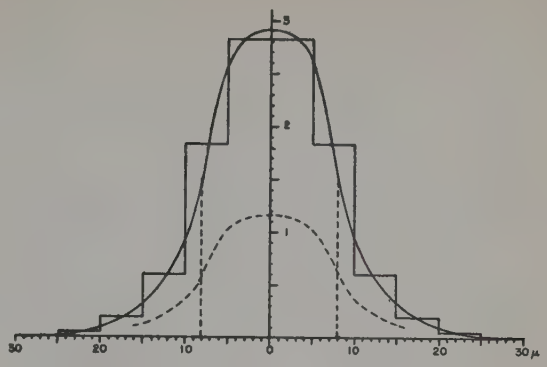

FIG. 8. Intensity of light in the image for the test of January 3, 1959.

evaluation of the test of June 14, it was decided to aluminize the mirror, and a satisfactory coat was obtained on June 24, 1959.

We wish to express appreciation to Dr. I. S. Bowen, Director of the Mount Wilson and Palomar Observatories, for making available to us data on the Hartmann tests of the 200-in. Hale Telescope.

REFERENCES

Bowen, I. S. 1950, *Publs. Astron. Soc. Pacific* **62**, 91.
Hartmann, J. 1904, *Z. Instrumentenk.* **24**, 1, 33, 97.
Plummer, H. C. 1898, *Astron. J.* **19**, 21.
Ross, F. E., 1924, *The Physics of the Developed Photograhpic Image* (New York: D. Van Nostrand Company).
Shane, C. D. 1958, *Astron. J.* **63**, 361.
Whitford, A. E. 1959, *Astron. J.* **64**, 290.

Asteroidal Fragments*

GERALD S. HAWKINS
Boston University, Boston, Massachusetts, and Harvard College Observatory, Cambridge, Massachusetts

(Received February 19, 1960)

The meteorite catalogue of Prior and Hey was used to determine the rate of fall and mass distribution of meteorites. An analysis for the United States and Europe shows that 3.3 meteorites with a mass $\geqslant 10$ kg reach the earth per day. The cumulative number with mass greater than or equal to a chosen value m varies as $1/m$. This law holds for stone finds and falls and iron falls. The iron finds include an excess of larger objects, attributed to selection effects on the ground. If this influx has been constant, the earth has collected the equivalent of an asteroid 14 km in diameter during the last 5×10^9 years. It is estimated that the aster consist of 16.7% by weight of nickel-iron, indicating a mary object that before breakup was intermediate in between the moon and Mars. The space density of meteorite shown to vary as (radius)$^{-4}$ and the total mass of meteorites v radius between 1 cm and 1 km is at least 5.6×10^{-24} g cm^{-3}. size distribution of particles produced by the crushing of roc similar to that found for meteorites and suggests that meteor undergo a considerable number of collisions in space.

INTRODUCTION

IF we accept the thesis that meteorites are remnants of a collision between two or more asteroids, then a study of meteorites will yield data on the original asteroids and will lead to an understanding of the collisional process in which they were destroyed. Meteorites are, of course, rare objects; and it is also rare for a person to see a meteorite enter the atmosphere and to witness its fall. Nevertheless, during the past 150 years enough information on meteorites has accumulated to justify some preliminary statistical research. This paper attempts to derive data on asteroids and asteroidal collisions from a study of meteorites.

The catalogue of Prior and Hey (1953) gives details on meteorites from all the continents of the world except Antarctica. The author considers this catalogue to be the most comprehensive and reliable one now available, and has used it as the primary source of data for the analyses that follow.

MASS DISTRIBUTION

The catalogue gives an account of 1447 meteorites from which a reliable estimate could be made of the mass of the material recovered at the surface of the earth. To determine the mass distribution it was convenient to choose a logarithmic sampling interval. That is to say, the meteorites were divided into categories according to mass as follows: 1.0 to 4.9 g, 5.0 to 24.9 g, 25.0 to 124.9 g, . . . , where the mass in each succeeding category increases by a factor of 5. The mass distribution was obtained separately for each of four classes of meteorites. The first division, into two groups, separated the meteorites composed almost entirely of iron from those composed of stony material; pallasites were grouped with the stones amd mesoiderites with the irons. Each of the two groups was then subdivided into "falls" (meteorites that were actually seen to fall), and "finds" (meteorites found on the earth's surface or in the subsoil).

* The research in this document was supported jointly by the United States Army, Navy, and Air Force under contract with the Massachusetts Institute of Technology.

The distribution of mass in the four classes is sho in Figs. 1 and 2, where we plot the number, N, meteorites with mass greater than or equal to a cho value, m kg. As the mass m increases, the distribut curve approaches a gradient of -1.0 ± 0.3 for classes except iron "finds." Thus we may write

$$\log N = N_0 - s\log m,$$

where logarithms are to the base 10, $s=1.0\pm0.3$ a N_0 is a constant. The curvature of the distribution small values of m is due to several causes. A sm meteorite, weighing a few grams, is not easily recover Even if an observer witnesses its entry into the atm phere, the specimen makes a relatively inconspicuo addition to the countryside. Smaller meteorites a probably dissipated by ablation in the atmosphe Although a large object, weighing several tons, mig lose less than 50% of its material by vaporization, smaller object loses a considerably greater fracti The mass distribution of the iron "finds" is anomalo in that the gradient is -0.5. This group therefore co tains a higher proportion of large objects. Since t gradient for iron "falls" is -1.0, we may presume th the discrepancy results from observational bias—lar

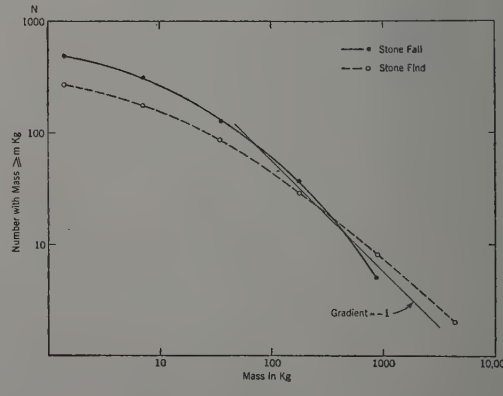

FIG. 1. The cumulative mass distribution of stone meteorites

n objects are more easily discovered, and they ather less rapidly than do large stone specimens. Equation (1) represents the mass distribution of teorites after passage through the earth's atmos-ere. To deduce from this the mass distribution of teorites in interplanetary space requires a correction the effects of ablation and fragmentation in the nosphere, and a correction for any selective bias that nherent in the original data. It is probably fair to ume as an approximation that these effects are in-endent of the mass of the object, at least for the ear portion of the observed distribution. Equation may then be taken to represent the mass distribu-n of asteroidal fragments, and we may write

$$\log N = N_\infty - s \log m_\infty, \qquad (2)$$

ere N_∞ is a constant, s defines the mass distribution, d m_∞ is the mass of the meteoroid in space. Differ-iation of Eq. (2) yields the incremental law,

$$dN = C d\rho/\rho^{3s+1}, \qquad (3)$$

ere C is a constant and ρ is the radius of the asteroid, sumed to be a spherical fragment. The quantity dN presents the number of meteorites with radii between nd $\rho+d\rho$. The mean value of the exponent in Eq. (2) therefore -4.0 and the limits of uncertainty are 3.1 and -4.9. One may deduce from direct observa-n of the asteroids an inverse 4th-power dependence d the exponent varies from -2.8 to -4.6 within the eroid zone. The meteorite (Hawkins 1959) and eroid (Kuiper *et al.* 1958) observations are therefore fair agreement and indicate that the exponent in the ius distribution law [Eq. (3)] is close to -4.0. otrowski (1953) deduced on theoretical grounds that q. (3) should show an inverse 3rd-power dependence radius if the number of collisions between the eroids has not been large.

It is of interest to estimate the relative abundance stone and iron fragments among the asteroids. To oid the problems associated with differential effects

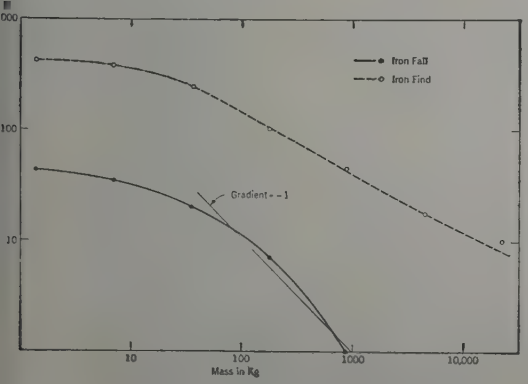

FIG. 2. The cumulative mass distribution of iron meteorites.

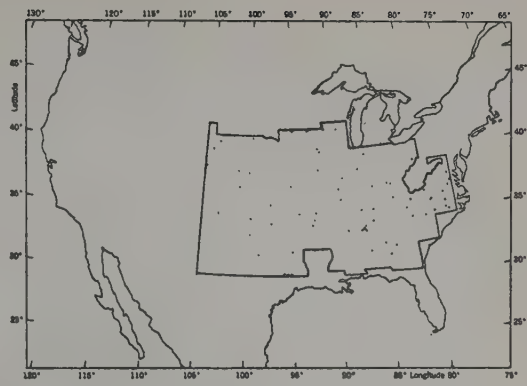

FIG. 3(a). Observed falls in United States.

FIG. 3(b). Observed falls in Europe.

of weathering, I have considered only the witnessed "falls." Figure 1 represents 590 stones with a total mass of 1.349×10^4 kg. Figure 2 gives the data for 50 iron falls with a total mass of 2.699×10^3 kg. The figures indicate that stony asteroids out-number the irons in the ratio 11.80:1, and that the mass of the asteroids comprises 16.7% of nickel-iron.

NUMBER OF METEORITES IN SPACE

Before estimating the number of meteorites per unit volume in the space surrounding the earth we must determine the influx rate at the surface of the earth. The catalogue of Prior and Hey (1953) gives the latitude, longitude, and date of observed falls. For this analysis I have chosen two areas where the terrain is mostly unforested and cultivated intensively. The first area is in the United States east of the Rocky Mountains; the boundaries are shown in Fig. 3(a); the second area covers most of Europe and is shown in Fig. 3(b). On these maps each dot represents the location of a meteorite fall. The number of falls observed per decade is shown in the histograms of Figs. 4(a) and 4(b). The number of falls observed per decade is clearly not constant in either area. This variation results in part from

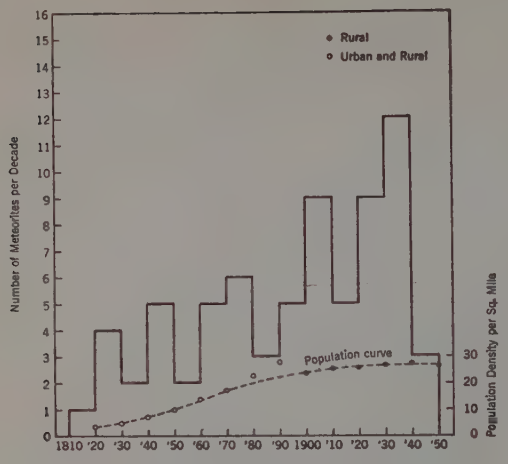

FIG. 4(a). Meteorite falls per decade in United States, and number of people per sq. mile.

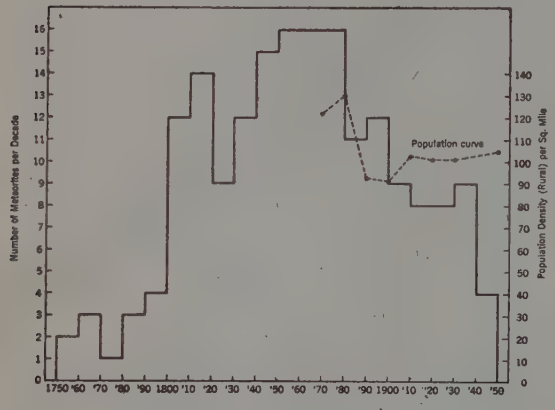

FIG. 4(b). Meteorite falls per decade in Europe, and number of people per sq. mile in England and Wales.

the irregular occurrence of meteorites but mostly from the changing numbers of people living in the selected area. The number of nonurban people living within the selected area is indicated in Fig. 4(a) and 4(b), which show that the number of falls observed per decade in the United States is apparently correlated with the size of the population, although the increase in observed meteorites is not so pronounced as the increase in population. The only figures on population growth readily available for Europe are those for the British Isles, but we may assume that these numbers are representative of Europe. The correlation between meteorite rate and density of population is present in Europe, but is not so good as in the United States; therefore, additional factors must be present. We can probably account for the sudden increase in the number of falls in 1800–1810 by the fact that the fall of stones at L'Aigle was authenticated by a scientific investigation. The phenomenon was given considerably publicity and the French Academy officially recognized

TABLE I. Rate of meteorite falls.

	Europe	United St
Mean number per decade	4.18	5.14
Peak number per decade	16	12
Area (sq km)	4.05×10^{6}	2.95×10
Mean influx (kg km^{-2} yr^{-1})	1.99×10^{-6}	8.06×10
Peak influx (kg km^{-2} yr^{-1})	7.62×10^{-6}	1.88×10
Mean influx (number km^{-2} hr^{-1})	1.18×10^{-11}	1.99×10
Peak influx (number km^{-2} hr^{-1})	4.51×10^{-11}	4.65×10

the source of the meteorites. It is unlikely that influx of meteorites actually decreased in Eu between 1860 and 1950, and one must conclude the apparent decrease in rate is due to a drift of rural population to the cities during the indust revolution and, perhaps, a waning of interest in m oritical phenomena. In view of these uncertainties a first approximation I have taken the influx rate t the highest rate observed in any ten-year period. T the rate for the United States is 12, and for Europ 16 meteorites per decade. The observational data each area are summarized in Table I.

It can be seen that the peak influx rate for United States and Europe is approximately 4.5×1 meteorites km^{-2} hr^{-1}. The close agreement is alm certainly fortuitous since one would expect an erro $+30\%$ from statistical variations, and the many servational uncertainties must also influence the res One can infer, however, that the peak rate would increase appreciably if the density of the populat were increased, because the observed rate for Eur is the same as that for the United States; yet population density is greater in Europe by a factor o

It is difficult to determine whether the peak r does indeed represent the actual influx. Many mete ites must fall in forest, woodland, lakes and in regi that are uninhabitable. From an earlier calculati Nininger (1933) determined a rate of 1.4×10^{-11} me orites km^{-2} hr^{-1}, and estimated that under the m favorable circumstances the observed rate might greater by a factor of 10. Nininger did not consider detail the increase of population, as has been done the present paper, but his factor presumably ma allowance for the population growth curve. From data in Table I it is probably reasonable to assume t with ideal terrain and an active populace the obser rate would be 2×10^{-10} meteorites km^{-2} hr^{-1}.

Even under such ideal conditions, the recovery small meteorites would still be difficult and the m distribution would no doubt follow the curve for "fa shown in Figs. 1 and 2. If we correct for the curvat in the observed mass distribution we find that a t of 640 observed falls corresponds to 740 meteor landing on the earth with mass m equal to or grea than 10 kg. The true influx rate of meteorites w $m \geqslant 10$ kg is therefore $2.0\times10^{-10}\times740/640=2.3\times1$ km^{-2} hr^{-1}. We may write the cumulative number N

orites landing with mass $\geqslant m$ as

$$\log N\ (\mathrm{km^{-2}\ hr^{-1}}) = -\log m - 8.64. \quad (4)$$

e mass m_∞ before ablation is difficult to determine he meteor theory (Levin 1946) indicates that for ors of the same velocity the ratio $m_\infty/m = \text{const} = f$. the number expressed in terms of initial mass m_∞ ne

$$\log N\ (\mathrm{km^{-2}\ hr^{-1}}) = -\log m_\infty - 8.64 + \log f. \quad (5)$$

value of f is difficult to determine; an estimate of has been made from a study of the Grant meteor- Fireman 1959), and a value of $f=700$ was obtained he Luhy (Ceplecha 1960) meteorite. In view of uncertainties we may tentatively adopt $f=10$ as ver limit.

suming that the mean geocentric velocity for mete- s is 17 km/sec (Whipple and Hughes 1955), we deduce the number of meteorites per cm³ in the e through which the earth passes. The number dN radius between ρ and $\rho+d\rho$ cm is given by the ession,

$$dN = 7.63 f \times 10^{-27} (d\rho/\rho^4)\ \mathrm{cm^{-3}}, \quad (6)$$

re a mean specific gravity of 3.5 g cm^{-3} is assumed. cumulative number N with radius $\geqslant \rho_1$ is then

$$N = \frac{2.54 f \times 10^{-27}}{\rho_1^3}\ \mathrm{cm^{-3}}. \quad (7)$$

o obtain the total mass per cm³ we must integrate quantity $m_\infty dN$. Again assuming the specific gravity eteorites to be 3.5, we find the total mass per cm³, m_∞, is given by the expression,

$$\sum m_\infty = 1.12 f \times 10^{-25} \log \frac{\rho_1}{\rho_2}\ \mathrm{g\ cm^{-3}}, \quad (8)$$

re ρ_1 and ρ_2 are the upper and lower limits on ius ρ.

he total mass falling on 1 cm² of the earth per sec iven by the equation,

$$\sum_{\oplus} m_\infty = 6.33 f \times 10^{-20} \log \frac{m_{\infty 2}}{m_{\infty 1}}\ (\mathrm{g\ cm^{-2}\ sec^{-1}}), \quad (9)$$

re $m_{\infty 2}$ and $m_{\infty 1}$ are the upper and lower limits of ss. The total mass reaching the earth in the form of d meteorites is, of course, in g cm^{-2} sec^{-1},

$$\frac{1}{f} \sum_{\oplus} m_\infty.$$

DISCUSSION

he observations of asteroids in space and meteor- on the ground indicate a fourth power law for the ribution according to size. Since meteorites and eroids are a product of collisions, it is of interest to compare this distribution with the results obtained in the crushing of terrestrial rock. The process of mineral dressing, whether it be by stamp mill, rod mill or standard tumbler, produces a continuous gradation of particle sizes. The results of mineral dressing are usually expressed by the comminution law (Gaudin 1944)

$$\log p = k \log x + \log A, \quad (10)$$

where p is the percentage of the total mass contained in particles with diameters between x_1 and x_2, after the crushing process. In Eq. (10), k and A are constants. The quantity x in the comminution law is a mean value of the sizing limits; the sizing interval is chosen to be logarithmic so that $\sqrt{2}x_1 = x_2$, $\sqrt{2}x_2 = x_3$, etc.

The number of meteorites as a function of mass may be written to correspond to the comminution law by the following transformations. Let us assume that dN particles in the meteorite sample have a radius between ρ and $\rho+d\rho$ and that the distribution is given by the expression,

$$dN = C d\rho/\rho^\alpha, \quad (11)$$

where C is a constant. We may convert ρ and $d\rho$ into the mass m and differential dm. Equation (11) then transforms into the expression

$$dN = B m^{-(\alpha+2)/3} dm, \quad (12)$$

where B is a constant. The total mass in the interval dN is

$$m dN = B m^{(1-\alpha)/3} dm. \quad (13)$$

The total mass p between the mass limits m_1 and m_2 is then found by integration:

$$p = \int_{m_1}^{m_2} B m^{(1-\alpha)/3} dm = B' [m_2^{(4-\alpha)/3} - m_1^{(4-\alpha)/3}]. \quad (14)$$

If a logarithmic mass interval is used in the sample, then $m_2 = \beta m_1$, where β is a constant. This leads to the expression,

$$p = B' m_1^{(4-\alpha)/3} [\beta^{(4-\alpha)/3} - 1]. \quad (15)$$

We may now express the distribution as a function of diameter x. Equation (15) becomes

$$p = A x^{4-\alpha}, \quad (16)$$

where A is a constant. Taking the logarithm of this equation produces the comminution law,

$$\log p = k \log x + \log A, \quad (17)$$

where $k = 4-\alpha$.

The integration involves a singularity when $\alpha=4$. By a separate integration for this singularity it can be shown that the relation $k=4-\alpha$ still holds when $\alpha=4$.

The law giving the number of meteorites as a function of size may now be compared directly with the comminution law of mineral dressing. In particular it should be noted that the meteorite and asteroidal law with $\alpha=4.0$ corresponds to a value of $k=0$.

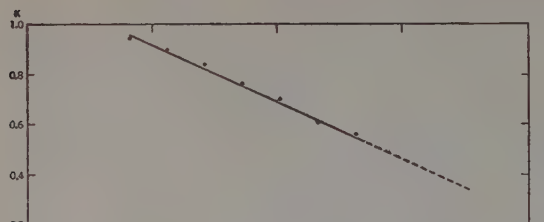

FIG. 5. The comminution parameter k as a function of time.

In rock crushing a deliberate attempt is made to avoid the production of small particles, and the primary objective is to produce particles of uniform size. In the early stages of a crushing process the value of k is close to unity, and an inverse cube law results for Eq. (11) with $\alpha=3$. Further grinding, however, reduces the value of k and produces an increasing number of small particles. This process is referred to as "over grinding." Figure 5 plots the value of k as a function of time for the grinding of quartz in a rod mill (Gaudin 1944). As the grinding continues, the value of k approaches zero and with a linear extrapolation we may deduce that $k=0$ after 600 hours of grinding. The tendency for k to decrease is noticeable in all crushing processes regardless of the mechanism involved. It is not possible to determine from the published data whether the relationship in Fig. 5 is linear or whether k approaches zero asymptotically. One may infer, however, that if $k=0$, and $\alpha=4$, then the debris has probably been subjected to a considerable amount of mechanical disturbance.

Low velocity collisions among asteroidal fragments are probably similar in action and effect to the grinding mechanisms used in dressing minerals. The observed mass distribution of meteorites and asteroids therefore indicates that these bodies have undergone a large number of collisions, and one may assume that this process of attrition is still in progress in the asteroid zone.

Since a large number of meteorites consist of metallic iron we must presume that one or more of the pre-collisional bodies were large enough to possess an iron core. The percentage of iron in the asteroid is given approximately by the ratio of iron to stone meteo falling on the earth. The percentage of iron wil underestimated if one or more of the asteroids invo in the collision did not possess an iron core. The centage will be overestimated if fragments of s meteorites are lost due to weathering and other s tion factors as indicated by the differences in Fig and 2. The analysis in this paper shows that the centage of iron by mass is 16.7%. This corresp (Urey 1951) to the composition expected from the of a body intermediate in size between Mars and moon. At least one of the original asteroids, t must have been between 2000 and 4000 km in diam

The influx laws [Eqs. (4) and (5)] are probably certain by ±50%, but there is agreement with influx law determined by another method. Haw (1959) deduced from the observed rate of bright balls that $\log N=\log m_\infty-7.98$. We may there adopt an influx law:

$$\log N=-\log m_\infty-7.5 \text{ km}^{-2} \text{ hr}^{-1}.$$

This law shows that the earth encounters one astero fragment with $m_\infty \geqslant 13\times10^6$ kg every 100 years.

If the influx rate has remained constant for the 5×10^9 years, Eq. (9) indicates that the earth collected 4.60×10^{18} g of meteoritic material du this period. This mass is equivalent to an asteroid v a diameter of about 14 km and a mean density of This is an insignificant fraction of the total mass in asteroid zone.

REFERENCES

Ceplecha, Z., 1960, *Bull. Astron. Inst. Czech.* **11**, 9.
Fireman, E. L., 1959, *Planet Space Sci.*, **1**, 66.
Gaudin, A., 1944, *Principles of Mineral Dressing* (McGraw-Book Company, Inc., New York).
Hawkins, G. S., 1959, *Astron. J.* **64**, 450.
Kuiper, G. P., Y. Fumita, T. Gehrels, I. Groeneveld, J. K G. Van Biesbroeck, and C. J. Van Houten, 1958, *Astrophys Suppl.* **32**, III, 289.
Levin, B. F., 1946, *Astron. J. USSR* **23**, 83.
Nininger, H. H., 1933, *Our Stone-Pelted Planet* (Hough Mifflin Company, Boston, Massachusetts).
Piotrowski, S. L., 1953, *Acta Astronomica*, Ser. **A. 5**, 115; private communication.
Prior, G. T. and M. H. Hey, 1953, *Catalogue of Meteorites* (Bri Museum, London).
Urey, H. C., Geochim, 1951, *Cosmochim. Acta* **1**, 209.
Whipple, F. L. and R. F. Hughes, 1955, *J. Atmosphys. Terr. P Spec. Suppl.* **2**, 149.

A Color-Magnitude Diagram of High Velocity Double Stars

GEORGE WALLERSTEIN AND JOHN WESTFALL
Berkeley Astronomical Department, University of California, Berkeley, California

(Received February 1, 1960)

A color-magnitude diagram of high velocity stars has been compiled using absolute magnitudes obtained from dynamical parallaxes. All visual binaries in Miss Roman's *Catalogue* (1955) which show sufficient orbital motion are included. The main sequence is well populated with stars redder than $B-V=0.55$. Of eight stars lying above the main sequence, five lie close to the giant branch of M67. Two stars lie significantly above that line and one lies below it. The system ADS 10938, which has been reported by Eggen and Sandage (1959) to be a member of the Groombridge 1830 group, is discussed in some detail.

1. INTRODUCTION

:VERAL authors have recently discussed color-magnitude diagrams of high velocity stars. Woolley Eggen (1958) divided the stars within 20 parsecs ıe sun into six groups according to galactic orbits. result of their diagrams was the confirmation of the ɔthesis that the stars of high space velocity relative he local standard of rest are old stars. This is :rally confirmed by Oke (1959) who used both ɔnometric and spectroscopic parallaxes. Although 's method of obtaining spectroscopic parallaxes ıs to be very accurate (Oke 1957), it is desirable to :oach the problem by an entirely independent hod. The purpose of this paper is to do so by em-ing dynamical parallaxes of visual double stars.

2. PROCEDURE

'e have considered all the visual double stars listed Miss Roman in her *Catalogue of High Velocity Stars* 55). Of 56 such systems, 21 show too little motion two show only rectilinear motion which is of no use s. The remaining 33 systems were divided into three ıps according to the reliability of the orbital data. first group contains stars which have shown suffi-tly great motion for their orbits to have been com-ed; some of these are admittedly rather preliminary. Data regarding these stars are listed in Table I. First we list the ADS number followed by $\Delta\theta$, the total observed change in position angle. In the third column is listed the (semi-major axis) (period)$^{-\frac{2}{3}}$. The next three columns contain the dynamical parallax which we have derived along with the trigonometric and spectroscopic parallaxes. The seventh column contains the $B-V$ for the brighter component. In a few cases the $B-V$ of the fainter star has been measured, in which case it is listed below that of the primary. The eighth column lists the absolute visual magnitude as determined from the dynamical parallax. Reference to the orbit used is listed in the final column.

In Table II we list data for systems that show too little motion for a reliable orbit but show sufficient curvature for a preliminary value of $aP^{-\frac{2}{3}}$ to be computed. It is well known that a given observed arc may be fitted by various ellipses for which the value of $aP^{-\frac{2}{3}}$ does not vary widely. We have confirmed this in each case.

The third group consists of slow-moving pairs which may be treated by the statistical methods originally proposed by both Russell and Hertzprung and fully discussed by Russell and Moore (1940). Data for these stars are listed in Table III. In the third and fourth columns of that table are listed the mean annual motion in position angle $\dot{\theta}$, in deg/yr and the mean separation ρ.

TABLE I. Data for stars with orbits.

ADS	$\Delta\theta$	$aP^{-\frac{2}{3}}$	π_{dyn}	π_{trig}	π_{sp}	$(B-V)_A$	$(Mv)_A$	Ref
2173	194°.6	0.0224	0″.019	0″.012	0″.014	0.66	5.2	a
3093 BC	167°.9	0.1738	0″.155	0″.200	0″.220	0.76	6.0	b
5469	70°.5	0.0241	0″.020	0″.012	0″.019	0.55	4.8	c
7251	31°.5	0.1884	0″.218	0″.163	0″.210	1.38	8.7	d
						1.34	8.8	
7724	18°.1	0.0343	0″.026	0″.019	0″.053	1.12	0.3	e
9380	330°.3	0.0258	0″.021	...	0″.025	0.56	4.4	f
9397	2001°.9	0.0448	0″.042	...	0″.0275	0.88	7.4	g
12 145 AB	384°.7	0.0237	0″.019	0″.007	0″.026	0.76	5.0	h
14 636	50°.6	0.2908	0″.237	0″.292	0″.330	1.19	7.1	i
						1.38	7.9	
17 175	1088°.4	0.0940	0″.077	0″.086	0″.066	0.62	5.2	j

Baize, M. P. 1954, *Circ. d'Information* No. 4.
Bos, W. H. van den. 1926, *Bull. Astron. Inst. Neth.* **3**, 128.
Muller, P. 1956, *Circ. d'Information* No. 9.
Güntzel-Linger, U. Von. 1955, *Astron. Nach.* **282**, 185.
Rabe, W. 1958, *Astron. Nach.* **283**, 97.
[f] Wierzbiński, S. 1955, *Circ. d'Information* No. 8.
[g] Bos, W. H. van den. 1954, *U. O. C.* **114**, 236.
[h] Baize, M. P. 1943, *J. d. O.* **26**, 95.
[i] De Caro, Vecca. 1948, *Catania Contr.* **62**, 63.
[j] Hall, R. G., Jr. 1949, *Astron. J.* **54**, 102.

TABLE II. Data for stars for which preliminary elements were computed.

ADS	$\Delta\theta$	$aP^{-\frac{2}{3}}$	π_{dyn}	π_{trig}	π_{sp}	$(B-V)_A$	$(Mv)_A$
2459	152°9	0.0182	0″015	0″006	0″032	1.05	1.3
7067	40°1	0.0819	0″079	0″089	0″063	1.38	7.8
9423	27°5	0.0185	0″014	0″005	0″0145	0.57	4.2
9939	16°7	0.0380	0″035	0″027	0″022	1.00	2.5
10 938	54°6	0.0144	0″012	0″020	0″011	0.56	5.2
12 557	63°2	0.0247	0″023	···	0″018	0.60	5.1
16 270	27°2	0.0466	0″039	0″026	0″038	0.61	5.2

The expression for the dynamical parallax is then

$$\pi_{dyn}=\frac{0.028\rho\dot{\theta}^{\frac{2}{3}}}{(m_1+m_2)^{\frac{1}{3}}}.$$

The reliability of individual parallaxes obtained from small motions by this method is considerably less than for the stars in the first two groups.

The fact that the cube root of the sum of the masses appears in the expression for the dynamical parallax makes it unnecessary to know the masses with high precision. We have obtained our masses in the following way. Using the spectroscopic parallax, we have entered the mass-luminosity relations of Van de Kamp (1958) for a preliminary mass from which a preliminary dynamical parallax was computed. The procedure was then iterated, using the dynamical parallax and the mass-luminosity relation until convergence was obtained. In all but 3 cases, a single iteration was satisfactory.

We have made the further assumption that stars lying above the main sequence should be assigned a mass of 1.2 M⊙. It may be argued at this point that we have assumed what we wish to prove; however, for only one pair the difference between the sum of the masses, as derived from the mass-luminosity relation and the adopted 2.4 M⊙, was greater than a factor of two, and again the cube root factor prevents the introduction of gross errors.

The observed colors must be corrected for the contribution to the total light by the companion. For main sequence stars this was done by assuming that the companion is also a main sequence star and using the slope of the main sequence as given by Johnson (19 Clearly for pairs of nearly equal magnitude or pairs a great difference of magnitude the correction is neg ble. In no case is the color correction greater than in $B-V$, but the color of the secondary is largely determined. Such a method cannot be used for gia Only in cases in which the magnitude differenc sufficiently large can it be assumed that the secon is a main sequence star. This is confirmed for one syst 39 Eri, for which separate spectra are available (Step son 1958). For the remaining four stars it was assu that the pairs lie along a sequence with the same s as the M67 giants. Separate spectra roughly con this for one system, γ Leo.

3. RESULTS AND DISCUSSION

In Fig. 1 we plot dynamical parallax against trig metric parallax for stars with trigonometric parall greater than 0″.04. The agreement seems to be as s factory as might be expected.

Figure 2 is our color-magnitude diagram. The represent the standard main sequence according Johnson (1957) and the giant branch of the gala cluster M67 according to Johnson and Sandage (19

The main sequence is well populated with stars re than $B-V=0.55$. The absence of bluer main sequ stars confirms the conclusion of Woolley and Eg (1958) that the high velocity stars are old. The sca above and below the main sequence is a little m than 0.5 mag., which is about the same as found Oke (1959).

Of eight stars lying above the main sequence fiv very close to the M67 line. The two stars above the line are θ UMa, whose $B-V=0.47$ (it is the bluest

TABLE III. Data for slow-moving pairs.

ADS	$\Delta\theta$	$\lvert\dot{\theta}\rvert$ (°/yr)	ρ	π_{dyn}	π_{trig}	π_{sp}	$(B-V)_A$	$(Mv)_A$
497	9°8	0.083	5″8	0″024	0″022	0″026	0.65	3.9
2757	7°2	0.067	8″5	0″032	0″037	0″042	0.77	4.9
3079	7°2	0.042	6″42	0″017	0″011	0″011	1.20	1.6
3900	13°7	0.282	3″9	0″049	0″071	0″066	1.03	6.6
4099	5°1	0.041	8″5	0″023	0″018	0″022	0.58	4.5
7420	25°8	0.318	4″7	0″057	0″052	0″056	0.47	1.9
8606	17°5	0.150	2″40	0″016	···	0″012	0.60	5.2
8959	6°2	0.054	4″45	0″015	0″003	0″0115	0.57	4.9
8981	10°9	0.100	2″55	0″012	0″027	0″0275	0.66	3.5
9000	6°3	0.046	3″3	0″009	0″004	0″012	1.13	0.4
9291	7°7	0.144	2″25	0″014	0″035	0″022	0.72	4.3
10 329	10°6	0.084	11″5	0″057	0″040	0″060	1.04	7.6
12 169	12°4	0.098	9″35	0″047	0″041	0″044	0.65	4.8
							0.64	5.0
14 123[a]	10°2	0.095	9″36	0″060	0″013	0″0019	0.88	7.5
14 738	16°5	0.218	1″38	0″011	···	0″017	0.52	3.6

[a] This system is probably optical. The spectral type of the primary is K3 III. It is not plotted in Fig. 2.

ur diagram), and γ Leo, whose $B-V=1.12$. The amical, spectroscopic, and trigonometric parallaxes UMa are in excellent agreement. One star, 39 Eri, below the M67 line. Several authors have recently ed attention to giants lying below the M67 line. An resting discussion of these stars which may differ n the M67 stars in age and/or chemical composition been published recently by Wilson (1959).

system of particular interest is ADS 10938=HD 810, which, according to Eggen and Sandage (1959), member of the Groombridge 1830 moving group. y derive a group parallax of ADS 10938 or 0".018 or 20. Our dynamical parallax, based upon a motion in 58 yr, is 0".012. This is a significant difference , if confirmed by further observations, indicates that star is not a member of the Groombridge 1830 group. r parallax combined with the color (corrected by 6 mag. for the companion) places it 0.6 mag. below main sequence, as compared with 1.1 mag. below as nd by Eggen and Sandage (1.4 mag. below had they rected the observed color for the companion).

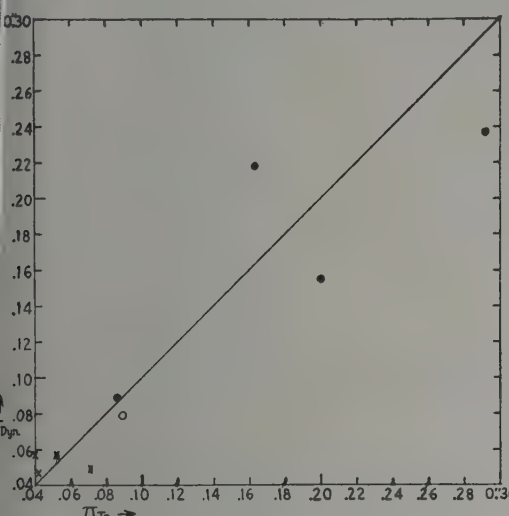

IG. 1. Comparison of dynamical and trigonometric parallaxes. e symbols are as follows: filled circles, stars from Table I; n circles, stars from Table II; crosses, stars from Table III.

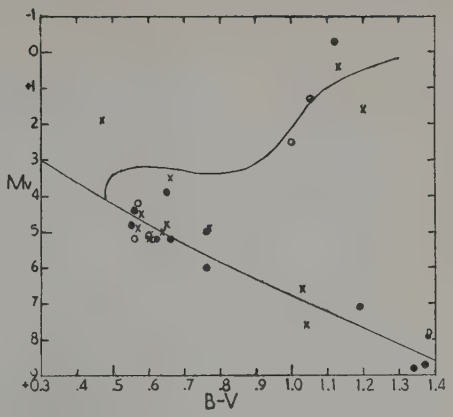

FIG. 2. Color-magnitude diagram of high velocity stars. Symbols are the same as in Fig. 1.

Finally it might be mentioned that we have attempted to divide our stars into groups according to galactic orbits; but, probably due to the small sampling, no significant differences could be noted between the stars of moderately high space velocity and those of very high space velocity.

We wish to thank Dr. Hamilton M. Jeffers for making available to us the data on double stars that is kept in the Lick Observatory punch card file. We are also grateful to Charles Worley for observing several stars.

REFERENCES

Eggen, O. J. and Sandage, A. R. 1959, *Monthly Notices Roy. Astron. Soc.* **119**, 255.
Johnson, H. L. 1957, *Astrophys. J.* **126**, 121.
Johnson, H. L. and Sandage, A. R. 1955, *Astrophys. J.* **121**, 616.
Oke, J. B. 1957, *Astrophys. J.* **126**, 509.
——. 1959, *Astrophys. J.* **130**, 487.
Roman, N. G. 1955, *Astrophys. J. Suppl.* **2**, 195.
Russell, H. N. and Moore, C. E. 1940, *The Masses of the Stars* (The University of Chicago Press, Chicago, Illinois).
Stephenson, C. B. 1958, Thesis, University of California, Berkeley, California.
Van de Kamp, P. 1958, *Handbuch der Physik* (Berlin: Springer-Verlag) **50**.
Wilson, O. C. 1959, *Publs. Astron. Soc. Pacific* **71**, 338.
Woolley, R. v. d. R. and Eggen, O. J. 1958, *Monthly Notices Roy. Astron. Soc.* **118**, 57.

Photometry of R Canis Majoris

ROBERT H. KOCH*
Flower and Cook Observatory, Philadelphia, Pennsylvania
(Received January 23, 1960)

Photoelectric light curves of R CMa have been obtained in three colors and have yielded a common solution of the orbital elements. Peculiarities of the light curves are pointed out and discussed.

1. INTRODUCTION

WOOD (1946) has summarized the history of R CMa (BD $-16°1898$, HD 57167, 1950.0: $\alpha=7^h18^m.4$, $\delta=-16°17'$) and has analyzed his photoelectric observations for the elements of the system. More recently, Kopal and Shapley (1956) have rediscussed Wood's light curve. Struve and Smith (1950) have observed and solved the radial velocity curve of the bright component. Several times of minimum light have been published, and the variable has figured in a number of discussions of the masses of double stars and of their period changes and stability. The spectral type of the bright component has been given as F1V by Fringant (1956) whose study indicates it to be a slightly reddened Population I star. Buscombe and Morris (1958), however, include R CMa in their finding list of southern high velocity stars.

2. OBSERVATIONS

With the 36-inch telescope of the Steward Observatory, 260 yellow, 258 blue, and 259 ultraviolet observations were obtained during the winter of 1955–1956. At the same time, 58 yellow, 68 blue, and 67 ultraviolet observations were taken with the 12.5-inch Calver telescope at the desert station of the Steward Observatory. In general, the Calver photometer, filters, photocell and amplifier are similar to those used with the larger telescope. The recorder is an Esterline-Angus permanent-magnet, moving-coil, direct-current milliammeter. The color responses of the two telescopes are not identical so that a transformation to the system of the Steward telescope is necessary. This is provided by the calibration of both telescopes on the U, B, V system of Johnson and Morgan (1953) and the requirements that the magnitudes and colors on this system be the same for both telescopes. Fitch (1957) has published the calibration for the 36-inch telescope and has also determined the calibration for the Calver telescope. The latter has not yet been published and is given below together with the probable error for each coefficient from a least-squares solution. In these equations $m_y{}^c$, $C_y{}^c$, and $C_u{}^c$ represent the magnitudes and colors on the natural Calver telescope system.

$$V=m_y{}^c+K+1.126-0.033\,C_y{}^c,$$
$$\pm 11 \quad \pm 11$$
$$(B\text{-}V)= +1.248+1.054\,C_y{}^c,$$
$$\pm 4 \quad \pm 4$$
$$(U\text{-}B)= -0.742+0.972\,C_u{}^c.$$
$$\pm 5 \quad \pm 6$$

The Calver observations are transformed to Steward system as follows. Let $\Delta m_y{}^c$, $\Delta m_b{}^c$ and Δ be the observed Calver magnitude differences in sense of variable star minus comparison star. Therefo

$$\Delta C_y{}^c=\Delta m_b{}^c-\Delta m_y{}^c,$$
$$\Delta C_u{}^c=\Delta m_u{}^c-\Delta m_b{}^c.$$

Similar equations can be written for the Stew telescope. Finally, let $\Delta m_y{}^s$, $\Delta m_b{}^s$ and $\Delta m_u{}^s$ repres the observed Calver magnitude differences transforn to the Steward system. The equations of transformat are:

$$\Delta m_y{}^s=\Delta m_y{}^c+0.095\Delta C_y{}^s-0.033\Delta C_y{}^c,$$
$$\Delta m_b{}^s=\Delta m_b{}^c-0.018\Delta C_y{}^s+0.021\Delta C_y{}^c,$$
$$\Delta m_u{}^s=\Delta m_u{}^c-0.018\Delta C_y{}^s+0.021\Delta C_y{}^c+0.014\Delta C_u{}^s$$
$$-0.028\Delta C$$

It can be seen that the color responses differ m conspicuously in the yellow.

For all observations the comparison star BD $-15°1734$. At least once a night this star checked against BD $-15°1732$. These compari stars were used by Wood, and so far have remai constant in light. All observations were corrected differential extinction using the following mean efficients: $0^m.220$ in yellow, $0^m.353$ in blue, and 0^m in the ultraviolet. All observations, transformed w necessary to the system of the 36-inch telescope, listed in Table I. Times are counted from Greenw Mean Noon and corrected to the sun. The yellow a ultraviolet observations are collected into light cur in Figs. 1 and 2.

3. EPOCH AND PERIOD

Wood has listed all observed heliocentric times minimum light published before 1946. Several ad

* Now at Amherst College Observatory, Amherst, Massachusetts.

TABLE Ia. Yellow Observations of R CMa.

$V-C$	JD ⊙ 2435000+	Phase	$V-C$	JD ⊙ 2435000+	Phase	$V-C$	JD ⊙ 2435000+	Phase
0m252	449.8330	0.3102	+0m258	483.9187	0.3168	+0m291	522.6967	0.4543
0.255	.8476	0.3231	0.232	491.7735	0.2317	0.295	.7050	0.4616
0.248	.8608	0.3347	0.274	.7881	0.2446	0.298	.7130	0.4686
0.268	.8733	0.3457	0.261	.7978	0.2531	0.311	.7216	0.4762
0.255	.8879	0.3586	0.260	.8079	0.2620	0.315	.7325	0.4858
0.260	.9046	0.3733	0.257	.8173	0.2703	0.321	.7408	0.4931
0.253	.9177	0.3848	0.255	.8267	0.2785	0.320	.7495	0.5007
0.267	.9289	0.3947	0.259	.8385	0.2889	0.311	.7589	0.5090
0.261	.9400	0.4044	0.270	.8527	0.3014	0.309	.7707	0.5194
0.271	.9511	0.4142	0.279	497.8357	0.5684	0.303	.7790	0.5267
0.277	.9671	0.4283	0.253	508.7493	0.1760	0.300	.7877	0.5344
0.282	.9789	0.4387	0.259	.7660	0.1907	0.291	.7957	0.5414
0.267	453.8134	0.8143	0.275	.7753	0.1999	0.273	.8054	0.5500
0.273	.8259	0.8253	0.268	.7847	0.2072	0.245	524.6046	0.1339
0.283	.8363	0.8345	0.265	.7941	0.2154	0.256	.6178	0.1455
0.277	.8474	0.8442	0.252	.8035	0.2237	0.254	.6262	0.1529
0.286	.8606	0.8559	0.259	.8128	0.2319	0.261	.6345	0.1602
0.271	.8745	0.8681	0.254	.8264	0.2439	0.261	.6425	0.1673
0.274	.8870	0.8791	0.258	.8357	0.2520	0.255	.6505	0.1743
0.286	.9009	0.8913	0.261	.8455	0.2607	0.258	.6585	0.1814
0.291	.9120	0.9011	0.253	.8559	0.2698	0.256	.6678	0.1895
0.282	.9273	0.9146	0.542	509.7316	0.0408	0.252	.6803	0.2005
0.325	.9460	9.9310	0.451	.7444	0.0520	0.268	.6887	0.2079
0.347	.9488	0.9335	0.392	.7531	0.0597	0.252	.6970	0.2152
0.419	.9606	0.9439	0.352	.7618	0.0674	0.260	.7046	0.2219
0.548	.9766	0.9580	0.307	.7705	0.0750	0.263	.7137	0.2300
0.632	.9877	0.9684	0.291	.7791	0.0826	0.258	.7216	0.2369
0.710	.9960	0.9751	0.272	.7828	0.0858	0.259	.7310	0.2452
0.280	456.9250	0.5536	0.276	.7972	0.0985	0.257	.7414	0.2543
0.265	.9410	0.5676	0.283	.8101	0.1099	0.258	.7494	0.2614
0.261	458.8011	0.2051	0.272	.8187	0.1174	0.259	.7574	0.2684
0.255	.8119	0.2146	0.277	.8276	0.1253	0.264	.7657	0.2757
0.261	.8216	0.2232	0.291	.8385	0.1349	0.260	.7744	0.2834
0.251	.8313	0.2317	0.286	511.7818	0.8456	0.269	.7862	0.2938
0.262	.8414	0.2406	0.284	.7964	0.8584	0.269	.7960	0.3024
0.250	.8508	0.2489	0.286	.8061	0.8670	0.261	528.6659	0.7091
0.268	.8647	0.2611	0.316	513.6842	0.5203	0.259	.6794	0.7210
0.258	.8751	0.2703	0.317	.6964	0.5310	0.267	.6884	0.7289
0.250	.8855	0.2794	0.315	.7051	0.5387	0.249	.6971	0.7366
0.250	.8959	0.2886	0.303	.7137	0.5463	0.255	.7058	0.7442
0.252	.9063	0.2977	0.269	.7224	0.5539	0.262	.7138	0.7513
0.268	.9167	0.3069	0.267	.7321	0.5625	0.267	.7225	0.7589
0.257	.9265	0.3155	0.264	514.6589	0.3784	0.274	.7343	0.7693
0.260	.9403	0.3277	0.264	.6717	0.3896	0.258	.7454	0.7791
0.256	.9508	0.3369	0.260	.6804	0.3973	0.263	.7544	0.7870
0.264	.9612	0.3461	0.255	.6912	0.4068	0.252	530.6074	0.4183
0.261	.9709	0.3546	0.266	.6998	0.4144	0.257	.6237	0.4327
0.859	460.8349	0.9956	0.285	518.6390	0.8822	0.247	531.6129	0.3035
0.848	.8474	0.0066	0.287	.6512	0.8929	0.248	.6254	0.3144
0.798	.8578	0.0157	0.286	.6602	0.9008	0.250	.6341	0.3219
0.727	.8677	0.0244	0.278	.6682	0.9079	0.256	.6426	0.3296
0.627	.8773	0.0328	0.295	.6762	0.9149	0.257	.6504	0.3365
0.529	.8884	0.0426	0.310	.6873	0.9247	0.260	.6605	0.3454
0.447	.8995	0.0524	0.342	.6963	0.9326	0.245	.6691	0.3529
0.380	.9092	0.0609	0.420	.7105	0.9451	0.255	.6785	0.3612
0.309	.9245	0.0744	0.484	.7189	0.9525	0.253	.6910	0.3722
0.287	.9342	0.0829	0.565	.7279	0.9604	0.254	.6997	0.3799
0.290	.9446	0.0921	0.621	.7362	0.9678	0.262	.7084	0.3875
0.290	.9544	0.1007	0.716	.7446	0.9751	0.263	.7167	0.3948
0.294	.9669	0.1117	0.785	.7546	0.9840	0.256	.7250	0.4019
0.263	482.8187	0.3485	0.856	.7630	0.9913	0.257	.7348	0.4108
0.249	.8330	0.3611	0.873	.7709	0.9983	0.397	534.6069	0.9392
0.267	.8431	0.3700	0.872	.7793	0.0057	0.485	.6201	0.9509
0.251	.8528	0.3786	0.807	.7876	0.0130	0.540	.6301	0.9597
0.260	.8628	0.3874	0.256	522.6113	0.3791	0.623	.6388	0.9673
0.258	.8733	0.3966	0.252	.6241	0.3903	0.683	.6475	0.9750
0.261	.8868	0.4085	0.259	.6325	0.3977	0.764	.6562	0.9826
0.269	.9042	0.4238	0.256	.6412	0.4054	0.838	.6652	0.9906
0.252	483.7909	0.2043	0.262	.6495	0.4127	0.861	.6742	0.9985
0.252	.8048	0.2166	0.263	.6575	0.4197	0.832	.6854	0.0083
0.255	.8145	0.2251	0.265	.6675	0.4286	0.757	.6961	0.0177
0.254	.8947	0.2957	0.280	.6797	0.4393	0.712	.7048	0.0254
+0.260	.9090	0.3083	+0.270	.6884	0.4470	+0.606	.7145	0.0339

TABLE Ia. (Continued)

$V-C$	JD ⊙ 2435000+	Phase	$V-C$	JD ⊙ 2435000+	Phase	$V-C$	JD ⊙ 2435000+	Phase
+0m530	534.7235	0.0418	+0m257	537.7070	0.6683	+0m292	542.7410	0.1062
0.468	.7319	0.0492	0.269	.7178	0.6778	0.290	.7515	0.1091
0.392	.7416	0.0578	0.253	.7289	0.6875	0.303	.7605	0.1170
0.354	.7506	0.0657	0.264	.7386	0.6961	0.275	.7744	0.1292
0.324	.7538	0.0685	0.278	.7480	0.7044	0.313	543.6191	0.8729
0.298	.7718	0.0843	0.277	.7601	0.7150	0.305	.6320	0.8842
0.270	.7805	0.0920	0.284	.7685	0.7224	0.308	.6427	0.8936
0.257	536.6136	0.7058	0.280	.7768	0.7297	0.290	.6504	0.9004
0.273	.6258	0.7165	0.313	538.6337	0.4841	0.294	.6618	0.9104
0.256	.6338	0.7236	0.320	.6483	0.4970	0.298	.6688	0.9166
0.261	.6421	0.7309	0.330	.6594	0.5067	0.327	.6795	0.9260
0.266	.6511	0.7388	0.323	.6677	0.5140	0.352	.6872	0.9328
0.276	.6629	0.7492	0.322	.6781	0.5232	0.531	.7163	0.9584
0.264	.6709	0.7562	0.327	.6861	0.5302	0.619	.7250	0.9661
0.269	.6789	0.7634	0.320	.6962	0.5391	0.735	.7368	0.9765
0.254	.6869	0.7703	0.303	.7049	0.5468	0.888	.7594	0.9964
0.264	.6949	0.7773	0.284	.7320	0.5706	0.864	.7674	0.0034
0.270	.7019	0.7835	0.276	.7413	0.5788	0.850	.7778	0.0126
0.268	.7112	0.7917	0.265	.7521	0.5883	0.765	.7858	0.0196
0.278	.7195	0.7993	0.278	.7636	0.5985	0.277	545.6204	0.6347
0.261	.7289	0.8073	0.279	.7747	0.6082	0.269	.6353	0.6478
0.278	.7369	0.8143	0.271	.7820	0.6147	0.274	.6433	0.6549
0.269	.7452	0.8216	0.875	542.6320	0.0039	0.268	.6541	0.6644
0.274	.7539	0.8293	0.839	.6431	0.0137	0.288	547.6272	0.4014
0.286	.7657	0.8397	0.699	.6581	0.0269	0.268	.6432	0.4154
0.274	.7747	0.8476	0.631	.6660	0.0338	0.283	.6547	0.4256
0.258	537.6393	0.6087	0.520	.6768	0.0434	0.288	.6640	0.4337
0.259	.6532	0.6209	0.464	.6841	0.0497	0.289	.6762	0.4445
0.246	.6632	0.6297	0.415	.6938	0.0583	0.305	.6873	0.4543
0.261	.6716	0.6371	0.349	.7022	0.0657	0.301	.6974	0.4641
0.275	.6799	0.6444	0.309	.7136	0.0757	0.311	.7043	0.4692
0.273	.6886	0.6521	0.287	.7226	0.0836	0.320	.7151	0.4787
+0.264	.6973	0.6597	+0.302	.7331	0.0929	+0.323	.7224	0.4852

tional times have been determined subsequently. These are listed in Table II with residuals computed from the elements of Dugan and Wright (1939). The run of the residuals from these elements for all published minima is shown in Fig. 3 and can presently be represented either by two more or less straight lines or by a sine curve with a semi-amplitude of 0d.032. When observed, secondary eclipse has always been located at the half-period point, and the absorption lines from a third body have never been detected. The peri is probably intrinsically variable.

The phases of the Tucson observations have be computed from Min. = 2422030.638+1.1359386 *E*. T small differences which these elements show wh compared with Wood's elements are necessary primary eclipse is to be symmetric about 0P.0. Observ tions in secondary eclipse show appreciable scatter b indicate that the minimum is not displaced from t half period point.

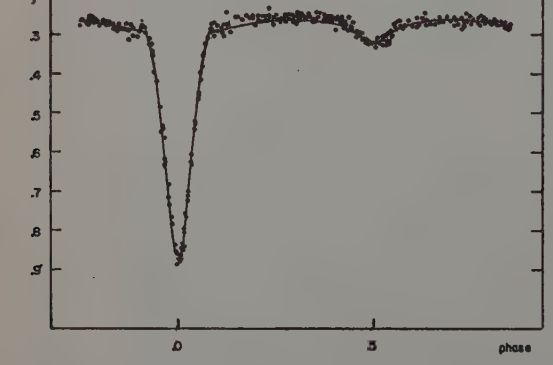

FIG. 1. The yellow observations of R CMa. The light curve is given in Table IV.

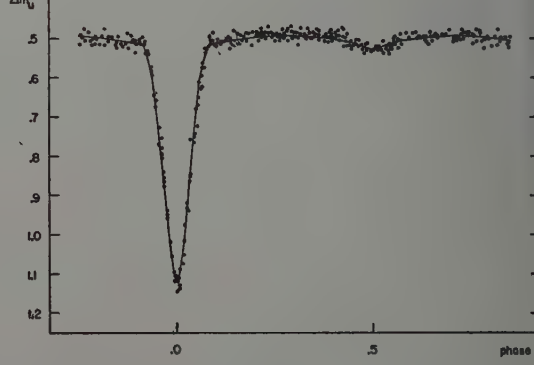

FIG. 2. The ultraviolet observations of R CMa. The light curve is given in Table IV.

TABLE Ib. Blue Observations of R CMa.

V−C	JD ⊙ 2435000+	Phase	V−C	JD ⊙ 2435000+	Phase	V−C	JD ⊙ 2435000+	Phase
0m483	449.8337	0.3109	+0m489	482.8635	0.3880	+0m491	522.6248	0.3910
0.487	.8483	0.3237	0.486	.8740	0.3972	0.500	.6332	0.3984
0.481	.8615	0.3353	0.500	.8875	0.4091	0.491	.6418	0.4059
0.503	.8740	0.3463	0.498	.9049	0.4244	0.505	.6502	0.4133
0.496	.8886	0.3592	0.489	483.7916	0.2049	0.494	.6582	0.4204
0.493	.9052	0.3738	0.493	.8055	0.2172	0.505	.6682	0.4292
0.501	.9184	0.3854	0.488	.8152	0.2257	0.514	.6804	0.4399
0.506	.9296	0.3953	0.490	.8954	0.2963	0.513	.6891	0.4476
0.490	.9407	0.4050	0.488	.9096	0.3088	0.523	.6974	0.4549
0.498	.9518	0.4148	0.487	.9194	0.3175	0.522	.7057	0.4622
0.507	.9677	0.4288	0.472	491.7742	0.2323	0.520	.7137	0.4692
0.510	.9796	0.4393	0.518	.7888	0.2452	0.526	.7223	0.4768
0.486	453.8141	0.8149	0.501	.7985	0.2537	0.531	.7332	0.4864
0.499	.8266	0.8259	0.488	.8086	0.2626	0.535	.7415	0.4937
0.512	.8370	0.8351	0.497	.8180	0.2709	0.538	.7502	0.5014
0.501	.8481	0.8449	0.496	.8273	0.2791	0.535	.7596	0.5096
0.496	.8613	0.8565	0.492	.8392	0.2895	0.528	.7714	0.5200
0.500	.8752	0.8687	0.507	.8534	0.3020	0.532	.7797	0.5273
0.507	.8877	0.8797	0.506	497.8364	0.5691	0.526	.7885	0.5351
0.503	.9016	0.8920	0.497	508.7500	0.1766	0.519	.7965	0.5421
0.511	.9127	0.9017	0.503	.7667	0.1913	0.514	.8061	0.5506
0.527	.9287	0.9158	0.490	.7760	0.1995	0.487	524.6053	0.1345
0.567	.9467	0.9317	0.494	.7854	0.2078	0.484	.6185	0.1461
0.592	.9495	0.9341	0.500	.7948	0.2160	0.489	.6269	0.1535
0.650	.9613	0.9445	0.495	.8041	0.2242	0.499	.6352	0.1608
0.787	.9773	0.9586	0.486	.8135	0.2325	0.499	.6432	0.1679
0.854	.9884	0.9684	0.491	.8271	0.2445	0.491	.6512	0.1749
0.937	.9967	0.9757	0.499	.8364	0.2527	0.489	.6591	0.1819
0.497	455.8549	0.6115	0.489	.8462	0.2613	0.490	.6685	0.1902
0.509	.8764	0.6304	0.490	.8566	0.2704	0.493	.6810	0.2012
0.497	.8910	0.6433	0.760	509.7322	0.0413	0.504	.6894	0.2086
0.512	456.9257	0.5542	0.669	.7451	0.0527	0.486	.6977	0.2159
0.465	458.8018	0.2057	0.610	.7538	0.0603	0.492	.7053	0.2226
0.481	.8126	0.2152	0.571	.7625	0.0680	0.490	.7144	0.2306
0.484	.8223	0.2238	0.526	.7712	0.0756	0.496	.7223	0.2375
0.483	.8320	0.2323	0.513	.7795	0.0829	0.499	.7317	0.2458
0.487	.8421	0.2412	0.505	.7885	0.0909	0.496	.7421	0.2550
0.481	.8515	0.2495	0.514	.7979	0.0991	0.498	.7501	0.2620
0.481	.8653	0.2616	0.510	.8107	0.1104	0.500	.7581	0.2690
0.490	.8758	0.2709	0.506	.8194	0.1181	0.496	.7664	0.2763
0.480	.8862	0.2800	0.508	.8285	0.1261	0.497	.7751	0.2840
0.471	.8966	0.2892	0.520	.8392	0.1355	0.505	.7869	0.2944
0.474	.9070	0.2984	0.530	511.7825	0.8462	0.504	.7966	0.3029
0.510	.9174	0.3075	0.518	.7971	0.8590	0.511	528.6666	0.7097
0.489	.9272	0.3161	0.505	.8068	0.8676	0.497	.6801	0.7216
0.488	.9410	0.3283	0.544	513.6849	0.5209	0.501	.6891	0.7295
0.486	.9515	0.3375	0.536	.6971	0.5316	0.496	.6978	0.7372
0.489	.9619	0.3467	0.537	.7057	0.5392	0.499	.7065	0.7449
0.494	.9716	0.3552	0.532	.7144	0.5469	0.486	.7145	0.7519
1.117	460.8356	0.9962	0.499	.7231	0.5545	0.485	.7232	0.7596
1.103	.8481	0.0072	0.492	.7328	0.5631	0.493	.7350	0.7699
1.037	.8585	0.0163	0.499	514.6596	0.3790	0.495	.7461	0.7797
0.954	.8682	0.0248	0.488	.6724	0.3913	0.497	.7565	0.7889
0.852	.8780	0.0335	0.483	.6811	0.3979	0.487	530.6081	0.4190
0.752	.8891	0.0432	0.489	.6918	0.4073	0.468	.6244	0.4333
0.657	.9002	0.0530	0.513	518.6397	0.8828	0.491	531.6136	0.3041
0.595	.9099	0.0615	0.513	.6518	0.8935	0.485	.6261	0.3151
0.540	.9252	0.0750	0.516	.6609	0.9015	0.483	.6348	0.3227
0.511	.9349	0.0836	0.514	.6689	0.9085	0.494	.6433	0.3302
0.512	.9453	0.0927	0.519	.6768	0.9155	0.496	.6511	0.3371
0.506	.9551	0.1013	0.536	.6880	0.9253	0.511	.6612	0.3460
0.533	.9676	0.1123	0.570	.6970	0.9332	0.482	.6698	0.3535
0.485	474.7751	0.2675	0.653	.7112	0.9457	0.498	.6792	0.3618
0.487	.7887	0.2795	0.732	.7196	0.9531	0.503	.6917	0.3728
0.484	.8040	0.2930	0.808	.7286	0.9611	0.494	.7004	0.3805
0.481	.8165	0.3040	0.874	.7369	0.9684	0.498	.7091	0.3881
0.488	.8304	0.3162	0.962	.7452	0.9757	0.506	.7174	0.3955
0.482	.8477	0.3315	1.036	.7553	0.9846	0.496	.7257	0.4028
0.478	.8606	0.3428	1.104	.7637	0.9920	0.496	.7355	0.4114
0.497	482.8194	0.3491	1.113	.7716	0.9989	0.632	534.6076	0.9398
0.481	.8337	0.3617	1.114	.7800	0.0063	0.719	.6208	0.9515
0.498	.8437	0.3705	1.055	.7883	0.0136	0.775	.6308	0.9603
0.488	.8535	0.3792	+0.485	522.6120	0.3797	+0.853	.6395	0.9679

TABLE Ib. (Continued)

V−C	JD ⊙ 2435000+	Phase	V−C	JD ⊙ 2435000+	Phase	V−C	JD ⊙ 2435000+	Phas
+0m918	534.6482	0.9756	+0m505	537.6626	0.6292	+0m519	542.7233	0.08
1.022	.6569	0.9832	0.504	.6709	0.6365	0.521	.7338	0.09
1.082	.6659	0.9912	0.507	.6792	0.6438	0.499	.7417	0.10
1.107	.6749	0.9990	0.510	.6879	0.6515	0.508	.7522	0.10
1.080	.6860	0.0088	0.505	.6966	0.6591	0.508	.7612	0.11
0.983	.6968	0.0183	0.494	.7063	0.6677	0.490	.7751	0.12
0.947	.7055	0.0260	0.503	.7171	0.6772	0.530	543.6198	0.87
0.843	.7138	0.0333	0.502	.7282	0.6869	0.519	.6327	0.88
0.753	.7242	0.0424	0.498	.7379	0.6955	0.537	.6434	0.89
0.698	.7326	0.0498	0.501	.7473	0.7037	0.525	.6511	0.90
0.613	.7423	0.0584	0.494	.7594	0.7144	0.514	.6626	0.91
0.577	.7513	0.0663	0.501	.7678	0.7218	0.517	.6695	0.91
0.543	.7544	0.0690	0.496	.7761	0.7291	0.547	.6802	0.92
0.516	.7725	0.0850	0.528	538.6323	0.4829	0.578	.6879	0.93
0.506	.7812	0.0926	0.537	.6490	0.4976	0.756	.7170	0.95
0.492	536.6143	0.7064	0.544	.6601	0.5073	0.848	.7257	0.96
0.495	.6265	0.7171	0.543	.6684	0.5146	0.950	.7361	0.97
0.482	.6345	0.7242	0.520	.6788	0.5238	1.093	.7587	0.99
0.499	.6428	0.7315	0.537	.6868	0.5308	1.093	.7667	0.00
0.499	.6518	0.7394	0.541	.6969	0.5397	1.071	.7785	0.01
0.508	.6636	0.7498	0.518	.7056	0.5474	0.988	.7851	0.01
0.495	.6716	0.7568	0.504	.7327	0.5713	0.508	545.6211	0.63
0.498	.6796	0.7639	0.498	.7420	0.5794	0.512	.6360	0.64
0.483	.6876	0.7709	0.511	.7528	0.5889	0.509	.6440	0.65
0.505	.6956	0.7780	0.497	.7642	0.5990	0.502	.6548	0.66
0.514	.7036	0.7850	0.494	.7754	0.6088	0.526	547.6279	0.40
0.505	.7119	0.7923	0.497	.7827	0.6153	0.532	.6456	0.41
0.508	.7202	0.7996	1.121	542.6327	0.0045	0.517	.6554	0.42
0.490	.7296	0.8079	1.056	.6438	0.0143	0.506	.6647	0.43
0.512	.7376	0.8149	0.930	.6574	0.0262	0.523	.6769	0.44
0.497	.7459	0.8222	0.881	.6653	0.0332	0.517	.6880	0.45
0.523	.7546	0.8299	0.747	.6761	0.0427	0.522	.6981	0.46
0.526	.7664	0.8403	0.695	.6834	0.0491	0.538	.7050	0.46
0.502	.7754	0.8482	0.633	.6945	0.0589	0.524	.7158	0.47
0.493	537.6400	0.6094	0.576	.7028	0.0662	+0.529	.7231	0.48
+0.504	.6539	0.6215	+0.534	.7143	0.0763			

4. VARIATIONS OUTSIDE ECLIPSE

From primary eclipse to secondary the observations of R CMa at each wavelength show very little change in brightness. At the other and lower maximum more scatter is apparent, and the light curves are constant in brightness. Immediately following prim eclipse the observations suggest a plateau of some in phase angle and then a rather abrupt rise to level of the first maximum. These effects are pronounced at the same locations before prim minimum. Transient "humps" have been observed both Wendell (1909) and Pickering (1904) after prim eclipse, but large anomalies of this kind are not kno to occur at other phases.

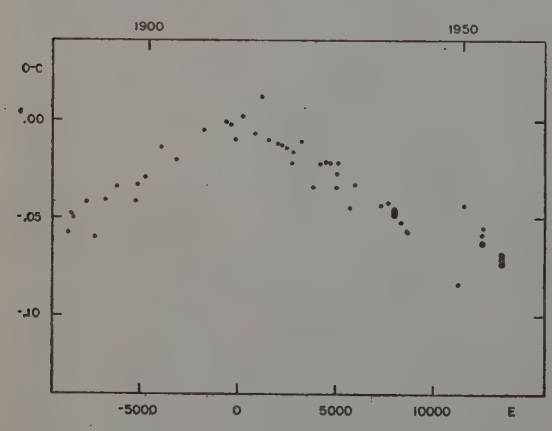

FIG. 3. Residuals from linear elements for R CMa. The six large points toward the right represent photoelectric determinations of primary minimum. One large open circle represents a photoelectric determination of secondary eclipse. All other points refer to the visual observations or estimates of primary tabulated by Wood in *Princeton Contr.* **21**.

The discordances between the maxima are so sev particularly in yellow light, that it is impossible represent the outside-eclipse variation by a Fou expansion up to and including the fourth harmo Over the first maximum it is equally impossible detect the customary and expected terms in reflec and ellipticity. The second maximum, however, be satisfactorily represented by:

$$\mathfrak{L}(\text{y, max. II}) = 0.9750 - 0.0106\cos\theta - 0.0123\cos 2\theta (\pm 0^{m}0$$

$$\mathfrak{L}(\text{b, max. II}) = 0.9693 - 0.0052\cos\theta - 0.0112\cos 2\theta (\pm 0^{m}0$$

$$\mathfrak{L}(\text{u, max. II}) = 0.9683 - 0.0078\cos\theta - 0.0110\cos 2\theta (\pm 0^{m}0$$

TABLE Ic. Violet Observations of R CMa.

$V-C$	JD ⊙ 2435000+	Phase	$V-C$	JD ⊙ 2435000+	Phase	$V-C$	JD ⊙ 2435000+	Phase
m484	449.8344	0.3115	+0m488	482.8542	0.3798	+0m494	522.6127	0.3803
.490	.8490	0.3243	0.483	.8642	0.3886	0.477	.6255	0.3916
.480	.8622	0.3359	0.492	.8746	0.3977	0.494	.6339	0.3990
.497	.8747	0.3469	0.479	.8882	0.4097	0.490	.6425	0.4065
.490	.8893	0.3598	0.476	.9056	0.4250	0.491	.6509	0.4139
.505	.9073	0.3756	0.490	483.7923	0.2056	0.495	.6589	0.4210
.508	.9191	0.3860	0.482	.8062	0.2178	0.499	.6689	0.4298
.501	.9302	0.3958	0.495	.8159	0.2263	0.506	.6811	0.4405
.497	.9414	0.4057	0.492	.8961	0.2969	0.519	.6898	0.4482
.496	.9525	0.4154	0.495	.9103	0.3094	0.514	.6981	0.4555
.505	.9684	0.4294	0.470	491.7749	0.2329	0.516	.7064	0.4628
.513	.9802	0.4398	0.494	.7895	0.2458	0.517	.7144	0.4698
.476	453.8148	0.8155	0.486	.7992	0.2543	0.532	.7230	0.4774
.495	.8273	0.8265	0.498	.8093	0.2632	0.529	.7339	0.4870
.494	.8377	0.8357	0.488	.8187	0.2715	0.531	.7422	0.4943
.509	.8488	0.8455	0.480	.8280	0.2797	0.528	.7509	0.5020
.512	.8620	0.8571	0.481	.8398	0.2901	0.522	.7602	0.5102
.488	.8759	0.8693	0.493	.8541	0.3027	0.527	.7721	0.5206
.494	.8884	0.8803	0.482	.8638	0.3112	0.533	.7803	0.5279
.506	.9023	0.8926	0.502	497.8371	0.5697	0.525	.7891	0.5356
.505	.9134	0.9023	0.508	508.7507	0.1772	0.512	.7971	0.5426
.535	.9315	0.9183	0.517	.7673	0.1918	0.500	.8068	0.5512
.586	.9474	0.9323	0.492	.7767	0.2001	0.500	524.6060	0.1351
.594	.9502	0.9347	0.507	.7861	0.2084	0.479	.6192	0.1468
.674	.9620	0.9451	0.494	.7955	0.2167	0.489	.6275	0.1541
.778	.9780	0.9592	0.484	.8048	0.2248	0.495	.6359	0.1615
.852	.9891	0.9690	0.485	.8142	0.2331	0.495	.6449	0.1694
.949	.9974	0.9763	0.490	.8278	0.2451	0.486	.6519	0.1755
.503	455.8771	0.6320	0.495	.8371	0.2533	0.486	.6598	0.1825
.485	.8937	0.6456	0.497	.8468	0.2618	0.482	.6692	0.1908
.493	456.9264	0.5548	0.492	.8573	0.2711	0.482	.6817	0.2018
.487	.9424	0.5689	0.758	509.7330	0.0420	0.494	.6900	0.2091
.493	458.8025	0.2064	0.669	.7458	0.0533	0.489	.6984	0.2165
.473	.8133	0.2159	0.621	.7545	0.0609	0.491	.7060	0.2232
.484	.8230	0.2244	0.571	.7632	0.0686	0.486	.7150	0.2311
.483	.8327	0.2329	0.528	.7719	0.0762	0.487	.7230	0.2381
.492	.8428	0.2418	0.515	.7805	0.0838	0.489	.7324	0.2464
.504	.8522	0.2501	0.505	.7892	0.0915	0.494	.7428	0.2556
.505	.8660	0.2623	0.515	.7986	0.0997	0.490	.7508	0.2626
.495	.8765	0.2715	0.512	.8114	0.1110	0.493	.7588	0.2697
.475	.8869	0.2807	0.504	.8201	0.1187	0.490	.7671	0.2770
.469	.8973	0.2898	0.501	.8291	0.1266	0.503	.7758	0.2846
.481	.9077	0.2990	0.525	.8399	0.1361	0.491	.7876	0.2950
.515	.9181	0.3081	0.521	511.7832	0.8468	0.485	.7973	0.3035
.487	.9278	0.3167	0.516	.7978	0.8597	0.496	528.6673	0.7103
.496	.9417	0.3289	0.513	.8075	0.8682	0.489	.6808	0.7222
.484	.9522	0.3381	0.528	513.6856	0.5215	0.483	.6898	0.7302
.483	.9626	0.3473	0.527	.6978	0.5323	0.481	.6985	0.7378
.475	.9723	0.3558	0.529	.7064	0.5398	0.482	.7072	0.7455
1.102	460.8363	0.9968	0.520	.7151	0.5475	0.490	.7152	0.7525
1.089	.8488	0.0078	0.505	.7238	0.5551	0.474	.7239	0.7602
1.014	.8592	0.0169	0.500	.7335	0.5637	0.480	.7357	0.7706
0.940	.8689	0.0254	0.489	514.6602	0.3795	0.512	.7468	0.7803
0.843	.8787	0.0341	0.493	.6731	0.3909	0.513	.7572	0.7895
0.741	.8898	0.0438	0.495	.6818	0.3985	0.470	530.6088	0.4196
0.649	.9009	0.0536	0.498	.6925	0.4080	0.487	.6251	0.4339
0.590	.9106	0.0622	0.508	518.6404	0.8834	0.485	531.6143	0.3047
0.529	.9259	0.0756	0.514	.6536	0.8950	0.486	.6268	0.3157
0.495	.9356	0.0842	0.507	.6616	0.9021	0.495	.6355	0.3234
0.514	.9460	0.0933	0.513	.6696	0.9091	0.490	.6440	0.3308
0.502	.9557	0.1019	0.513	.6775	0.9161	0.496	.6532	0.3389
0.508	.9682	0.1129	0.531	.6887	0.9259	0.496	.6618	0.3465
0.478	474.7758	0.2682	0.571	.6977	0.9339	0.487	.6705	0.3542
0.475	.7894	0.2801	0.659	.7119	0.9464	0.480	.6799	0.3624
0.497	.8047	0.2936	0.726	.7202	0.9537	0.499	.6924	0.3734
0.486	.8172	0.3046	0.806	.7293	0.9617	0.496	.7011	0.3811
0.472	.8310	0.3168	0.863	.7376	0.9690	0.492	.7098	0.3888
0.474	.8484	0.3321	0.959	.7459	0.9763	0.487	.7181	0.3961
0.465	.8613	0.3434	1.053	.7560	0.9852	0.485	.7264	0.4034
0.487	.9307	0.4045	1.119	.7643	0.9925	0.489	.7362	0.4120
0.498	482.8201	0.3498	1.142	.7723	0.9995	0.645	534.6083	0.9405
0.500	.8344	0.3624	1.130	.7807	0.0069	0.761	.6215	0.9519
0.500	.8444	0.3712	+1.050	.7890	0.0142	+0.790	.6315	0.9609

TABLE Ic. (Continued)

$V-C$	JD ⊙ 2435000+	Phase	$V-C$	JD ⊙ 2435000+	Phase	$V-C$	JD ⊙ 2435000+	Pha
+0m876	534.6402	0.9686	+0m499	537.6546	0.6221	+0m516	542.7240	0.08
0.939	.6489	0.9762	0.496	.6619	0.6286	0.511	.7344	0.09
1.018	.6576	0.9839	0.496	.6702	0.6359	0.511	.7424	0.10
1.094	.6666	0.9918	0.512	.6785	0.6432	0.509	.7528	0.11
1.120	.6756	0.9997	0.503	.6872	0.6508	0.507	.7619	0.11
1.070	.6867	0.0094	0.489	.6959	0.6585	0.498	.7758	0.13
0.974	.6975	0.0189	0.491	.7056	0.6670	0.528	543.6205	0.87
0.920	.7062	0.0266	0.489	.7164	0.6765	0.504	.6334	0.88
0.849	.7152	0.0345	0.487	.7275	0.6863	0.538	.6441	0.89
0.763	.7249	0.0431	0.477	.7372	0.6949	0.503	.6518	0.90
0.721	.7333	0.0505	0.506	.7466	0.7031	0.499	.6632	0.91
0.612	.7430	0.0590	0.504	.7587	0.7138	0.509	.6702	0.91
0.562	.7520	0.0669	0.503	.7671	0.7212	0.540	.6809	0.92
0.526	.7551	0.0696	0.500	.7754	0.7285	0.584	.6886	0.93
0.504	.7732	0.0856	0.519	538.6344	0.4847	0.751	.7177	0.95
0.485	.7819	0.0932	0.516	.6497	0.4982	0.839	.7264	0.96
0.499	536.6150	0.7070	0.517	.6608	0.5080	0.939	.7354	0.97
0.496	.6272	0.7177	0.520	.6691	0.5153	1.106	.7580	0.99
0.477	.6352	0.7248	0.508	.6795	0.5244	1.111	.7660	0.00
0.496	.6435	0.7321	0.526	.6875	0.5315	1.071	.7792	0.01
0.491	.6553	0.7425	0.538	.6976	0.5404	0.973	.7844	0.01
0.511	.6643	0.7504	0.524	.7063	0.5480	0.508	545.6218	0.63
0.492	.6723	0.7574	0.512	.7333	0.5718	0.494	.6367	0.64
0.503	.6803	0.7645	0.484	.7427	0.5801	0.493	.6447	0.65
0.484	.6883	0.7715	0.497	.7535	0.5896	0.494	.6555	0.66
0.504	.6963	0.7786	0.485	.7649	0.5996	0.498	547.6297	0.40
0.501	.7043	0.7856	0.485	.7761	0.6095	0.501	.6446	0.41
0.500	.7126	0.7929	0.497	.7833	0.6158	0.517	.6560	0.42
0.517	.7209	0.8002	1.138	542.6334	0.0051	0.516	.6654	0.43
0.491	.7303	0.8085	0.932	.6567	0.0256	0.524	.6790	0.44
0.517	.7383	0.8155	0.866	.6647	0.0327	0.509	.6887	0.45
0.507	.7466	0.8229	0.747	.6754	0.0421	0.508	.6988	0.46
0.492	.7553	0.8305	0.678	.6827	0.0485	0.527	.7057	0.47
0.511	.7671	0.8409	0.625	.6952	0.0595	0.512	.7165	0.48
0.495	.7761	0.8488	0.571	.7035	0.0668	+0.511	.7238	0.48
+0.497	537.6417	0.6108	+0.531	.7150	0.0769			

After each of these determinations there is given the probable residual of a single observation from the computed variation. Terms in $\cos 3\theta$ and $\cos 4\theta$ and all the harmonics of $\sin\theta$ are negligibly small.

The variation in blue light is quite similar to that found by Wood from his observations taken with a Kunz cell without filters. Similarly, the variation in yellow light resembles that found by Dugan (1924) from his visual observations.

5. RECTIFICATION AND SOLUTION

With the maxima so asymmetric, it becomes questionable whether the light curves can be rectified with confidence. For a first attempt the more-or- constant light levels of the first maxima were assu to give the true outside-eclipse luminosities. On assumption, however, the eclipse curves yielded solutions. In terms of the parameters of the Princ nomographs the shape curves and depth lines c not be made to intersect.

For a second trial, rectification coefficients determined solely from the outside-eclipse variation the second maxima. These were first based on orbital inclination determined by Wood but eventually improved to a slight degree by the vergence of successive solutions.

TABLE II. Times of Minimum Light, R CMa.

JD ⊙ 2400000+	E	$O-C$	Method	Reference
28596.3573	+ 7380	−0d0438	vis. est.	Lause (1949)
28922.3745	7667	0.0424	vis. est.	Lause (1949)
32999.235	11256	0.083	vis. est.	Pohl (1951)
33367.320	11580	0.044	vis. est.	Pohl (1951)
34453.271	12536	0.055	vis. est.	Wroblewski (1954)
34454.404	12537	0.058	vis. est.	Pohl (1955)
34481.6617	12561	0.0627	pe.	Fitch (unpublished)
35515.360	13471	0.073	pe.	Lenouvel & Fiogère (1957)
35522.745	13477.5	0.072	pe.	Koch
35534.6755	+13488	−0.0685	pe.	Koch

final rectifications were made according to:

$$r(y)=0.0120+0.0106\cos\theta+0.0039\cos2\theta,$$

$$r(b)=0.0084+0.0052\cos\theta+0.0027\cos2\theta,$$

$$r(u)=0.0068+0.0078\cos\theta+0.0022\cos2\theta,$$

$$r'(y)=\frac{g'(y)}{0.9870-0.0084\cos2\theta},\quad Nz(y)=0.0662,$$

$$r'(b)=\frac{g'(b)}{0.9777-0.0085\cos2\theta},\quad Nz(b)=0.0570,$$

$$r'(u)=\frac{g'(u)}{0.9751-0.0088\cos2\theta},\quad Nz(u)=0.0542.$$

the mean darkening coefficient, values of 0.4, 8, and 1.0 were investigated. At each wavelength n coefficient of 0.8 proved to be significantly than any other value. No attempt was made to ine the coefficient more closely, and secondary is not deep enough to distinguish different ings for the two components. The common n for the three light curves is given in Table III. ough primary eclipse, systematic deviations from olution are rather troublesome in violet light. deviations, however, were not considered serious nt to cast doubt on the validity of a common n for all three light curves. Within the minima obable residual for a single observation is $\pm0^m.007$ w, $\pm0^m.008$ in blue and $\pm0^m.007$ in violet. ratios of the mean surface brightnesses indicate nperature of the cool star to be similar to that of dwarf.

n the solution, light curves were computed. are tabulated in Table IV, and on Figs. 1 and 2 llow and violet curves are drawn against the ations.

6. DISCUSSION

entire light curve of R CMa was first observed endell. His observations were analyzed by Shapley (1915) for stars moving in elliptical orbits. The orbit of R CMa is almost certainly circular so that Shapley's solution is not directly comparable with the later ones. It was decided to analyze Wendell's curve from the beginning for circular elements and 0.4 limb darkening. The scatter of the observations is large, but appreciable ellipticity and reflection effects were found. The rectified eclipses yielded a determinate solution.

Table III. Solution of light curves, R CMa.

			y	b	u
x	0.8				
k	0.819	$(1-l_0)^{pr}$	0.393	0.404	0.409
$\alpha_o^{tr}=\alpha_o^{pr}$	0.556	$(1-l_0)^{sc}$	0.036	0.020	0.013
$\alpha_o^{oc}=\alpha_o^{sc}$	0.627	L_g	0.942	0.969	0.980
a_g	0.302	L_s	0.058	0.031	0.020
b_g	0.299	L_g'	0.936	0.963	0.972
a_s	0.248	L_s'	0.027	0.014	0.011
b_s	0.245	J_g'/J_s	23.4	44.8	60.4
j	77°.0	z	0.021	0.018	0.017

Selected parameters of the best individual solutions for all the light curves are listed in Table V, first for the yellow observations and then for the blue ones. For the Tucson observations the orbital inclination, the dimensions of the small star, and the geometric ellipticities of figure are all in good agreement with previous determinations. The dimensions of the large, hot component, on the other hand, are on the order of 20% greater than the sizes found from the light curves of 1899 and 1920. They are about 10% larger than the values found in 1939. Only part of these discrepancies can be removed by juggling the depths of the eclipses within the scatter of the observations. Examination of all the light curves suggests strongly that these changes are not due to an actual expansion of the hot component but can probably be traced to real, though small, variations in the depths and shapes of the minima. At least one instance of such changes can be detected in the new light curves, for the descending branch of secondary eclipse is definitely brighter point for point than is the ascending branch.

Interpretation of the new light curves in terms of a plausible model has not been very successful. A

Table IV. Computed Light Curves, R CMa.

Phase	Δm_y	Δm_b	Δm_u	Phase	Δm_y	Δm_b	Δm_u
$0^p.000$	$+0^m.865$	$+1^m.103$	$+1^m.111$	$\pm0^p.250$	$+0^m.264$	$+0^m.496$	$+0^m.493$
±0.005	0.859	1.096	1.103	0.300	0.263	0.497	0.492
0.010	0.837	1.073	1.080	0.350	0.267	0.502	0.496
0.020	0.761	0.995	1.001	0.400	0.272	0.508	0.501
0.030	0.659	0.892	0.896	0.420	0.276	0.511	0.504
0.040	0.557	0.787	0.790	0.430	0.280	0.513	0.506
0.050	0.463	0.692	0.694	0.440	0.285	0.518	0.509
0.060	0.387	0.615	0.614	0.450	0.291	0.522	0.512
0.070	0.331	0.559	0.557	0.460	0.299	0.526	0.515
0.080	0.301	0.526	0.525	0.470	0.308	0.531	0.518
0.100	0.291	0.518	0.516	0.480	0.314	0.534	0.520
0.150	0.281	0.508	0.506	0.490	0.318	0.536	0.522
±0.200	+0.270	+0.500	+0.497	0.495	0.319	0.537	0.523
				±0.500	+0.320	+0.538	+0.523

TABLE V. Solutions for R CMa.

Observer	Wendell	Dugan	Koch	Wood	Koch
Date	1898–99	1916–23	1955–56	1939	1955–56
Wavelength	5500 A	5500 A	5300 A	4500 A	4200 A
$(1-l_0)^{pr}$	0.380	0.373	0.393	0.405	0.404
$(1-l_0)^{sc}$	0.040	0.028	0.036	0.035	0.020
j	77°.4	76°.6	77°.0	76°.7	77°.0
r_g	0.260	0.253	0.302	0.275	0.302
r_s	0.247	0.244	0.248	0.255	0.248
D	0^d.170	0^d.165	0^d.194	0^d.182	0^d.194

beginning toward this end is possible, however, if it is assumed that the excess light observed after primary eclipse remained stationary in the frame of reference rotating with the system and that the periods of rotation and revolution for the stars are synchronized. That this postulate may express the actual situation can be seen if we inspect Fig. 1. In this case for yellow light, the change of light level and the disparity of the maxima are so cleanly marked that any departure from synchronism would have conspicuously increased the scatter of the observations. It can be noted further that the amount of excess light at least does not increase with decreasing wavelength, and that this same excess light comes into view as we begin to see the interior hemisphere of the cool star and the exterior hemisphere of the hot star. Finally, the light distribution after primary eclipse appears due to circular rather than elliptical isophotes on the stars. In sum, these characteristics can be tentatively interpreted as evidence of a sharply defined edge of a hot, emitting area on the inside hemisphere of the cool star rotating into view at about forty-five degrees orbital longitude. There is one conspicuous difficulty in accepting this analysis. To account for the rest of the observed light curve an unknown number and orientation of dark and bright spots would have to follow this emitting edge so that as it rotated out of sight a drop of 0^m.03 for the yellow light curve would not be detected. If the advancing edge of the disturbed area is the same size at all wavelengths, a temperature of 6000°K for this edge would account for the rise after primary eclipse.

It may now be possible to distinguish two [illegible] complications which occur on R CMa. The first i[s] emission effect on the order of 0^m.1 in the visual r[egion] established independently by Wendell and Pick[ering] in 1898–1899. This has been observed to vanis[h] appear in less than a month's time. The second i[s] smaller-scale emission lasting at least three m[onths] and described in this paper. This distinction, of c[ourse] may be artificial. It is almost a certainty, how[ever] that the depths of the eclipses and the shapes o[f] minima vary as a result of these complications [and] others yet unrecognized. This being so, an un[com]plicated, definitive light curve of R CMa has per[haps] not yet been observed.

7. SUMMARY AND ACKNOWLEDGMENTS

In all areas R CMa remains an important sy[stem] for future work: a better parallax is necessary, [and] simultaneous photometry and spectroscopy are ne[eded] to attack the observed changes in the light curves [and] the radial velocity curve. Observation of times of [maxi]mum light should also be continued faithfully.

The people and institutions cited in my p[aper] [*Astron. J.* **65**, 127 (1960)] on AO Cas are agai[n] be recognized as aiding the present piece of w[ork]. Special thanks are also due to Dr. W. S. Fitch fo[r] permission to use the unpublished material refe[rred] to herein.

REFERENCES

Buscombe, W. and Morris, P. M. 1958, *Mem. Mt. Stromlo* **3**, 15.
Dugan, R. S. 1924, *Princeton Contr.* **6**, 49.
Dugan, R. S. and Wright, F. W. 1939, *Princeton Contr.* **1[9]**
Fitch, W. S. 1957, *Astron. J.* **62**, 108.
Fringant, A. M. 1956, *Contr. de l'Inst. d'Astron. de Paris* **S[er. A]** No. 216.
Johnson, H. L. and Morgan, W. W. 1953, *Astrophys. J.* **117**
Kopal, Z. and Shapley, M. B. 1956, *Jod. Bank Ann.* **1**, 210.
Lause, F. 1949, *Astron. Nach.* **277**, 40.
Lenouvel, F. and Fiogère, Cl. 1957, *J. O.* **40**, 41.
Pickering, E. C. 1904, *Harvard Ann.* **46**, 184.
Pohl, E. 1951, *Astron. Nach.* **279**, 178.
——. 1955, *Astron. Nach.* **282**, 235.
Shapley, H. 1915, *Princeton Contr.* **3**, 82.
Struve, O. and Smith, B. 1950, *Astrophys. J.* **111**, 27.
Wendell, O. C. 1909, *Harvard Ann.* **69**, 66.
Wood, F. B. 1946, *Princeton Contr.* **21**, 31.
Wroblewski, A. 1954, *Rocznik Astron. Obs. Krakow* **25**, 83.

Be Stars in Galactic Clusters

A. J. MEADOWS
University of Illinois Observatory, Urbana, Illinois
(Received February 15, 1960)

The proportion of Be to B stars is considered for ten galactic clusters. It is shown that this ratio is considerably higher in some of the clusters than for the galaxy as a whole. It is suggested that an overbundance of Be stars indicates higher than average rotational velocities for all the B stars in the cluster.

HE determination of rotational velocities for cluster stars is important for two main reasons. y, variations of these velocities from cluster to r may indicate differences in origin or evolution system and, secondly, stars with very high ro- al velocities may evolve in a different manner ıse of mass loss and, perhaps, mixing) from the nary models which have hitherto been investi- theoretically. Relatively few rotational velocities been determined in galactic clusters. It therefore worthwhile to approach the problem from a more ative standpoint, using the data at present avail- The obvious method of investigation is to con- the distribution in clusters of stars with peculiar a, where the peculiarity is believed to depend on otational velocity. In this connection Be stars r to be the most useful, since it seems well estab- that their spectral peculiarities are due to high on rates (e.g., Slettebak 1949). Thus if Be stars und to be over- or under-abundant in clusters, it possible to draw conclusions correspondingly as rotational velocity distribution in the clusters. xample, Struve (1945) has pointed out that Be are overabundant in the Pleiades, where meas- nts have shown that the rotational velocities of rs may be above the average. This qualitative od has one advantage over rotational velocity obtained from linewidth measurements. In the case only velocities in the line of sight are meas- so that somewhat arbitrary assumptions must be concerning the inclination of the rotational axes. resence of Be stars should, however, be detectable ver their inclination.

OBSERVATIONAL DATA

Table I gives the number of Be and B stars in clusters for which reasonably up to date information is available. Only stars of luminosity classes IV and V have been considered, since emission in B giants may be effected by causes other than rotation. An asterisk before a cluster indicates that a quarter, or more, of the B stars observed have been found to have broad spectral lines (presumably due to rotation). The lifetimes of NGC 2264 and NGC 6530 are taken from Walker (1956, 1957) and the lifetimes of the remaining clusters from von Hoerner (1957). The three final clusters do not have determined ages.

The average B/Be ratio for the foregoing ten clusters is 5.5 for the range B0–B3 and 20.0 for the range B4–B8. This should be compared with the average for normal field stars (Struve 1951) of 10.1 for the range B0–B3 and 76.6 for the range B4–B8. Thus, the number of Be stars in the considered clusters is much greater than would be expected. There is, however, considerable variation within the group. Thus the Scorpio-Centaurus cluster has an average B/Be ratio differing little from the normal, whereas, in the Pleiades, the difference is very large.

Two other observations, not mentioned in Table I, are of importance. Firstly, there seems to be a tendency in some clusters for the Be stars to occur near the center of the cluster. Struve (1945) has already pointed this out for the Pleiades, but it is also true, for example, of NGC 6530, where the five Be stars are closely grouped near the center of the cluster (which contains well over a hundred stars). Secondly, the clusters with highest ratios of Be to B stars are, in the main, associ-

TABLE I.

Cluster	Age (in years)	Number of Be stars B0–B3	Number of Be stars B4–B8	Number of B stars B0–B3	Number of B stars B4–B9	Ratio B/Be B0–B3	Ratio B/Be B4–B9
*NGC 2264	3×10^6	0	0	5	10	...	...
*NGC 6530	3×10^6	5	0	14	17	2.8	...
*Scorpio-Centaurus	4×10^6	5	0	52	29	10.4	...
*h and χ Persei	4.4×10^6	5	1	20	17	4.0	17.0
NGC 457	1.5×10^7	2	0	9	21	4.5	...
α Persei	2×10^7	1	1	5	15	5.0	15.0
*Pleiades	8×10^7	0	5	0	25	...	5.0
NGC 2244	...	4	0	10	2	2.5	...
NGC 6087	...	0	2	0	14	...	7.0
M 25	...	0	0	1	25	...	...

ated with considerable nebulosity (e.g., NGC 6530, Pleiades, NGC 2244).

DISCUSSION

The data given indicate an overabundance of Be stars in the ten clusters considered. On the assumption that such an excess is an indication of rotational velocities above the average, we would expect the B stars in NGC 2244, NGC 6530, $h+\chi$ Persei, and the Pleiades to have rotation rates higher than the average. The only one of these clusters for which rotational velocities have so far been measured is the Pleiades (Struve 1945, van Dien 1948). Here, the mean rotational velocity of the eleven brightest cluster stars is 177 km/sec, compared with the galactic average for BV and BIV stars, of the same spectral types, of 159 km/sec (e.g., Boiarchuk and Kopilov 1958). However the fainter B stars in the Pleiades give a slightly lower average velocity. Hence, the result here is inconclusive. The only other cluster containing B stars for which extensive measurements are available is Scorpio-Centaurus (Huang and Struve 1954). The B/Be ratio for this cluster is close to normal and the measured rotational velocities are also close to the galactic average. Indeed, Huang and Struve state that the average rotational velocity may be lower f cluster stars than for field stars.

Struve (1945) has suggested that the higher ties found in the Pleiades may be due to the in matter from the surrounding interstellar materia would seem to receive some confirmation from t servation, mentioned above, of a possible corre between nebulosity and the number of Be star cluster. On the other hand, such a theory wou explain the presence in clusters of rotational vel below the average. Two explanations of such an appear possible; either (a) the rotational velociti actually low due to the mode of formation of the c (Huang and Struve 1954), or (b), there is a ten for the rotational axes to be orientated, for exa by an interstellar magnetic field.

REFERENCES

Boiarchuk, A. A. and Kopilov, I. M. 1958, *Astron. Zhur.* 3
Huang, S. and Struve O. 1954, *Ann. d'Astron.* **17**, 85.
Slettebak, A. 1949, *Astrophys. J.* **110**, 498.
Struve, O. 1945, *Pop. Astron.* **53**, 201, 259.
Struve, O. 1951, *Astrophysics* (ed. J. A. Hynek), p. 86.
Van Dien, E. 1948, *J. Roy. Astron. Soc. Can.* **42**, 249.
Von Hoerner, S. 1957, *Z. Astrophys.* **42**, 273.
Walker, M. F. 1956, *Astrophys. J. Suppl.* **2**, 365.
Walker, M. F. 1957, *Astrophys. J.* **125**, 636.

Some Remarks on Optical Properties of Saturn's Rings

M. S. BOBROV
U.S.S.R. Academy of Sciences, Moscow, Russia
(Received October 20, 1959)

Some optical properties of Saturn's rings are discussed in connection with the papers of F. A. Franklin and A. F. Cook (1958a, 1958b). Special attention is paid to the objection of these authors to Bobrov's conclusion about nondiffractional character of the light scattering by B-ring. It is shown that this objection is unfounded.

CENTLY F. A. Franklin and A. F. Cook have ublished two interesting papers (1958a, 1958b) g optical properties of Saturn's rings. The authors scuss some of my results on this subject.

nany aspects of the problem our views coincide. in and Cook's point of departure is that the most iate problem in the study of the rings involves a n between the diffraction and the shadowing neses. I believe that it is quite true. In my paper 0 (page 8), the same idea was formulated in the ng words: "The choice between the theory of ger and the diffraction theory is adequate to the on of the problem of the size of particles and of the of the rings." On the question of optical thickness ing and large-particle interpretation of the phase of this ring we have also rather similar opinions. he same time some details of Franklin and Cook's igations seem to be doubtful and need further sion. There is also a certain misunderstanding the sense of one equation used by me and quoted ese authors (1958a).

nklin and Cook object to the value $x(\pi)=5.3$ d by me (1952), $x(\pi)$ being the ratio of the back- red light to its average value and π being the ring angle. They see my mistake in using equation

$$r=0.72/\sin A, \tag{1}$$

0.72 is the absolute brightness (I/F in Chan- khar's notations) of Saturn's B-ring and A denotes levation angle of the sun above the ring-plane. klin and Cook suppose that Eq. (1) was used by order to reduce the brightness illuminated by the at an angle A to one illuminated by light rays ndicular to the ring plane. In fact it is not so. tion (1) is only an auxiliary formula for transition the absolute brightness $b=I/F$ to the so-called tness coefficient r which is the ratio of the intensity ht scattered by a given surface to one scattered he same conditions) by an orthotropic white surface olev 1956). The transition from b to r was expedient se Sobolev's tables (Sobolev 1949) were computed (By the way, the authors' remark that Sobolev's ulas neglect the small contribution of higher-order ering is not correct. Sobolev's formulas and tables into account the higher-order scattering computed Eddington's method.) One may obtain $x(\pi)\sim 5$ in another way, without using Eq. (1). According to Chandrasekhar (1950, §62) the following formula is valid for isotropic scattering:

$$I(0,\mu)=\frac{1}{4}\tilde{\omega}_0 F\frac{\mu_0}{\mu+\mu_0}[X(\mu)X(\mu_0)-Y(\mu)Y(\mu_0)]. \tag{2}$$

Assume that the first-order scattering is anisotropic with the phase function $x(\theta)$, where θ is the scattering angle. In the case when $x(\pi)\gg 1$, the contribution of the higher-order scattering into total intensity of the light scattered in the direction $\theta=\pi$ is rather small. So we may assume that the higher-order scattering is approximately isotropic. Taking also in Eq. (2) $\mu_0=\mu$ we receive the expression

$$b=\frac{I}{F}=\frac{1}{8}\tilde{\omega}_0\{[x(\pi)-1](1-e^{-2\tau/\mu})+X^2(\mu)-Y^2(\mu)\}. \tag{3}$$

Now adopt $b=0.72$, $\tilde{\omega}_0=1$, $\mu=\cos 25°=0.4225$, $\tau=1$. Then $X(\mu)=1.5385$, $Y(\mu)=0.3911$ (Chandrasekhar *et al.*, 1952) and Eq. (3) gives $x(\pi)=4.6$. For optical thickness $\tau=0.5$ Eq. (3) gives $x(\pi)=5.6$. The value $x(\pi)=5.3$ quoted above was derived by me with the aid of Sobolev's tables and formulas for $b=0.72$, $\tilde{\omega}_0=1$, $\tau=0.7$. The agreement among these three values of $x(\pi)$ is good. Sobolev's formulas permit also to take into account the anisotropy of higher-order scattering. The computations show that for this case the correction has an order of a few percent. It should be emphasized that such a manner of computing the value of $x(\pi)$ is nearly free from arbitrary hypotheses (about the form of the phase function, etc.) dealing chiefly with observable magnitudes. The result changes insufficiently if we take $\tilde{\omega}<1$ or $\tau\gg 1$.

The final conclusion is that at this point the criticism of Franklin and Cook (1958a) is unfounded. For the B-ring of Saturn, $x(\pi)$ has an order of 4–5. This value is evidently too high for the diffraction scattering and the large-particle treatment must be given preference.

Now, some words about the observed phase curves of Saturn's rings. The authors (1958a) consider them as very doubtful. Possibly they are not acquainted with the recent results of Lebedinets (1957) who obtained the phase curve of B-ring very accurately by photographic method. He used Professor Barabasheff's and

his own negatives. The phase curve of Lebedinets is in good agreement with the curves of Schoenberg (1933). My opinion is that further work in this direction is still desirable but that the main features of the B-ring curve are now quite clear.

Finally, I should like to make some remarks about the optical thickness τ_B of B-ring. The value τ_B is still very uncertain. Franklin and Cook's estimation of this magnitude is based on two results. The first was obtained by Reid *et al.* (1920) and by Bhaskaran and Bappu (1920) who watched the occultation of the star Lpz 4091 ($7^m.6$) by rings and disk of Saturn on March 14, 1920. Unfortunately the star intersected the ring system just before the disappearance behind Saturn's limb. Under these conditions the irradiation effects are of great importance (for a more detailed discussion see Bobrov 1956, p. 906). Both groups of observers believed that they saw the star through the ring B but more likely they were mistaken.

The second result used by Franklin and Cook was that of Barnard (1890) who observed the eclipse of Iapetus by the shadow of the rings. Oncoming daylight prevented Barnard from following the satellite more than just into the penumbra of ring B. In this situation the estimation of τ_B is rather difficult, but Franklin and Cook succeeded in developing an interesting method for the estimation of τ_B according to Barnard's data, finding $\tau_B = 0.58$. Unfortunately this method permits deriving of the optical thickness only for the zone near the inner edge of the B-ring where the matter is obviously more rarefied than in the bright zone of this ring. So one may conclude that the value 0.58 does not represent the real magnitude of τ_B which must be significantly greater.

Not long ago M. B. B. Heath (1958) reported that on April 28, 1957 J. E. Westfall had observed the oc tation of BD $-20°4568$ ($8^m.0$) by A- and B-rings. elevation of the earth above the ring-plane was According to this observation the two narrow zone the B-ring are undoubtedly not quite opaque: near outer edge of the ring and near the middle of the r The approximate width of the zones is $0''.5$ and 0 respectively, while the width of the B-ring is appr mately $3''.9$. The lack of data on atmospheric turbule prevents estimation of τ_B with accuracy.

These results show that for the evaluation of further observations of occultations are needed. electrophotometric design with a very small diaphra is possibly the best for this purpose. To avoid consi able errors due to the uncertainty of seeing conditi the observer must estimate the size of the star im during the occultation (for instance in Pickering Danjon-Couder scale).

REFERENCES

Barnard, E. E. 1890. *Monthly Notices Roy. Astron. Soc.* **50**, 1
Bhaskaran, T. P. 1920. *Monthly Notices Roy. Astron. Soc.* **80**,
Bobrov, M. S. 1940. *Astron. J. U.S.S.R.*, **17**, No. 6.
——. 1952. *ibid.* **29**, No. 3.
——. 1956. *ibid.* **33**, No. 6.
Chandrasekhar, S. 1950. *Radiation Transfer.*
Chandrasekhar, S., Elbert, D., and Franklin, A. 1952. *Astrop J.* **115**, 244.
Franklin, F. A., and Cook, A. F. 1958a. *Astron. J.* **63**, No. 9.
——. 1958b. *Smithsonian Contr. to Astrophys.* **2**, No. 13, 377.
Heath, M. B. B. 1958. *J. Brit. Astron. Assoc.* **68**, No. 2, 57.
Lebedinets, V. N. 1957. *Trans. Kharkov Astron. Obs.* **12**, 167.
Reid, W., Dutton, C. L. O'B. and Mc. Intyre, W. G. 1920. *J. Astron. Assoc.* **30**, 230, 306; **31**, 37.
Schoenberg, E. 1933. *Vierteljahresschr. Astron. Ges.* **68**, 387.
Sobolev, V. V. 1949. *Scientific Papers of Leningrad Univers series of math. sci.* No. 18, p. 17.
——. 1956. *Radiation transfer in the atmospheres of the stars planets*, pp. 40–41.